Plants (*Plantae* (= Archaeplastida))

Glaucophyta, Rhodoplantae, Viridiplantae

origin – more than
1 billion years ago

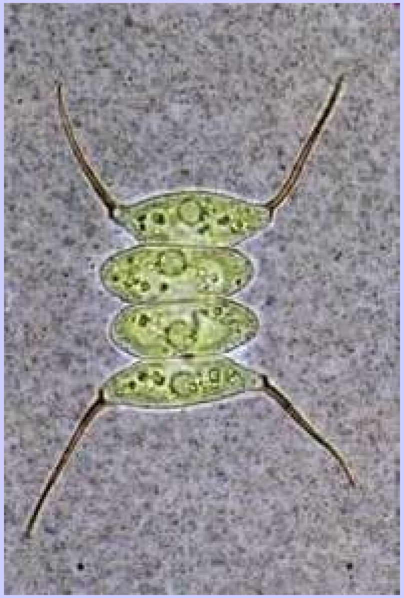

common features of plant lineages

traditional view on evolution
of Archaeplastida

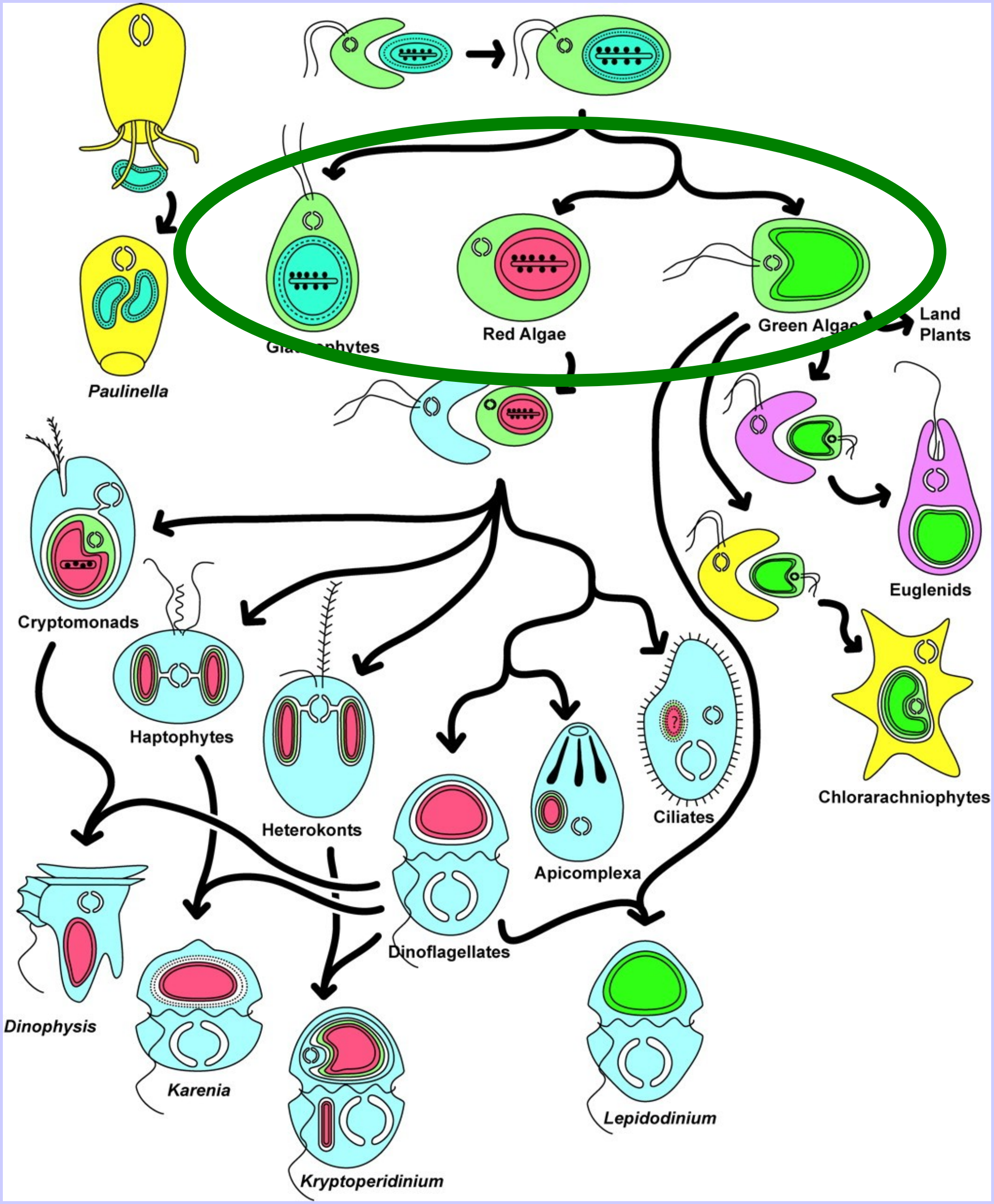

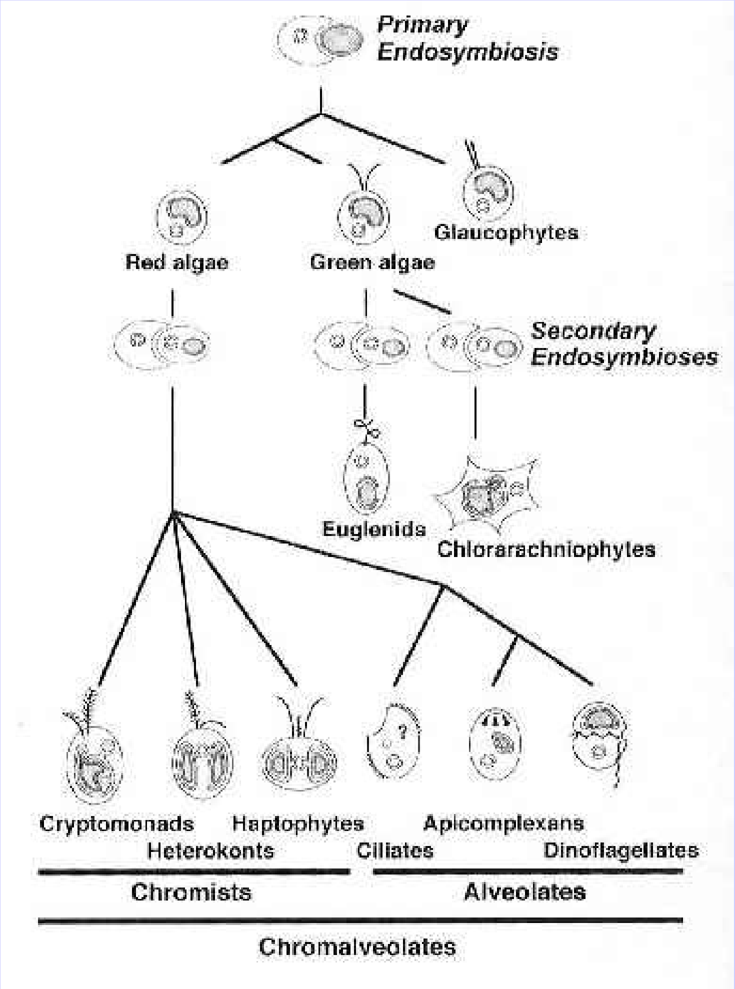

Keeling, 2004

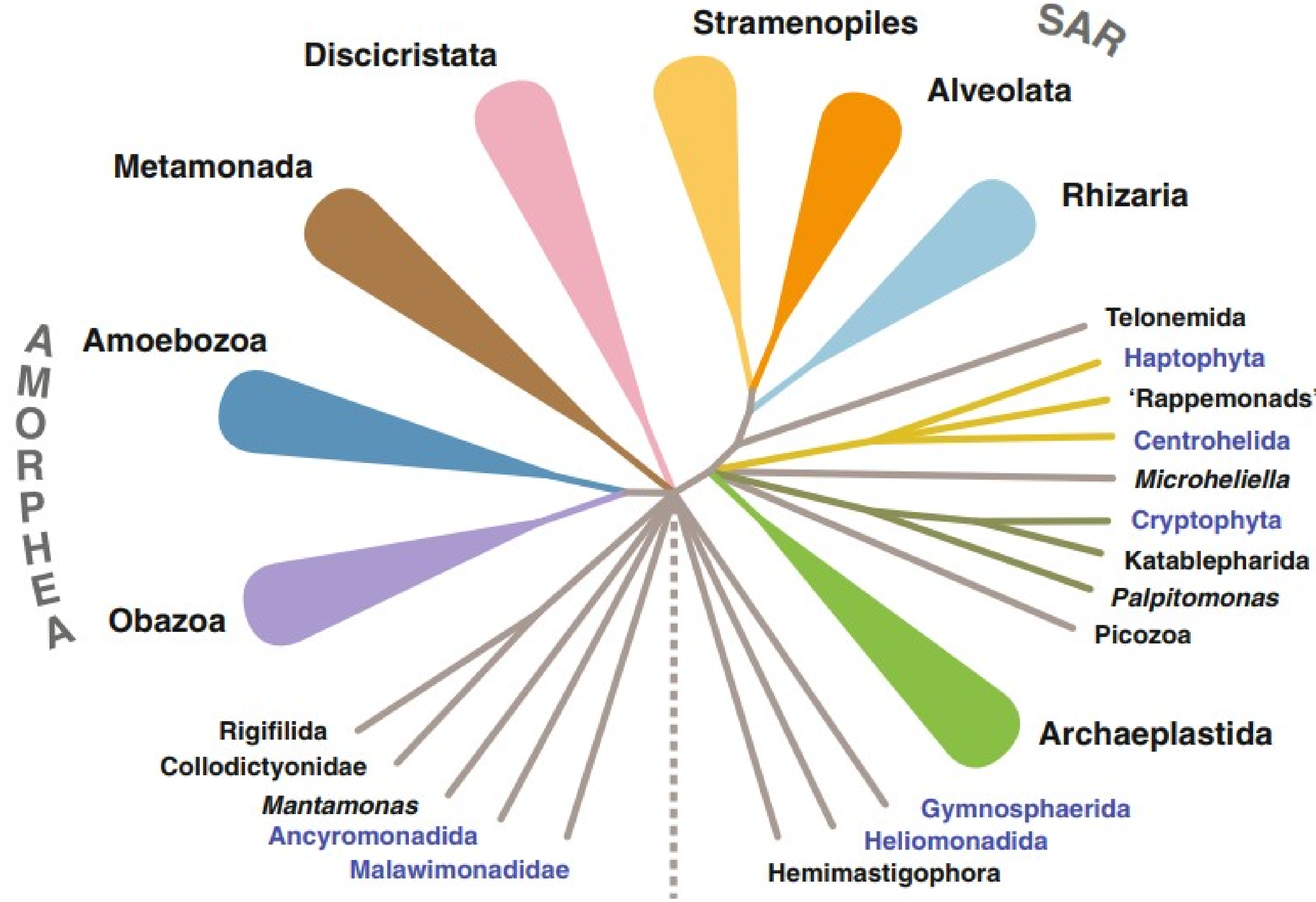

Fig. 1 Phylogeny of eukaryotes, based primarily on Brown et al. (2013), Cavalier-Smith et al. (2014), Kamikawa et al. (2014), Yabuki et al. (2014), Burki et al. (2016), and Leger et al. (2017). Groups with bulbous branches are examined in more detail in Figs. 2–5. Groups with narrow branches do not belong to well-established supergroups and are not illustrated separately; those covered in the Handbook are shown in *blue* and are as follows: ▶ Cryptophyta; ▶ Haptophyta; ▶ Centrohelida; ▶ Ancyromonadida; ▶ Malawimonadidae; ▶ Gymnosphaerida; ▶ Heliomonadida

Handbook of Protists, 2017

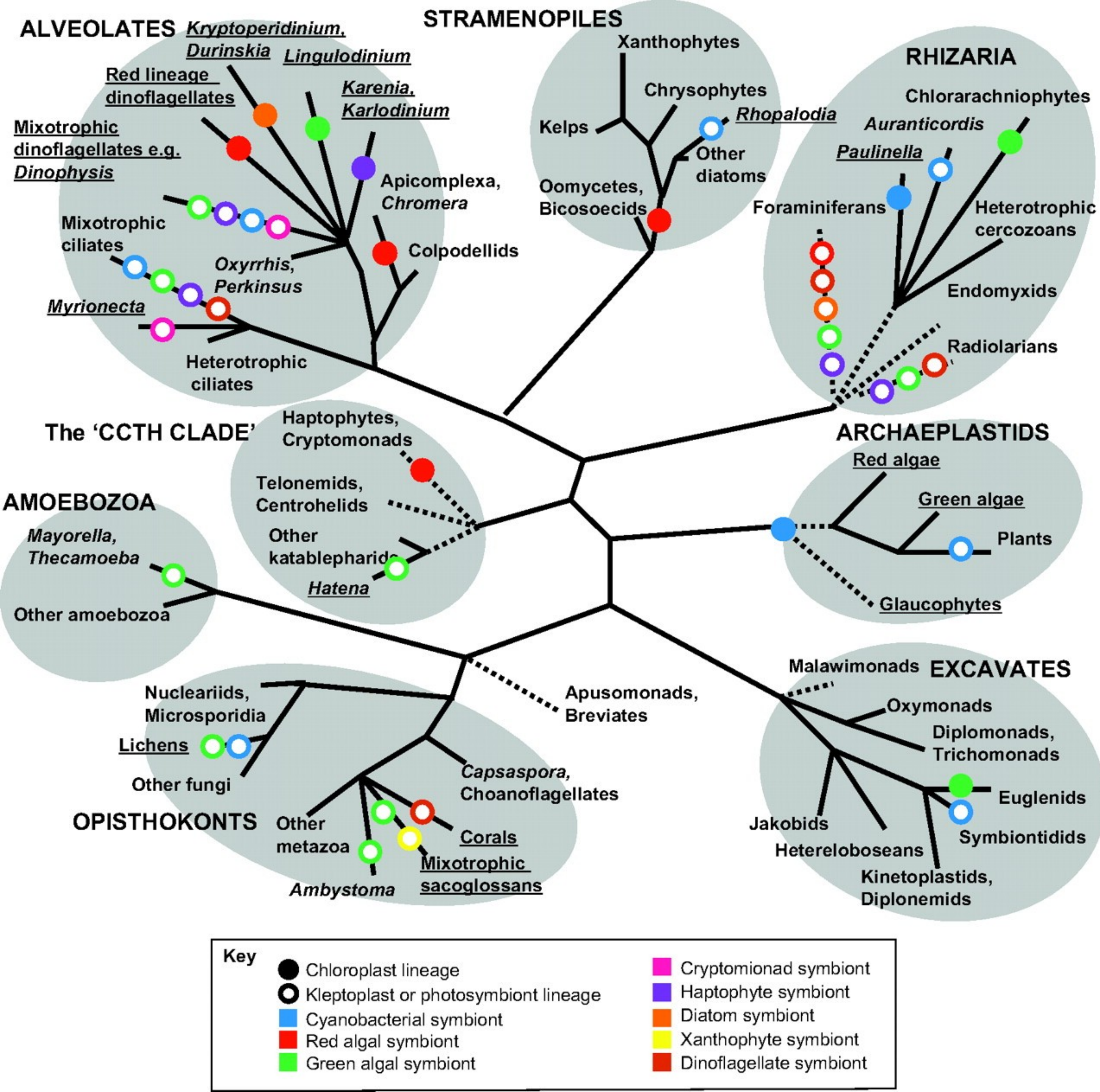

Dorrell et al., 2012, J Cell Sci

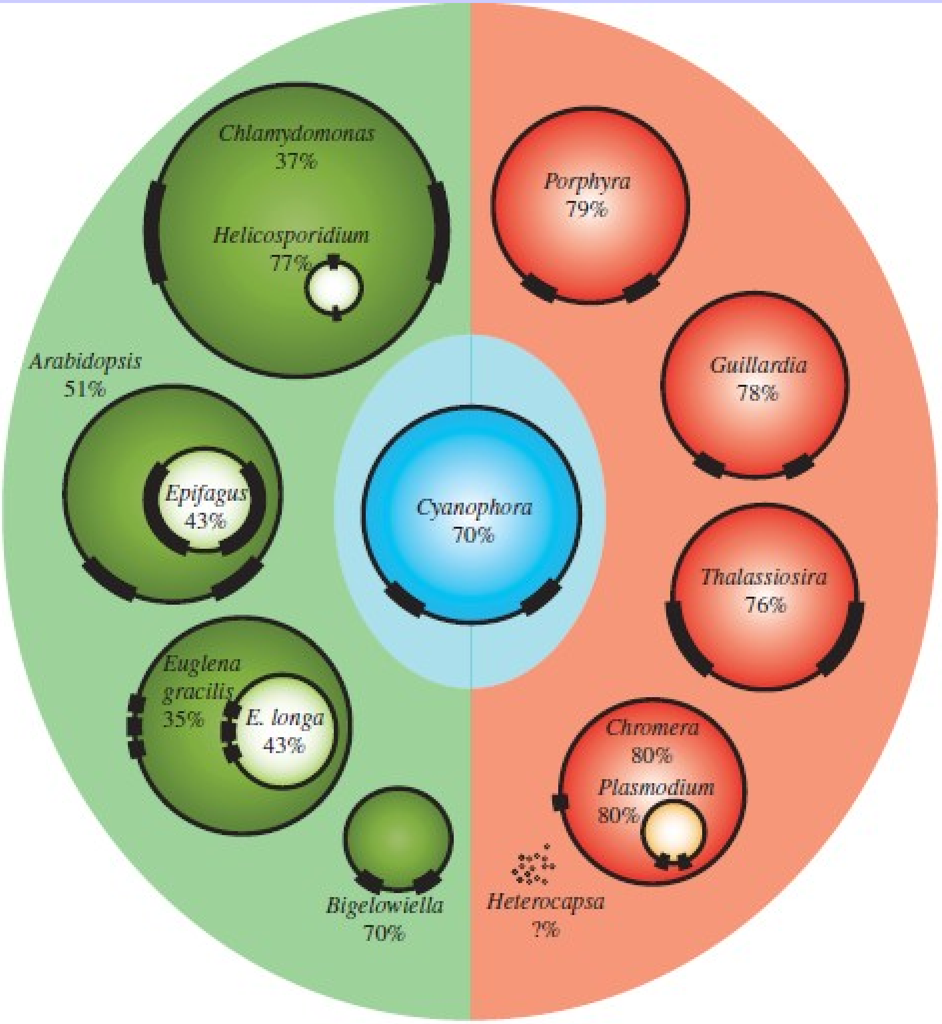

Figure 3. Plastid genome structure variation in photosynthetic and non-photosynthetic lineages. Genomes from the green lineage are on the left, the red lineage on the right and the glaucophyte genome is shown in the centre in blue. Inverted repeats encoding rRNA operons are shown as thickened lines. Numbers with names indicate the per cent of the genome that encodes proteins. Where both are available, a genome from a non-photosynthetic species is shown within that of a photosynthetic relative to show the scale of reduction. In general, plastid genomes map as circles and have an inverted repeat that encodes the ribosomal RNA operon. The major exception to this is the plastid genome of dinoflagellates, which has been reduced in coding capacity and broken down to single gene mini-circles. In some rare cases, the repeat and/or operon has been lost (e.g. in *Helicosporidium* and *Chromera*), or the rRNA operon is encoded in tandem (e.g. in *Euglena*). Non-photosynthetic plastids are greatly reduced in size, but tend to retain the overall structure of their photosynthetic counterparts.

Keeling, 2010, Phil. Trans. R. Soc. B 365: 729–748.

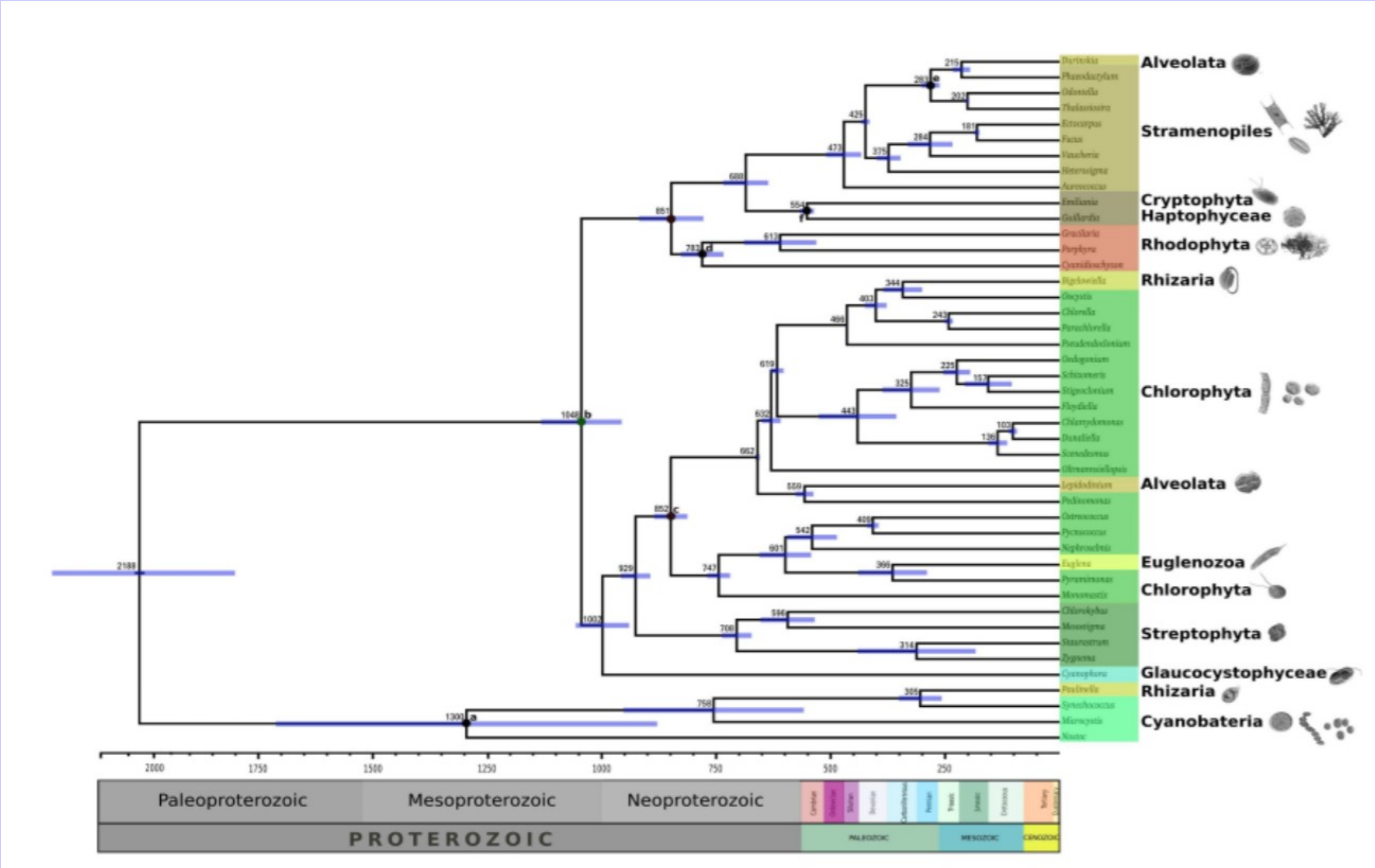

Evanovich et al, biorxiv
the plastid-encoded timeline

Glaucophyta

Glaucocystis nostochinearum

cocoid cells with flagellar remnants and contractile vacuoles

traditionally – 6 species, but only iconotypes are available…

uncertain (and possibly non-existent *Glaucocystopsis africana*)

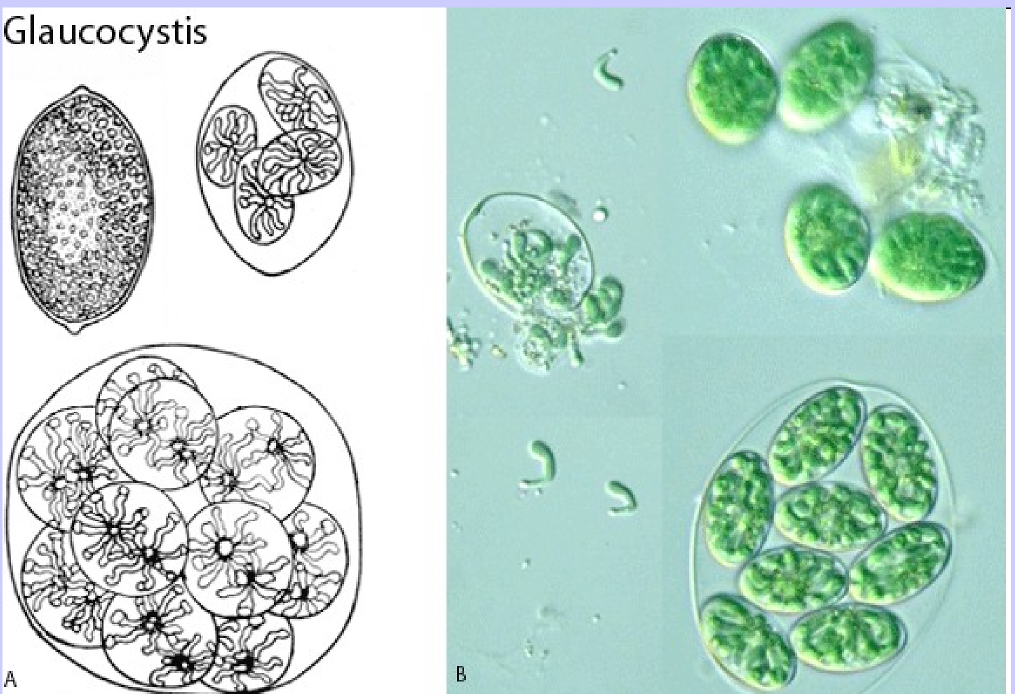

A after Prescott (1951)
B © Y.Tsukii, see http://protist.i.hosei.ac.jp/Protist_menuE.html

muroplasts = cyanelles, no traces of sex

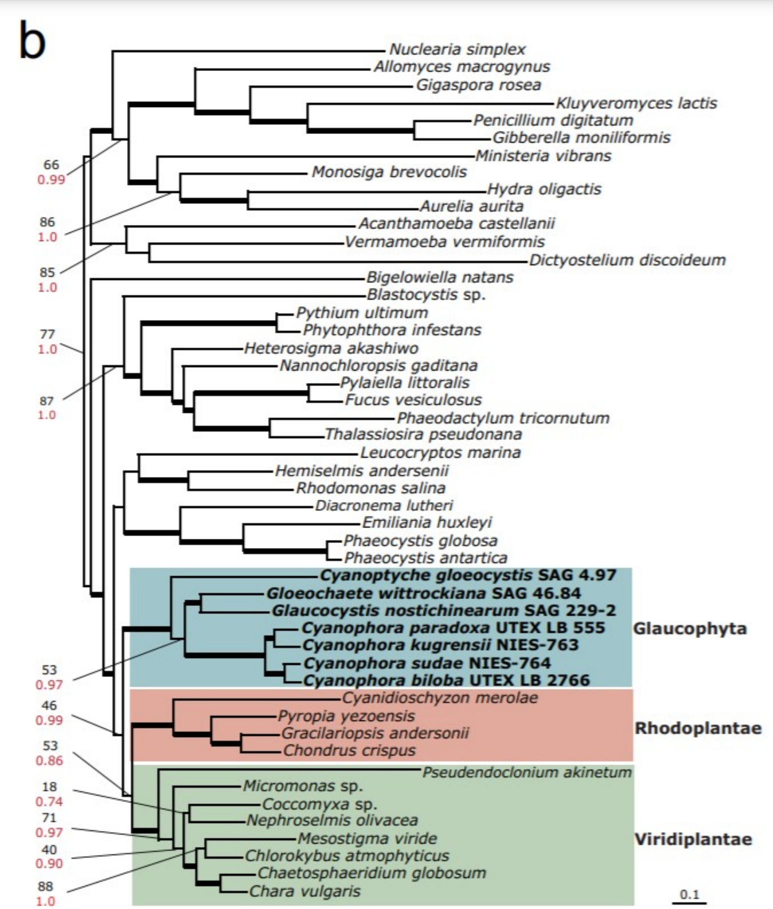

mitochondrial genomic data

Jackson et al., 2015

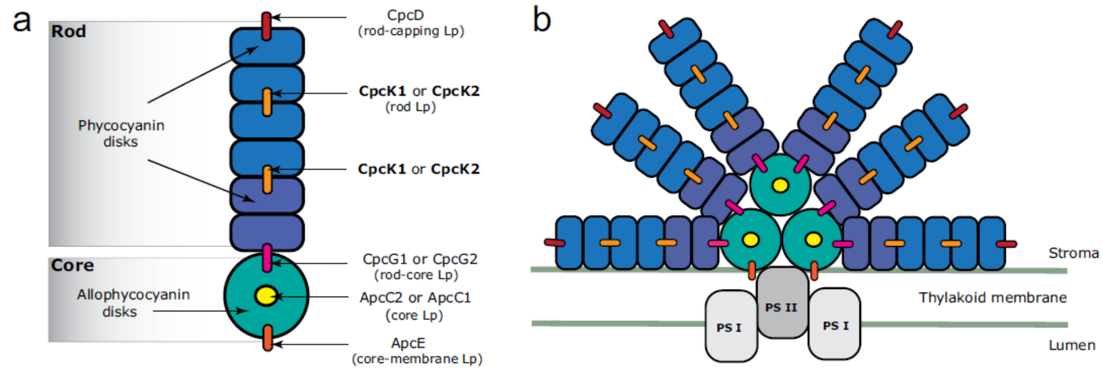

Fig. 5 Schematic model of the *Cyanophora paradoxa* phycobilisome antenna complex. A single rod and core section (**a**) illustrates the suggested arrangement of the phycobilisome cylinders (shapes in blue and turquoise) and the skeleton formed by the different linker proteins (Lp) of *Cyanophora*. The proteins CpcK1 or CpcK2 are novel rod linker proteins probably participating in the connection of phycocyanin disks, substituting for the typical cyanobacterial-like rod-linker protein CpcC, which is apparently absent in *Cyanophora*. The fan-like structure of the phycobilisome complex attached to the stromal side of the thylakoidal membrane (**b**) shows the core composed of three allophycocyanin cylinders (turquoise) with their longitudinal axes organized in a triangular arrangement. Six rods composed of six phycocyanin cylinders (blue) are attached to the core. The light energy efficiently captured by the phycobilosme antenna is then transferred to the reaction centers of the photosystems II (PS II) and I (PS I). This illustration is based on the model suggested by Watanabe et al. [40].

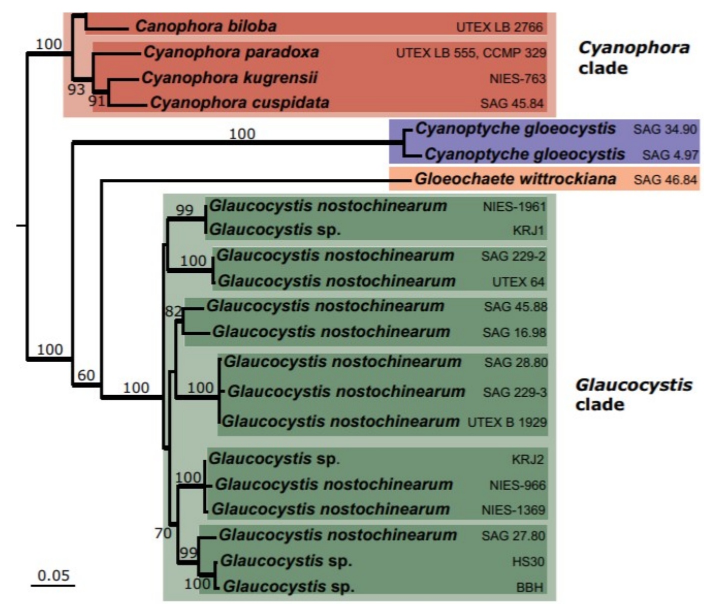

Fig. 4 Cryptic species diversity in *Cyanophora* and *Glaucocystis*. Maximum likelihood (ML) phylogenetic tree estimated from a concatenated data set of *psbA* (plastid gene), *cob* (mitochondrial gene) and the nuclear 5.8S and 18S rRNAs sequences. Numbers near nodes indicate bootstrap proportion support values >50% and thick branches indicate Bayesian posterior probabilities ≥0.95. Tree branch lengths are proportional to the number of substitutions per site indicated by the scale bar (see Chong et al. [38] for detailed methods).

Cyanophora paradoxa

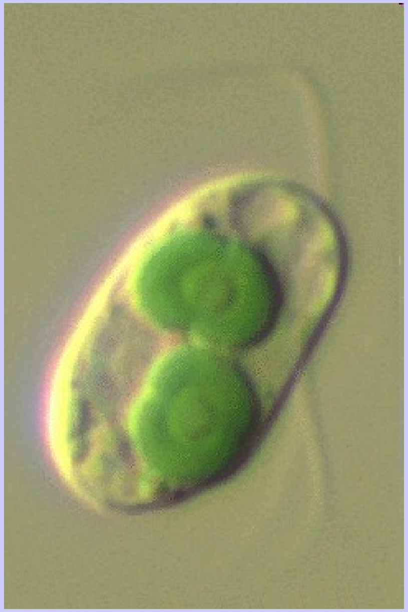

freshwater phytoplankton
eso-/eutrophic habitats
originally described from Ukraine,
additional records (UK, USA, Japan)

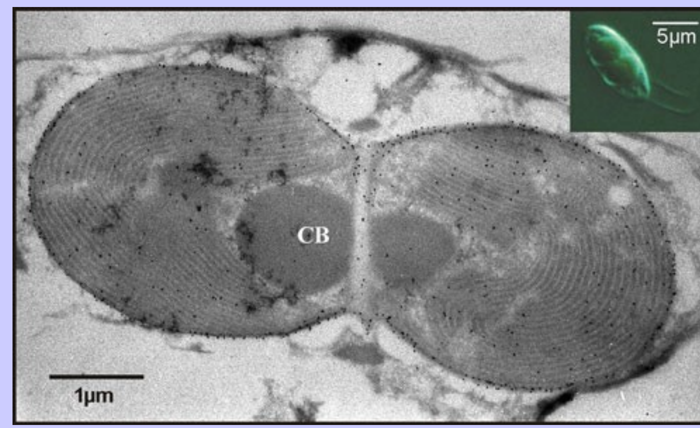

C. tetracyanea (from soil, a strain deposited in NIES)
But is it really a good species? *[We will see shortly...]*

Handbook of Protists, 2017

Cyanophora biloba (vs. *C. paradoxa*)

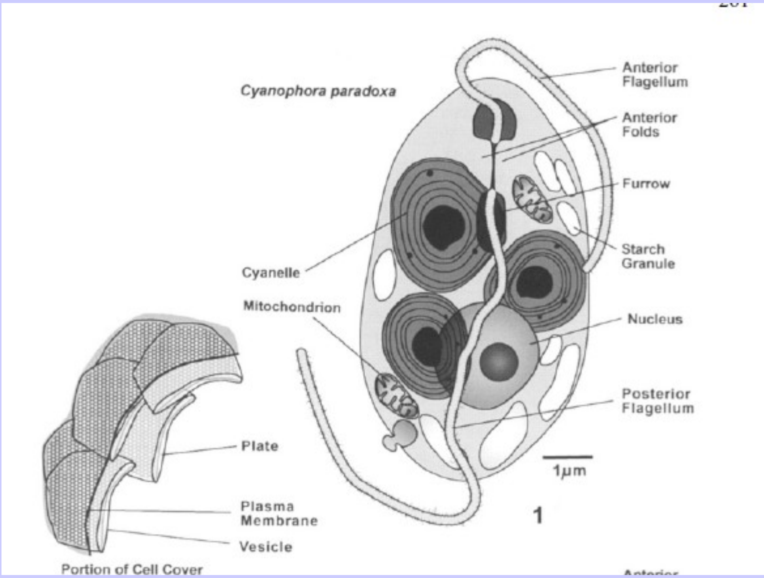

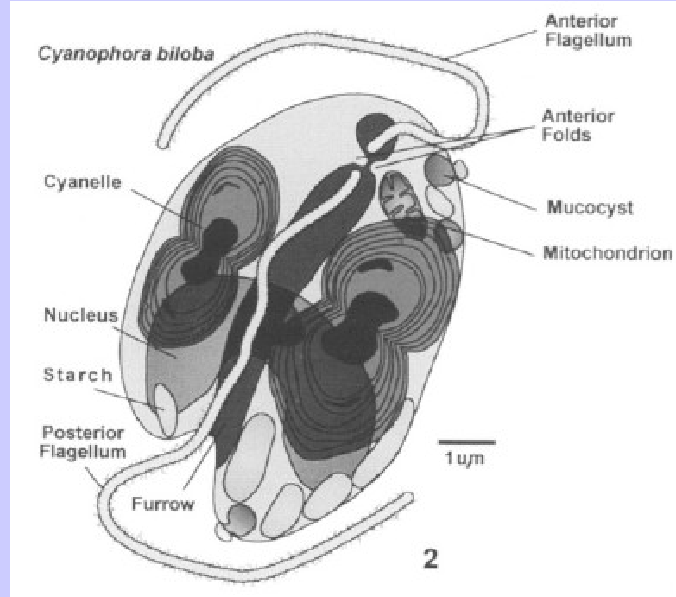

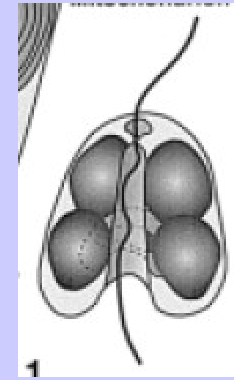

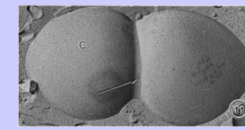

bilobate cells – one cyanelle in each lobe

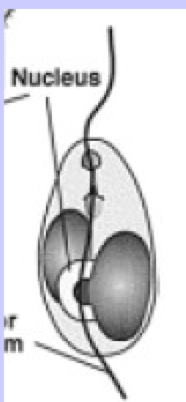

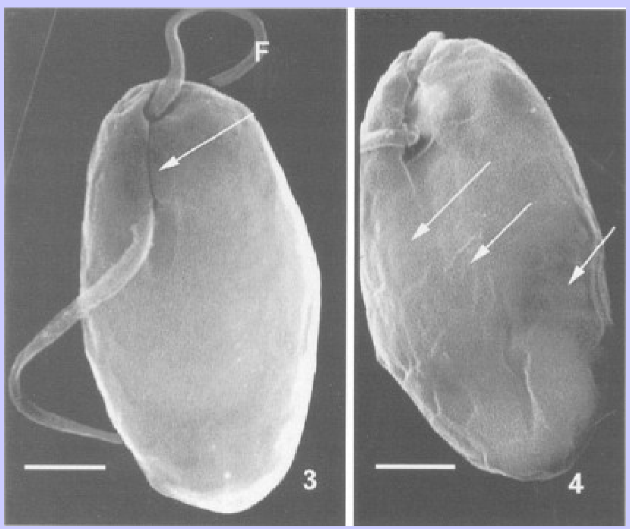

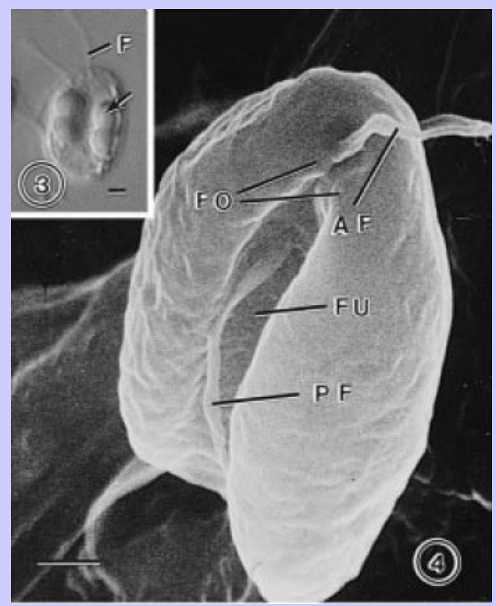

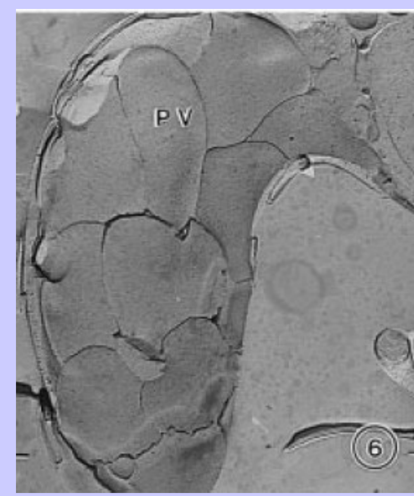

plates on cell surface, subapical flagellates

C. biloba – plankton ephemerous alpine pond (bloom)

Kugrens et al., 1999, J. Phycol. 35: 844-854.
Kugrens, 2002, Symbiosis 4

infrageneric taxonomy of *Cyanophora*

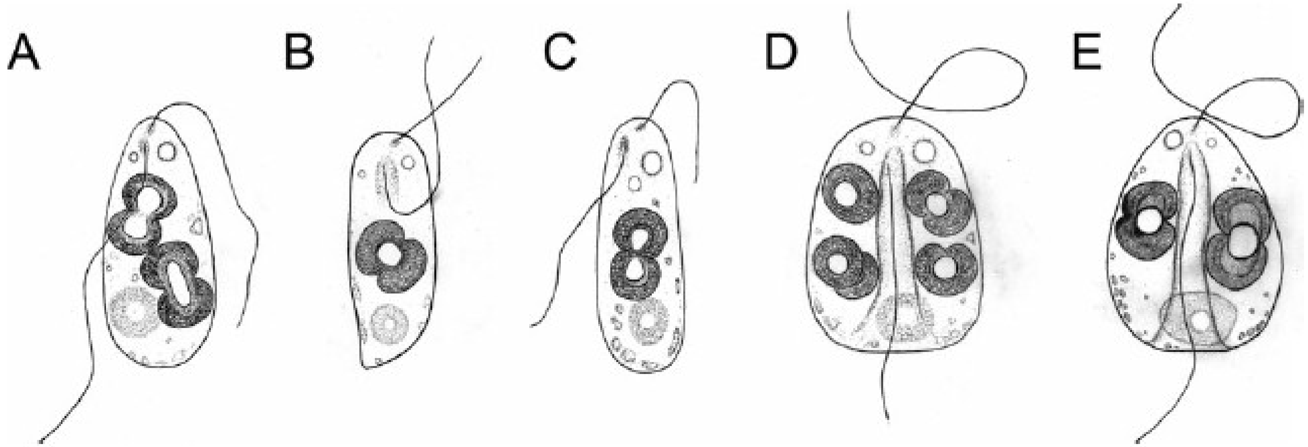

FIG. 1. Light microscope drawings of the vegetative cells of five *Cyanophora* species. (A) *C. paradoxa* Korshikov. (B) *C. cuspidata* Tos. Takah. & Nozaki sp. nov. (C) *C. kugrensii* Tos.Takah. & Nozaki sp. nov. (D) *C. sudae* Tos.Takah. & Nozaki sp. nov. (E) *C. biloba* Kugrens, B.L.Clay, C.J.Mey. & R.E.Lee. Drawings are not to scale.

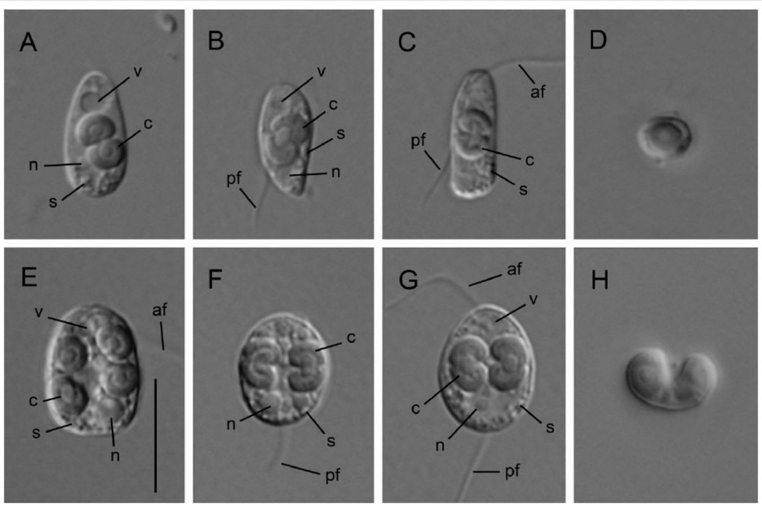

FIG. 2. Differential interference contrast microscopy of vegetative cells of five *Cyanophora* species, shown at the same magnification throughout; scale bar = 10 µm. af, anterior flagellum; pf, posterior flagellum; c, plastid; n, nucleus; s, starch grain. (A) Side view of a cell of *C. paradoxa* Korshikov strain CCAP 981/1. (B) Side view of a cell of *C. cuspidata* Tos.Takah. & Nozaki sp. nov. strain 101. (C) Side view of a cell of *C. kugrensii* Tos.Takah. & Nozaki sp. nov. strain NIES-763. (D) Optical section of antapical view of a cell without a deep furrow in *C. cuspidata* strain 101. (E and F) *C. sudae* Tos.Takah. & Nozaki sp. nov. strain NIES-764. (E) Front view showing four plastids. (F) Front view with two dividing plastids. Note that plastid divisions are transverse. (G) Front view with two dividing plastids in *C. biloba* Kugrens, B.L.Clay, C.J.Mey. & R.E.Lee strain UTEX 2766. Note that plastid divisions are transverse. (H) Optical section of antapical view of a cell with a deep furrow in *C. sudae* strain NIES-764.

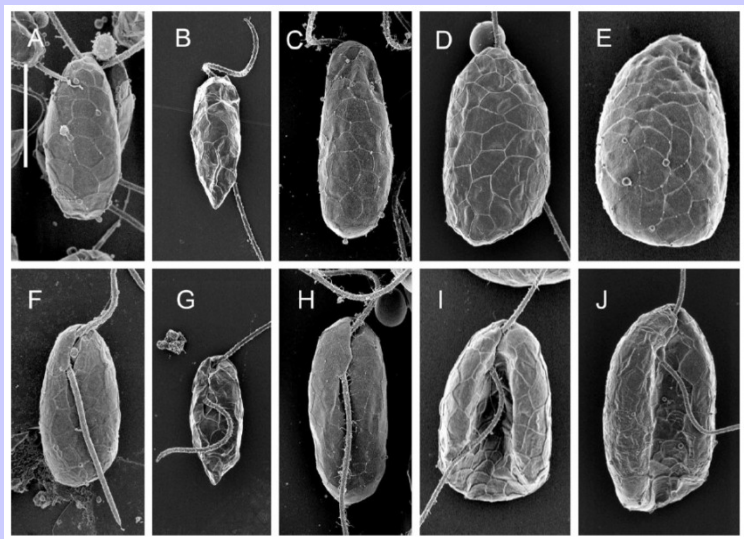

FIG. 3. Field-emission scanning electron microscope images of the dorsal and ventral sides of vegetative cells of five *Cyanophora* species. All images are at the same magnification; scale bar = 5 µm. Upper and lower panels show dorsal sides, showing fenestrations aligned by ridges, and ventral sides, showing anterior folds with flagella, respectively. Note the flagella attached to the right part of the anterior fold. (A and F) *C. paradoxa* Korshikov strain CCAP 981/1, with a rounded posterior end. (B and G) *C. cuspidata* Tos.Takah. & Nozaki sp. nov. strain 101, showing a pointed posterior end. (C and H) *C. kugrensii* Tos.Takah. & Nozaki sp. nov. strain NIES-763, with a rounded posterior end. (D and I) *C. sudae* Tos.Takah. & Nozaki sp. nov. strain NIES-764, showing a deep furrow (I). (E and J) *C. biloba* Kugrens, B.L.Clay, C.J.Mey. & R.E.Lee strain UTEX 2766, showing a deep furrow (J).

Takahashi et al., 2014, J. Phycol. 50

five *Cyanophora* species recognized by genetic and morphological features

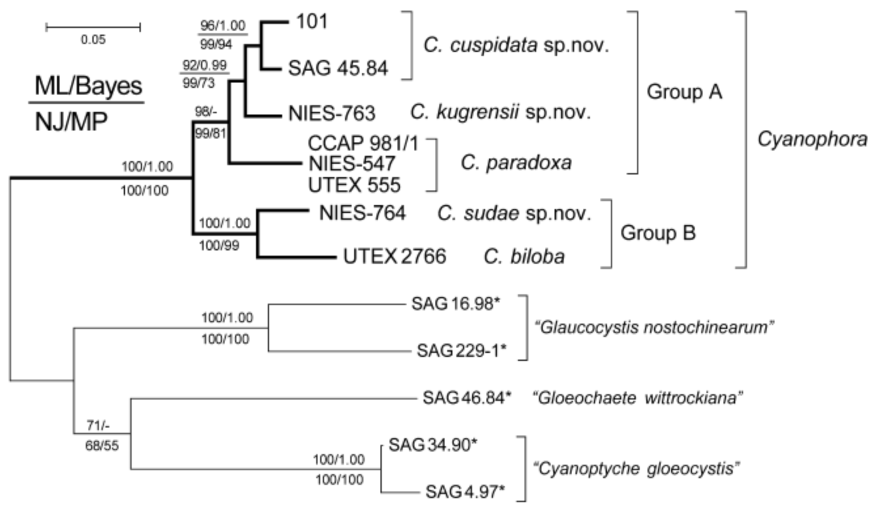

FIG. 5. Maximum likelihood (ML) tree based on analyses of 1,460 base pairs of the coding regions of the plastid *psaB* genes, from eight strains of five *Cyanophora* species and five strains of other glaucophyte genera (Table S1). Asterisks indicate strains that have not been identified to species level based on detailed taxonomic studies using light and electron microscopy and molecular data. Branch lengths are proportional to the genetic distances, which are indicated by the scale bar above the tree. Groups A and B represent morphologically distinct groups (Table 1). Numbers above branches represent ≥50% bootstrap values (based on 1,000 replications) of the ML analyses (left) and posterior probabilities (0.95 or more) by Bayesian inference (right). Numbers at the left and right sides below branches are ≥50% bootstrap values (based on 1,000 replications) of neighbor-joining and maximum-parsimony analyses, respectively. For details of the phylogenetic methods, see Materials and Methods in the text.

TABLE 1. Comparison of the morphological characteristics of *Cyanophora* species examined in cultures of the present study.

Species	*C. paradoxa*	*C. cuspidata* sp. nov.	*C. kugrensii* sp. nov.	*C. sudae* sp. nov.	*C. biloba*
Cell shape	Ovoid without a deep longitudinal furrow	Obovoid to ellipsoidal without a deep longitudinal furrow	Elongate-ovoid without a deep longitudinal furrow	Dorsoventrally compressed to form a broad, bean-shape	Dorsoventrally compressed to form a broad, bean-shape
Cell size	~7–15 μm long × ~3–6 μm wide	~5–12 μm long × ~2–5 μm wide	~5–15 μm long × ~2–6 μm wide	~9–12 μm long × ~4–9 μm wide	~9–12 μm long × ~4–9 μm wide
Formation of posterior pointed end (tail)	Absent	Present	Absent	Absent	Absent
Plastid number	Generally 1–2	Generally 1–2	Generally 1–2	2–8, generally 4	2–4, generally 2
Fenestrations in cell surface ornamentation	Angular or often crescent-shaped	Angular or often crescent-shaped	Angular or often crescent-shaped	Pentagonal to hexagonal	Triangular to pentagonal or often crescent-shaped
Strains examined	CCAP 981/1, UTEX 555 and NIES-547	101 (= NIES-3645), SAG 45.84	NIES-763	NIES-764	UTEX 2766
Morphological group	Group A	Group A	Group A	Group B	Group B

Takahashi et al., 2014, J. Phycol. 50

molecular diversity within the genera *Cyanophora* and *Glaucocystis*

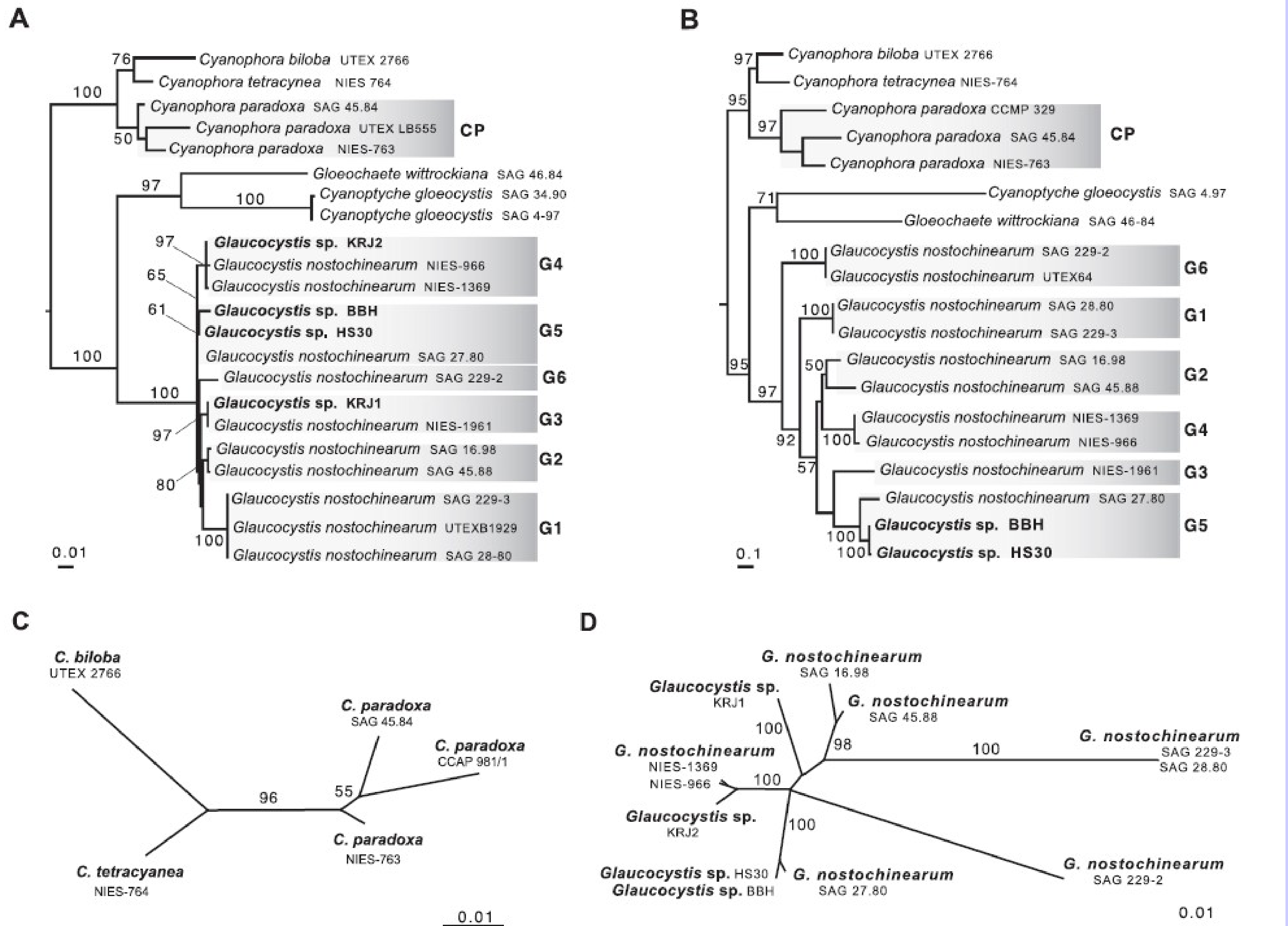

Fig. 1. Maximum likelihood analyses of glaucophyte molecular markers. Maximum likelihood (ML) trees estimated from (A) the plastid loci *psb*A, (B) the mitochondrial gene cytochrome *b* (*cob*) from diverse glaucophyte genera, and the nuclear ITS region of (C) *Cyanophora* and (D) *Glaucocystis* species/strains, respectively. The *psb*A and *cob* ML trees are rooted using the *Cyanophora* clade as outgroup. Numbers near nodes indicate PhyML bootstrap proportion support (only values >50% are shown). Branch lengths are proportional to the number of substitutions per site (scale bar corresponds to 0.1 substitutions per site). Putative genetic groups are indicated in the *Cyanophora paradoxa* (CP) and within *Glaucocystis* (G*n*) branches.

Chong et al., 2014, Mol. Phyl. Evol. 76: 181-188.

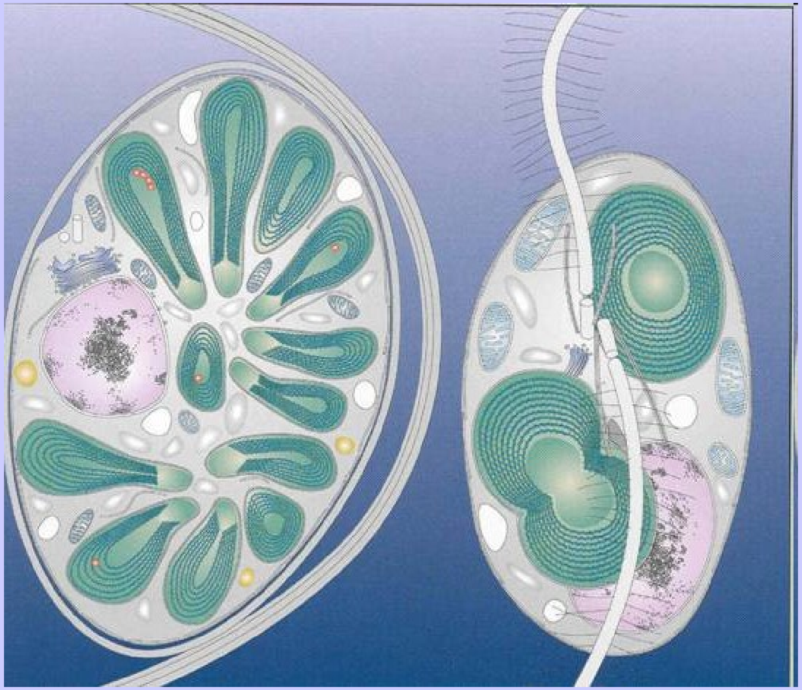

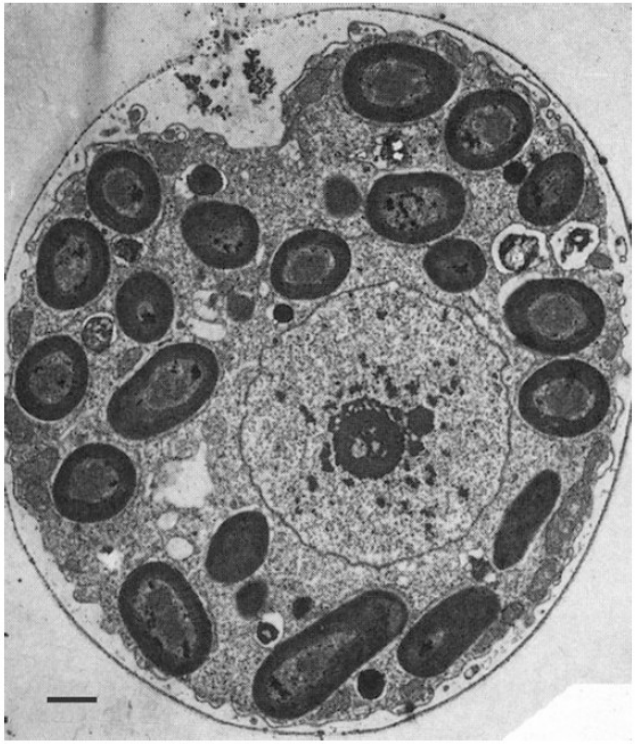

Fig. 3 *Gloeochaete wittrockiana*, strain SAG 46.84 (Kies strain IABH 2323), in longitudinal section, with apical depression, numerous muroplasts, and in the center of the cell a conspicuous nucleus with a nucleolus. Transmission electron micrograph. *Scale line* = 1 μm (Taken from Kies and Kremer (1990))

Fig. 5 Muroplasts of *Gloeochaete wittrockiana*, strain SAG 46.84 (Kies strain IABH 2323) with concentric thylakoid membranes. The central part contains a large polyhedral body confined by an electron-dense layer. Transmission electron micrograph. *Scale line* = 1 μm (Taken from Kies and Kremer (1990))

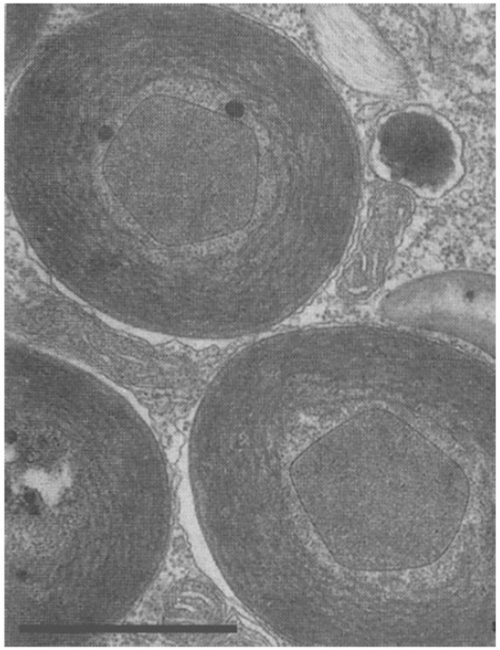

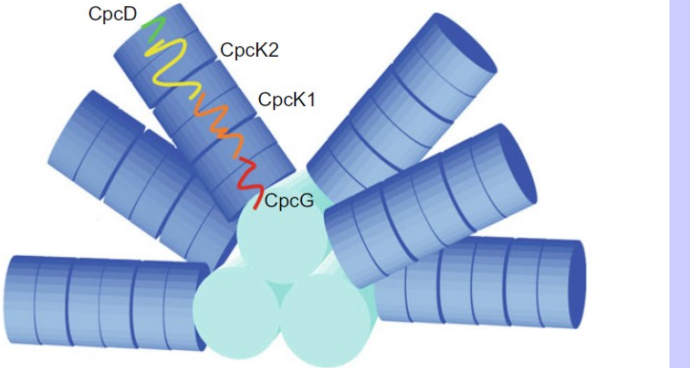

Fig. 12 Complete model of the *Cyanophora* phycobilisome according to Steiner et al. *Blue*, phycocyanin rods; *cyan*, allophycocyanin core; *green*, *yellow*, *orange*, and *red*, linker proteins

Handbook of Protists, 2017

Gloeochaete wittrockiana

Fig. 2 Two cells of *Gloeochaete wittrockiana*, strain SAG 46.84 (Kies strain IAB 2323). Each cell contains two long pseudocilia. Interference contrast light micrograph. Scale line=10 µm

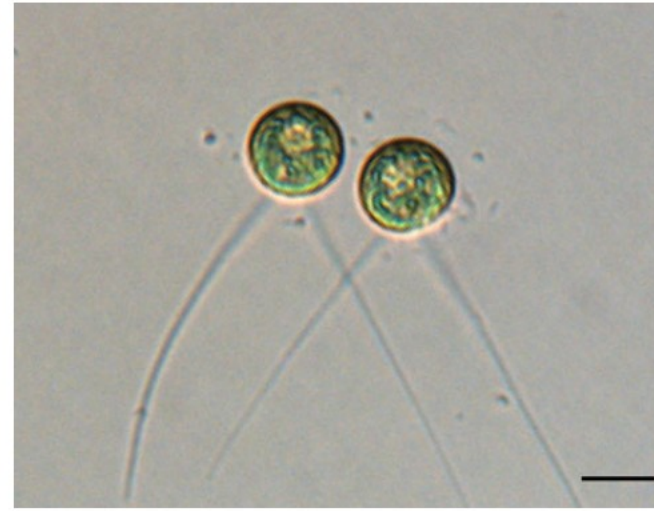

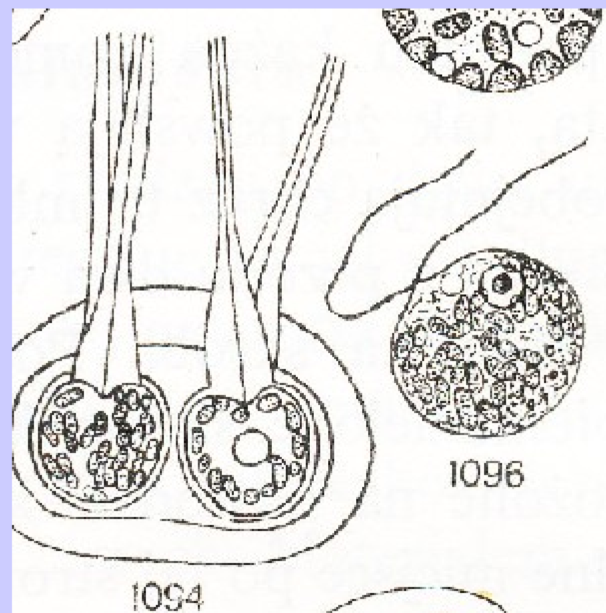

freshwater epiphyton, benthos, mesotrophic habitats

Cyanoptyche gloeocystis

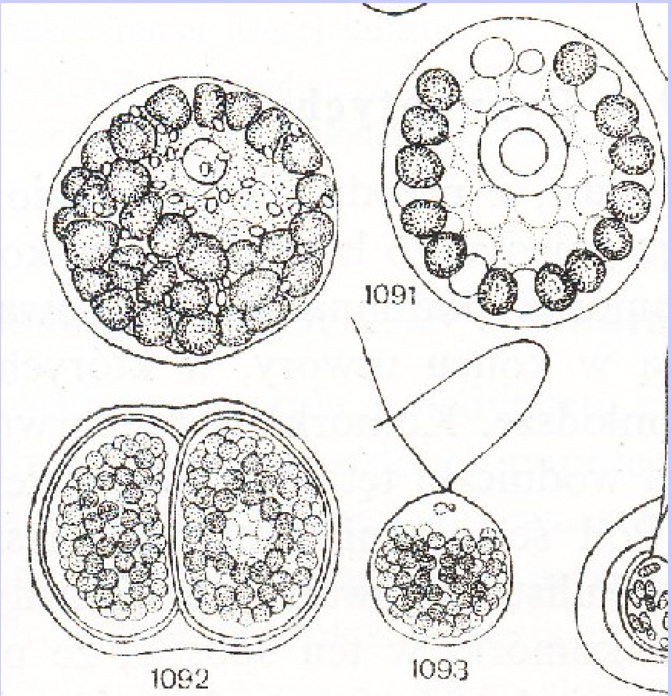

- described by Pascher from peat bog pool in Doksy
- known from other peat bogs (Ukraine, Poland, Canada)
- two strains exist (SAG) – as an epiphyte from a pool in Prater (Wien) + from Portugal

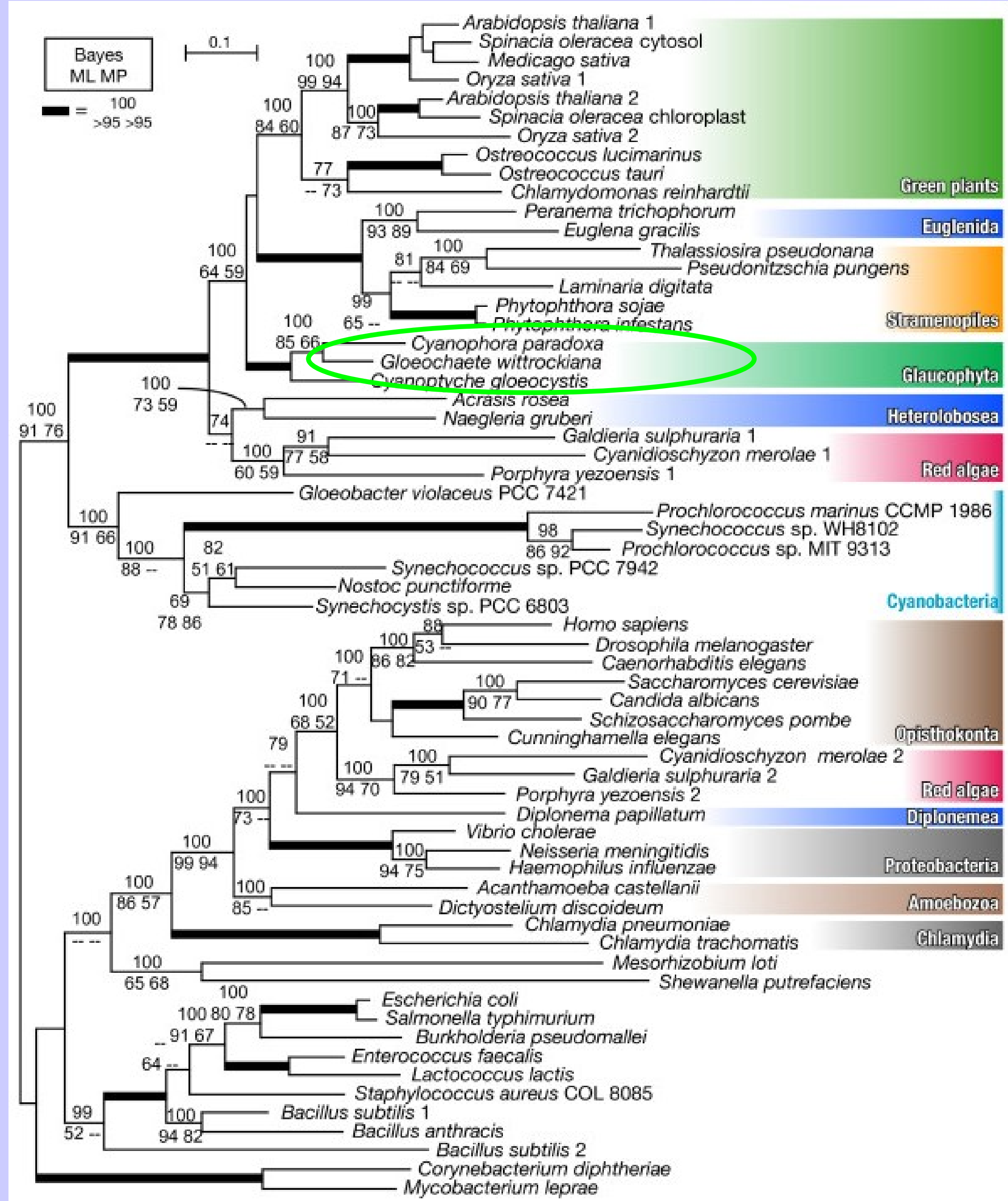

Maruyama et al., 2008, BMC Evol. Biol. 8:151.

unclear and/or erroneously described glaucophytes

Chalarodora azurea

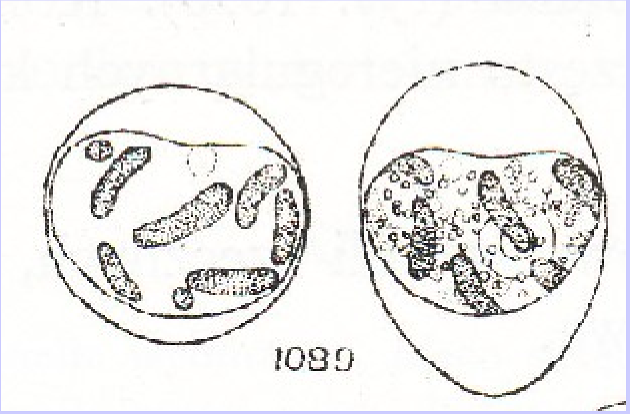

described by Pascher as an epiphyte of *Potamogeton* leaves

Glaucosphaera vacuolata
(red alga from Porphyridiophyceae)

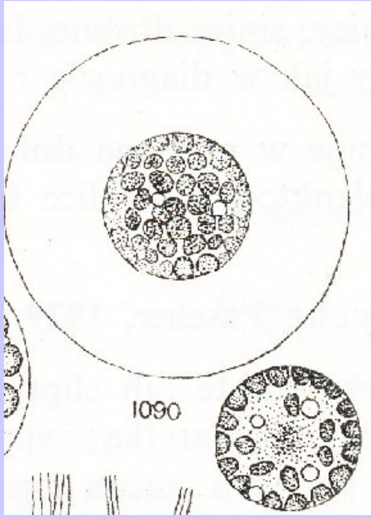

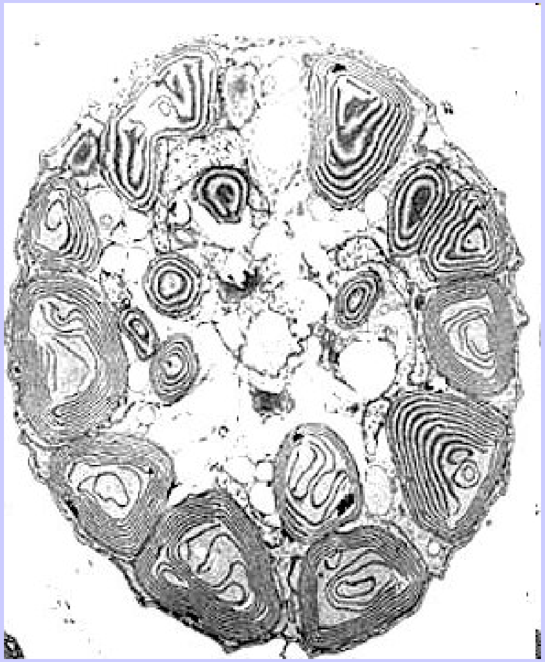

thrives in soil

the red plant lineage – subkingdom ***Rhodoplantae***

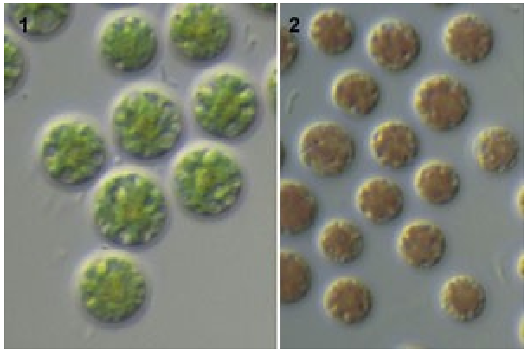

<u>evolutionarily important features</u>: Golgi apparatus associated with ER, mitochondrion, and nuclear membrane, presence/absence of thylakoidal lamella beneath plastid membrane (relation to evolution of secondary rhodoplasts), phycobilins, absence of any flagellates stages (but *Rhodelphis* !)

Basic Rhodophytan Characteristics

1. Eucaryotic cells
2. Phycobilin pigments present as phycobilisomes on the thylakoids
3. Nuclear membrane present throughout mitosis
4. Floridean starch granules located outside the chloroplasts
5. Single thylakoid bands in the chloroplasts
6. Absence of flagella or cilia

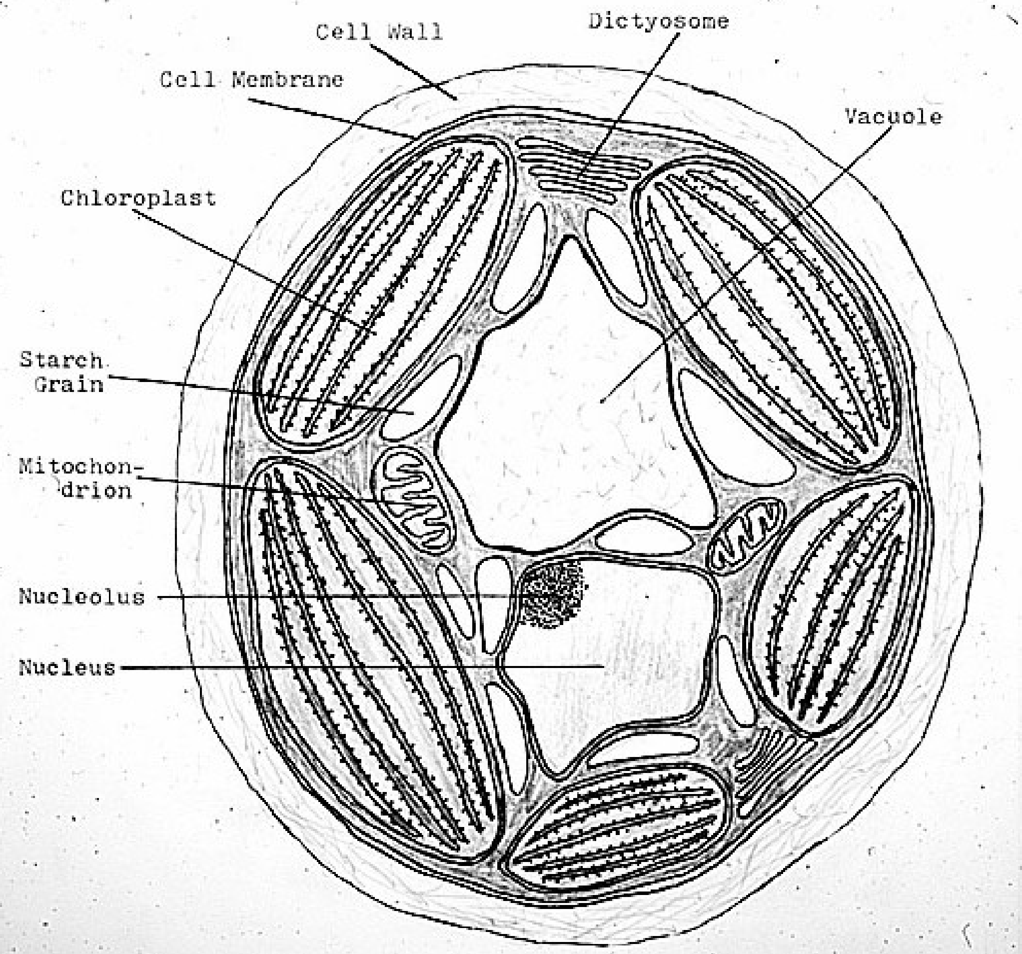

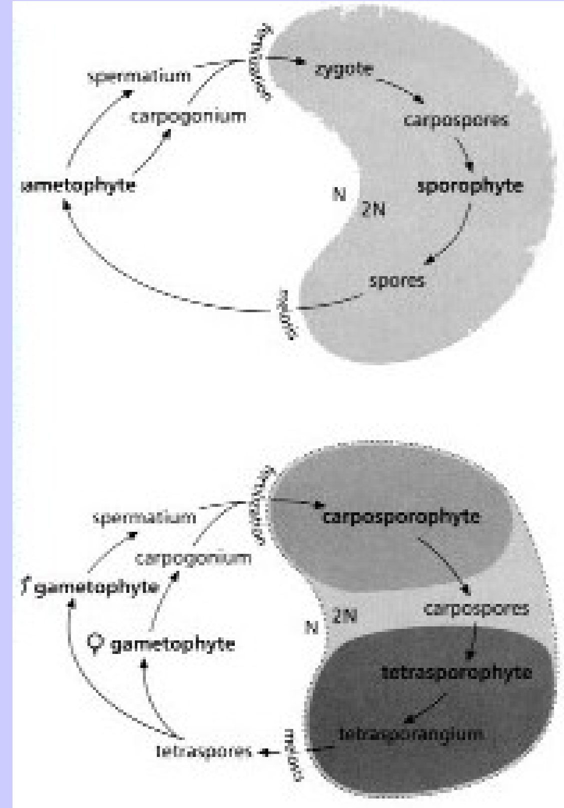

biphasic life cycle – ancestral
triphasic – evolutionarily advanced

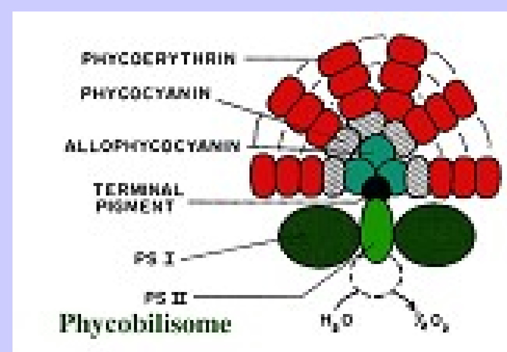

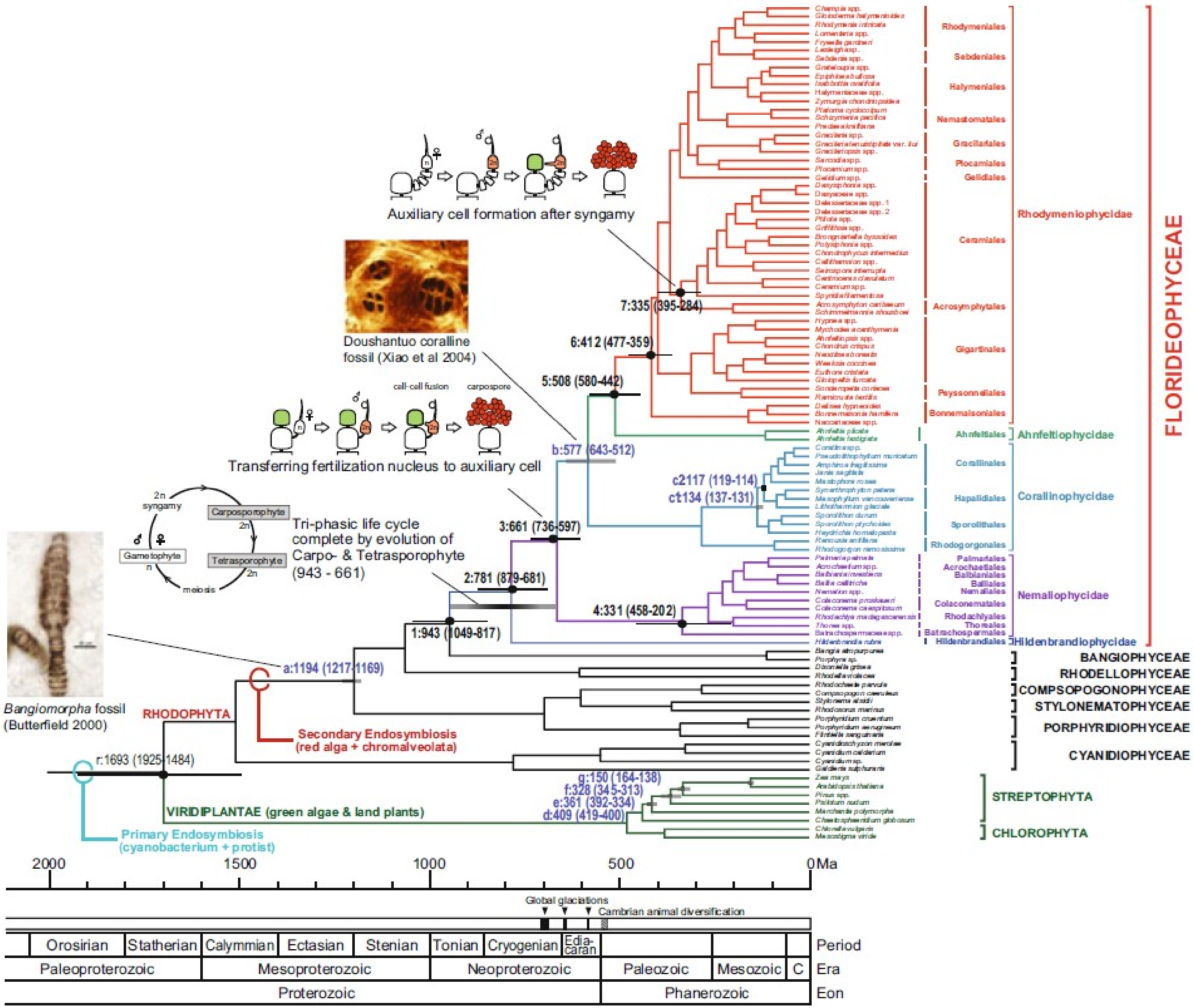

Fig. 6 Divergence time and evolution of the red algae. Primary and secondary endosymbiosis events are indicated with *cyan* and *red lines*, respectively. The three key evolutionary events are indicated with diagrams at the estimated evolutionary timeline. Triphasic life cycle, postfertilization "cell-to-cell fusion" mechanisms between carpogonium (fertilized egg) and an auxiliary cell, and the formation of an auxiliary cell after fertilization (syngamy) are indicated (Modified from Yang et al. 2016)

Yoon et al., 2017,
In: Handbook of Protists

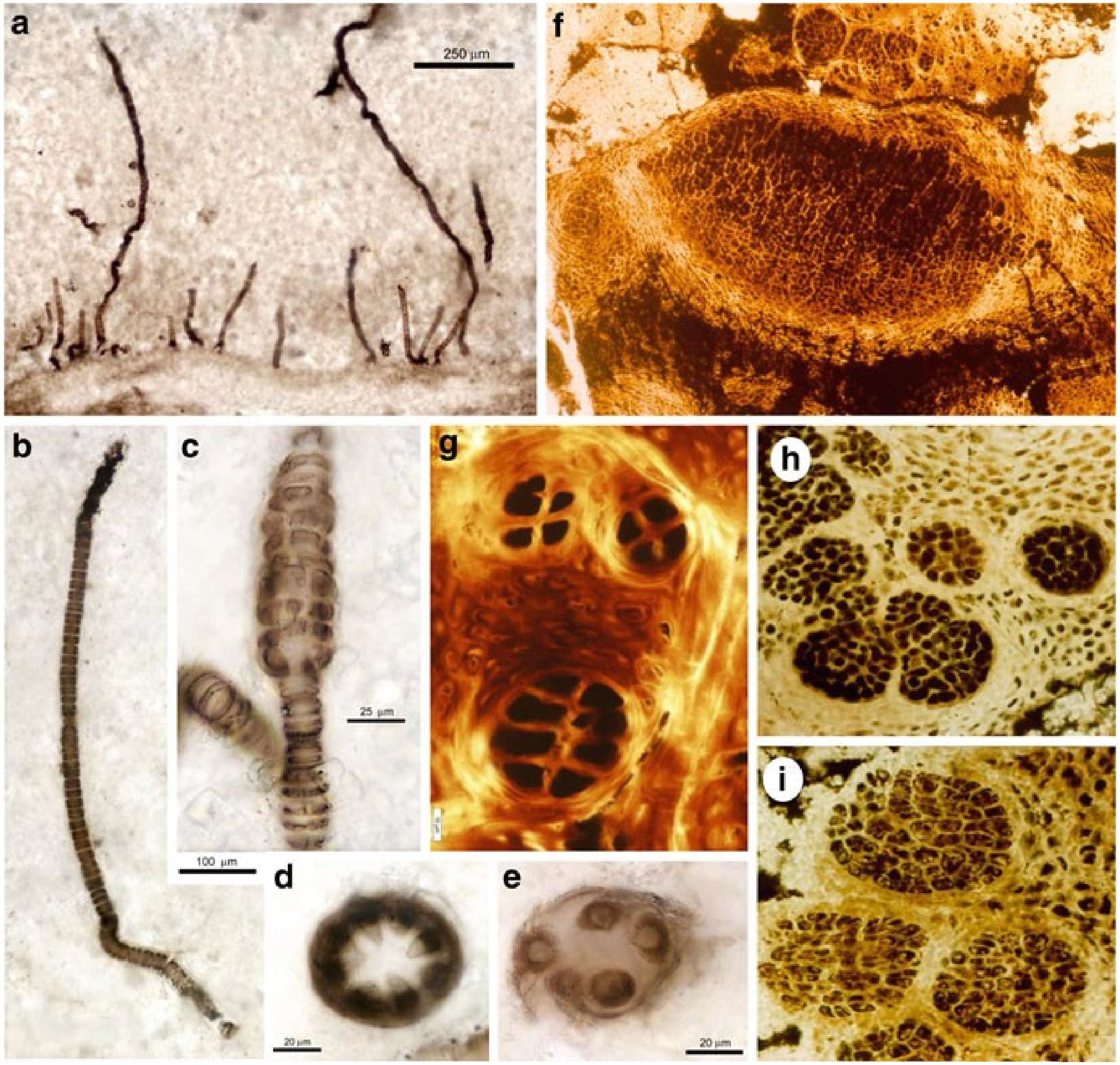

Fig. 5 Proterozoic red algal fossils. (**a–e**) *Bangiomorpha pubescens* fossils from the ca. 1200 million-year-old Hunting Formation, Somerset Island, arctic Canada (Courtesy of N. J. Butterfield). (**a**) Population of *Bangiomorpha* that clustered with up to 15 individuals. (**b**) Two paired cells reflecting transverse intercalary cell division. (**c**) Mature thallus showing both uniseriate and multiseriate portions of a filament. (**d**) Transverse cross-section of a multiseriate filament showing eight radially arranged wedge-shaped cells. (**e**) Spore-like spheroidal cells within multiseriate filaments from transverse cross-section. (**f–i**) Coralline fossils from the late Neoproterozoic 570 Ma Doushantuo Formation at Weng'an, southern China (Courtesy of S. Xiao). (**f**) A spermatangia-like reproductive structure with filaments. (**g**) Tetraspores and octaspores embedded in algal thallus showing possible tetrasporangium with subtending stalk cells. (**h, i**) Carposporangia

Yoon et al., 2017,
In: Handbook of Protists

synopsis of the contemporary formal classification:
(**834** genera in **90** families in **32** orders in **7** classes in **2** divisions)

subkingdom: **Rhodoplantae**

division: **Cyanidiophyta**

class: **Cyanidiophyceae** (3 genera)

division: **Rhodophyta**

class: **Rhodellophyceae** (2 genera)

class: **Stylonematophyceae** (12 genera)

class: **Porphyridiophyceae** (8 genera)

class: **Compsopogonophyceae** (14 genera)

class: **Bangiophyceae** (6 genera)

class: **Florideophyceae** (789 genera)

Schneider & Wynne, 2007, Bot. Mar. 50: 197–249.

How many extant species?

4000 to 6000 described

real number possibly up to 20 000

(Adl et al., 2007, Syst. Biol.)

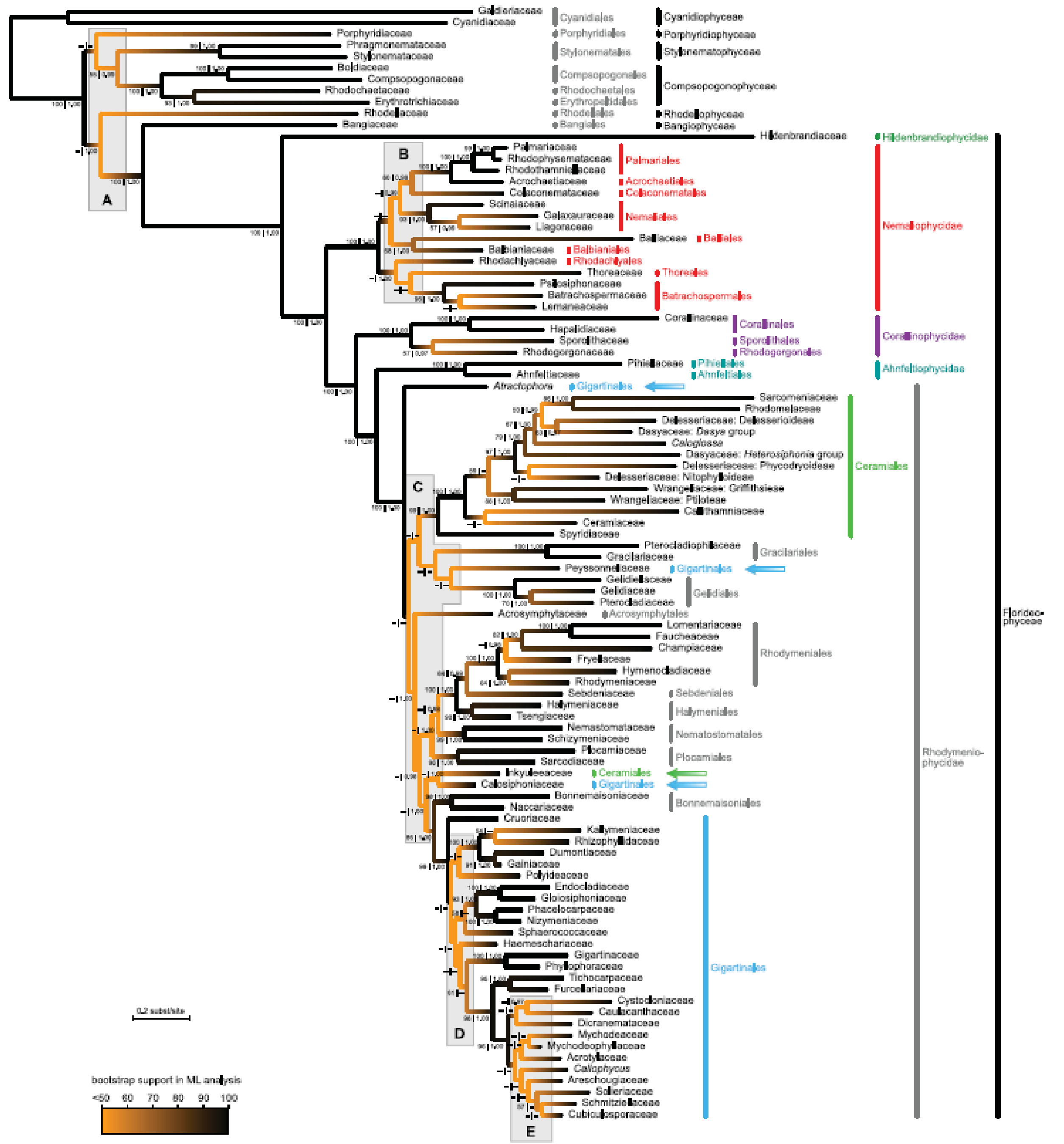

Figure 2 Red algal tree of life with current taxonomic classification. The tree was reconstructed using Bayesian phylogenetic inference of DNA data mined from GenBank (Figure 1). Branch colors indicate statistical support of the clades: whereas black branches are strongly

Verbruggen et al., 2010, BMC Evol Biol mitochondrial genome analysis

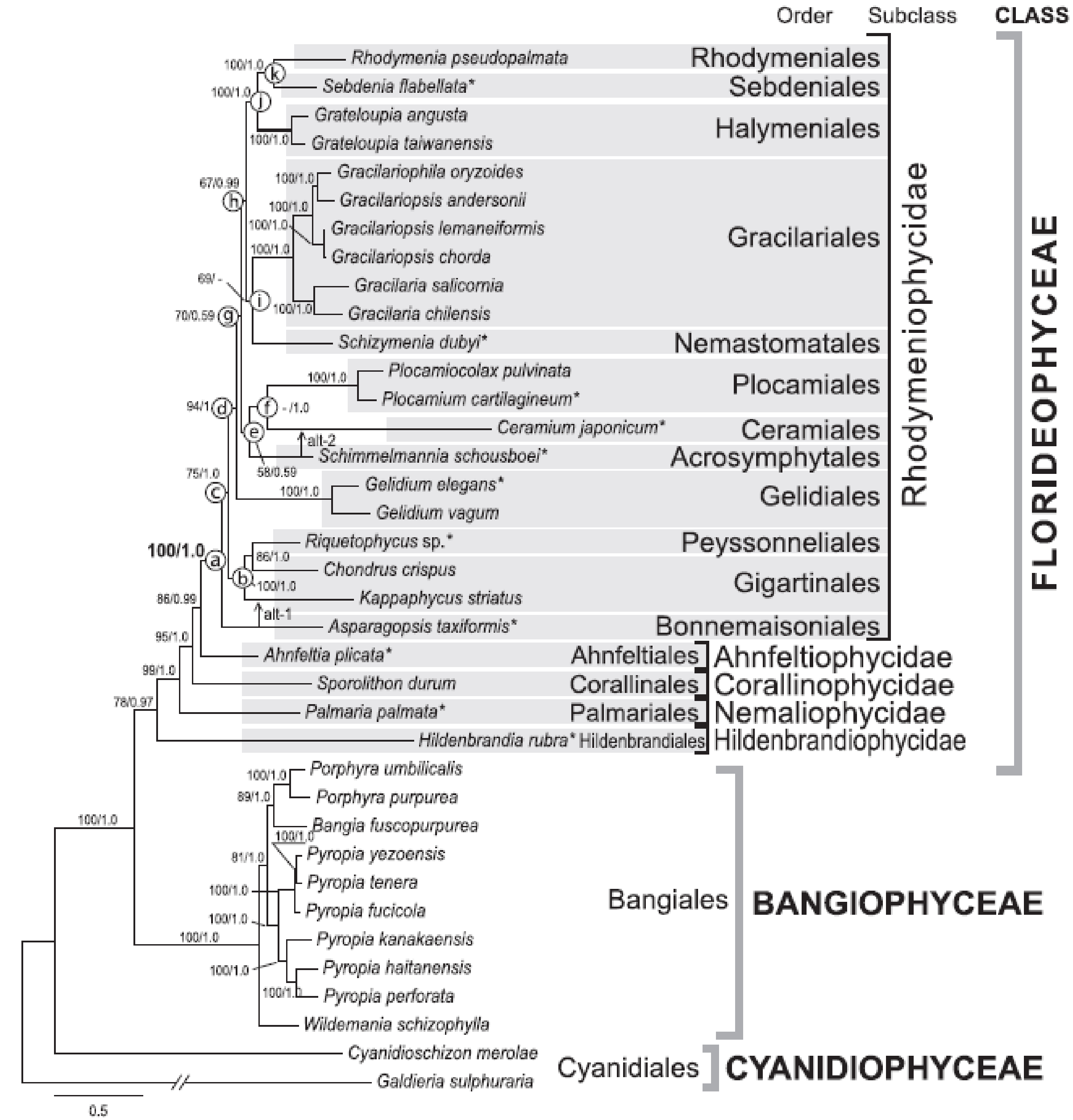

Fig. 1.—Phylogeny of the red algae (Rhodophyta) based on mt genome data. Tree constructed using the ML method based on 24 concatenated genes (6,345 amino acids from 24 protein coding). The support values for each node are calculated from MLB and BPP. Asterisks after species names indicate newly determined mt genomes, followed by red algal order, subclass, and class system. Alternative tree branch position of species (alt) indicated by dot line with arrow, that is, alt-1 for *Asparagopsis* and alt-2 for *Schimmelmannia*. Alternative topologies are available in supplementary figure S3, Supplementary Material online.

Yang et al., 2015, GBE

Cyanidiophyta

Cyanidium

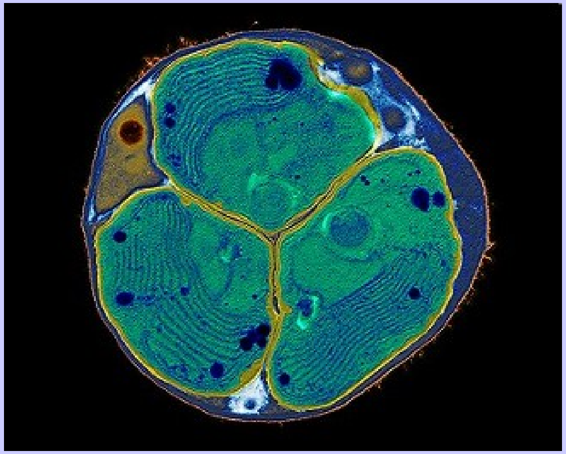

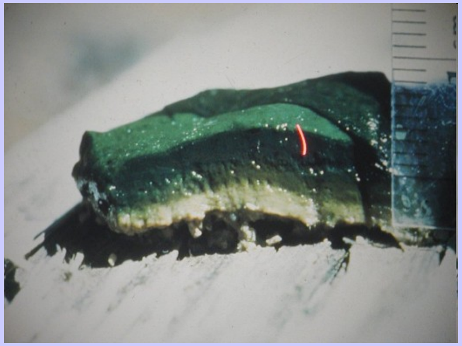

Yellowstone Nat. Park

an organism most similar to the ancestors of stramenopile plastids?

C. caldarium - hot (up to 57 C and acid soils/waters

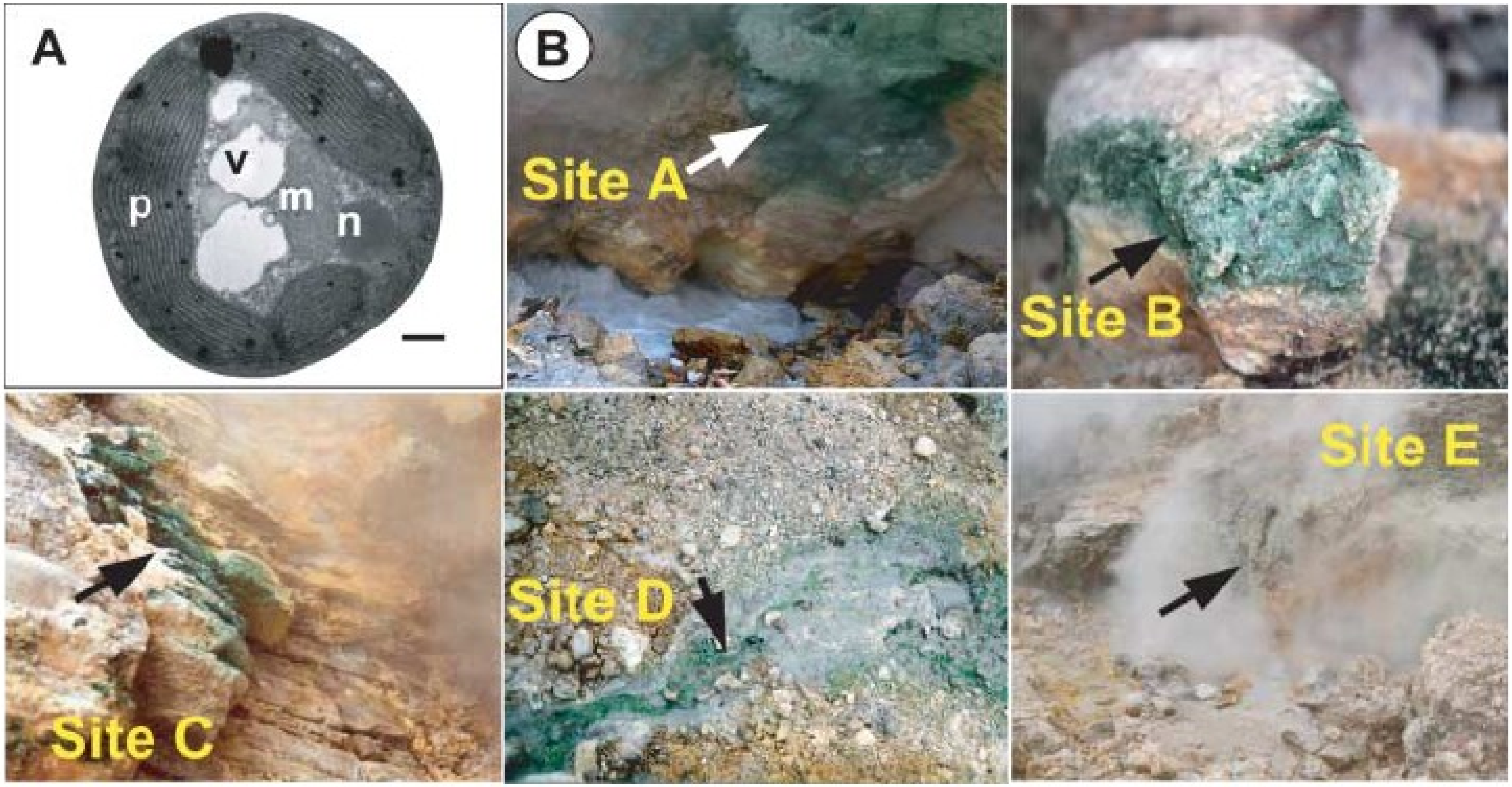

Fig. 1 The Cyanidiales red algae. (A) TEM micrograph of a crypto-endolithic strain of *Galdieria sulphuraria*. The abbreviations denote the following: m = mitochondrion, n = nucleus, p = plastid, v = vacuole. Scale bars = 1 μm. (B) The environmental Sites A–E used to collect Cyanidiales at Pisciarelli in the Phlegrean Fields, Italy (see text for details).

- probably four lineages (*Cyanidium, Galidieria, Cyanidioschizon, „Galdieria*" *maxima*)
- precambrian cyanophyte ancestor possibly lived in thermal and acidic habitats
- invasions to terrestrial and benthic habitats are evolutionarily derived
- Cyanidium generic lineage seemingly has tens of species

Ciniglia et al., 2004 Mol. Ecol. 13:1827-1838.

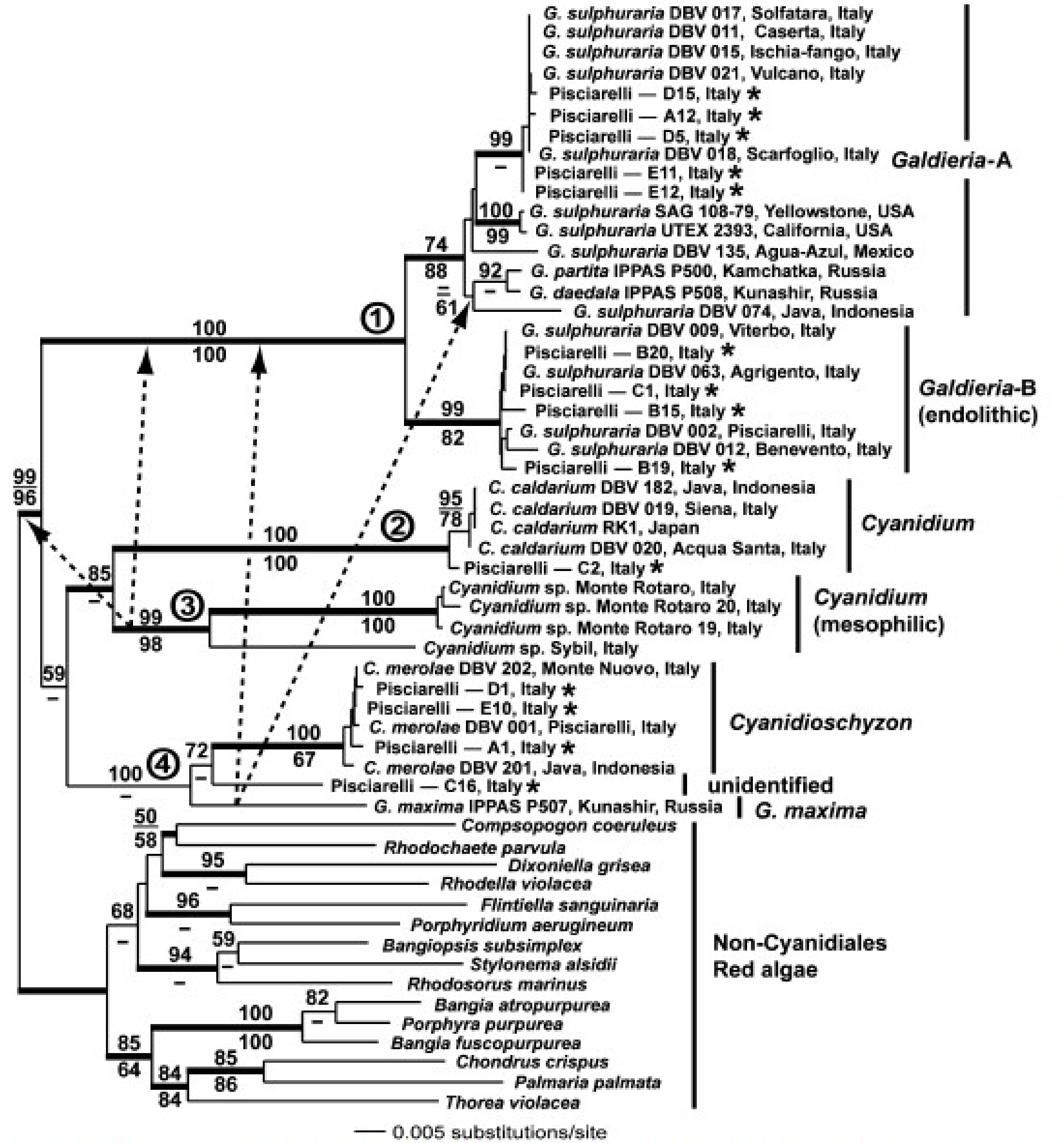

Fig. 3 Phylogeny of the Cyanidiales inferred from a minimum evolution (ME) analysis using the LogDet transformation of the *rbc*L sequences. Results of a ME-LogDet bootstrap analysis are shown above the branches, whereas the bootstrap values from a protein maximum likelihood analysis using the JTT evolutionary model are shown below the branches. Only bootstrap values > 60% are shown.

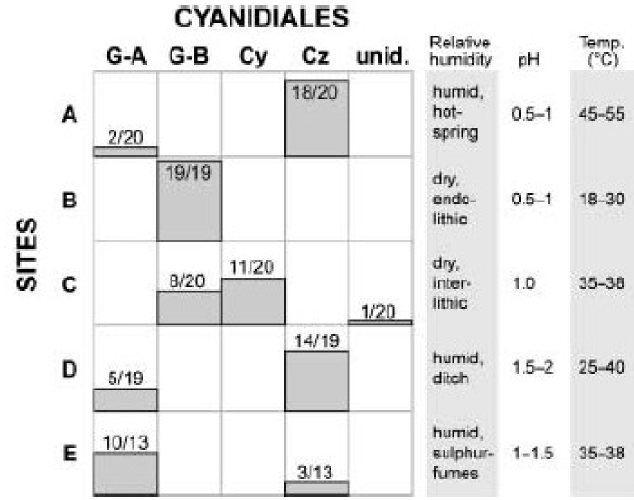

Fig. 4 Results of the environmental survey showing the distribution of Cyanidiales species/lineages clones with respect to the eco-physiological conditions at Pisciarelli, Italy. Up to 20 clones were sampled from each site. In this figure, G-A is *Galdieria*-A, G-B is *Galdieria*-B, Cy is *Cyanidium*, Cz is *Cyanidioschyzon* and unid. is unidentified taxa.

Ciniglia et al., 2004 Mol. Ecol. 13:1827-1838.

monospecific cave biofilms in **extremely shaded microhabitats**

Figure 2 Atacama cave description. **a** East entrance. **b** View towards the bottom (north) of the cave. The biofilm area studied is located on the left side wall. **c** Detail of *Cyanidium* biofilm. **d** Biofilm on rocks at the bottom of the cave. Note the biofilm development only on the rock face oriented towards the east entrance. In both **a**, **b**, and **c**, the different geological origin of the walls and ceiling of the cave can be observed

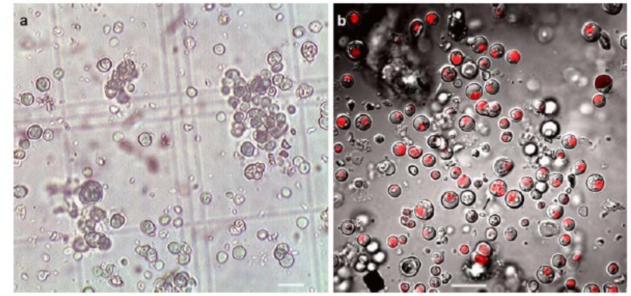

Figure 3 Micrographs of *Cyanidium* sp. cells found in biofilms of the Atacama cave. **a** Bright field micrograph of *Cyanidium* sp. composed of single photosynthetic cells and small fragmented colonies. *Scale bar* = 10 μm. **b** Merged CLSM micrograph of aqueous suspension of *Cyanidium* cells extracted from the cave biofilm. The differential interference contrast image was merged with the red fluorescence (excitation/emission 543 nm/long pass filter <570 nm) due to the autofluorescence emitted by the cell chloroplast containing chlorophyll. *Scale bar*=10 μm. The *arrows* in **b** indicate endospore-containing cells

Table 3 Lighting profile along the length of the cave. The light available for photosynthesis was determined with a photosynthetic photon flux density measuring device outside and inside the cave at different places in both the western an eastern walls of the cave

Distance from cave entrance (m)	March 2008				June 2008	
	PPFD ($\mu mol\ m^{-2}\ s^{-1}$)		Percentage of outside light		PPFD ($\mu mol\ m^{-2}\ s^{-1}$)	Percentage of outside light
	Western wall	Eastern wall	Western wall	Eastern wall	Western wall	Western wall
0	1,668	1,668	100	100	1,250	100
5	25	12	1.50	0.72	158	12.64
10	6	3	0.36	0.18	54	4.32
15	6	0	0.36	0	21	1.68
20	3	0	0.18	0	7	0.56
25	2	0	0.12	0	2	0.16
30	1	0	0.06	0	1	0.08

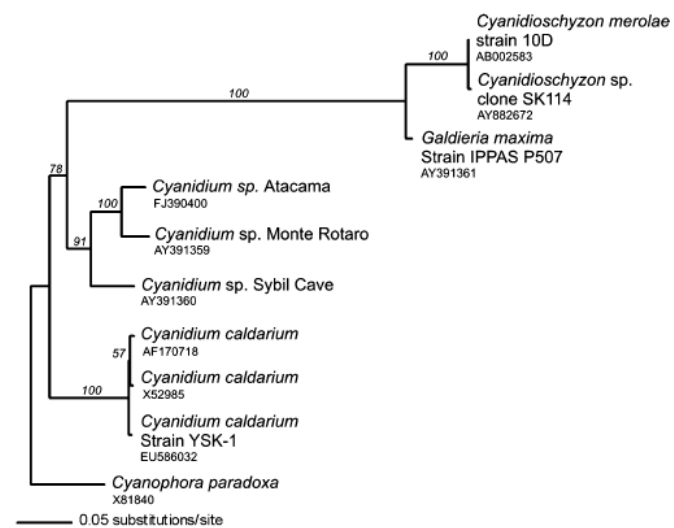

ML, plastid encoded 16S rDNA

Azua-Bustos et al., 2009, Microb. Ecol., 58:485–496.

Galdieria

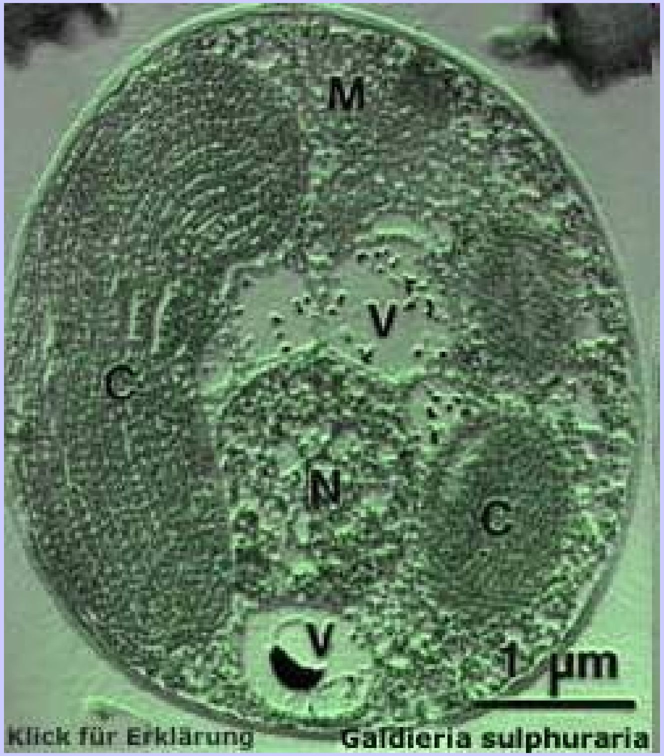

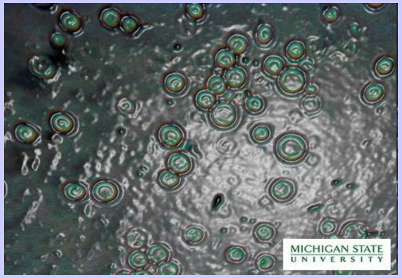

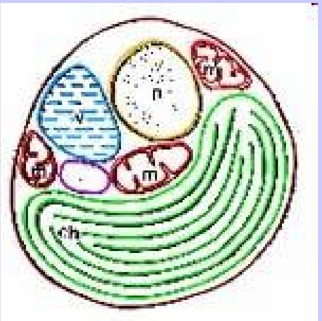

extremely acidic habitats

C. merolae
- a single nucleus, mitochondrion, plastid, peroxysome
- one of the most ancestrall plastids, at all
- all the DNA-containing organelles divide simultaneously

Cyanidioschyzon

C. merolae
acid hot water - pH < 2 a 45 °C

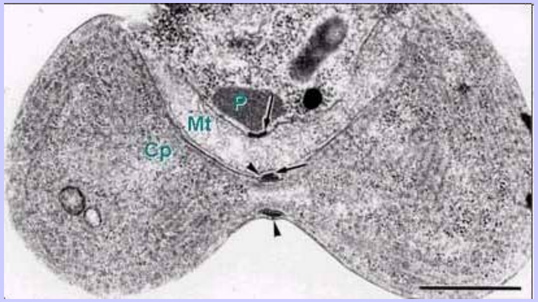

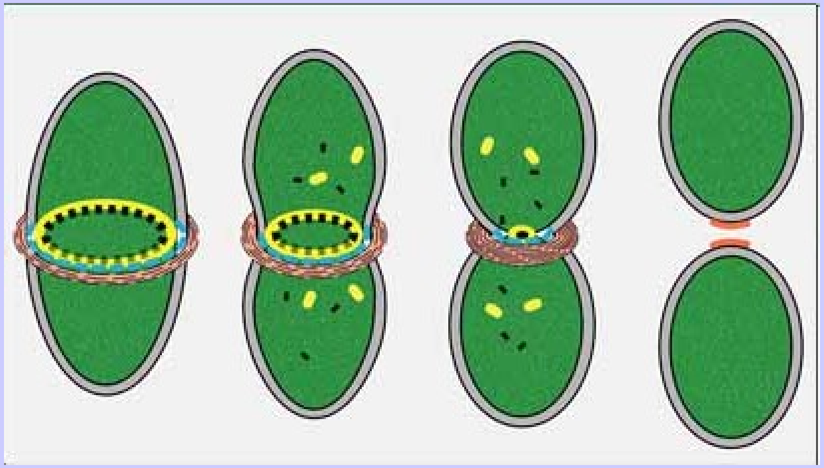

plastid division ring

unipolar cells in Cyanidioschyzon

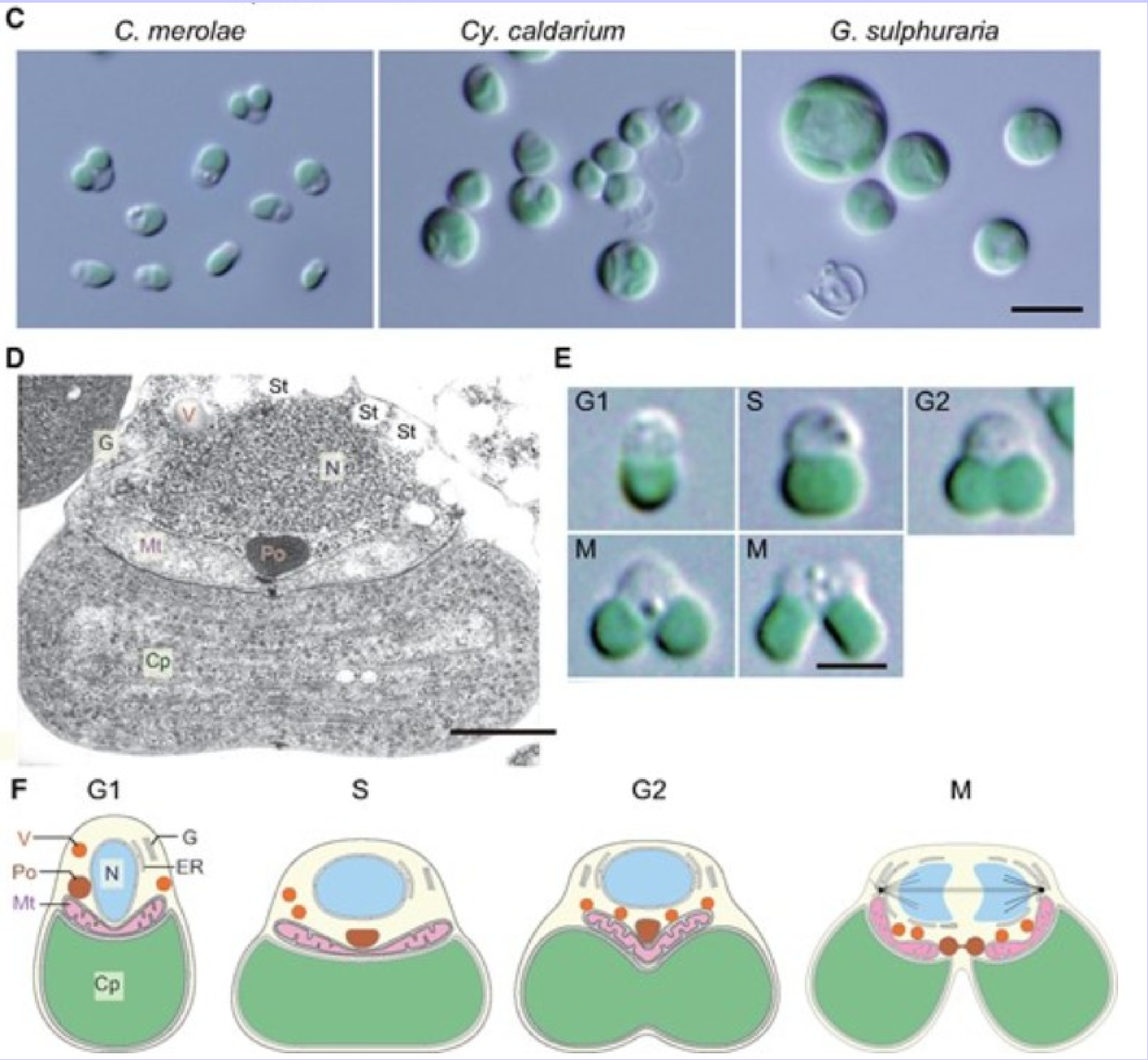

Miyagishima & Tanaka, 2021

thermophilic *Galdieria* in anthropogenic habitats

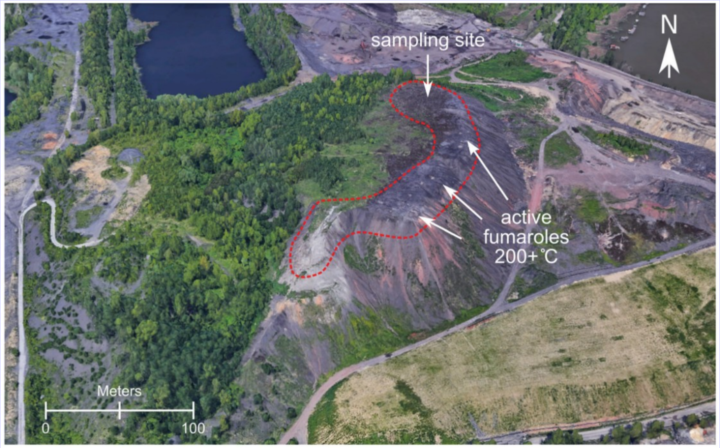

Fig. 1. Sampling site: Heřmanice spoil heap in Ostrava, Czech Republic.

Fig. 2. Sampling site: coal is still burning under the ground (a, b). *Galdiera* was found growing on the tree residuals (c, d, e) where hot fumes were coming out. Image (f) shows *Galdieria* cells from the field sample. Scale bar 20 μm.

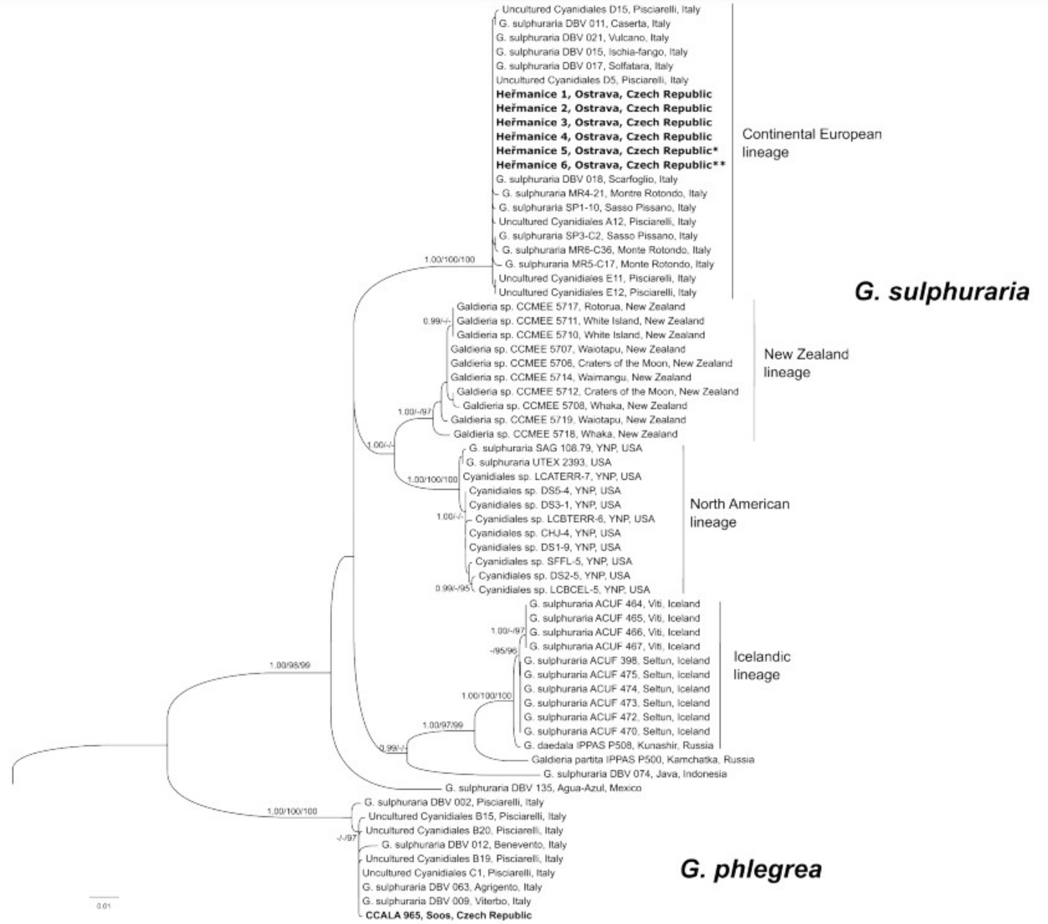

Fig. 6. Phylogenetic tree inferred from maximum likelihood (ML) analysis of *rbc*L gene sequences (with a hidden outgroup). Only Bayesian posterior probabilities ≥ 0.99 and bootstrap values (ML/MP) ≥ 95% are shown. Ostrava sequences from environmental samples are marked with asterisks (*2016, **2015).

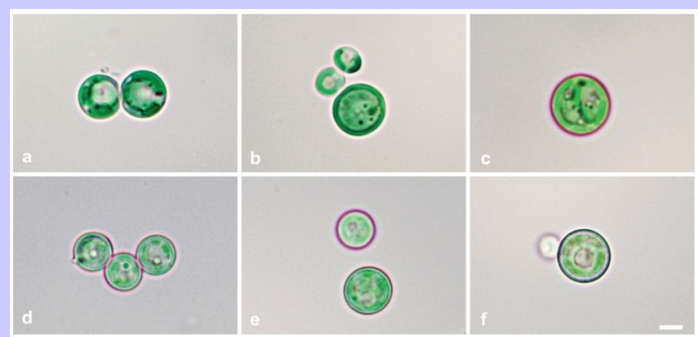

Fig. 3. Morphology of two *Galdieria* species: (a–c) *G. sulphuraria* from Ostrava, (d–f) *G. phlegrea* CCALA 965 from Soos.

Barcyte et al., 2018, Fottea

Rhodophyta

Rhodellophyceae

Glaucosphaera vacuolata – see before/above

Rhodella

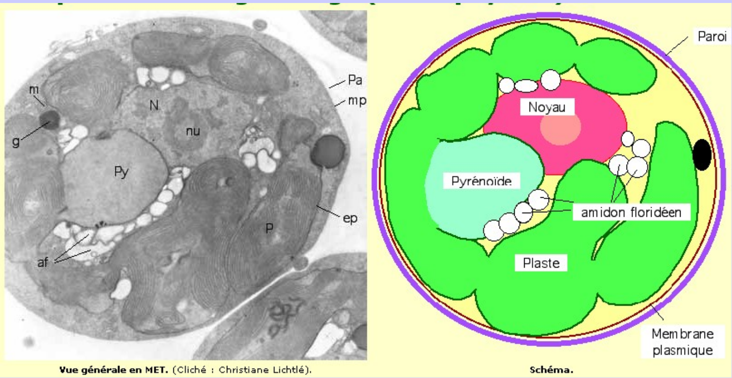

marine littoral – epiphyton, microbenthos

Figs 1–4. Cell structure of *Corynoplastis japonica* gen. et sp. nov. 1. Medial differential interference contrast optics (DIC) images of two young cells showing the somewhat radial nature of the chloroplast(s). Nuclei are eccentric-peripheral, each with a prominent nucleolus (arrows). Scale bar, 7.5 µm. 2. Non-medial DIC image of cell showing an eccentric nucleus with prominent nucleolus (arrow) and the complex chloroplast(s). Scale bar, 5 µm. 3. Confocal image of a cell stained with Hoechst 33258 to reveal DNA in the nucleus, chloroplast lobes and mitochondria. In the eccentric nucleus heterochromatin is evident along with a non-staining central nucleolus (arrow). Brightly autofluorescent chloroplast lobes extend into the cell center, which is only faintly autofluorescent due to the presence of pyrenoids and a small, central region of cytoplasm. Fusion of chloroplast lobes is evident at the cell periphery (*). Scale bar, 3.5 µm. 4. Low magnification electron micrograph of non-medial section showing eccentric nucleus and central pyrenoid region (*). Thin, seemingly unconnected chloroplast lobes (arrow) extend from the cell periphery to the cell center. Numerous, small electron dense starch grains are scattered throughout the cell. Scale bar, 1.5 µm.

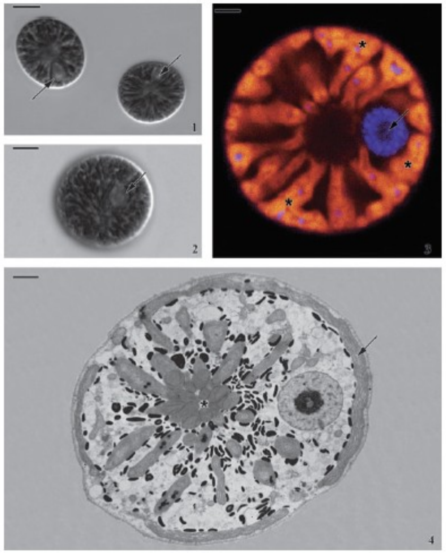

Corynoplastis japonica

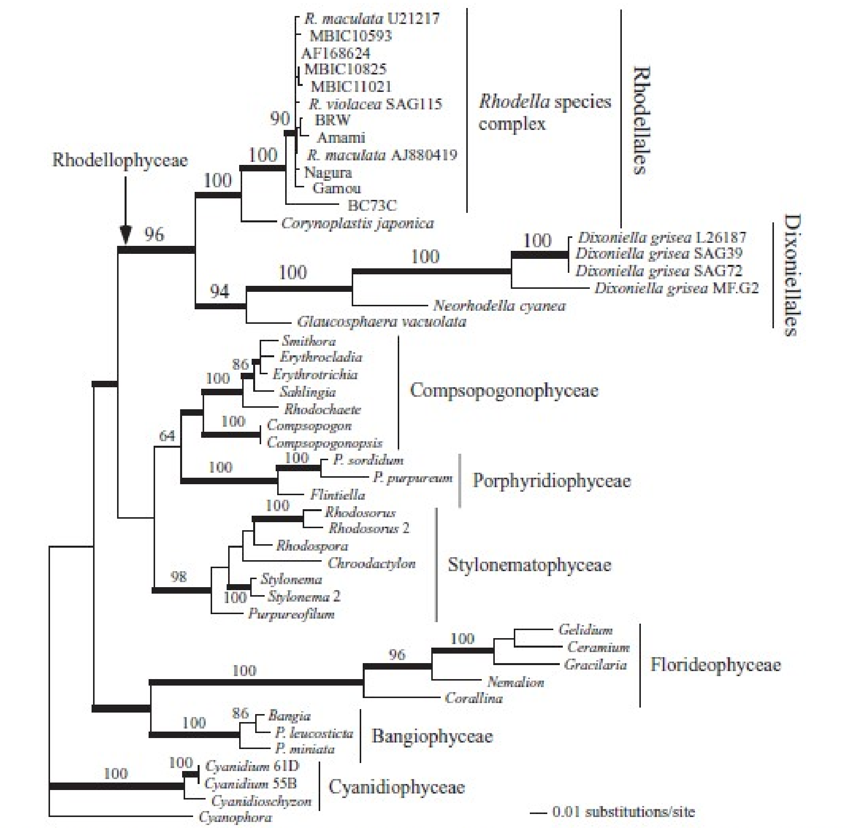

Fig. 15. Maximum likelihood (ML) topology of small subunit (SSU) DNA sequence data. Bayesian Inference (BI) posterior probabilities over 0.95 as thick lines, maximum-parsimony (MP) bootstrap values >50% above branches. Information on samples is in Table 2. The classes Bangiophyceae, Compsopogonophyceae, Cyanidiophyceae, Florideophyceae, Porphyridiophyceae, Rhodellophyceae and Stylonematophyceae are indicated as are the orders Dixoniellales and Rhodellales.

group synapomorphy:
Rhodellophyceae contain mannitol

Yokoyama et al., 2009, Phycol. Res., 57: 278–289

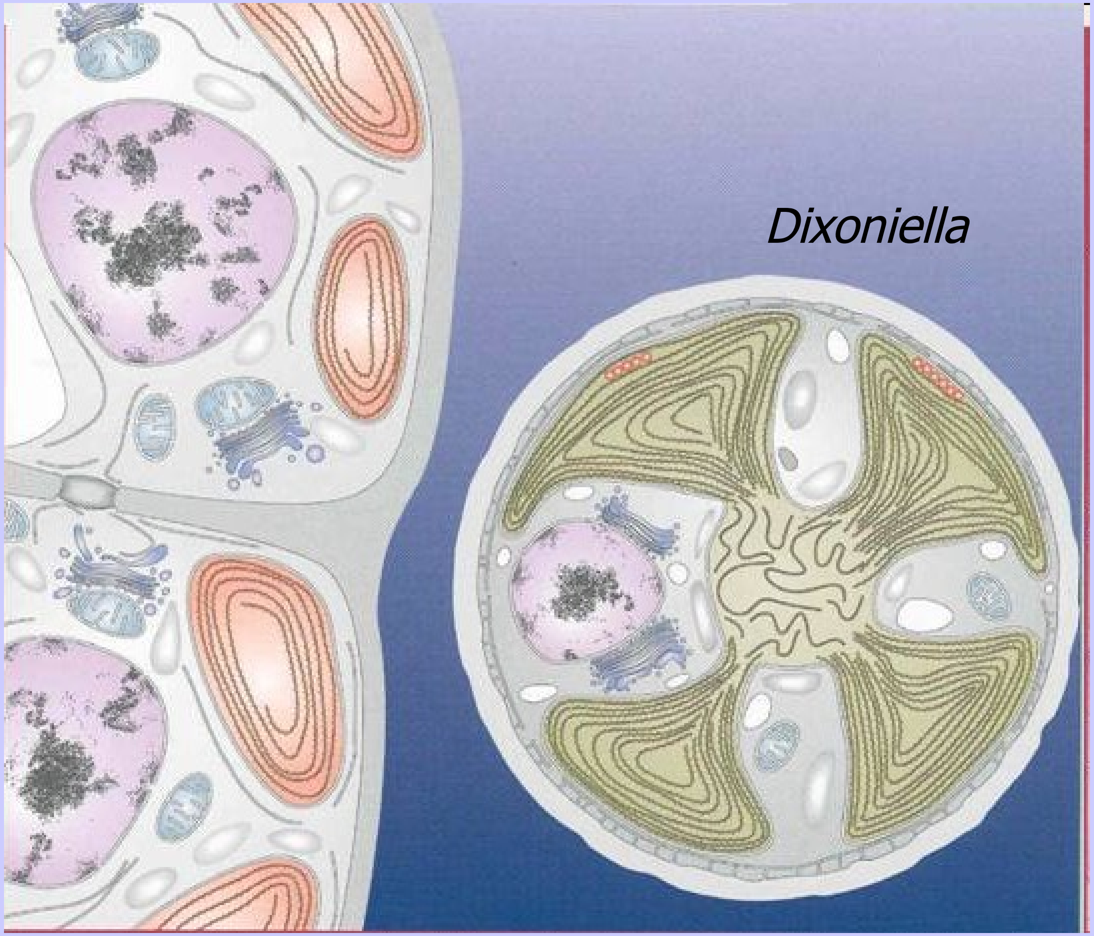
Dixoniella

Stylonematophyceae

Chroodactylon (= Asterocytis)

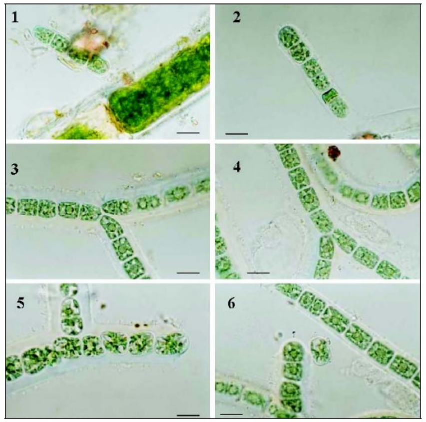

Figs 1–6. *Chroodactylon ornatum* (C. Agardh) Basson, specimens from the Botanical Garden in Cracow: 1, 2 – attached pseudofilaments; 3–5 – types of branched pseudofilaments; 6 – part of the pseudofilaments and a single cell. Scale bar 10 μm.

Chroothece

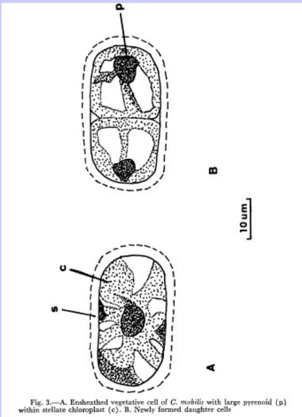

Fig. 3.—A. Ensheathed vegetative cell of *C. mobilis* with large pyrenoid (p) within stellate chloroplast (c). B. Newly formed daughter cells

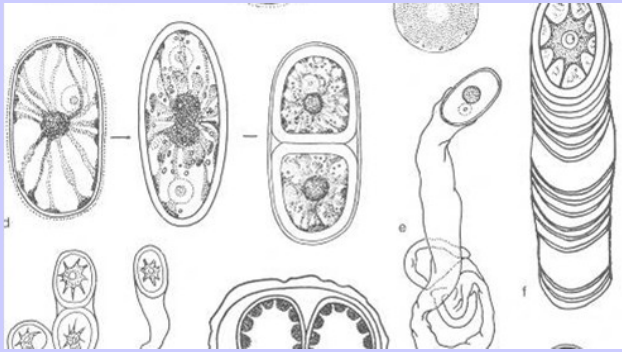

soil crusts, hydro-terrestrial habitats

freshwater and marine habitats
epiphyon

Purpureofilum

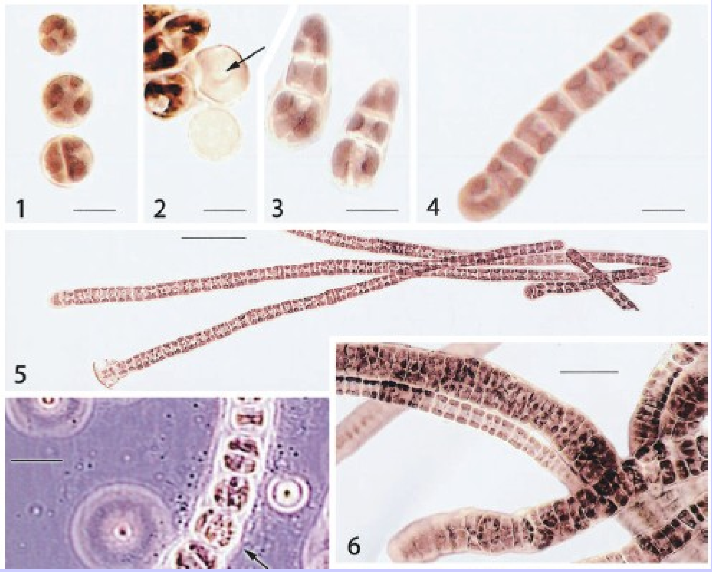

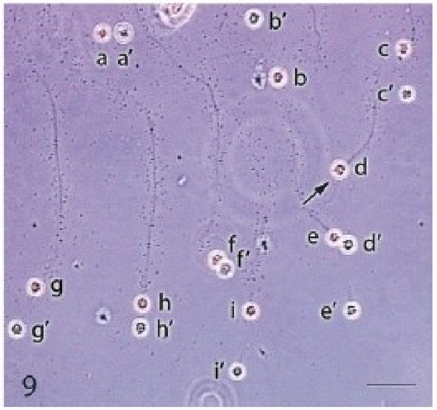

mobile monospores

epiphyte of filamentous algae in mangrove habitats

Wolowski et al., 2007, Biologia 62: 646—649.

Table 1. Comparison of morphological, cytological and biochemical characters of genera in the Stylonematales

Genus and species	Habitat	Thallus	Basal system	Reproduction	Spore movement	Chloroplast	LMWC	Reference
Purpureofilum apyrenoidigerum gen. et sp. nov.	Epiphytic on mangrove algae	Uniseriate to multiseriate, branched, to 1 mm	Unicellular	Vegetative cells discharge directly	Smooth, directed with tails or irregular shuffling without tails	Multiple-lobed single chloroplast without pyrenoid,	Digeneaside sorbitol	o
Bangiopsis subsimplex	On rock, intertidal	Uniseriate to multiseriate, branched, to 10 mm tall	Initially unicellular becoming multicellular	Vegetative cells discharge directly	Irregular, shuffling without tails or brief movement with tails	Single stellate with central pyrenoid	Digeneaside, sorbitol	a,g,i,o
Goniotrichopsis sublittoralis	Epiphytic, subtidal	Uniseriate to multiseriate, branched, to 10 mm tall	Unicellular	Vegetative cells discharge directly	Not observed in culture	Numerous discoid without pyrenoid	Unknown	c,j,l
Chroodactylon ornatum (C. Agardh) Basson	Epiphytic, intertidal and subtidal	Uniseriate, branched, to 5 mm	Unicellular	Vegetative cells discharge directly	Not observed in culture	Single stellate with central pyrenoid blue-green	Sorbitol	a,e,f,h,n
Stylonema alsidii	Epiphytic, intertidal and subtidal	Uniseriate, branched, to 5 mm	Unicellular	Vegetative cells discharge directly	Rapid directional or irregular shuffling, no tails	Single stellate with central pyrenoid	Digeneaside, sorbitol	a,e,f h,n
Stylonema cornu-cervi Reinsch	Epiphytic, intertidal and subtidal	Multiseriate, branched, to 5 mm	Unicellular	Vegetative cells discharge directly	Not observed in culture	Single stellate with central pyrenoid	Digeneaside, sorbitol	e,f,n
Neevea repens Batters	Endozoic in ascidians and bryozoans, subtidal	Uniseriate, multiseriate, branched, to 0.5 mm	n.a.	Vegetative cells discharge directly	Not known	Multiple discoid without pyrenoid bluegreen	Unknown	b,c,k
Empselium rubrum	Epiphytic, subtidal	Uniseriate to multiseriate, ± branches, to 150 μm tall	Unicellular	Not known	Not known	Single parietal band shaped without pyrenoid	Unknown	c
Rhodosorus marinus	Epiphytic, intertidal and subtidal, planktonic	Unicellular	n.a.	Cell division	Protoplast rotation only	Several parietal lobes, central pyrenoid	Digeneaside, Sorbitol	d,e,f,h,m

West et al., 2005, Phycol. Res. 53: 49–66.

Bangiopsis

intertidal benthos

tropics, subtropics

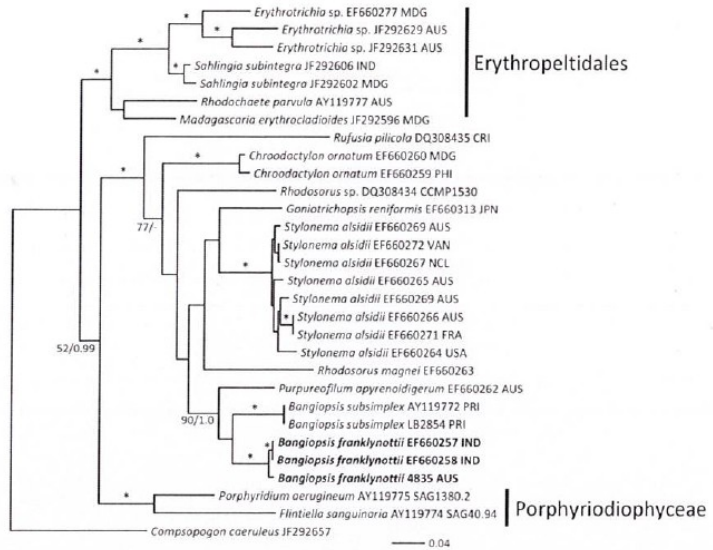

Fig. 2. Maximum-likelihood (ML) topology (-log Ln = -9142.548) of *rbc*L gene data of select Stylonematophyceae, Porphyridiophyceae and Compsopogonophyceae. *Composopogon caeruleus* was used as an outgroup. * ≥95% ML bootstrap values and ≥0.95 Bayesian posterior probabilities. Other values associated with branches = RaxML bootstrap percentage/Bayesian posterior probabilities. Abbreviations following the species names and culture numbers: MDG, Madagascar; AUS, Australia; IND, India; CRI, Costa Rica; PHI, Philippines; JPN, Japan; VAN, Vanuatu; NCL, New Caledonia; FRA, France; USA, United States; PRI, Puerto Rico. Scale bar represents substitutions/site.

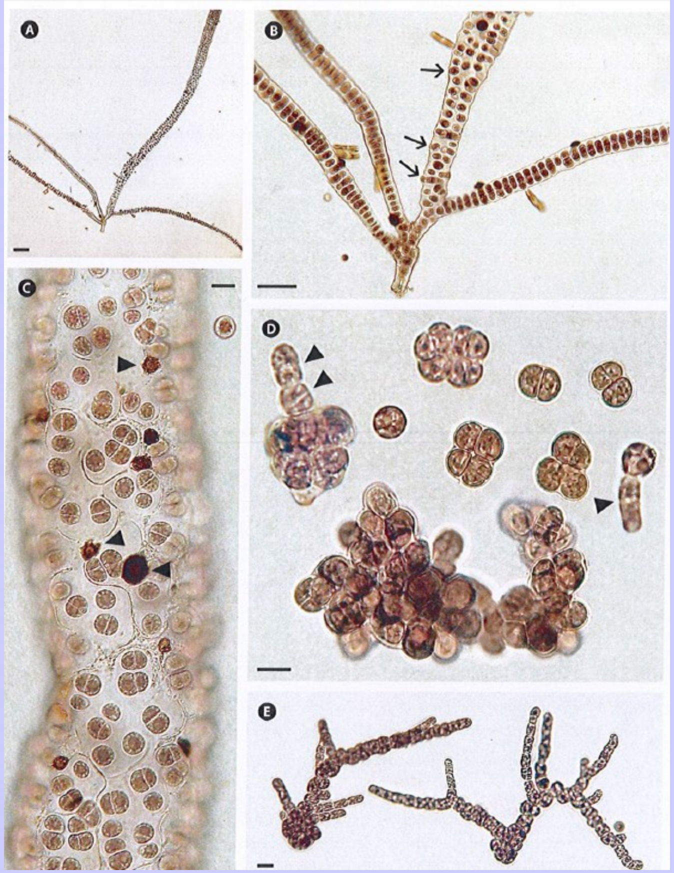

West et al., 2014, Algae 29: 101-109.

Porphyridiophyceae

Kyliniella

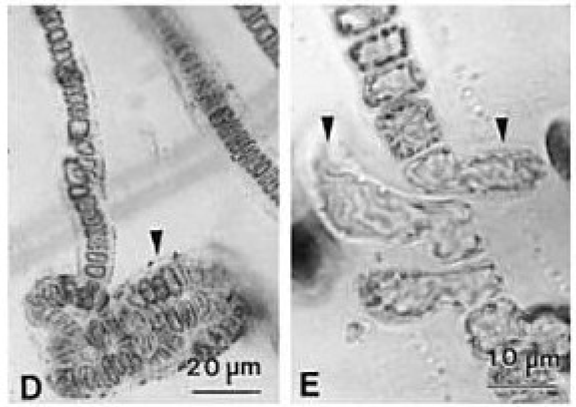

epiphyte in streams, N. Am.

Porphyridium

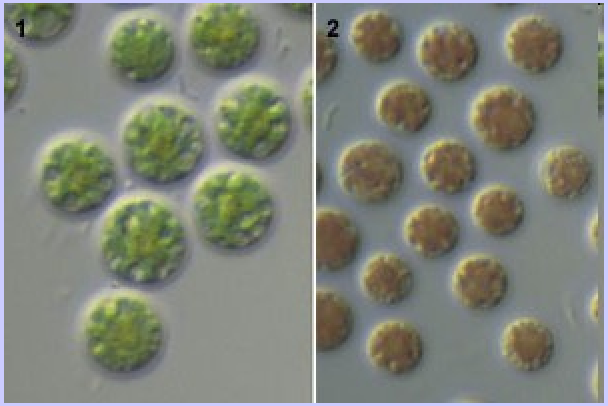

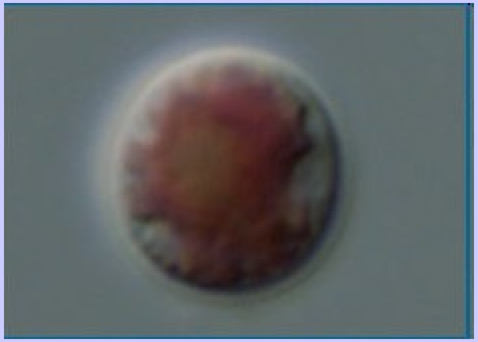

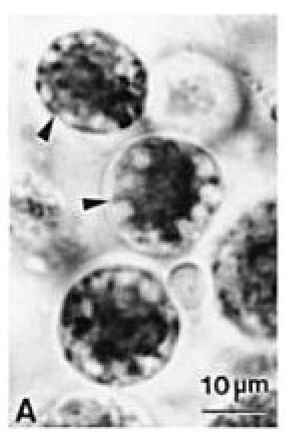

soil crusts, benthos

additional genera, i.e. *Phragmonema, Glauconema*

Compsopogonophyceae

Compsopogon

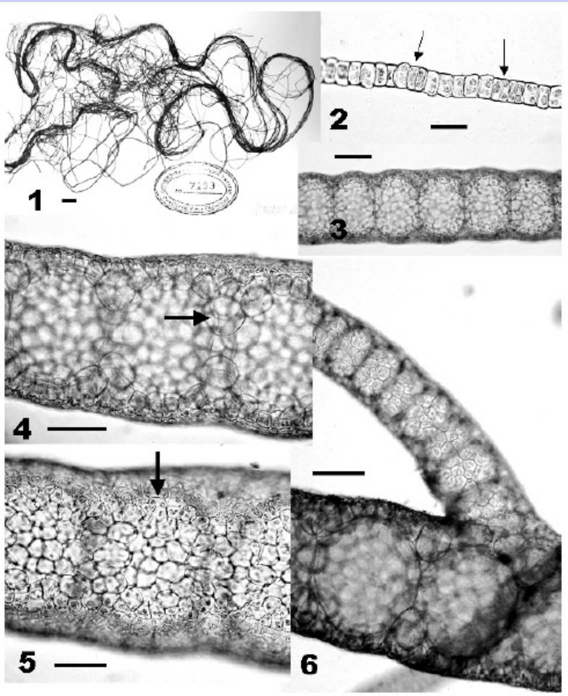

Fig. 1 Herbarium specimen of *Compsopogon coeruleus* from Wainivesi River, Tailevu, Fiji, 30 May 2001. SUVA-A 7199. Scale = 1 cm. **Fig. 2** Uniseriate terminal portion of branch, showing recent intercalary cell divisions

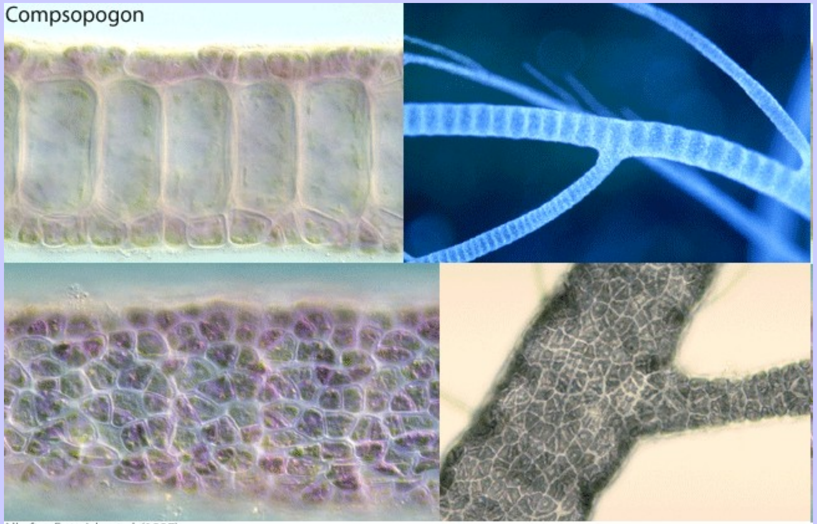

All after Entwisle et al. (1997)

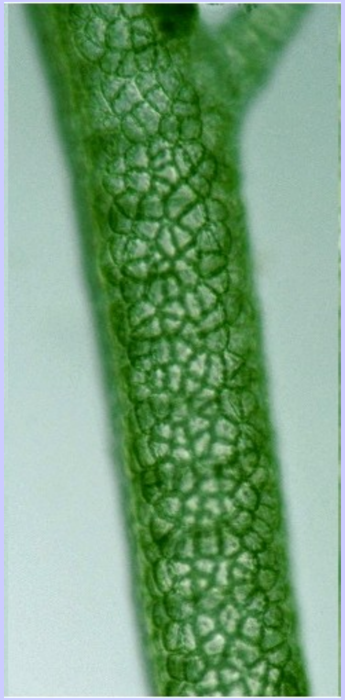

aquariums - nuisance alga

epiphytic growths in (sub-)tropical freshwater habitats
(in USA ca till Virginia and Kentucky – most often *C. coeruleus*)

subtropical Europe (E, F, MT, GB (?))

southern Pacific – ingredient for local puddings
(served with fish)

South & Skelton, 2002, N.Z. J. Mar. Fresh. Res. 36: 879–881.

Pulvinus

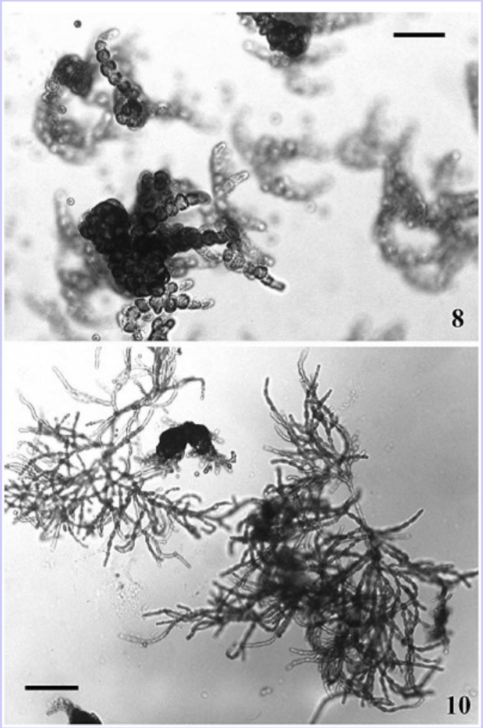

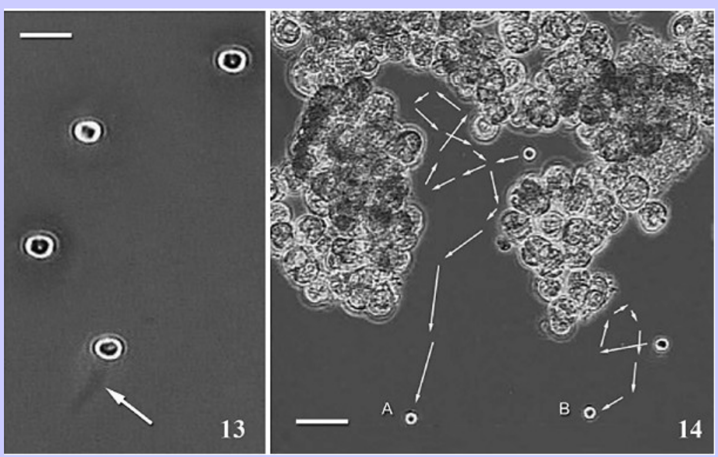

mobile monospores

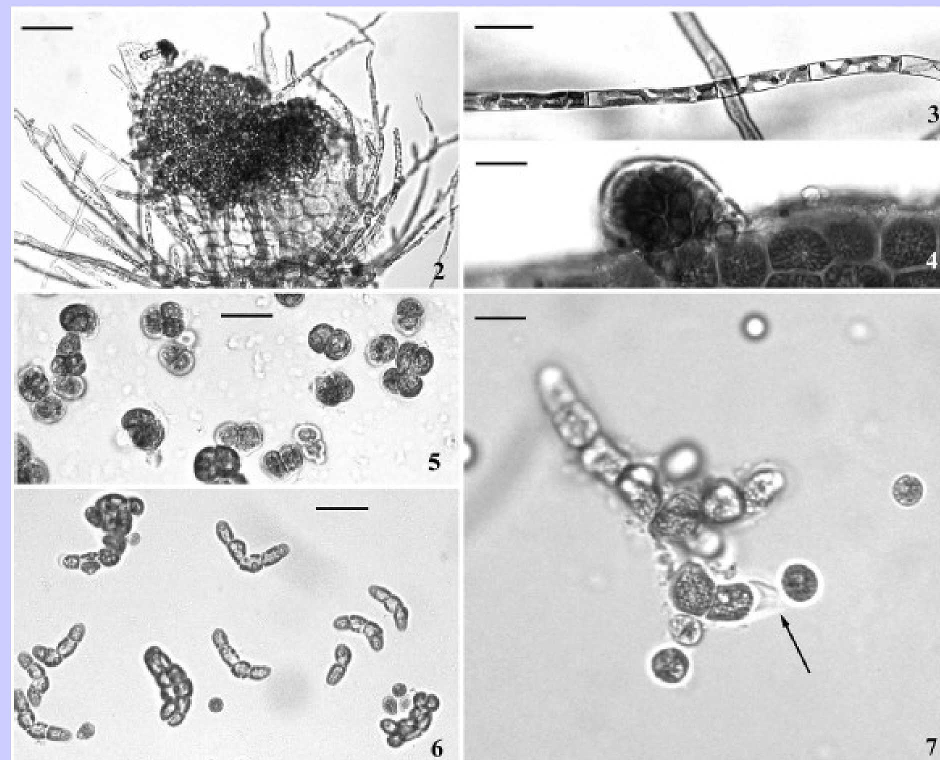

West et al., 2007, Phycologia 46: 237-246.

P. veneticus – epiphyte known from Vanutatu

Compsopogon seemingly has rather low global genetic diversity

(especially in comparison with many other microalgal lineages...)

(six morphological species synonymized within that study...)

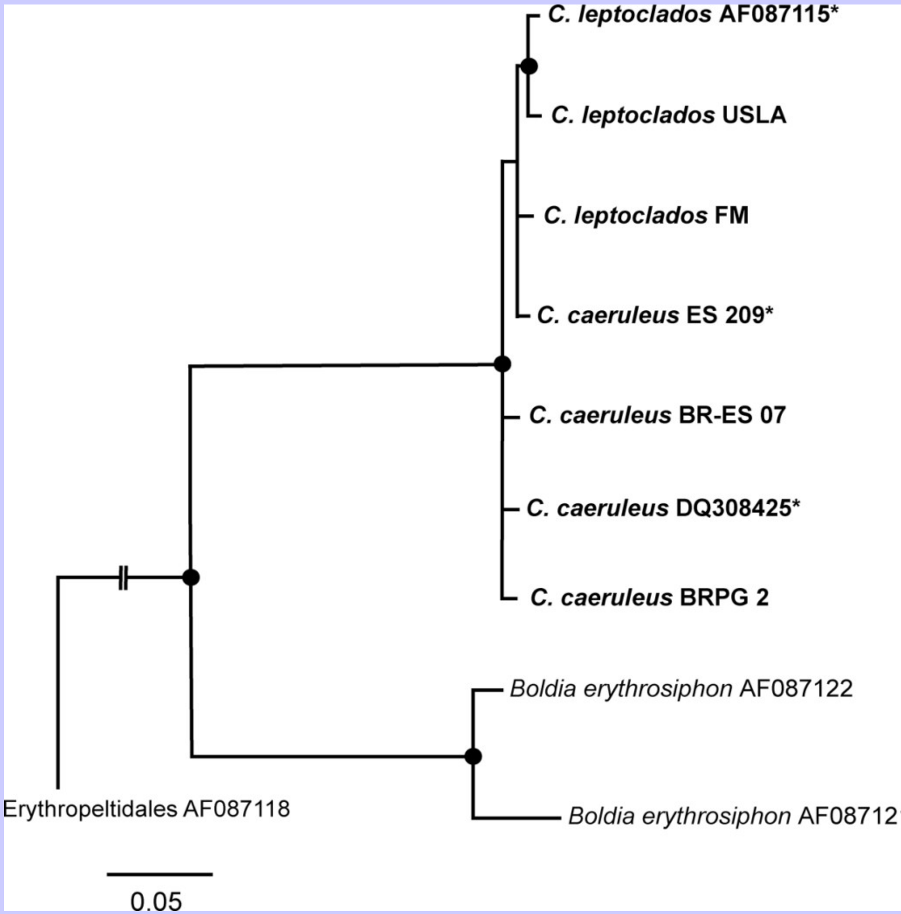

plastic encoded rbcL based phylogeny

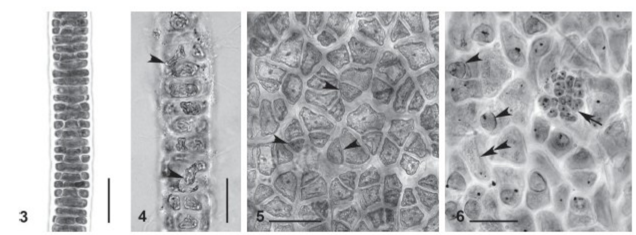

Figs 3–6. *Compsopogon caeruleus*: photomicrographs of important morphological features for both the 'caeruleus' and 'leptoclados' morphologies. Location codes as in Table 1. **3.** Early cortication of 'caeruleus' morphology showing regular cortication. Specimen from BR-ES7. **4.** Early cortication of 'leptoclados' morphology showing irregular cortication and rhizoidal cells (arrowheads). Specimen from BR-CL. **5.** Surface view of 'caeruleus' morphology showing regular (polygonal) cortical cells and monosporangia (arrowheads). Specimen from BR-ES3. **6.** Surface view of 'leptoclados' morphology showing monosporangia (arrowheads), microsporangia (arrow) and rhizoidal cell (double arrowhead). Specimen from BR-CL. Scale bars = 50 μm.

Why?
a)asexual reproduction – monospores
b)relatively wide niche

Necchi et al., 2013, Eur. J. Phycol. 48: 152-162.

Boldia

B. erythrosiphon
streams – eastern N. Am.
(Alabamy to Quebec)
very often on freshwater snails

Boldia on snails

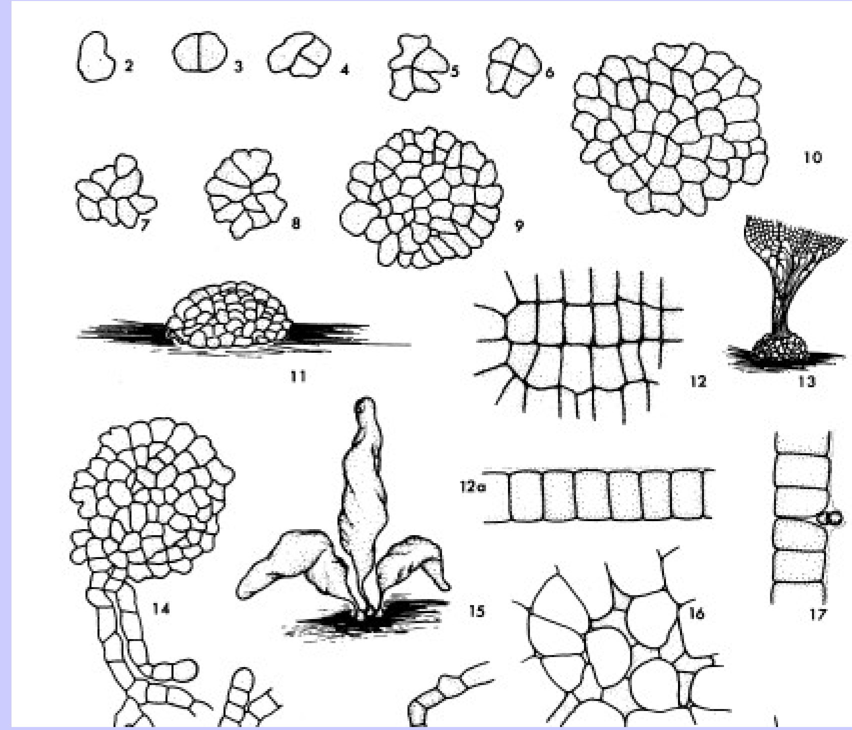

thallus ontogenesis

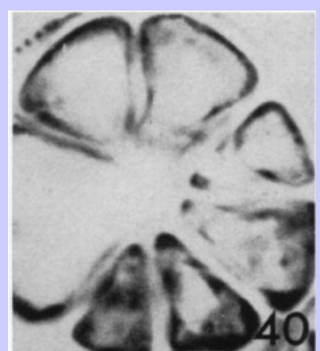

Nichols, 1964, Am. J. Bot. 51: 653-659 .

Erythrotrichia – filamentous thallus
Erythrocladia – pseudoparenchymatous thallus

epiphytic marine algae

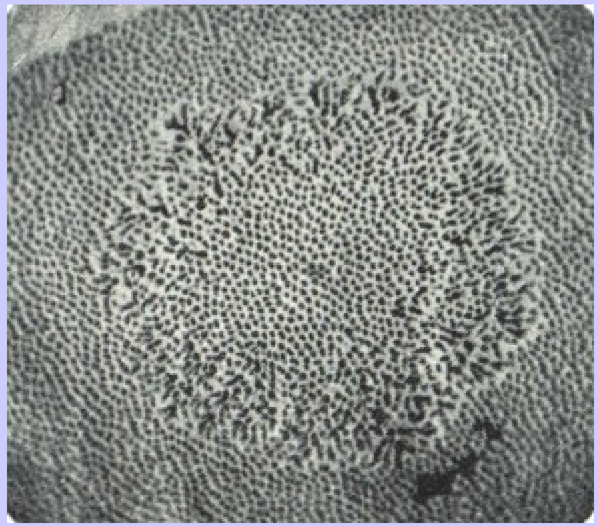

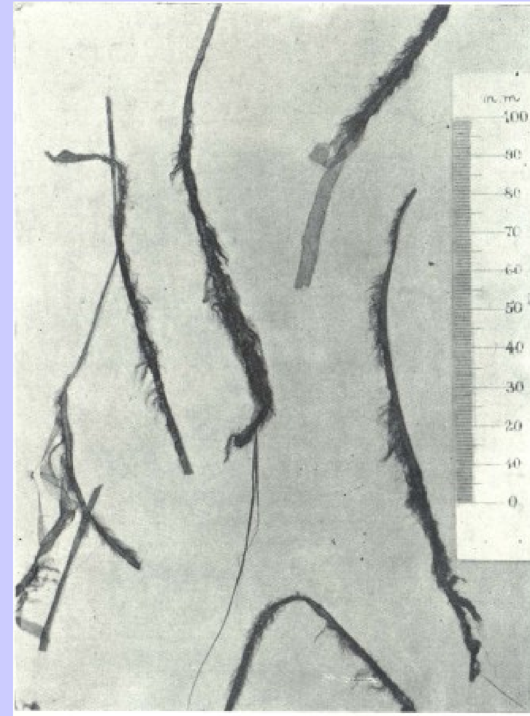

Photo, C. M. Gray.
FIG. 18.—*Erythrotrichia ciliaris* (?) on Zostera sp.

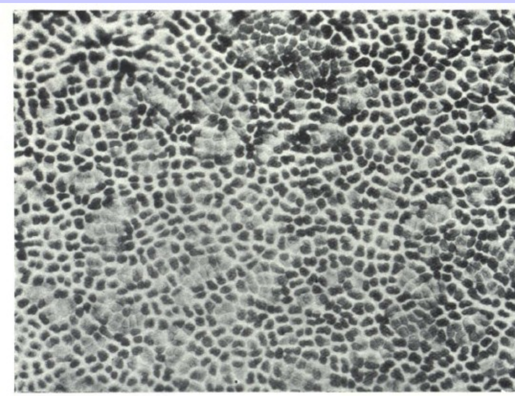

Photo, C. M. Gray.
FIG. 22.—Cells of *Erythrocladia insignis* streaming into an area, already occupied by *Porphyra*. The smaller darker cells are those of *Erythrocladia*, the larger paler ones are those of *P. umbilicalis*, var. *Novae Zelandiae*, x 150.

Erythrocladia – rarely in freshwater (NL)

Bangiophyceae

- formerly – two morphologically defined genera (*Bangia* and *Porphyra*)
- class-level definition: important life cycle synapomorphies
- phylogenetic diversity – across traditional morphologies
- primary evolution centre (coastal habitats, southern hemisphere, NZ/Australia)
- rarely also in freshwater habitats
- cosmopolitan distribution in marine habitats

- several recently described monophyletic genera

Porphyra-like morphology

Bangia-like morphology

phylogenetic revision of Bangiales

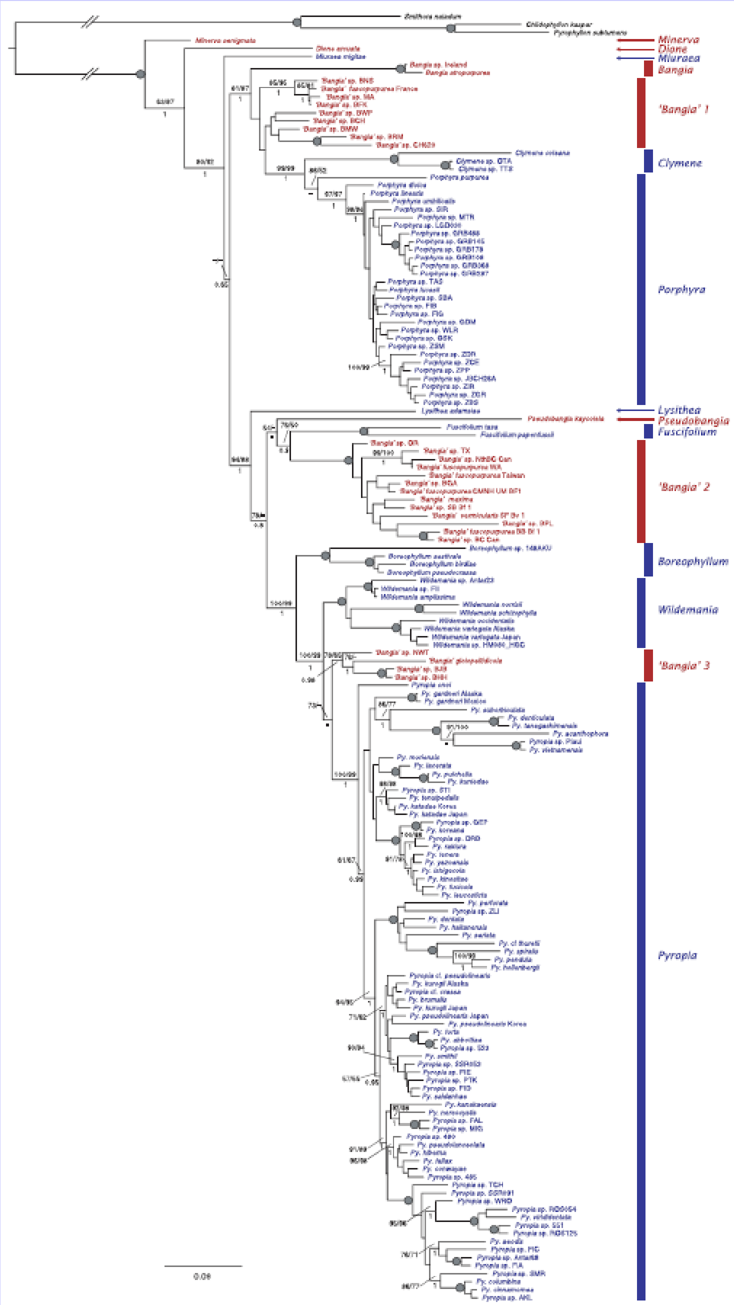

FIG. 1. Maximum-likelihood phylogram of 157 Bangiales taxa calculated from the concatenated nuclear SSU ribosomal RNA (nrSSU) and RUBISCO LSU (*rbc*L) data set under RAxML. Bootstrap values for RAxML and GARLI are shown above, and Bayesian PP values below the nodes. Some internal support values are omitted for clarity. Gray circles indicate nodes supported at 100% RAxML/100% GARLI/1 PP. Genera are indicated by lines, and monotypic genera by arrows. Names of filamentous taxa are shown in red, and those of foliose taxa in blue.

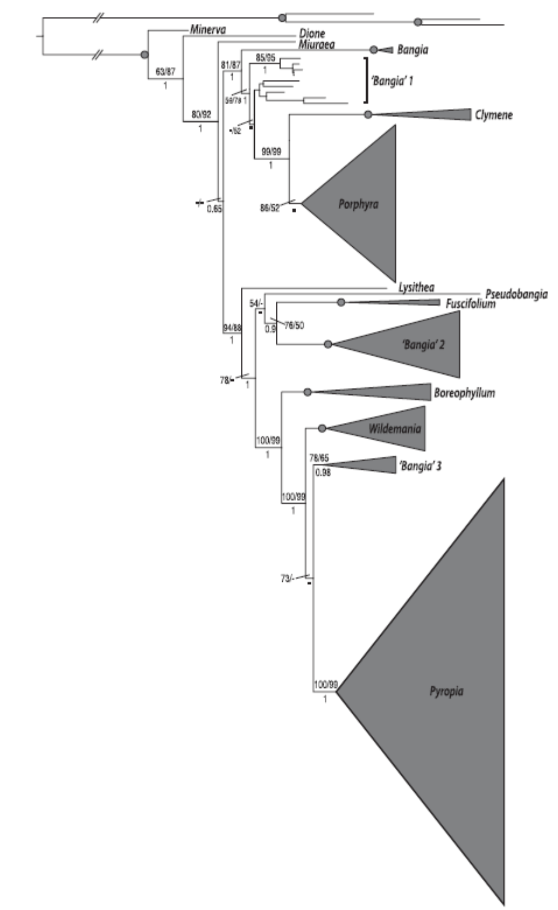

FIG. 2. Cartoon of the RAxML maximum-likelihood phylogram of 157 Bangiales taxa calculated from the concatenated nuclear SSU ribosomal RNA (nrSSU) and RUBISCO LSU (*rbc*L) data set showing existing and proposed new genera with support for nodes along the backbone of the tree. Gray circles indicate nodes supported at 100/100/1.

Sutherland et al., 2011, J. Phycol. 47

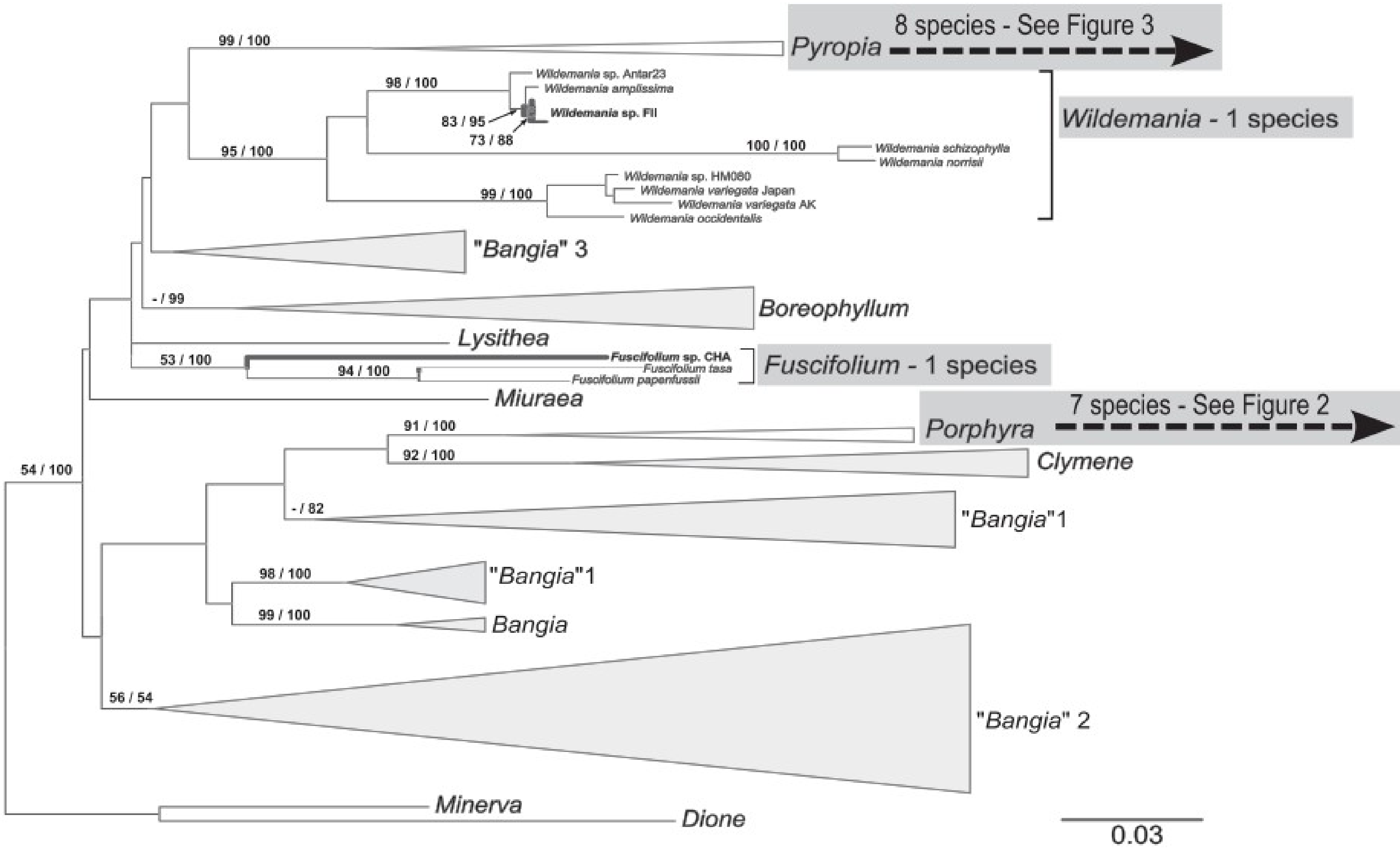

Fig. 1. Maximum Likelihood (ML) rooted tree for *rbc*L sequences (875 bp) of Bangiales. *Minerva* and *Dione* were used as outgroups. For each node, ML bootstrap values and Bayesian Posterior Probabilities are indicated (ML/BPP). Only high support values (>75) are shown; '-' = clade not observed in the Bayesian Inference. Next to collapsed branches are abbreviated genera names (as defined in Sutherland et al., 2011). Species of Chilean foliose Bangiales are shaded in gray. Since only the COI marker was sequenced for the *Porphyra* specimens assigned to the CHD group, only seven Chilean *Porphyra* were actually retrieved in the *rbc*L tree.

Guillemin et al., 2016, Mol. Phyl. Evol.

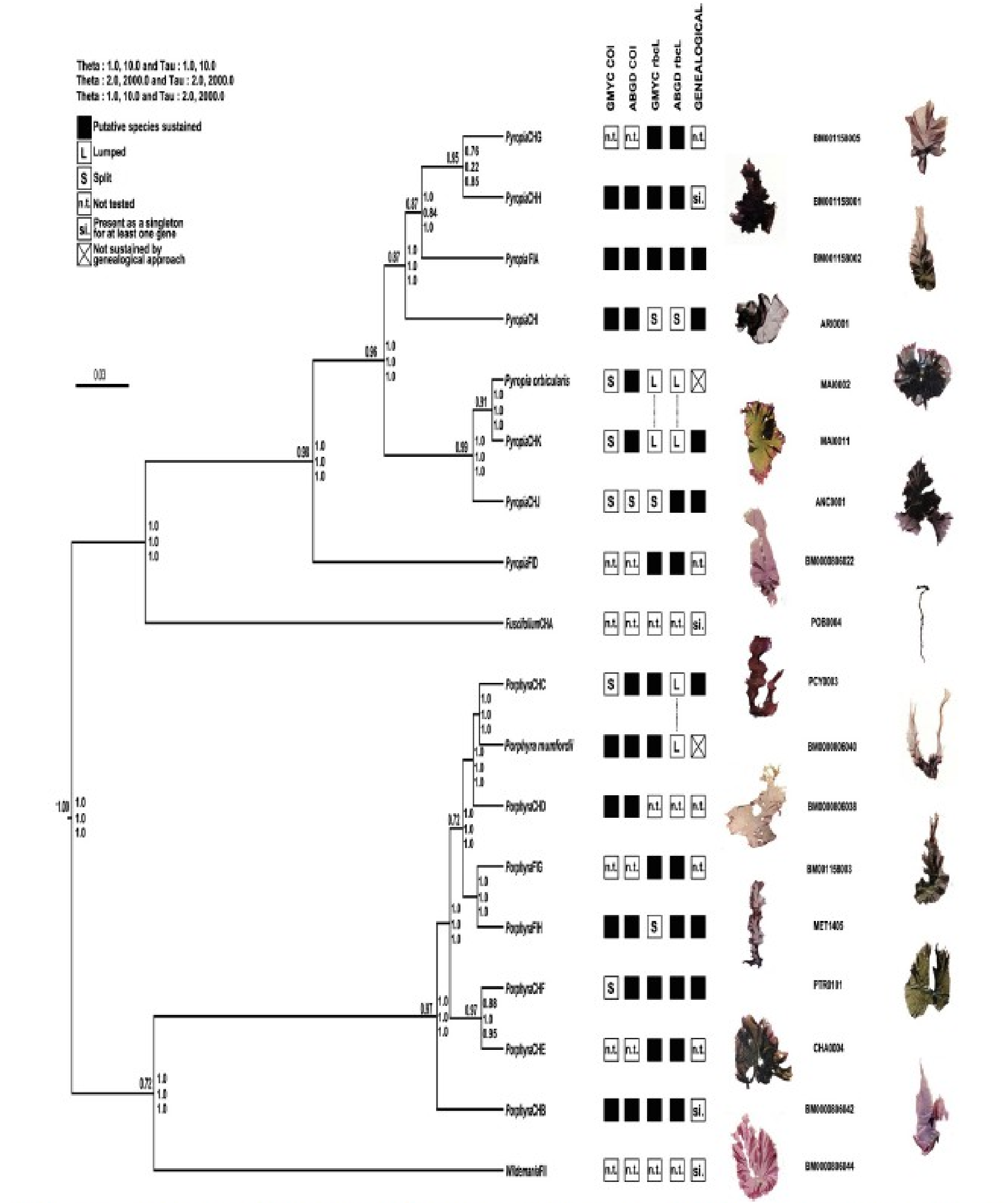

Fig. 2. Bayesian species tree inferred using *BEAST with numbers above branches representing posterior probability values (only values greater than 0.70 are shown). Speciation posterior probabilities from BP&P were calculated using three different prior combinations: 1st – large ancestral Ne and deep divergences (θ G(1, 10) and $\tau0$ G(1, 10); top); 2nd – small ancestral Ne and shallow divergences (θ G(2, 2000) and $\tau0$ G(2, 2000); middle) and 3rd – large ancestral Ne and shallow divergences (θ G(1, 10) and $\tau0$ G(2, 2000); bottom). Supports based on five different methods employed for species delimitation are given for the 18 Chilean Bangiales: $GMYC_{Multiple}$ for the COI, ABDG for the COI, $GMYC_{Multiple}$ for the *rbc*L, ABGD for the *rbc*L and genealogical concordance. A picture of a representative specimen is given on the right part of the figure for each species.

Guillemin et al., 2016, Mol. Phyl. Evol.

morphological type "***Porphyra***"

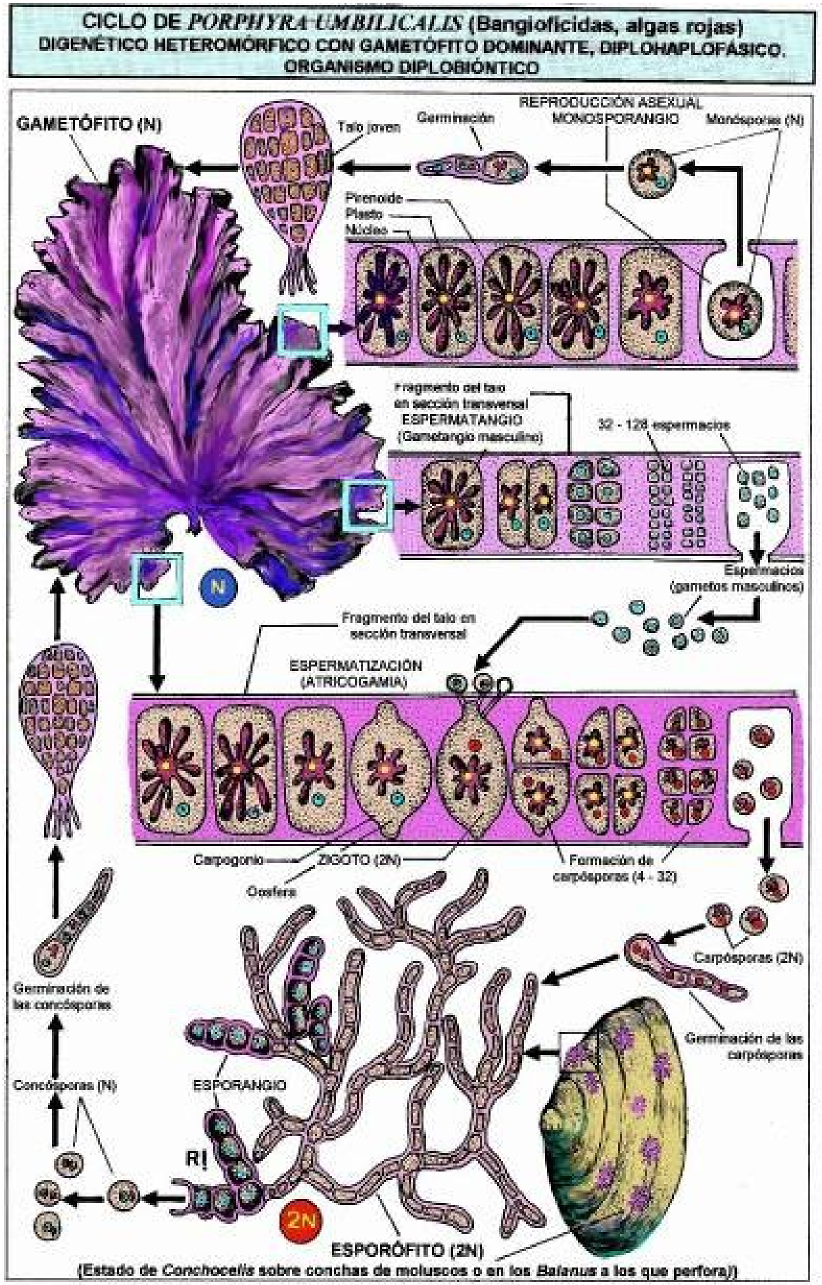

(sub-)tropical to subarctic seas
polyphyletic; ca 80 species desribed, so far

polyploid life history in Porphyra

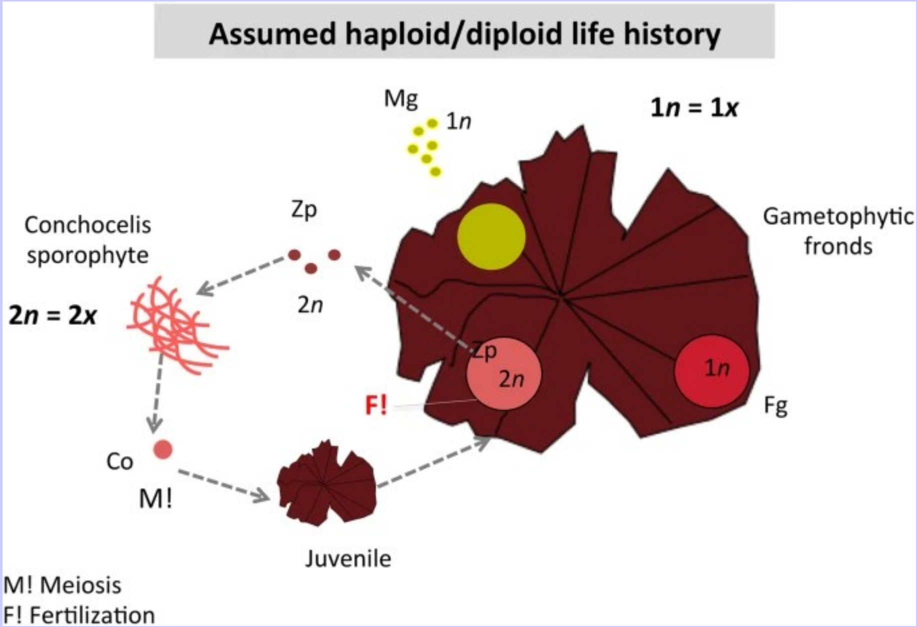

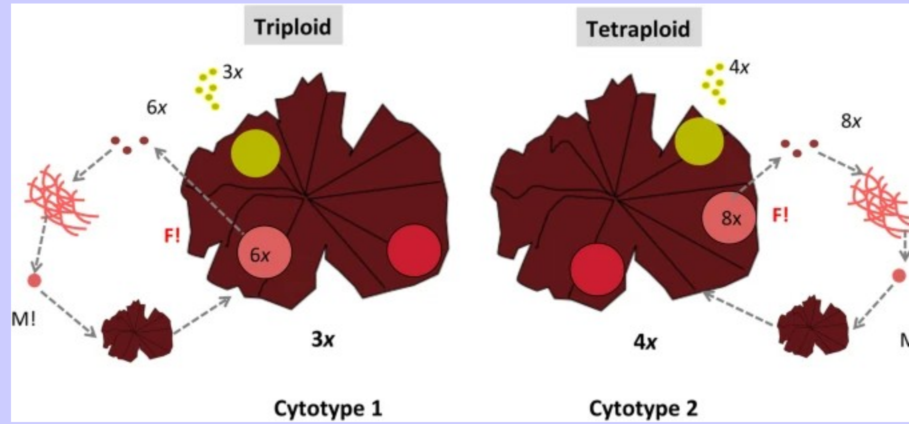

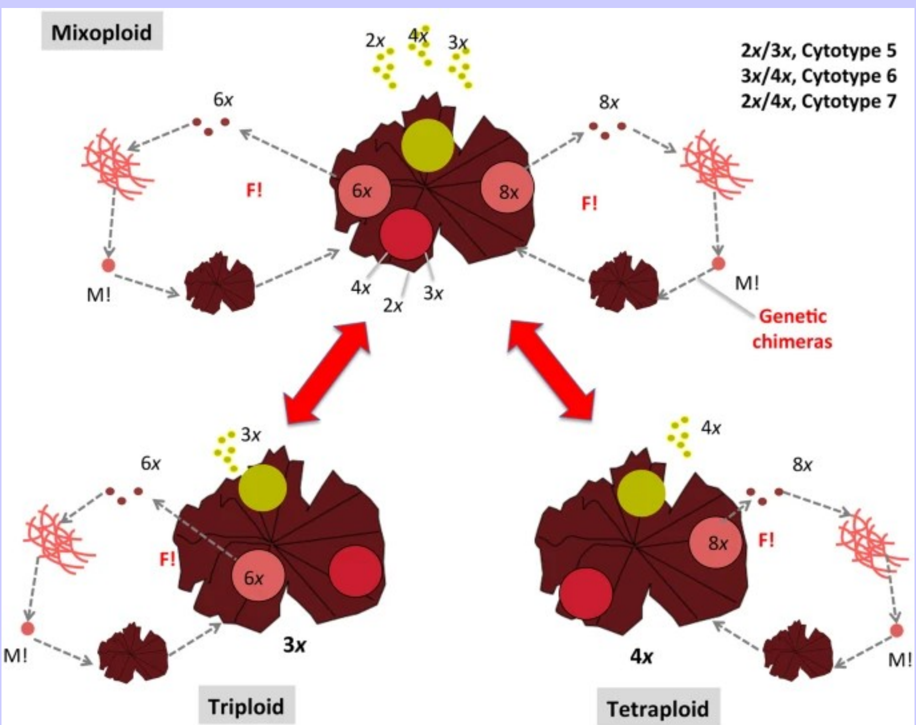

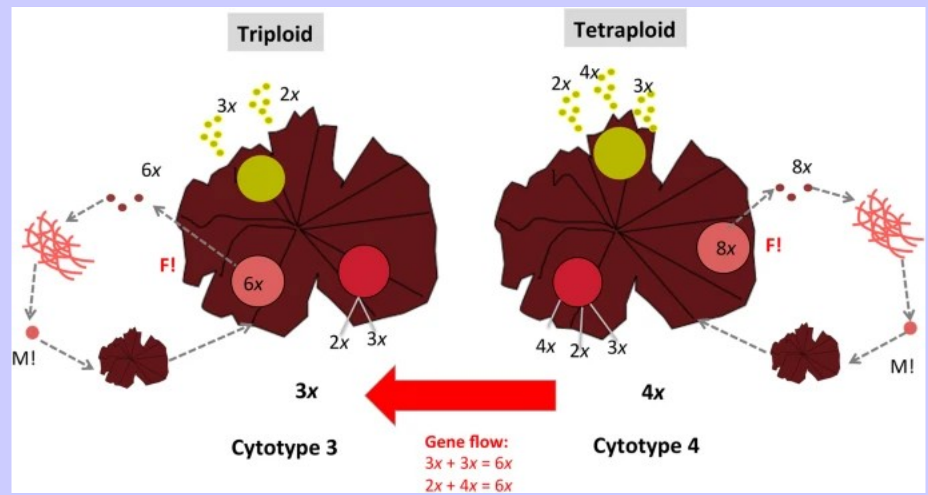

Varela-Álvarez et al., 2018

marine porphyroid genera

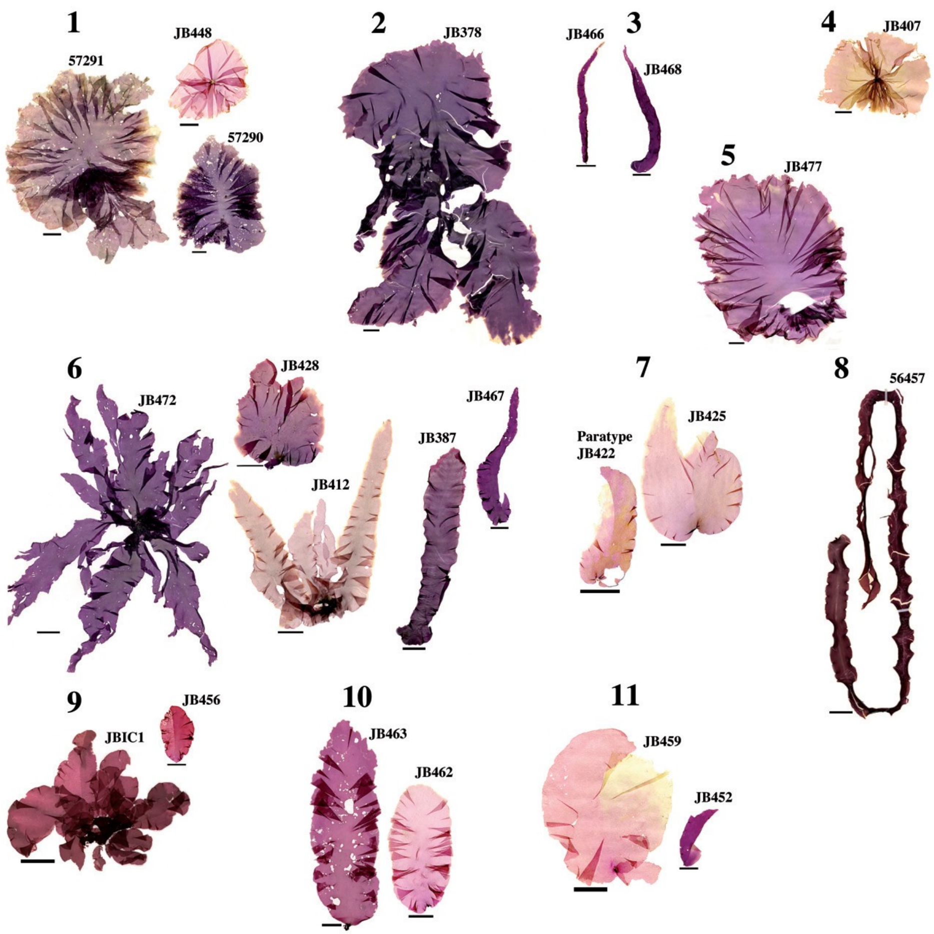

Boreophyllum, Porphyra, Pyropia, Wildemania

relatively homogeneous vegetative
morphology across genera

profound plasticity

Mols-Mortensen et al., 2012, Eur. J. Phycol. 47 morphological differentiation of *Pyropia* species - an example from Chilean coast

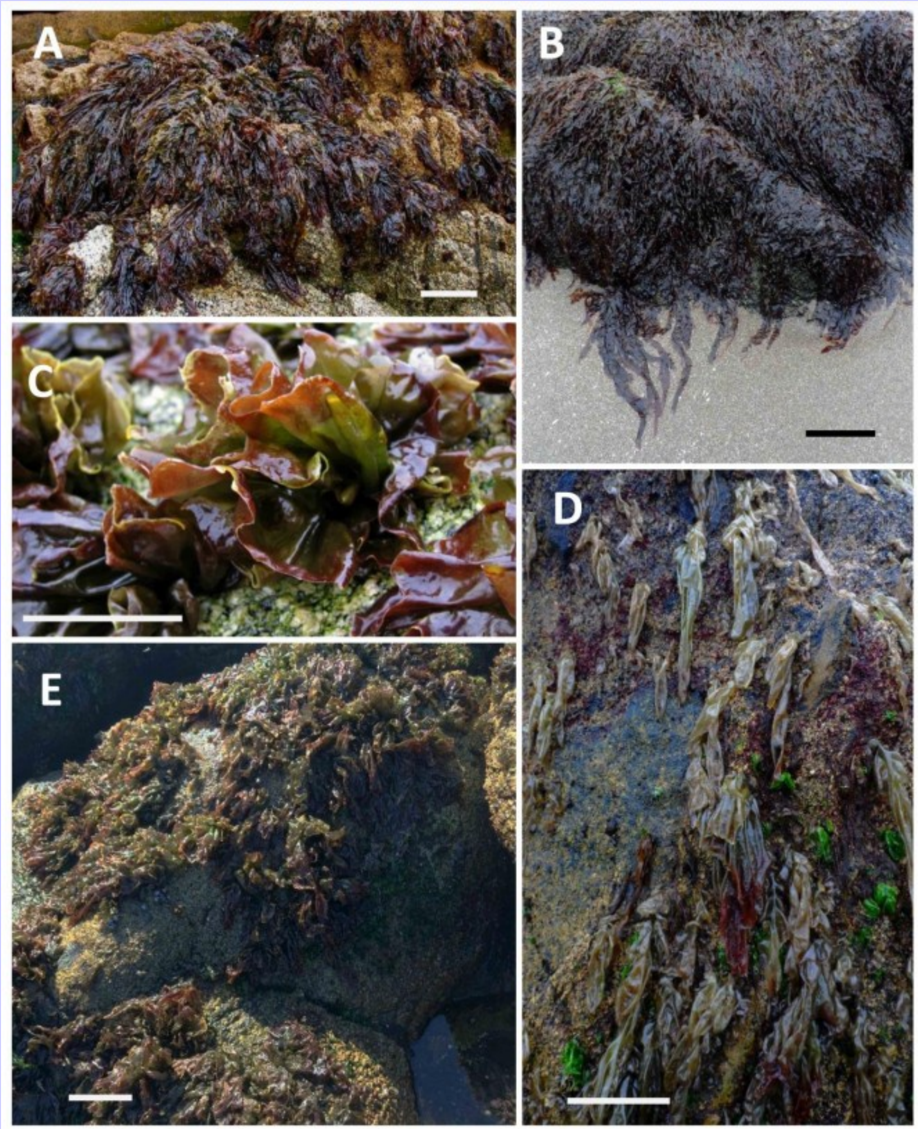

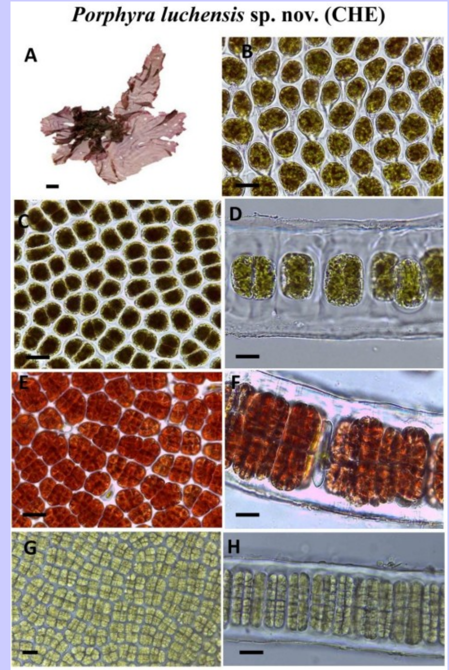

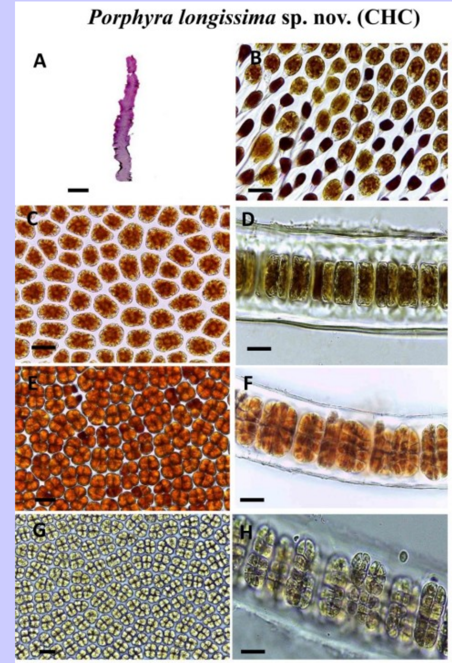

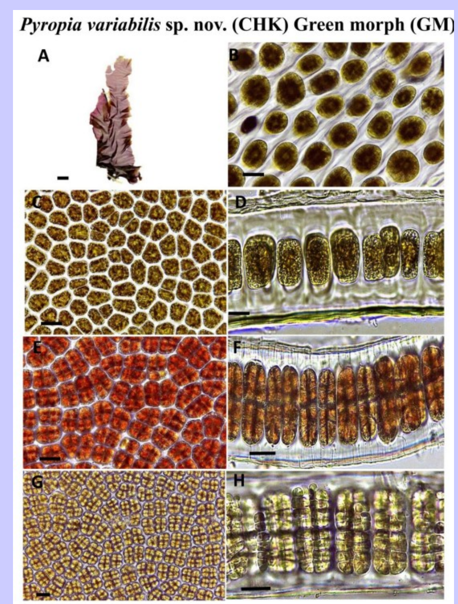

Meynard et al., 2019, J. Phycol.

open-air aquacultures; closed mass cultivation systems

laver (GB, Wales), nori (JP), hai-tai, zicai (CH), gim, zakai (KR), karengo (NZ):
– *P. umbilicalis, P. yezoensis, P. tenera, Pyropia columbina*

gametophyte harvest after about 45 days since germination

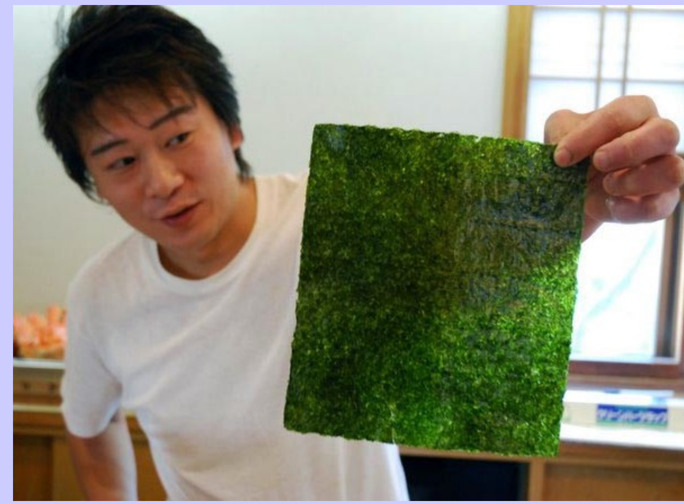

seeding of conchospores in the lab

annual production amounts to ca. 50 bill. CZK

seedling centre

Conchocelis stage on shells

seeding nets

Porphyra harvest

www.seaweed.ie

World Production of Seaweed (Algo Rhythme, No. 31, CEVA, Pluebian, France)

Country / Area	Algae / Seaweed(fresh weight million t)	World Production (%)
China	4.093	59
Korea	0.771	11
Japan	0.737	10
Phillipines	0.404	6
FAR EAST COUNTRIES (TOTAL)	6.263	90
Norway	0.185	2.6
Chile	0.182	2.6
USA	0.116	1.6
France	0.079	1.1
EUROPEAN COUNTRIES	0.302	4.3
TOTAL	6.941	100
Ireland	0.032	0.46

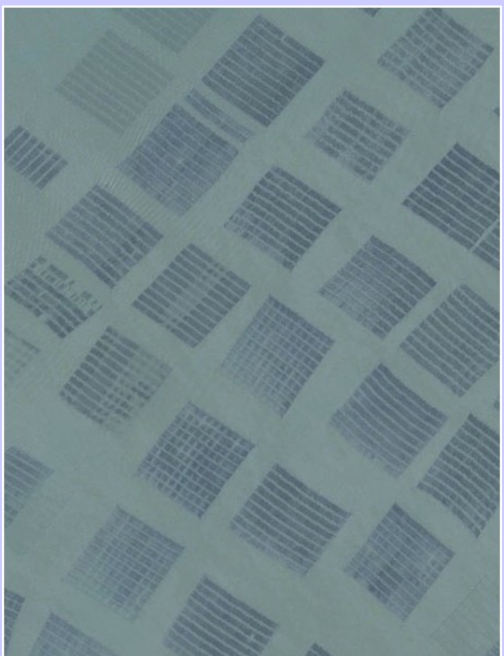

IMAGE: Seaweed farming rafts off the coast of the Chinese province of Jiangsu, south of the city of Qingdao, Bing Maps, via Mammoth.

www.seaweed.ie

bangioid lineages

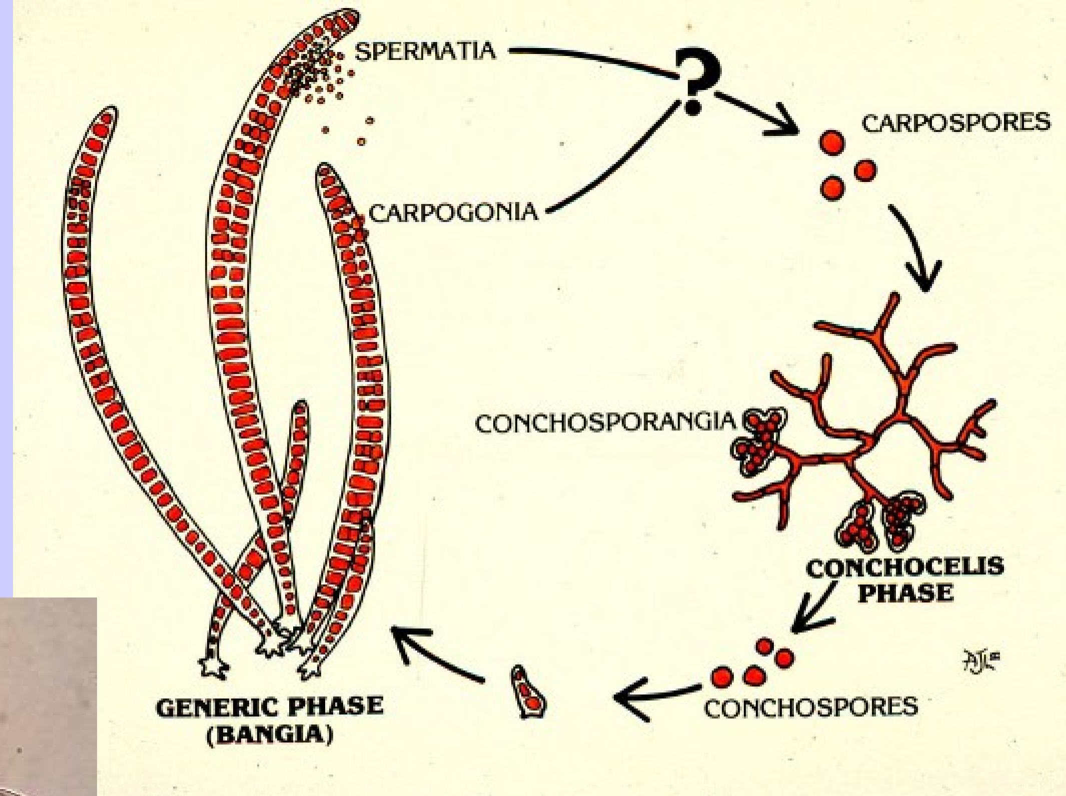

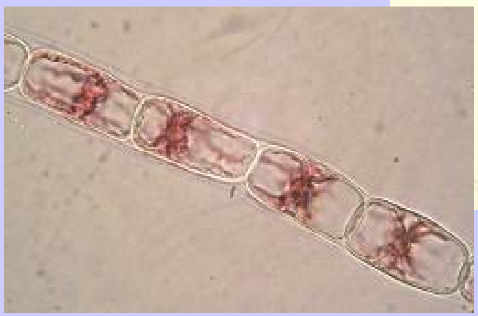

marine littoral, streams, wterfalls, clean lakes; polyphyletic genus

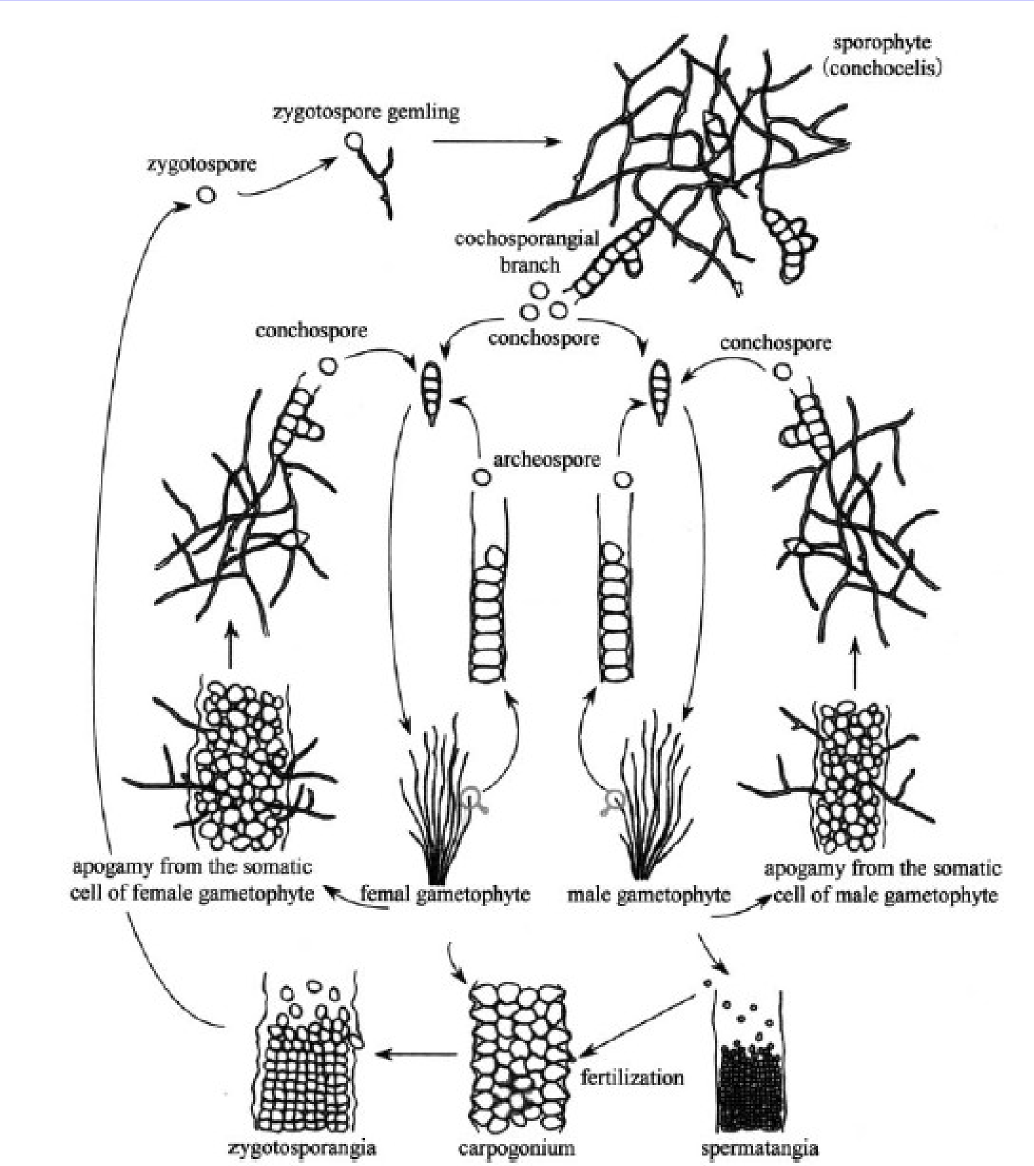

Fig. 8 Summarized life history of *Bangia atropurpurea* from Fukaura, Japan.

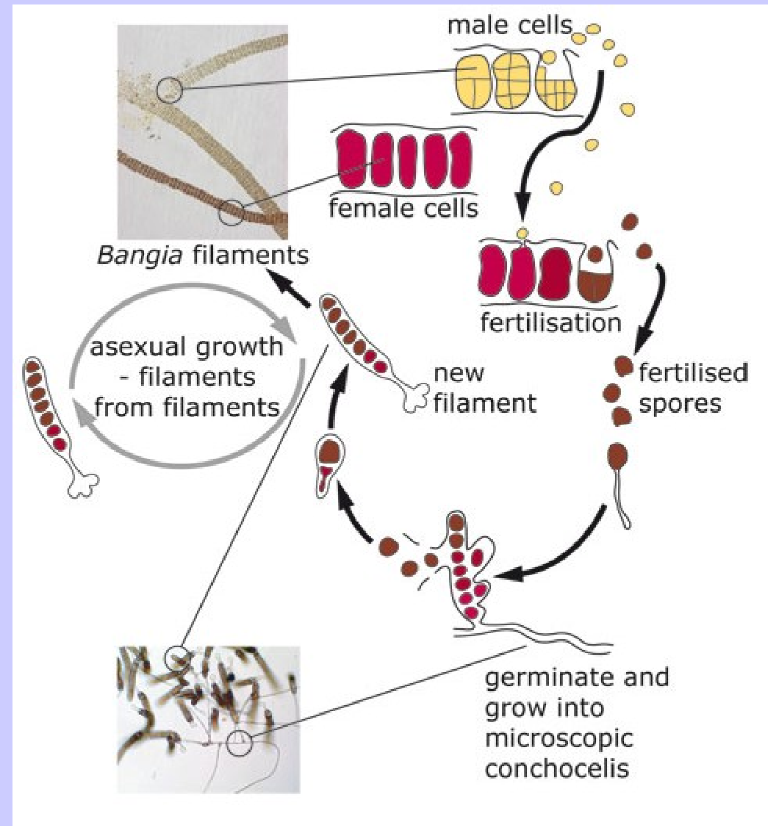

The biphasic life history of *Bangia*. (Graphic: Tracy Farr)

Bangia life cycle

Notoya & Iijima, 2003, Fisheries Sci.

marine bangioid lineages

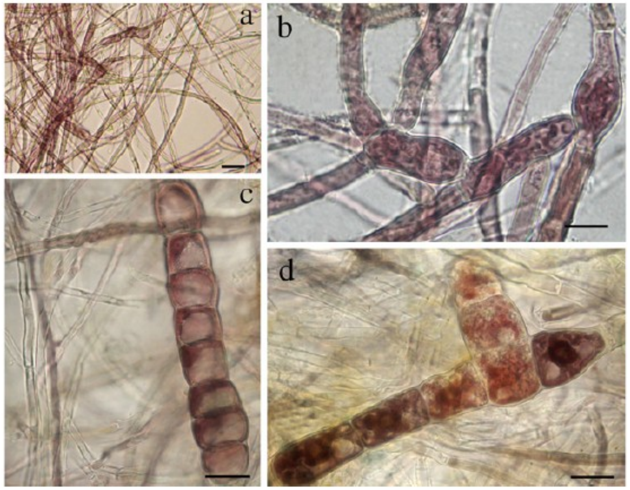

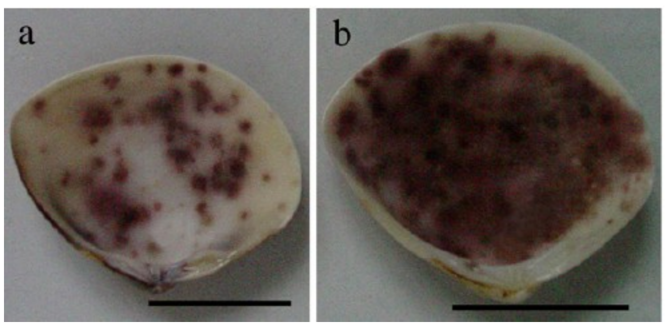

Conchocelis stages, often forming epizoic populations in shells

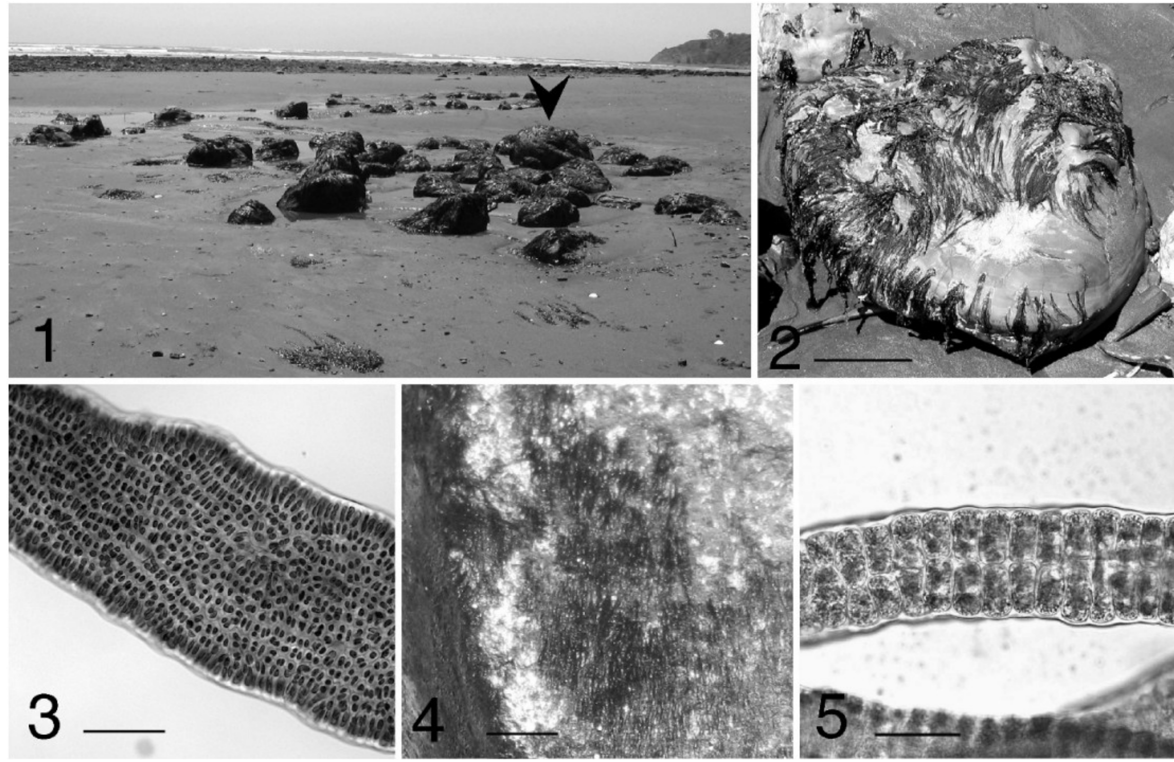

very often in supralittoral

B. fuscopurpurea
ushike-nori [JP]
hangmaocai [CN]

Lynch et al., 2008, Phycologia
Wang et al., 2008, Aquaculture

freshwater *Bangia*
(B. atropurpurea, Bangiadulcis)

a frequent member of phytobenthos in large oligotrophic lakes (Ohrid Lake, Lago di Garda)

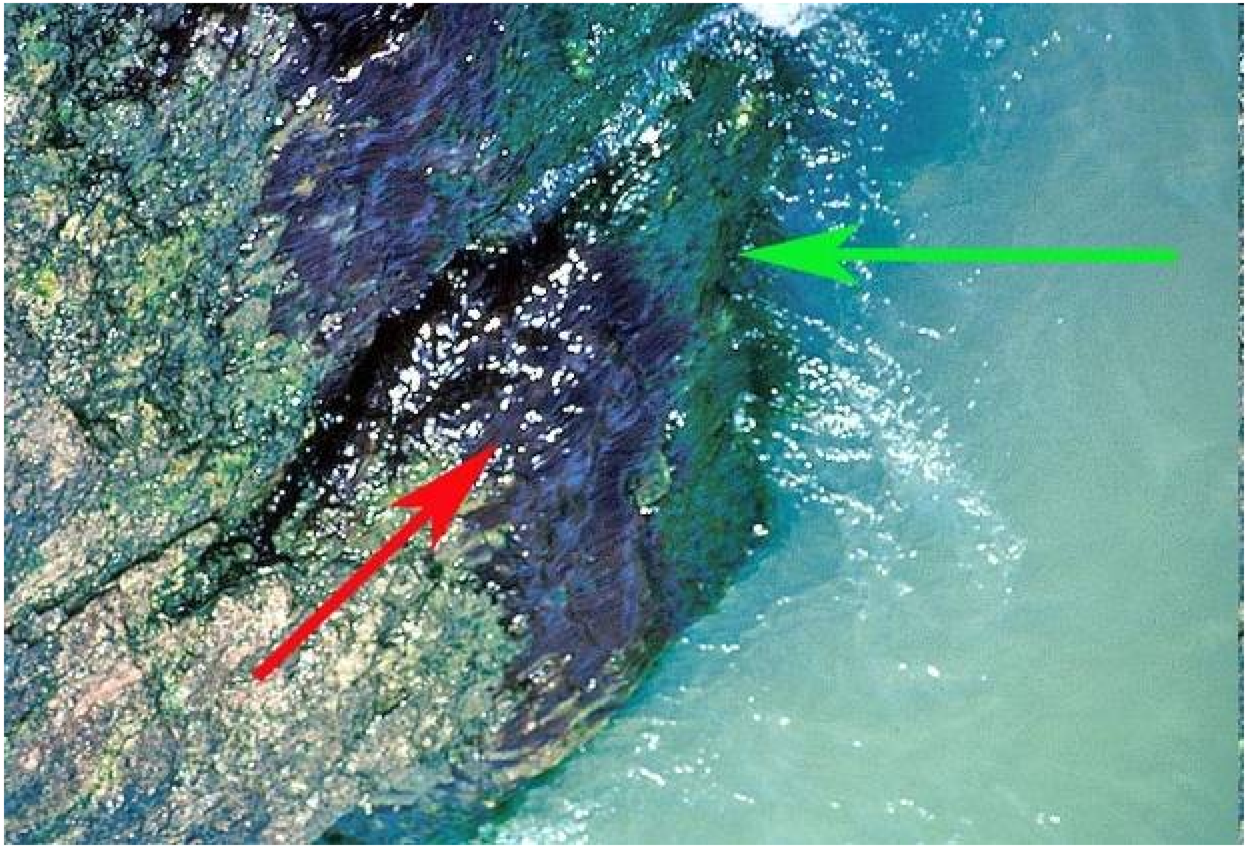

an invasive species in some lakes (e.g. Lake Erie)

bangias in littoral of
clean lakes
(such as Ohrid lake)

freshwater bangias
(Eu, S.Am., JP) recently
re-classified as
monophyletic genus
Bangiadulcis

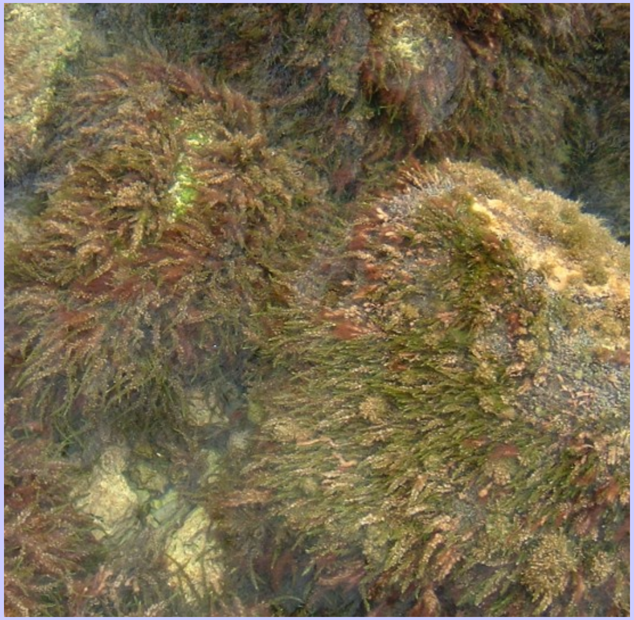

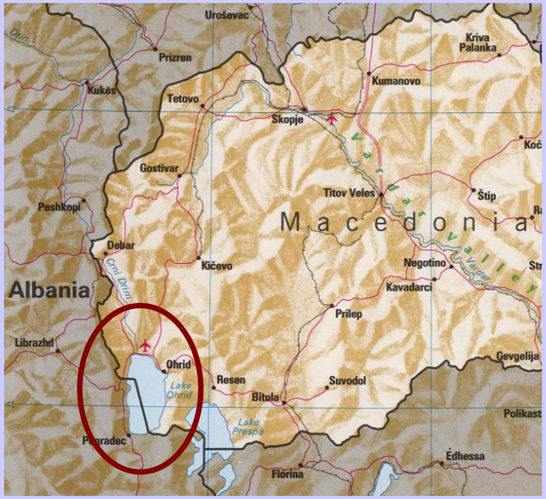

Dione a *Minerva* – two most ancestral genera in Bangiales (formerly classified as (a bit strangely looking) *Bangia*)

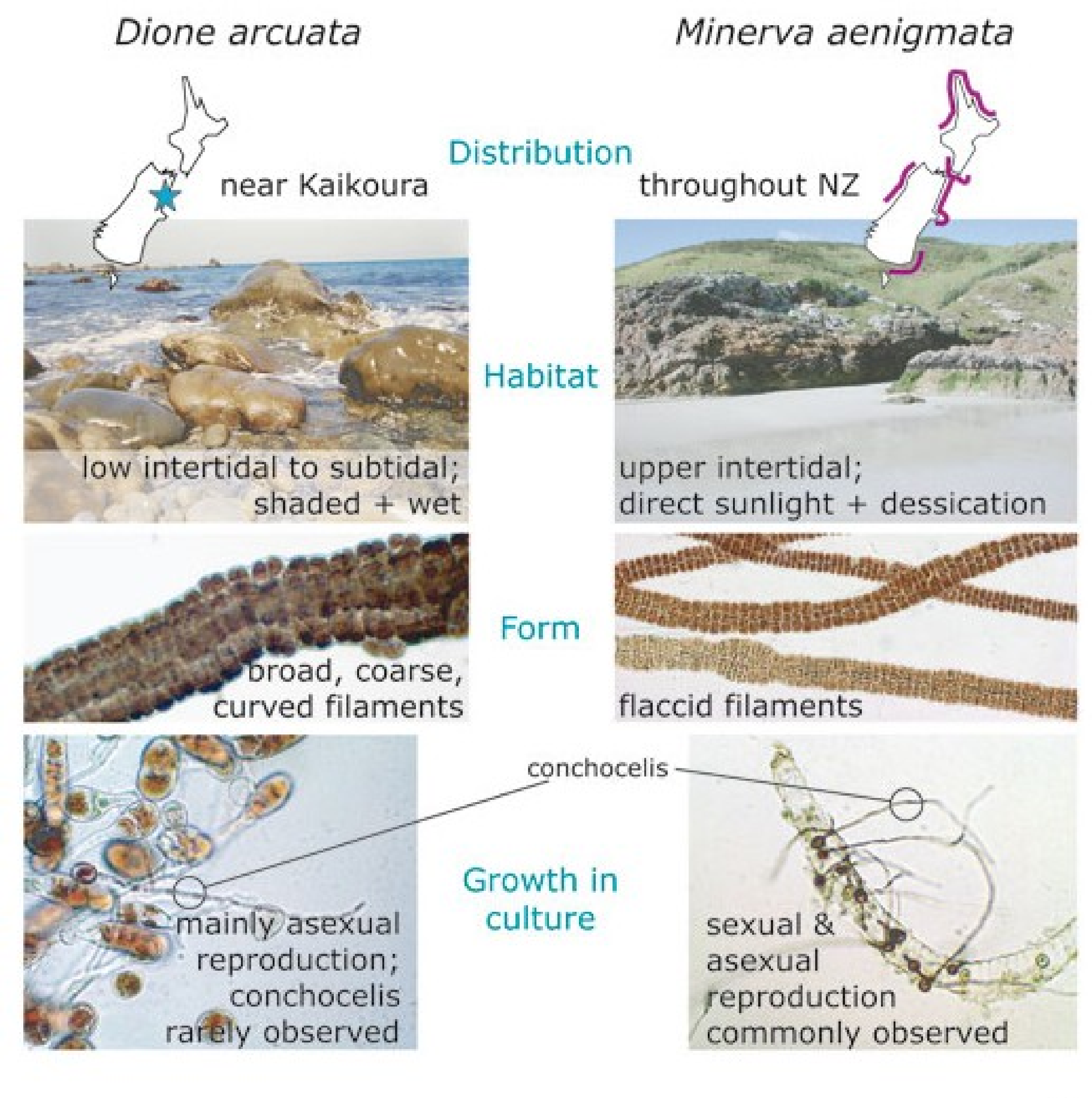

A comparison of the two new Bangiales species. (Graphic: Tracy Farr)
Image 3 of 3

distribution – N.Z.

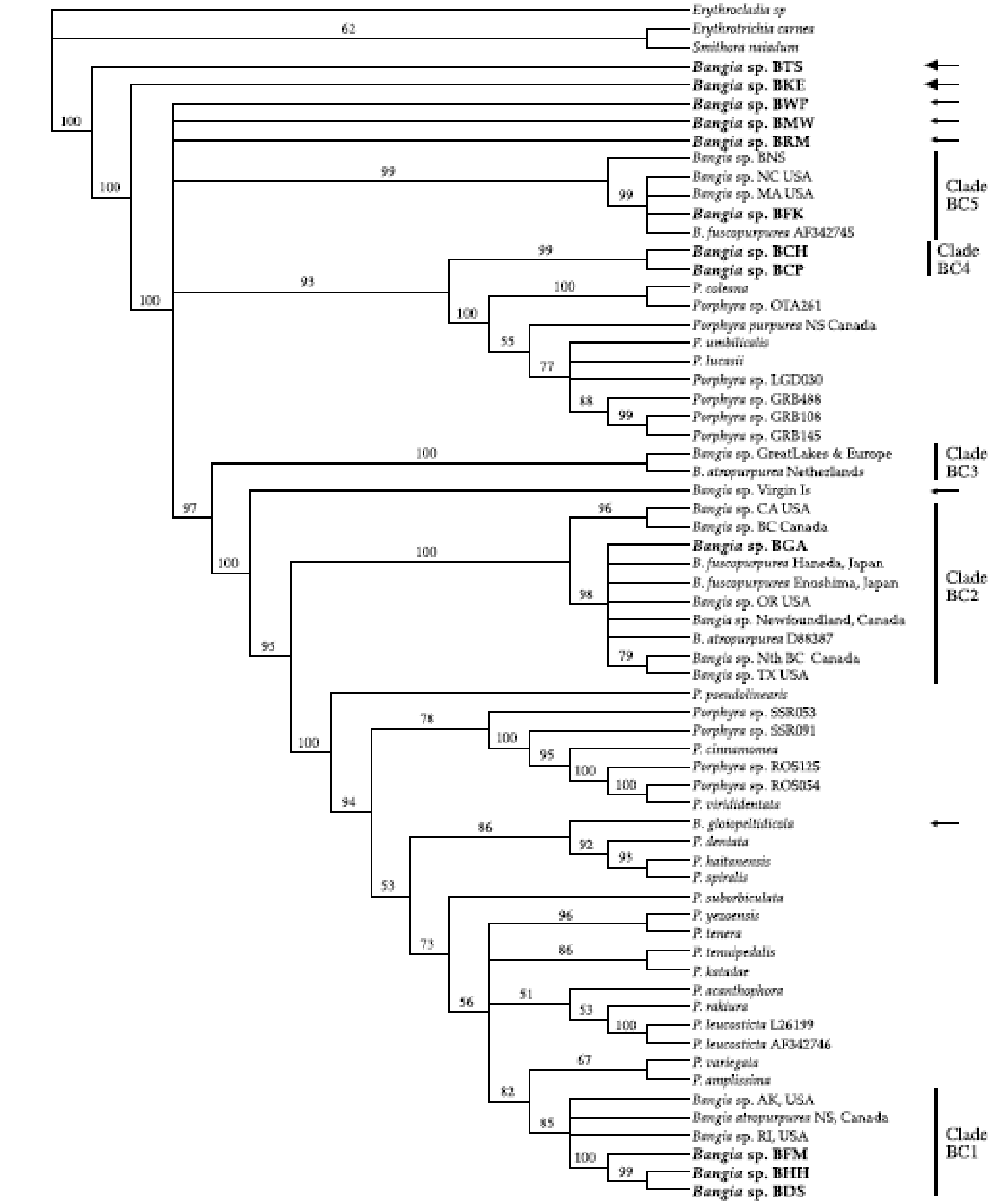

Fig. 2. Phylogenetic tree found under Bayesian analysis. Numbers above the nodes represent the marginal posterior probability of each clade under Bayesian analysis. Sequence and species identification and labelling of clades and taxa are as for Fig. 1.

presumed southern hemisphere origin of the Bangiales

Bangia s.l. – highest phylogenetic diversity in N.Z. coastal habitats

Broom et al., 2004, Mol Phyl Evol

Florideophyceae

five subclasses:

Hildebrandiophycideae
Nemaliophycideae
Corallinophycideae
Ahnfeltiophycideae
Rhodymeniophycideae

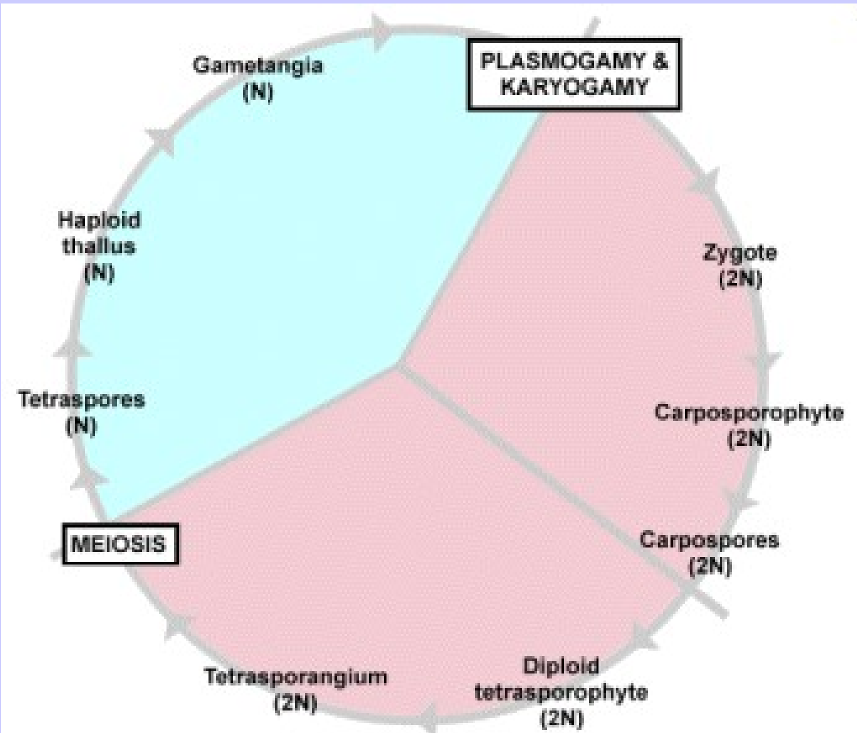

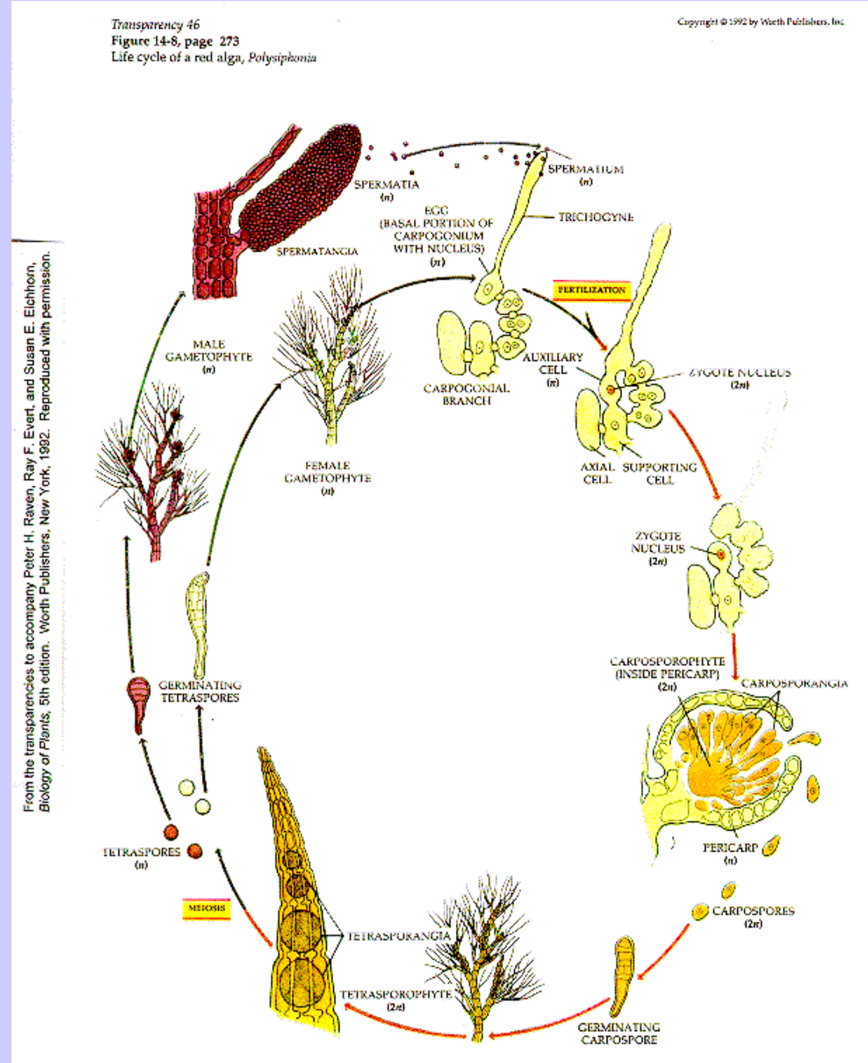

age: fossils – at least 600 mil years [sic], extant genera – up to 350 mil years

so far ca. 9000 species, most of them marine

typical life cycle features: absence of flagellated stages, oogamic sexual process

Taxonomic structure of Florideophyceae

5 subclasses *(current no. species)*:

Hildenbrandiophycidae *(19)*

Ahnfeltiophycidae *(12)*

Nemaliophycidae *(ca 900)*
[selected orders: Batrachospermales, Nemaliales, Thoreales]

Corallinophycidae *(ca 900)*
[selected orders: Corallinales, Sporolithales, Hapalidiales]

Rhodymeniophycidae *(ca 5300)*
[selected orders: Ceramiales, Gelidiales, Gracilariales, Gigartinales, Halymeniales, Plocamiales, Rhodymeniales]

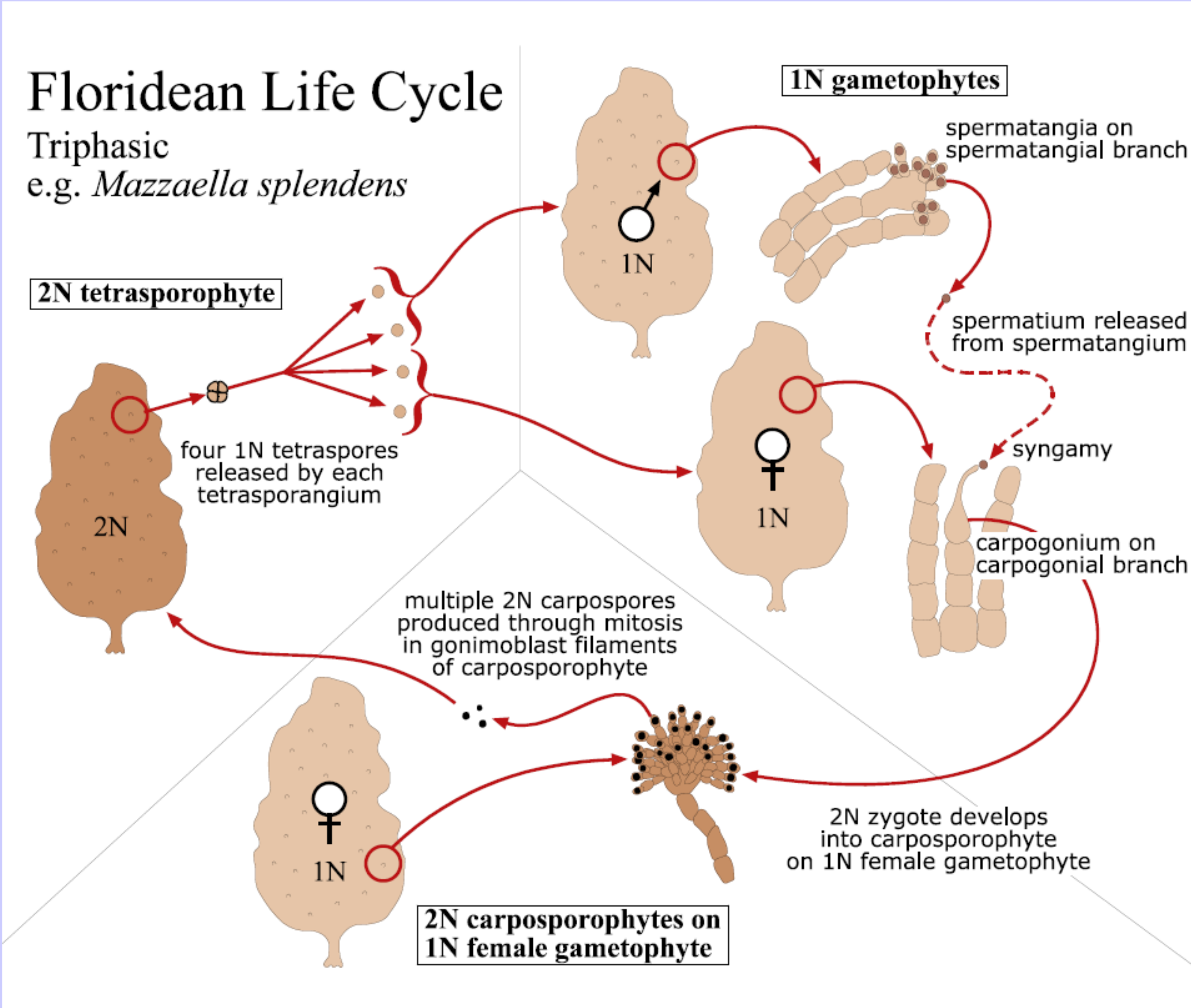
Floridean Life Cycle
Triphasic
e.g. *Mazzaella splendens*
1N gametophytes
spermatangia on spermatangial branch
2N tetrasporophyte
1N
spermatium released from spermatangium
four 1N tetraspores released by each tetrasporangium
2N
syngamy
1N
carpogonium on carpogonial branch
multiple 2N carpospores produced through mitosis in gonimoblast filaments of carposporophyte
2N zygote develops into carposporophyte on 1N female gametophyte
1N
2N carposporophytes on 1N female gametophyte

florideophycean phylogeny

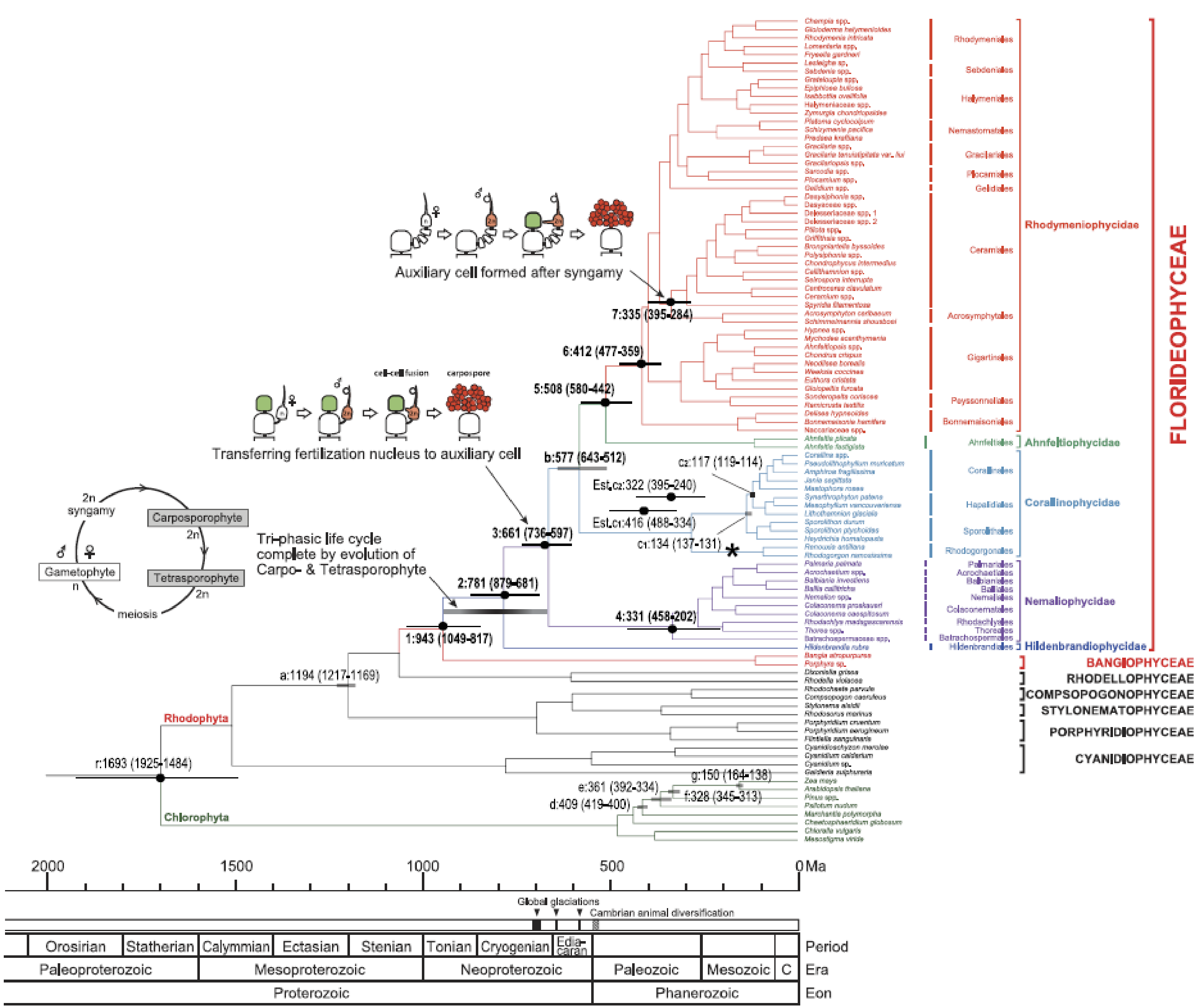

Figure 1. Divergence time and evolution of the Florideophyceae. Estimated times of major divergences based on multigene relaxed clock analysis using the best RAxML tree. Branch lengths are proportional to divergence

- major divergences in this Florideophyceae: emergence of Hildenbrandiophycidae [ca. 781 (681–879) Ma], Nemaliophycidae [ca. 661 (597–736) Ma], Corallinophycidae [ca. 579 (543–617) Ma], and the split of Ahnfeltiophycidae and Rhodymeniophycidae [ca. 508 (442–580) Ma]

- extant diversity seems to reflect largely Phanerozoic diversification

- divergences within Florideophyceae were accompanied by evolutionary changes in the carposporophyte stage, leading to a successful strategy for maximizing spore production from each fertilization event

Yang et al., 2016, Sci Rep

pit connection - primary [and secondary]

pit plugs

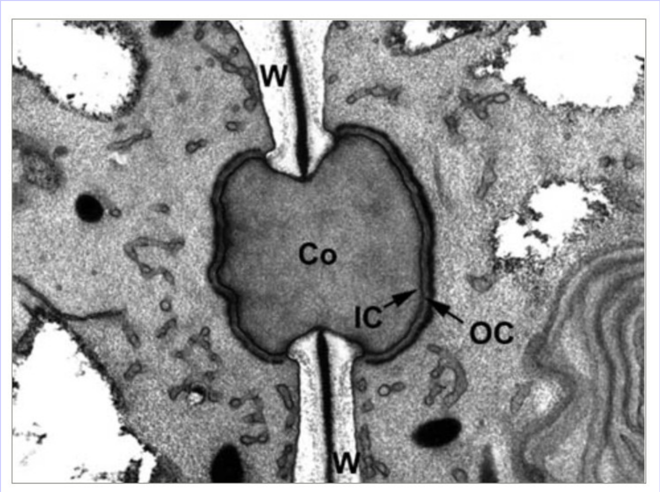

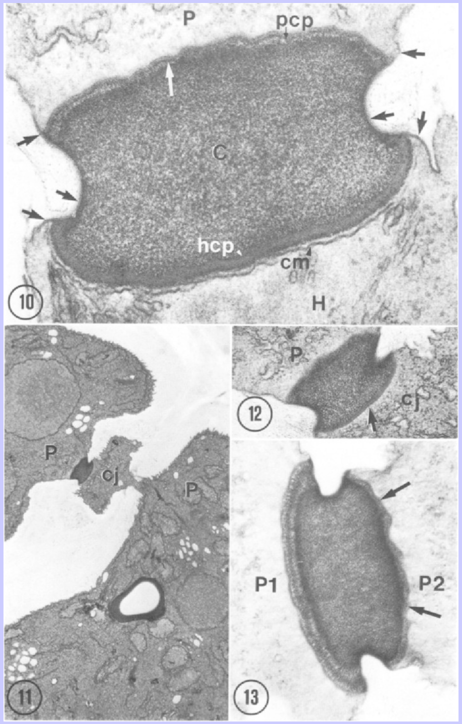

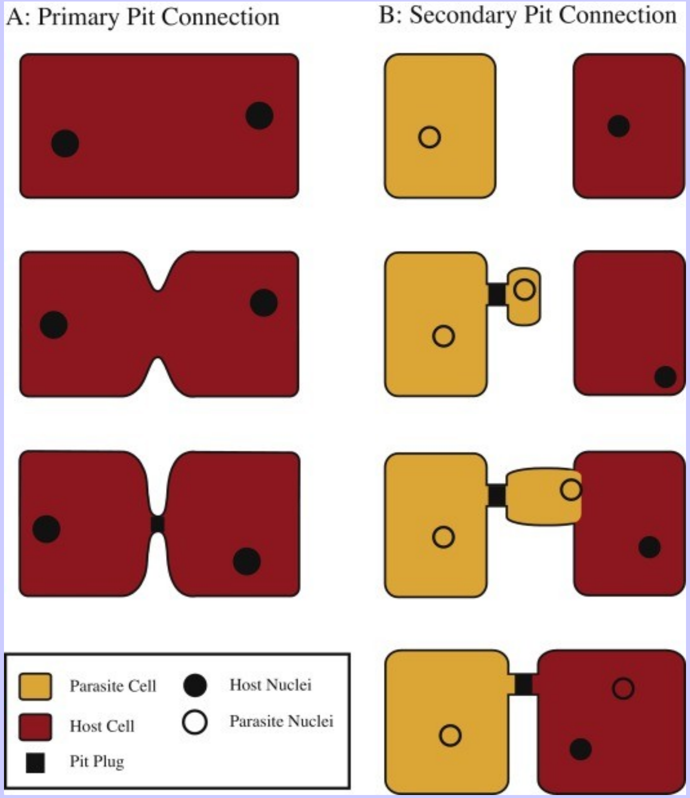

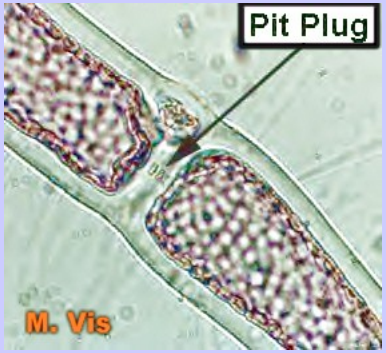

fertilization -

auxiliary cells and
ooblast filaments,

gonimoblasts
carpospores

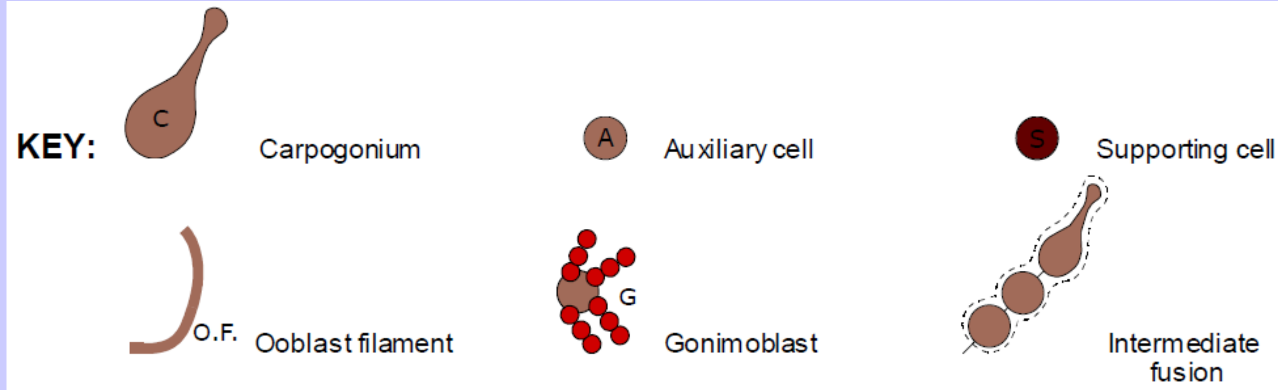

Nemaliophycideae

Order Nemaliales

- gonimoblasts initiated from carpogonium
- usually no auxiliary cell; carpogonium may fuse with nutritive cells *

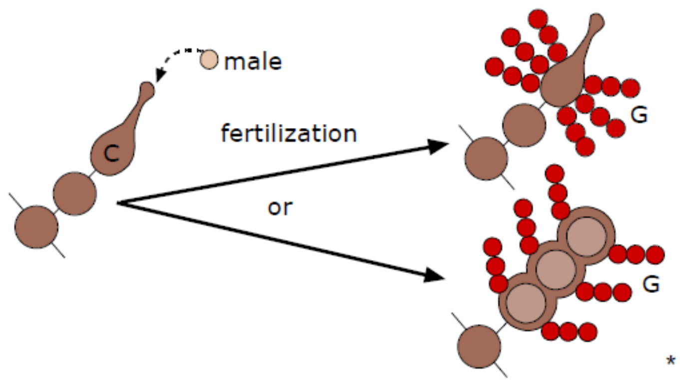

e.g. *Nemalion, Cumagloia*

Corallinophycideae

Order Corallinales

- carpogonial branches in conceptacles
- post-fertilization fusion of cells in carpogonial branch

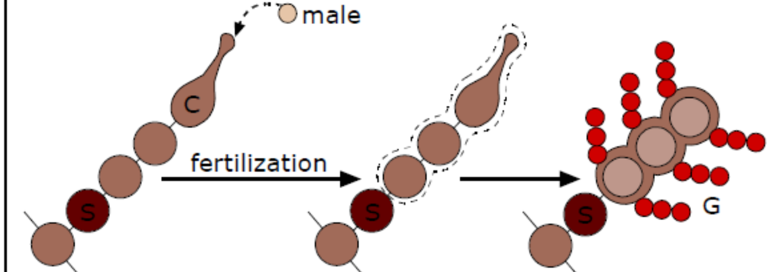

e.g. *Calliarthron, Bosiella*

Order Gigartinales (includes former Cryptonemiales)

- auxiliary cell in various locations—but not as in Rhodymeniales or Ceramiales

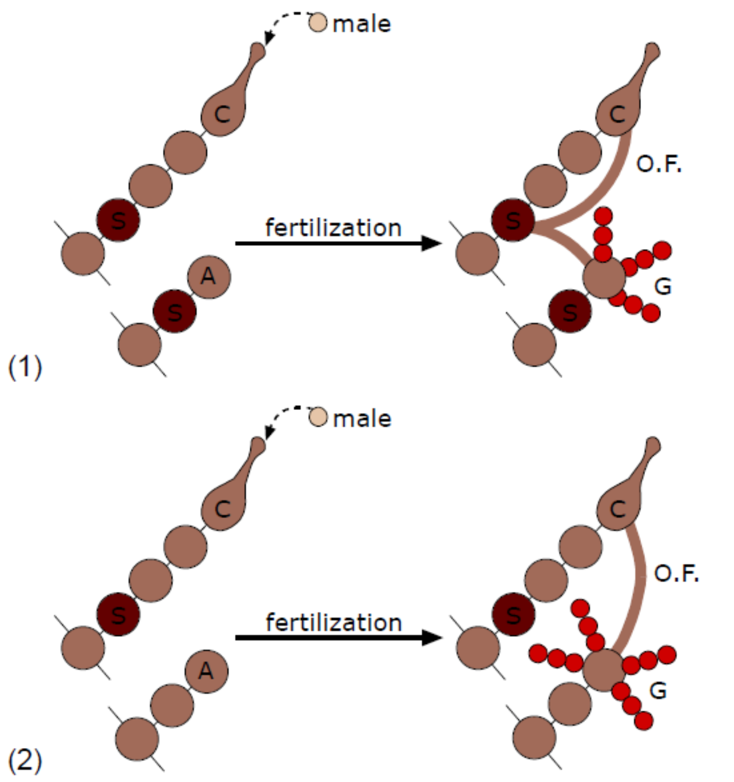

e.g. *Gigartina*

Order Ceramiales ▪ auxiliary cell develops from supporting cell of carpogonial branch <u>after</u> fertiliation (supporting cell is a pericentral cell)	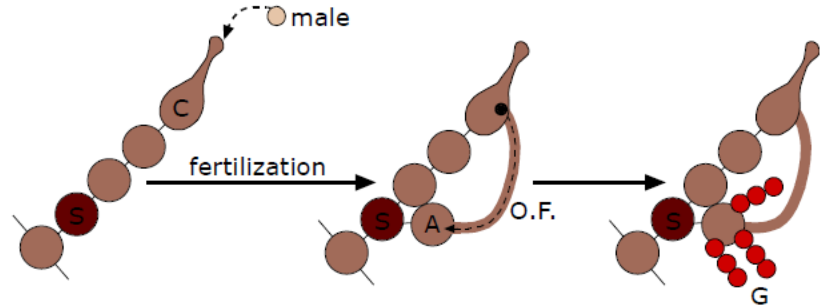 e.g. *Polysiphonia*

Order Rhodymeniales ▪ auxiliary cell filament born on a supporting cell of carpogonial filament ▪ auxiliary cell formed <u>before</u> fertilization ▪ fusion of carpogonium and auxiliary cell to form gonimoblast	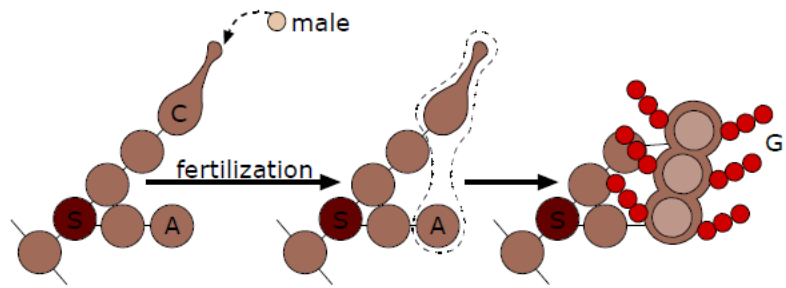 e.g. *Rhodymenia*

Hildenbrandiophycideae

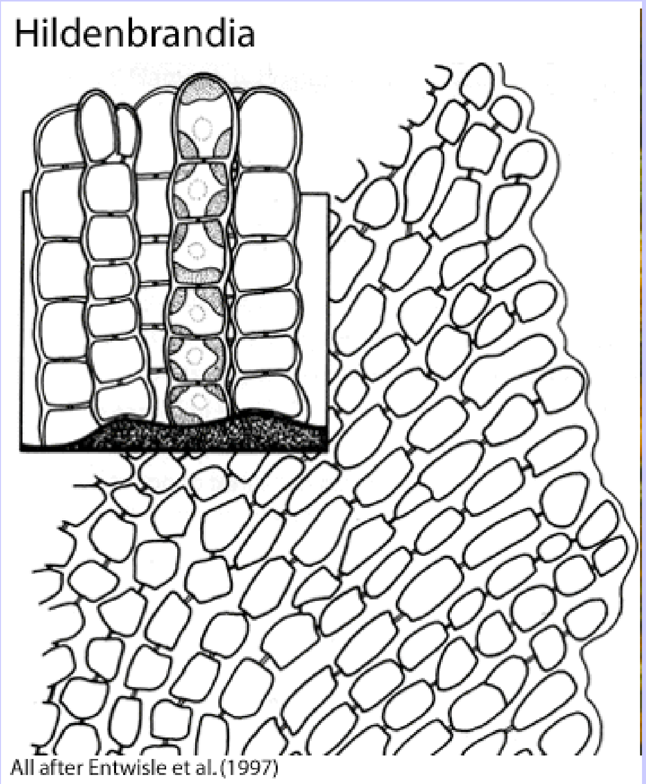

evolutionary radiation – marine habitats - many taxa, possibly just a single invasion into freshwater ecosystems

asexual: tetrasporangia in marine taxa, sexual process *gemmae* in freshwater taxa

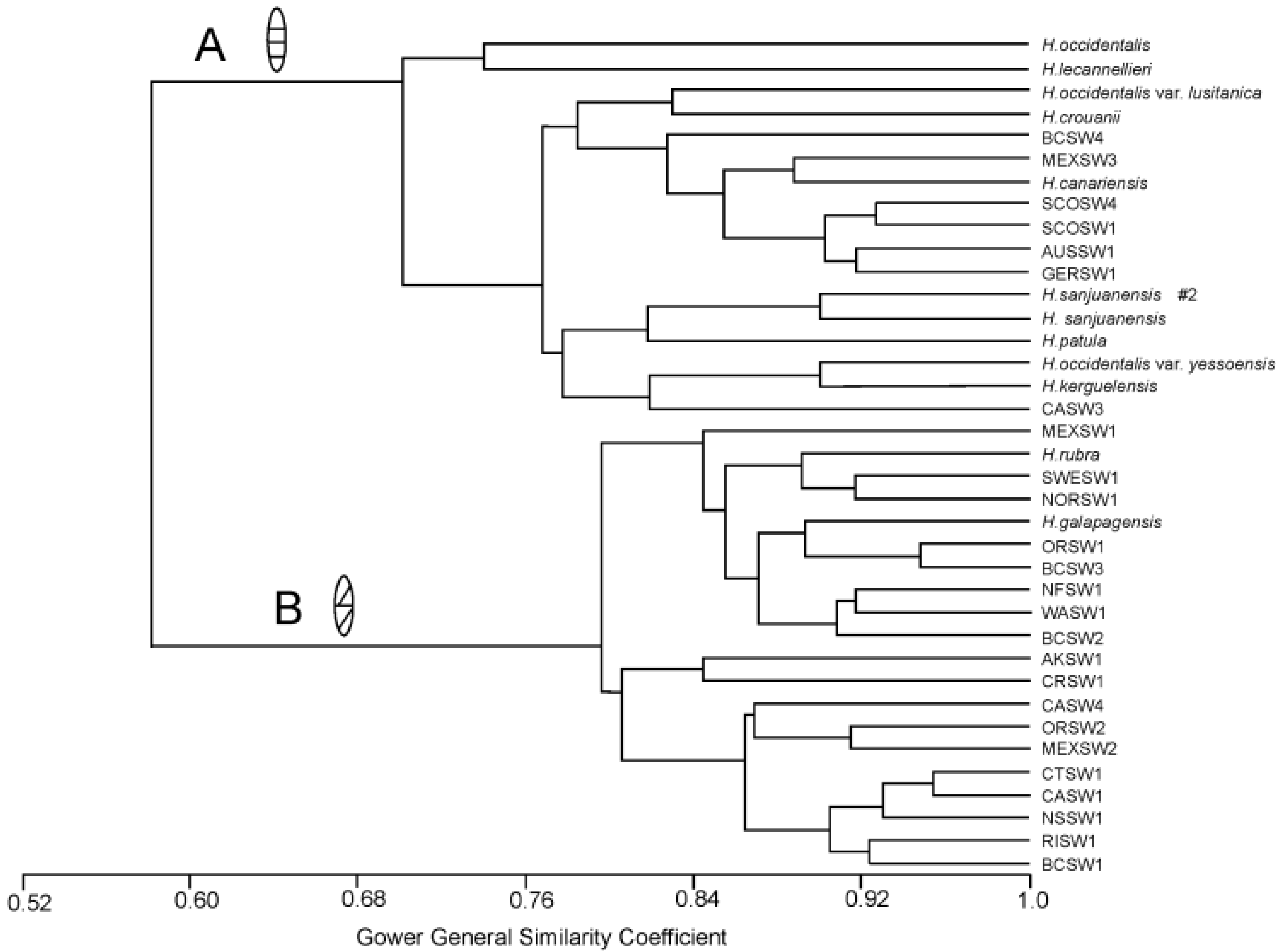

FIG. 1. Cluster dendrogram of all marine specimens (including type and historically significant specimens) for which reproductive character data were available, based on all characters. Two groups are evident, corresponding to specimens with parallel tetrasporangial division pattern (A) and those with nonparallel tetrasporangial divisions (B). The numerical scale indicates the level of similarity at which clusters are formed, according to the Gower similarity coefficient.

Sherwood & Sheath, 2003, J. Phycol. 39: 409–422.

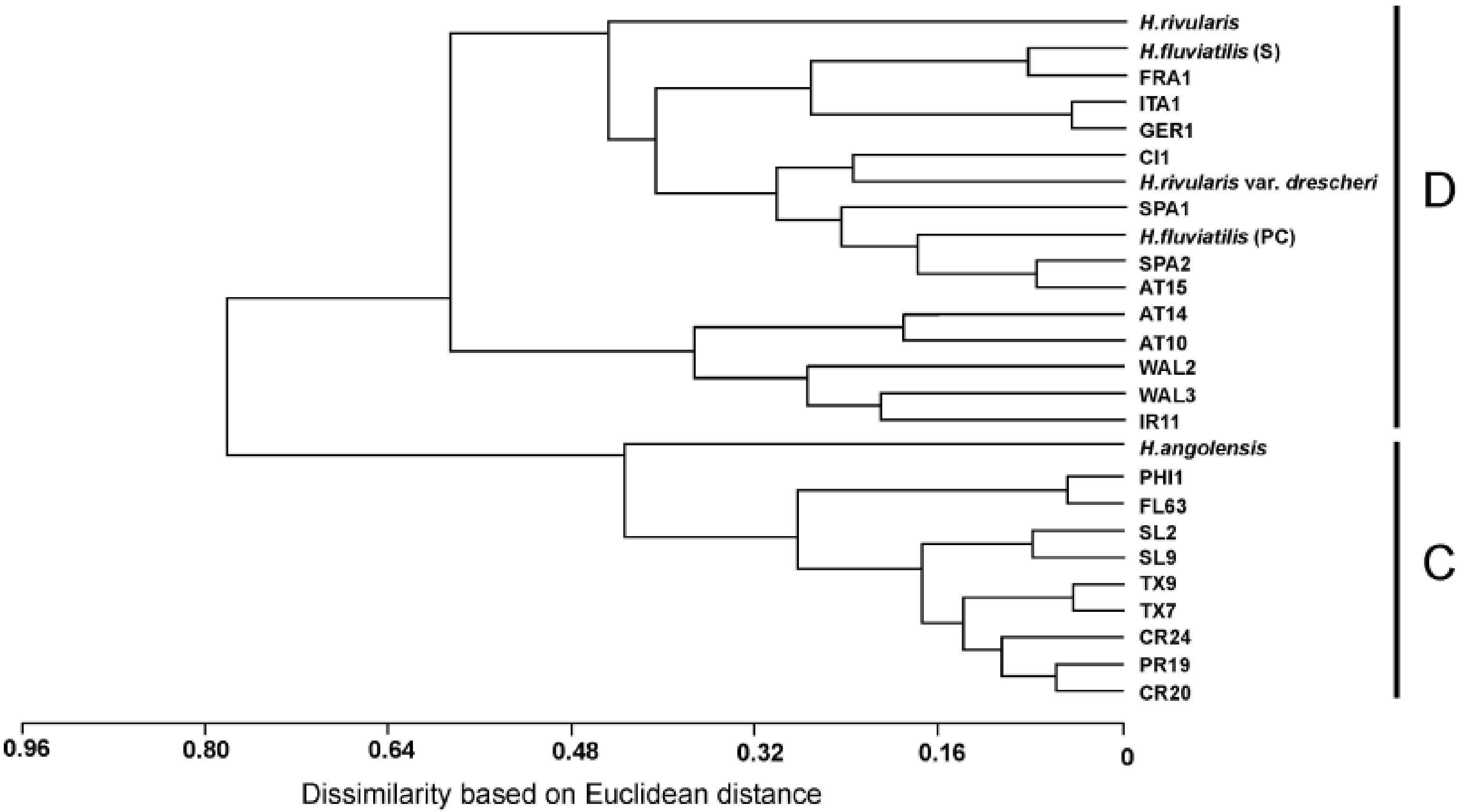

FIG. 2. Cluster dendrogram of all freshwater specimens (including type specimens and historically significant specimens). Two groups are evident, corresponding to those specimens from North America/Philippines (C) and Europe/Canary Islands (D). The numerical scale indicates the level of dissimilarity based on Euclidean distances.


Foto: Yvonne N.

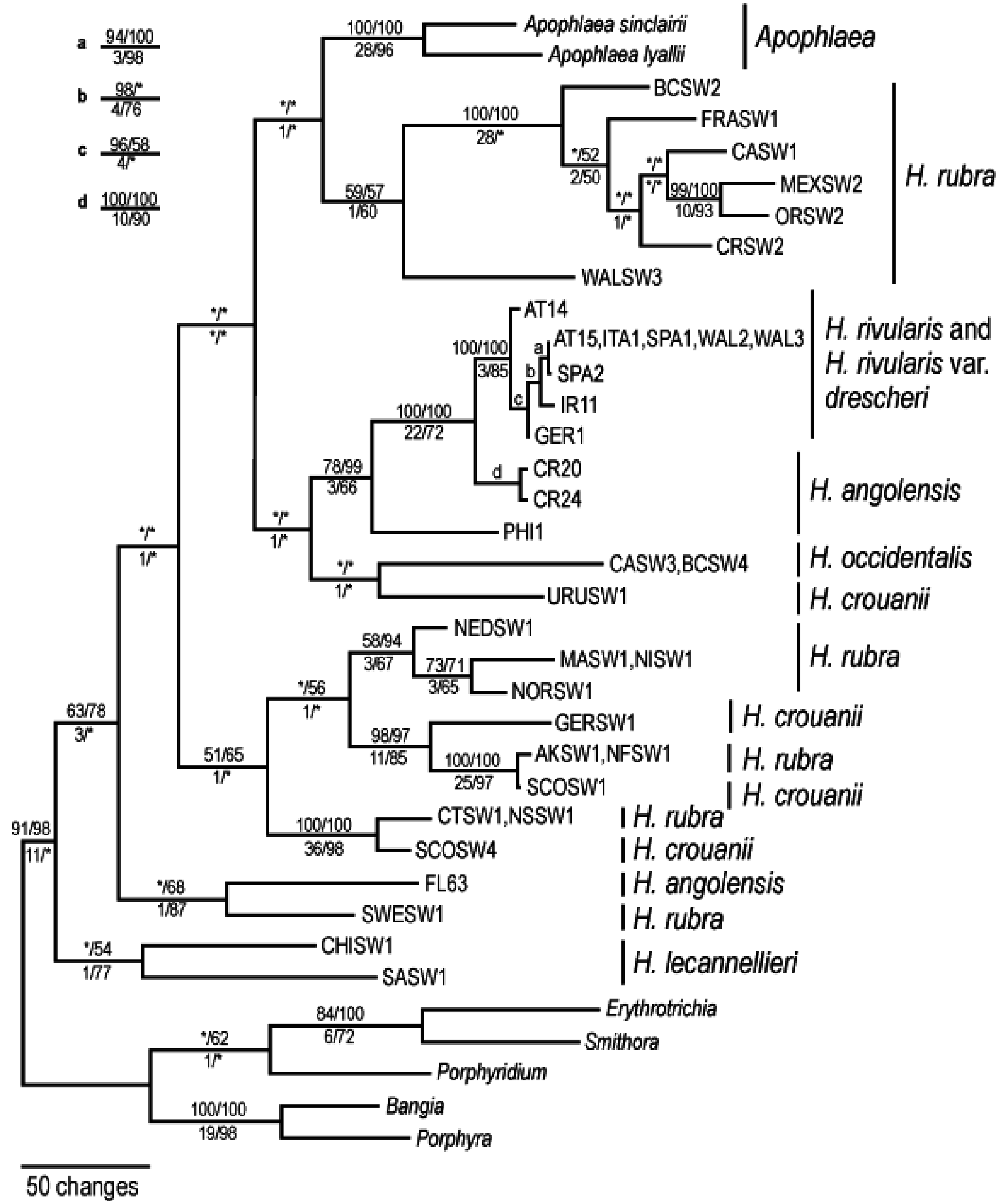

FIG. 4. The single most-parsimonious tree (showing branch lengths) generated by parsimony analysis of the *rbc*L gene for representatives of the Hildenbrandiales. Support measures are included for all forms of phylogenetic analysis (MP, NJ, and QP), where appropriate, as follows: MP bootstrap values above branch and left of slash, decay values below branch and left of slash, NJ bootstrap values above branch and right of slash, QP values below branch and right of slash. Some sets of support values are indicated on the tree as a letter, and corresponding values are shown to the upper left of the diagram. Asterisks indicate a lack of support at that node for the corresponding measure.

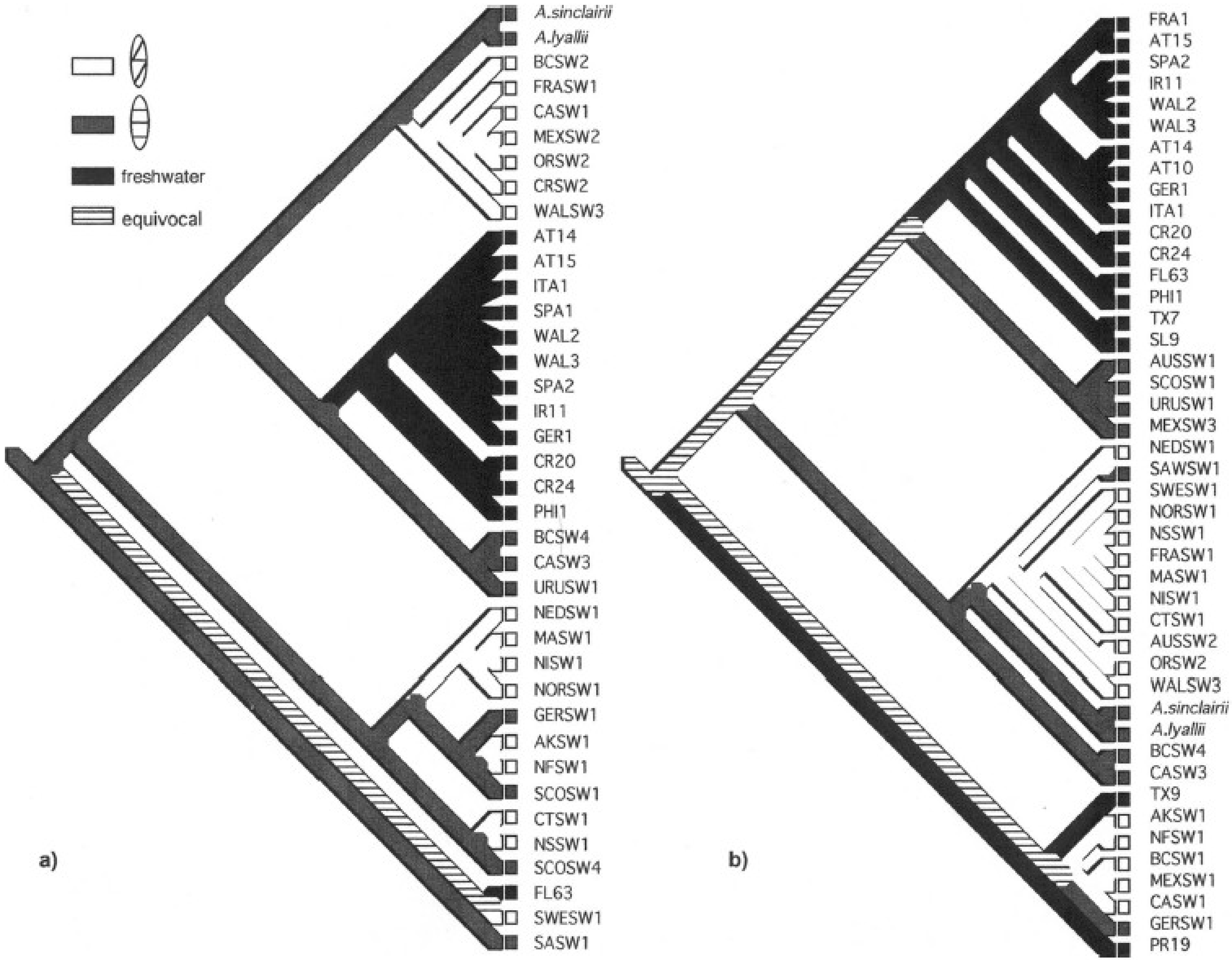

FIG. 5. (a) Cladogram based on the 18S rRNA gene for representatives of the Hildenbrandiales with tetrasporangial morphology mapped on the topology of one of the four most-parsimonious trees. (b) Cladogram based on the *rbc*L gene for representatives of the Hildenbrandiales with tetrasporangial morphology mapped on the topology of the single most parsimonious tree.

Sherwood & Sheath, 2003, J. Phycol. 39: 409–422.

Nemaliophycidae

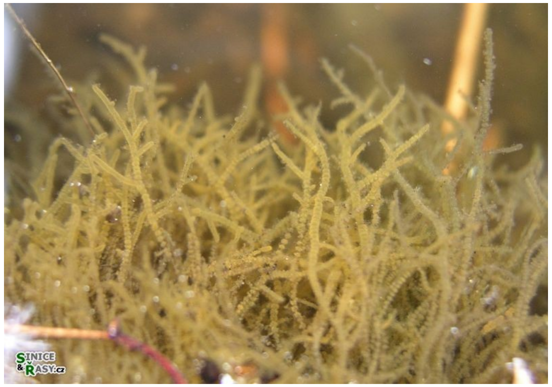

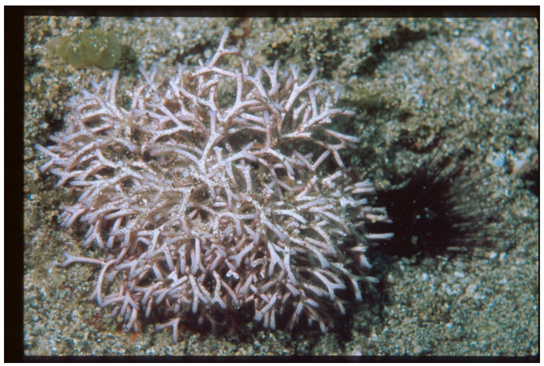

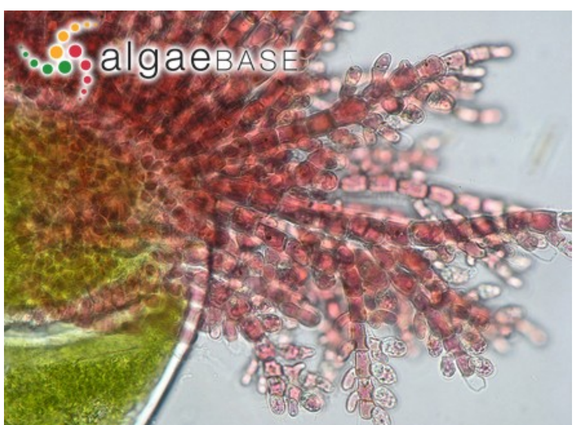

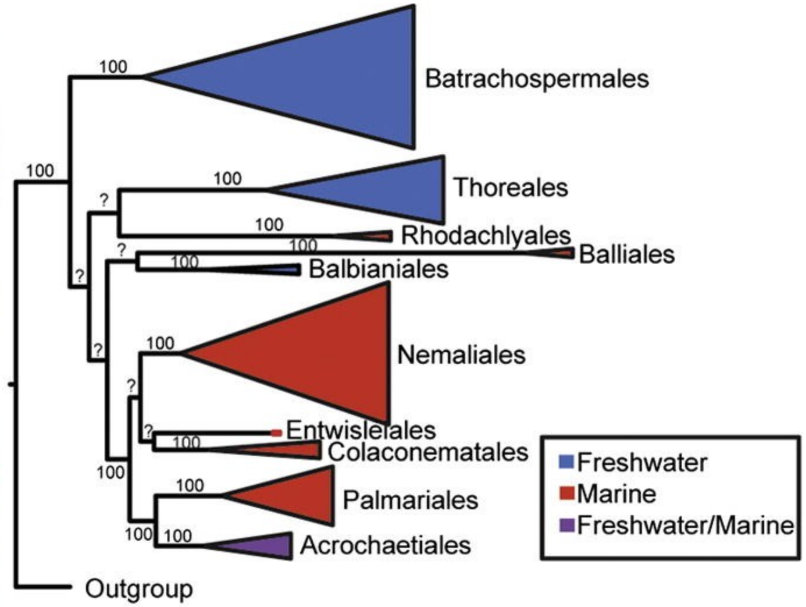

most freshwater red algae belong to this lineage

Lam et al., 2016, Mol. Phyl. Evol.
algaebase.org
sinicearasy.cz

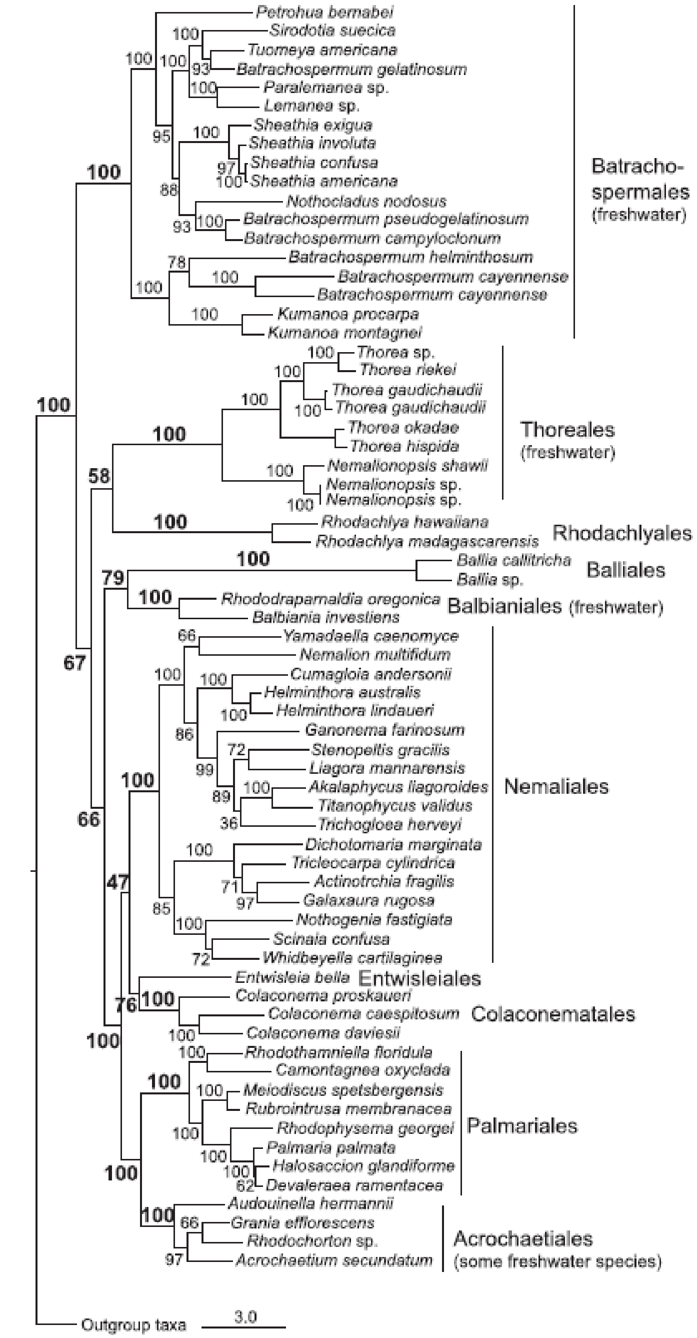

Fig. 1. ML tree (ln −209655.052203) with outgroups pruned for presentation. Numbers on branches are bootstrap support values. Values in bold are those for order monophyly and relationships among orders. Orders that are strictly freshwater or have a few freshwater species are noted; all other orders are marine.

Lam et al., 2015, Mol Phyl Evol

Acrochaetiales

Acrochaetium
stellate rhodoplasts, epiphytes, in coastal areas

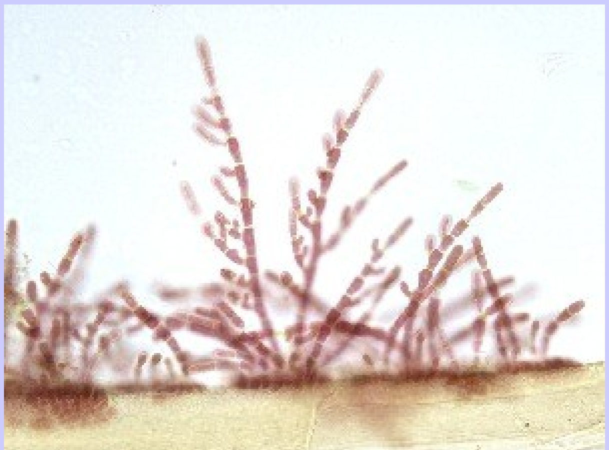

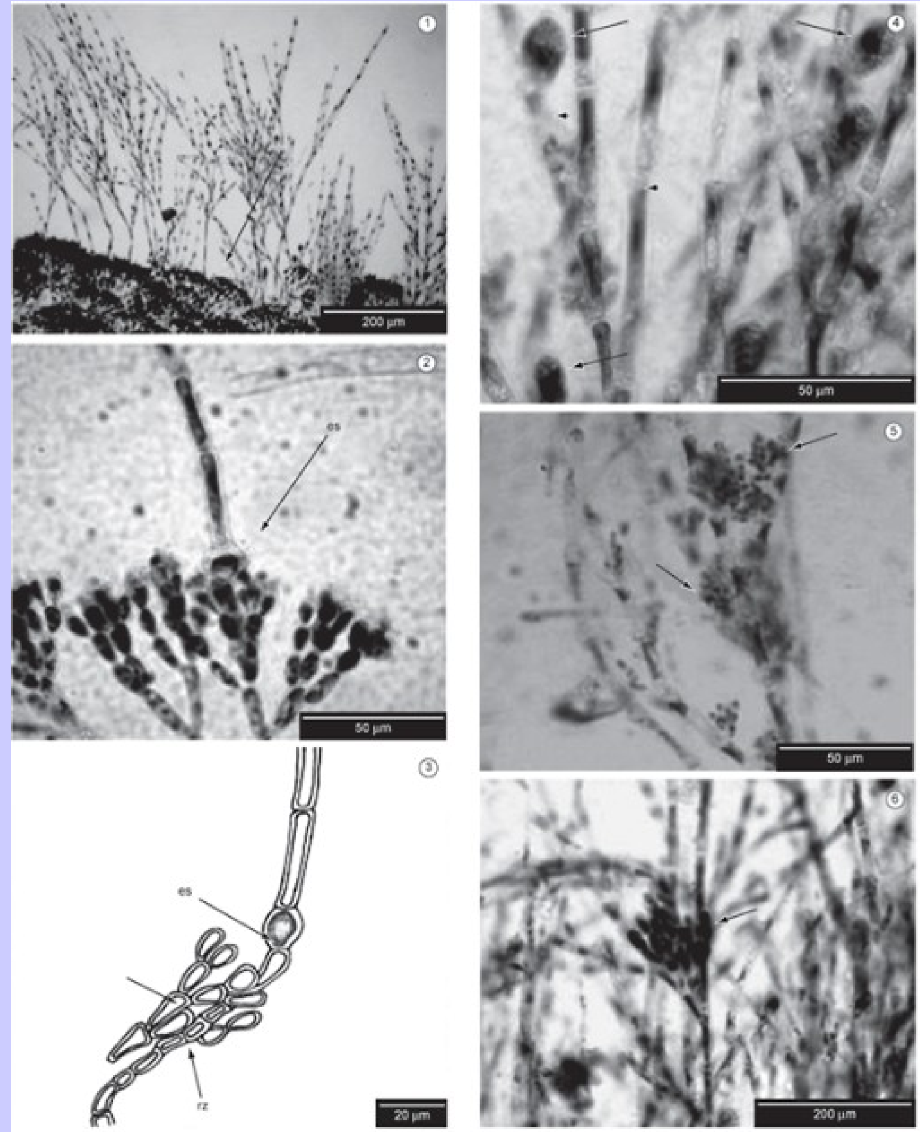

Figuras 1 -6. *Acrochaetium corymbiferum*: 1) aspecto geral do talo crescendo sobre *Liagora valida* (seta); 2) esporo persistente na região basal (es); 3) ilustração do esporo persistente na região basal do filamento (es) com rizóide (rz) penetrando na alga hospedeira(seta); 4)detalhe dos filamentos(cabeça de seta)com monosporângios (setas); 5) filamentos com espermatângios (setas); e 6) filamento com grupo de carposporângios (seta) organizados em forma corimbosa.

Figures 1-6. *Acrochaetium corymbiferum*: 1) plant over *Liagora valida* (arrow); 2) persistent spore in the basal region of the filament; 3) spore in basal region (es) with rhizoids (rz) penetrating into the host algae (arrow); 4) detail of the filaments (arrow head) with monosporangia (arrow); 5) filaments with spermatangia (arrow); and 6) filaments with carposporangia group (arrow) in corymbose shape.

Palmaria

epiphytic (e.g. on kelp macroalgae) or epilithic, cold seas, palmate thallus

algaebase.org

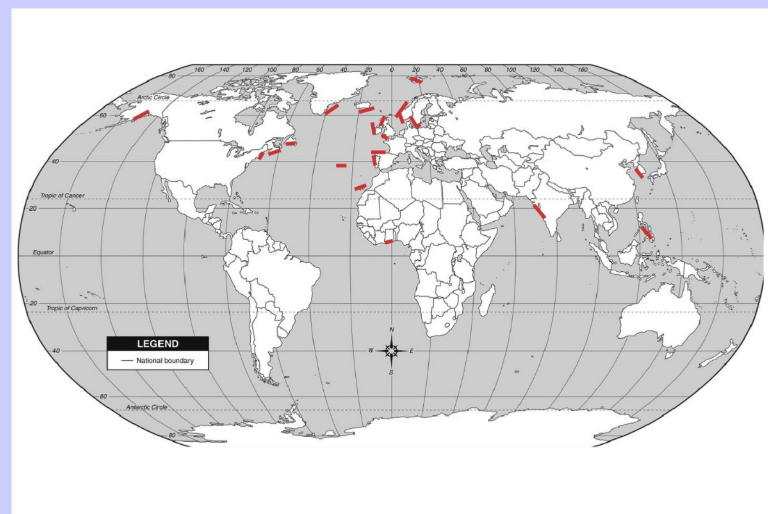

P. palmata

Audouinella (= Chantransia)

numerous discoid plastids

relatively tolerant to pollution
(e.g. Vltava river in Prague)

typical monosporangia – monospores
(and sexual process)

freshwater taxa, but also sporophyte stages of the genera Batrachospermum and Lemanea

Rhodochorton

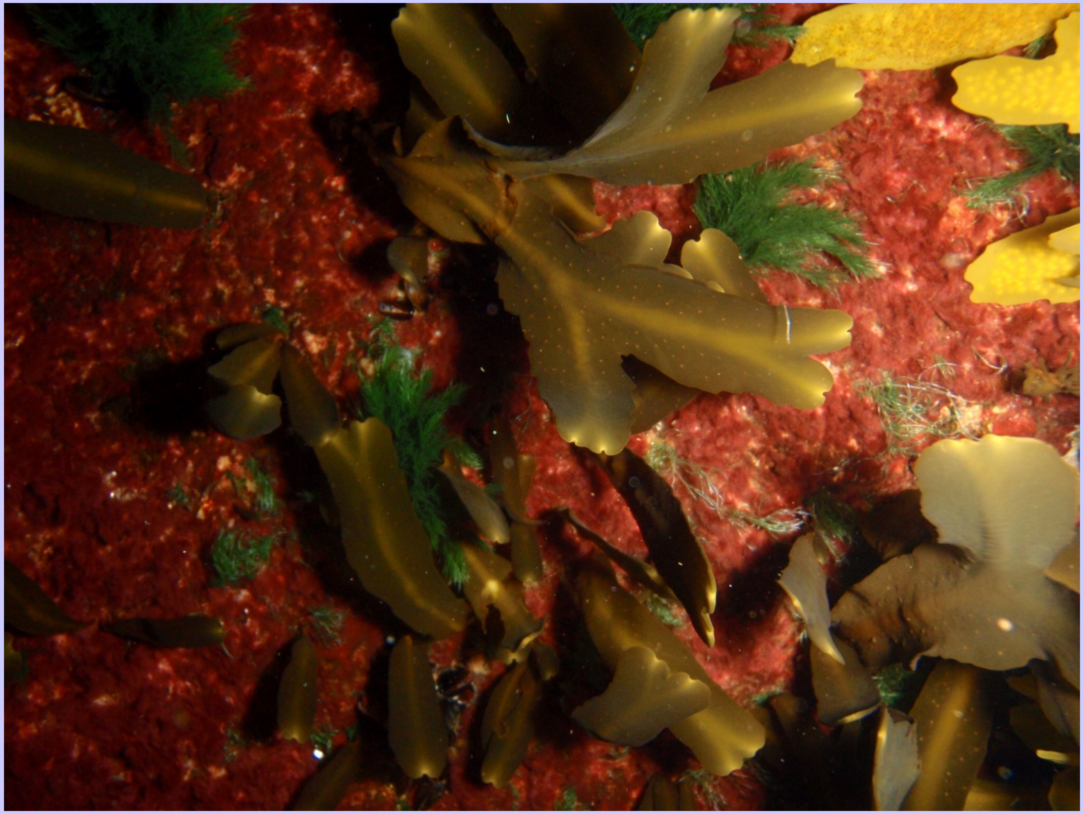

R. purpureum beneath F. serratus in the Baltic proper

Batrachospermales – a major freshwater florideophyte lineage

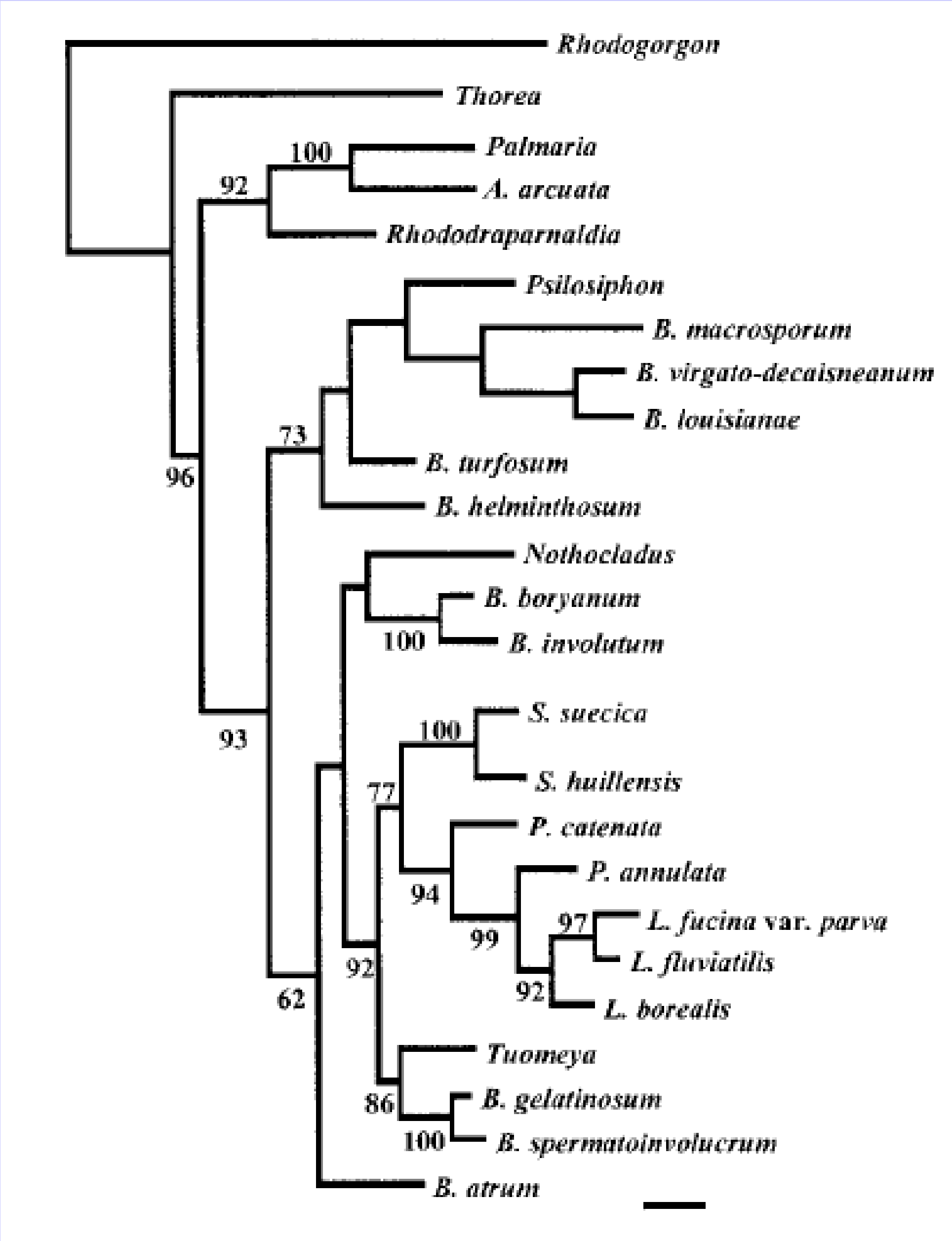

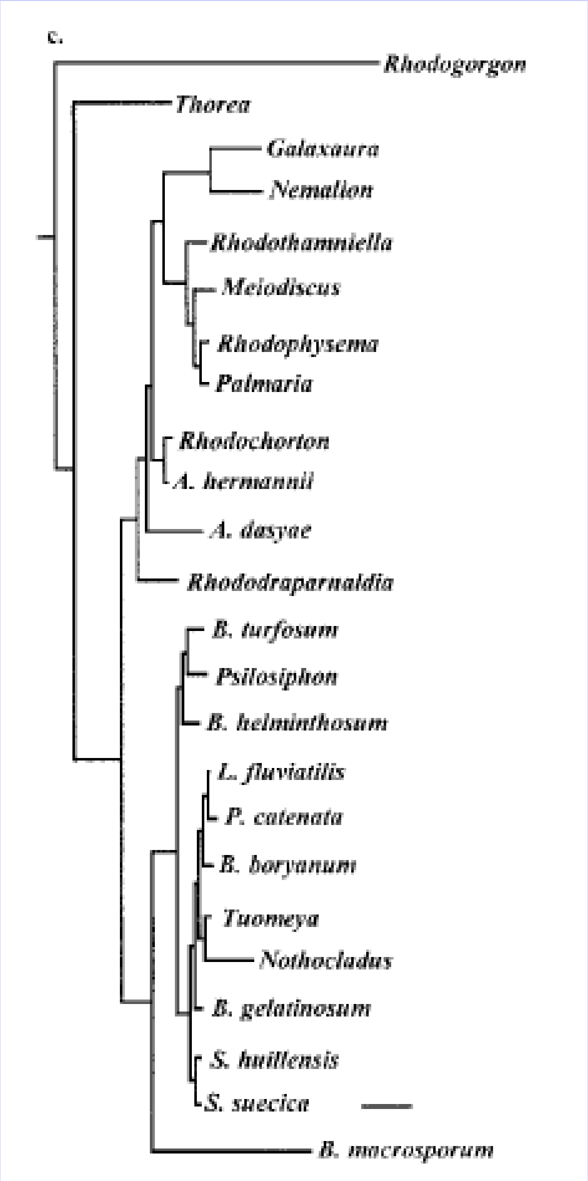

SSU, ML tree – monophyly of the order

Vis et al., 1998, J Phycol 34: 341–350 SSU+rbcL origin of *Lemanea*-like morphologies from *Batrachospermum*-like ancestors

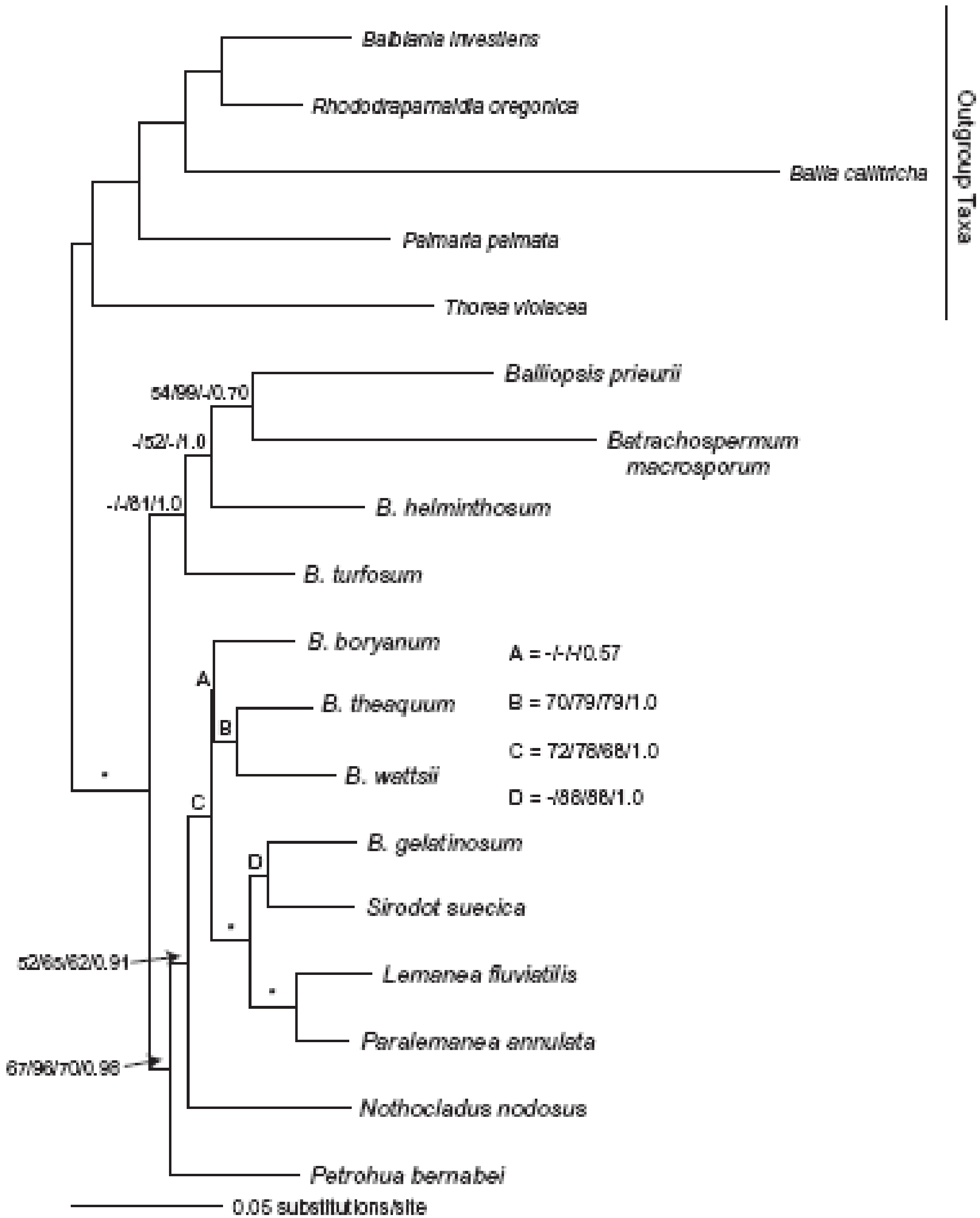

Fig 1. Maximum likelihood (ML) (–*ln* likelihood = 19 251.89892) topology for analyses of the combined data. Support values are presented as follows: maximum parsimony (MP) bootstrap/minimum evolution (ME) bootstrap/ML bootstrap/Bayesian posterior probabilities. * = 100% bootstrap support or 1.0 probability with all analysis methods. – = <50% bootstrap support or <0.50 probability.

Vis et al., 2007, Phycol Res 55: 103-112.

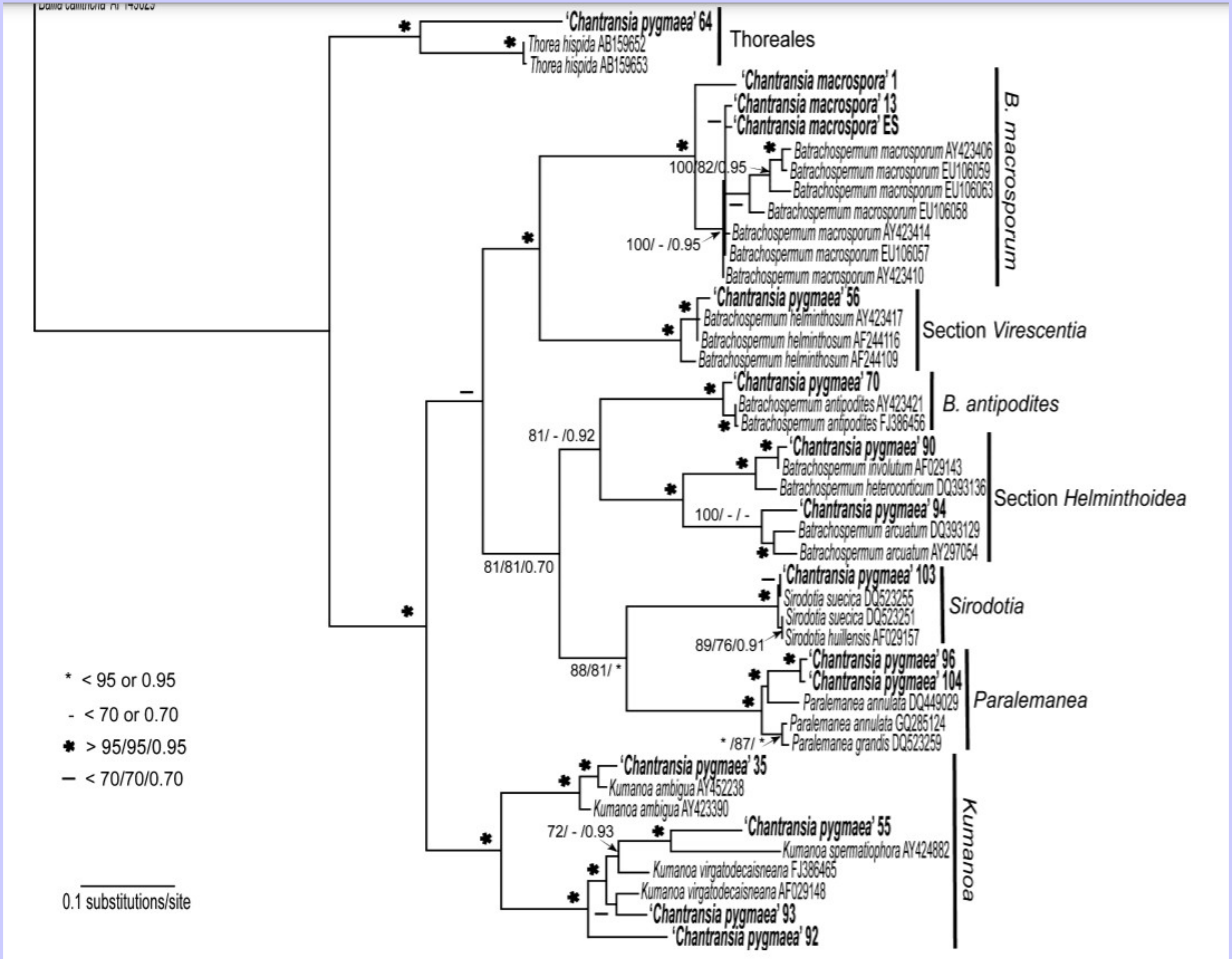

FIG. 1. Maximum-likelihood (ML) *rbc*L tree (−ln *L* likelihood = 9300.5723) showing the relationships of the "Chantransia" stage samples sequenced in this study (larger and boldface) to previously sequenced taxa of Batrachospermales and Thoreales. Support values for all analyses are shown on the branches as follows: maximum-parsimony bootstrap/ML bootstrap/Bayesian posterior probabilities.

sporophyte stages in Batrachospermales and Thoreales

Necchi jr, Oliveira, 2012, J. Phycol.

Batrachospermum

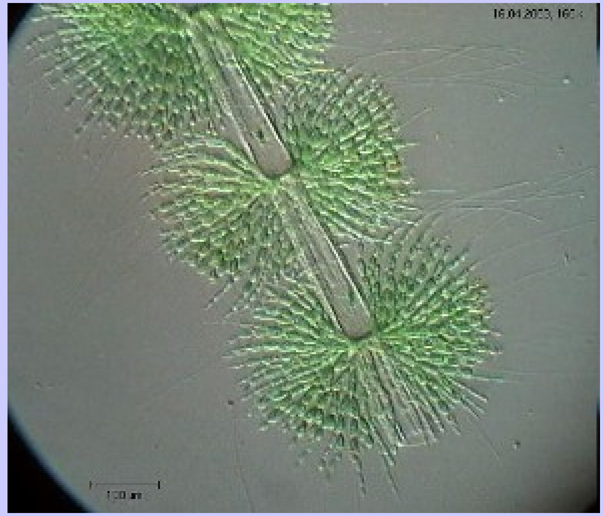

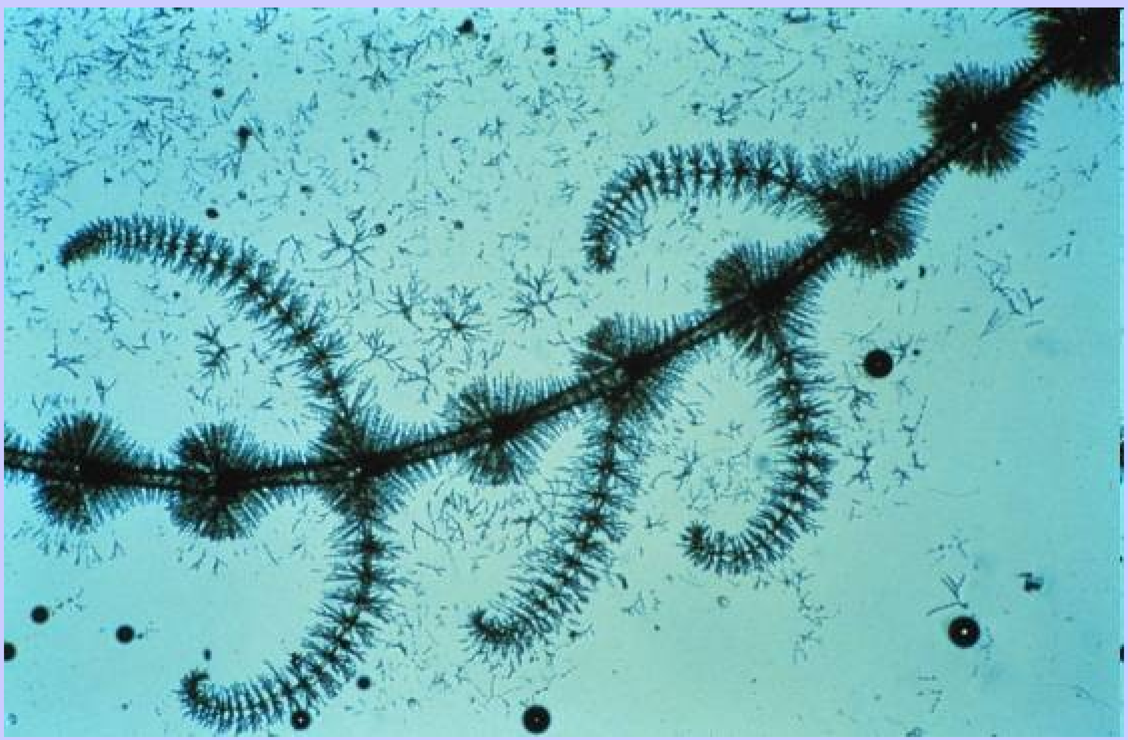

Life history of *Batrachospermum*. The macroscopic gametophyte produces male reproductive cells, spermatangia, and/or female reproductive structures, carpogonia. A spermatium fertilizes the carpogonium by attaching to the trichogyne. Following fertilization, a carposporophyte develops from the carpogonium. The carposporophyte produces carpospores, which germinate into the microscopic, filamentous chantransia. Vegetative meiosis occurs in the apical portions of the chantransia filaments, and a new haploid gametophyte is produced.
(Adapted from http://www.pmf.unsa.ba/biologija/talofiti/rhodophyta4.jpg.)

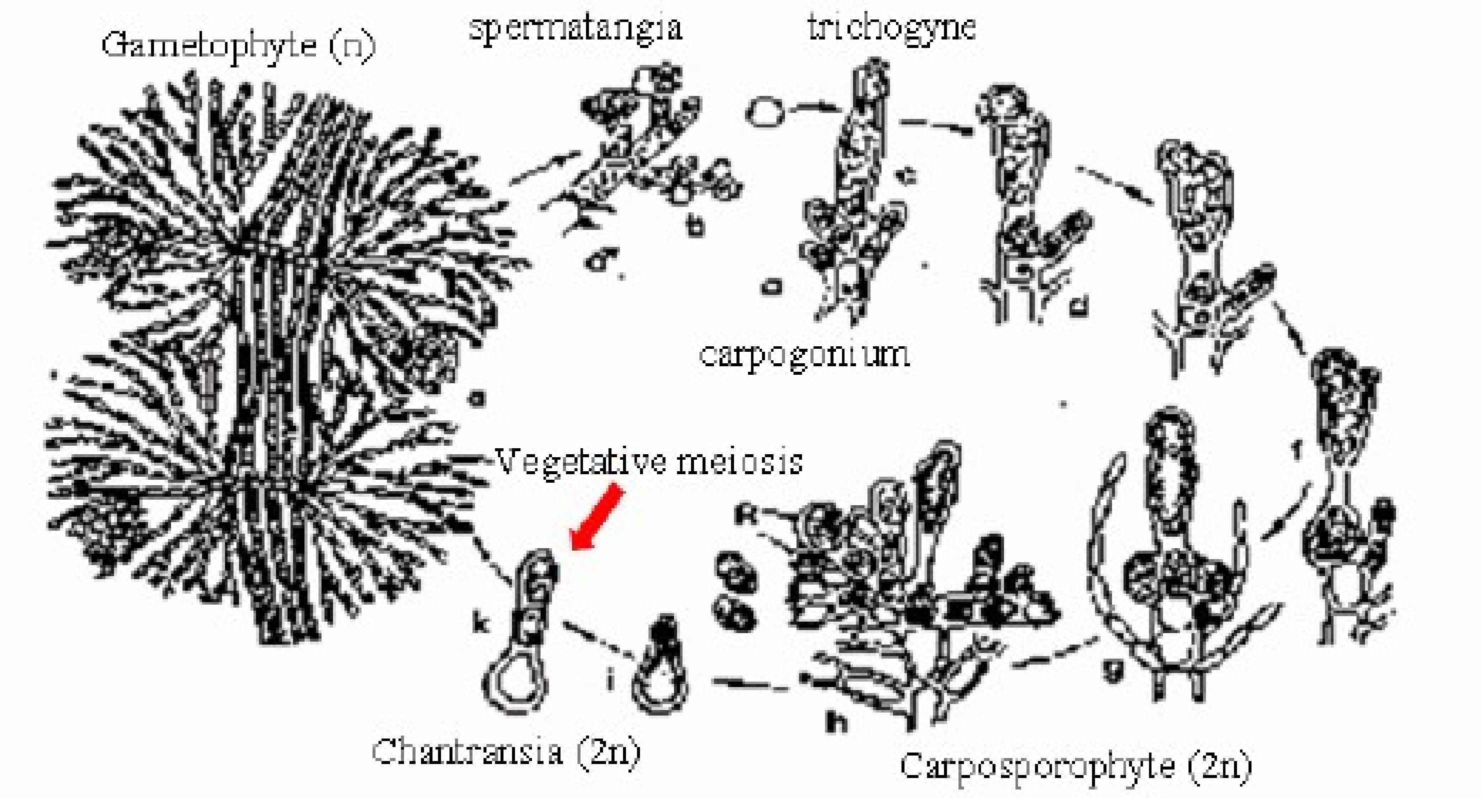

Stewart, 2006

Schematic diagram of *Batrachospermum* gametophyte thallus: A. Whorl composed of vegetative fascicle branches. B. Axial cell. C. Carposporophyte. D. Detail of carposporophyte showing carposporangia (arrowheads) on gonimoblast filaments (double arrowhead). E. Carpogonium with magnified detail showing carpogonial branch (arrowhead), carpogonium (double arrowhead), trichogyne with attached spermatium (large arrowhead) and involucral filaments (double large arrowhead). F. Spermatangia at the tips of fascicle branches (arrowheads). G. Detail of axial cell with cortical cells (arrowhead), proximal cells (double arrowheads) and pericentral cells (large arrow).

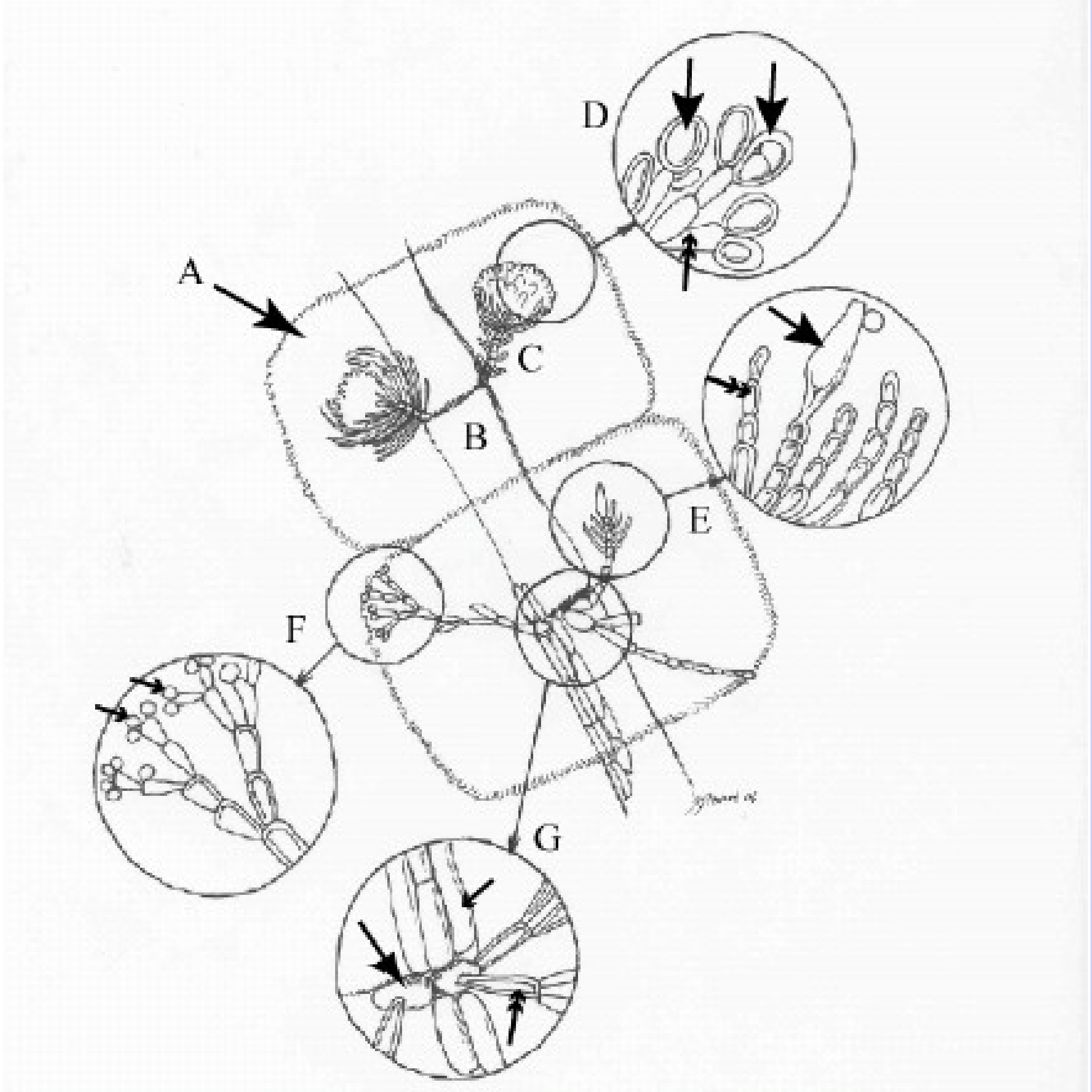

Stewart, 2006

Salient features of *Batrachospermum* species investigated: A. *B. pseudogelatinosum* (NZ1), axial cells and fascicle whorls with prominent, globose carposporophytes (arrowhead). Scale bar = 120 µm. B. *B. pseudogelatinosum* (NZ1) trichogyne, showing a variant that resembles *B. gelatinosum*. Scale bar = 8 µm. C. *B. campyloclonum* (NZ150), showing fascicle whorl with large, globose carposporophytes. Scale bar = 150 µm. D. *B. campyloclonum* clavate trichogyne. Scale bar = 7µm. E. *B. kraftii* (NZ7) showing characteristic scimitar-shaped trichogyne. Scale bar = 9 µm. F. *B. bourrellyi* (TJE3280) showing contorted or bent trichogyne. Scale bar = 10 µm. G. *B. theaquum* (TJE3050a) showing elongate, club-shaped trichogyne. Scale bar = 12 µm.

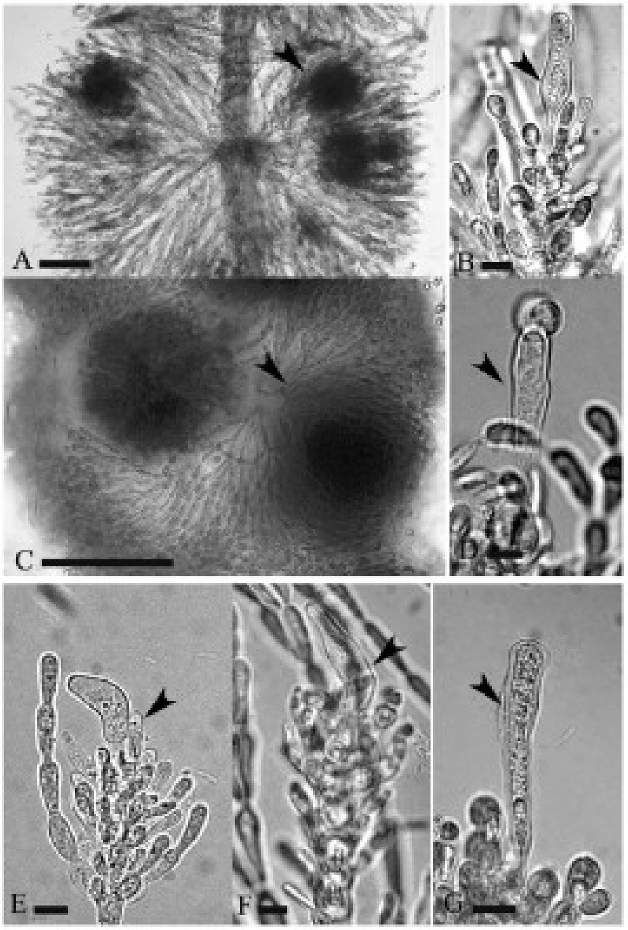

Stewart, 2006

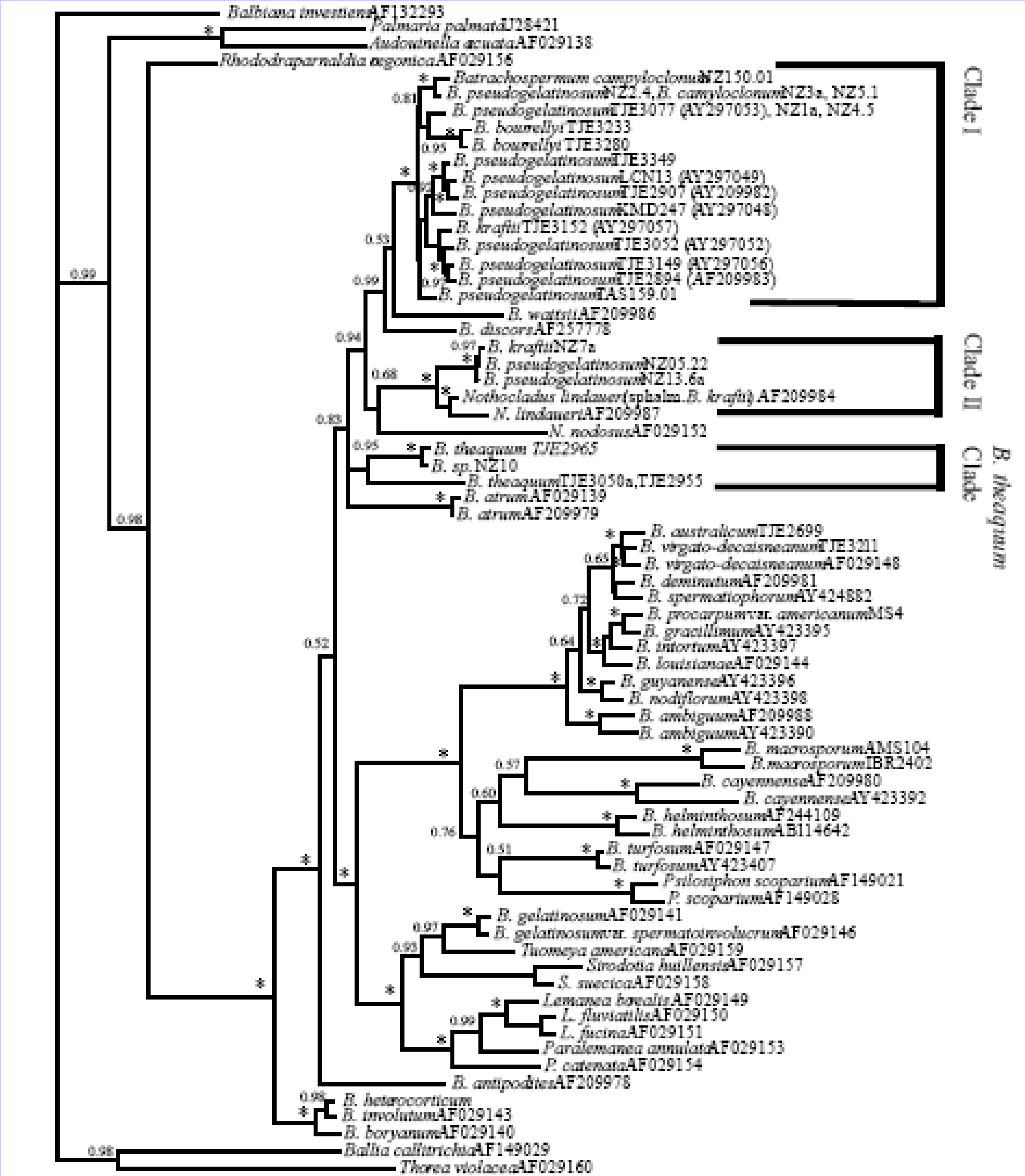

complicated species concepts in Batrachospermum...

rbcL, Bayesian tree

Stewart, 2006

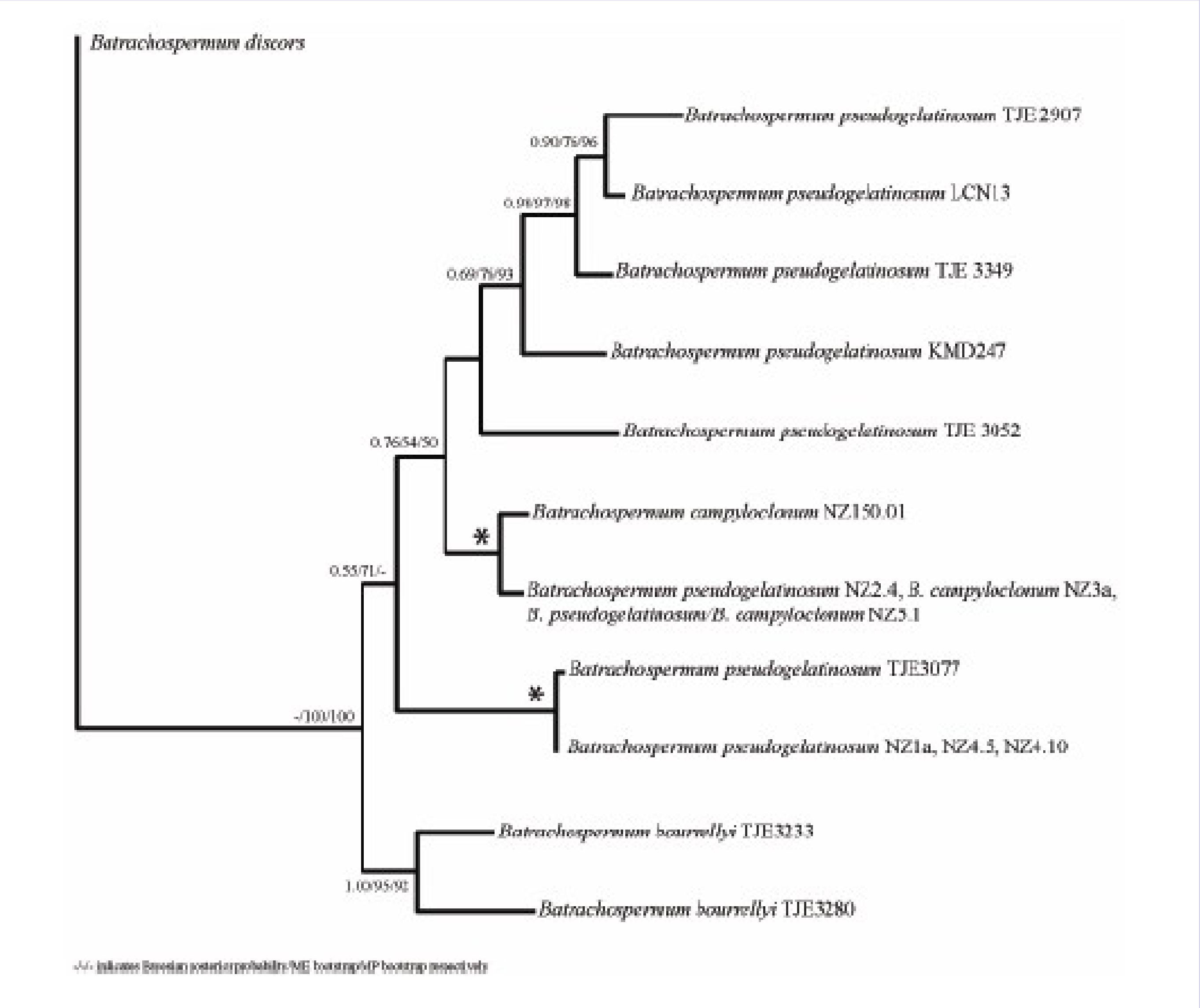

cox2-3 strom, AU-NZ taxa

Stewart, 2006

B. macrosporum

infraspecific differentiation on a continental scale

FIG. 1. Map of North and South America showing the sampling locations of *Batrachospermum macrosporum*. For more details regarding locations and abbreviations see Table S1 in the supplementary material.

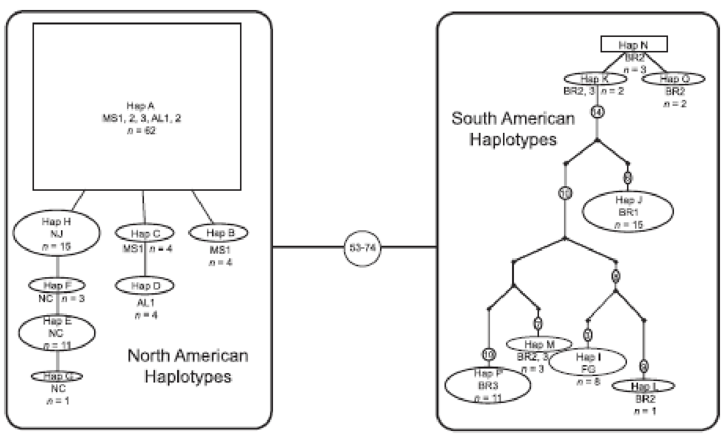

FIG. 2. Minimum spanning networks of *Batrachospermum macrosporum cox2-3* spacer haplotypes from North and South America. *n* = sample numbers. A single line indicates one mutational step, filled circles represent missing intermediates, and circles with numbers specify multiple intermediate steps. The rectangle around haplotypes A and N signifies these as the most probable outgroups calculated using the TCS software. Haplotype and location designations as given in Table S1 (see the supplementary material).

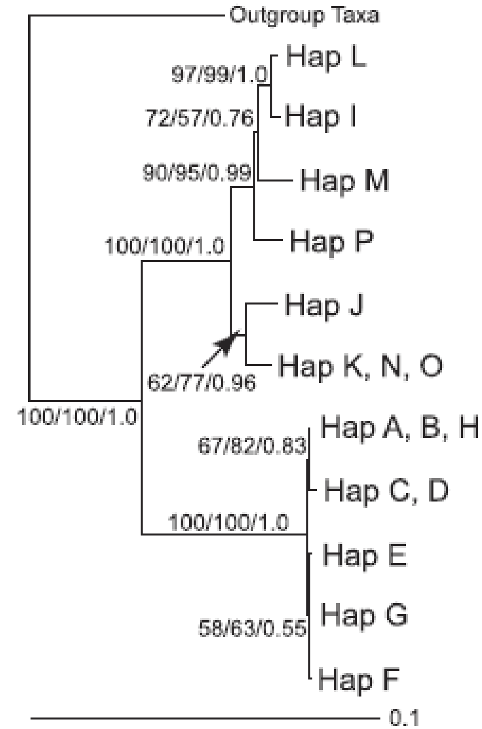

FIG. 3. Tree from ML (–Ln 7801.18755) analysis of *rbc*L gene sequence data showing the relationship among *Batrachospermum macrosporum* haplotypes. Haplotype designations as given in Table S1 (see the supplementary material). Support values for all analyses are shown as follows: MP bootstrap/ME bootstrap/Bayesian posterior probabilities.

larger differentiation of S. Am. populations indicates that Amazon region may be one of the primary diversity centers

Vis et al., 2008, J Phycol 44: 882-888

Lemanea

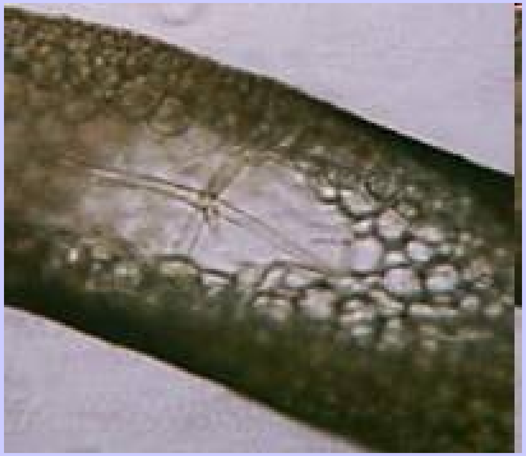

Sirodotia, Tuomeya

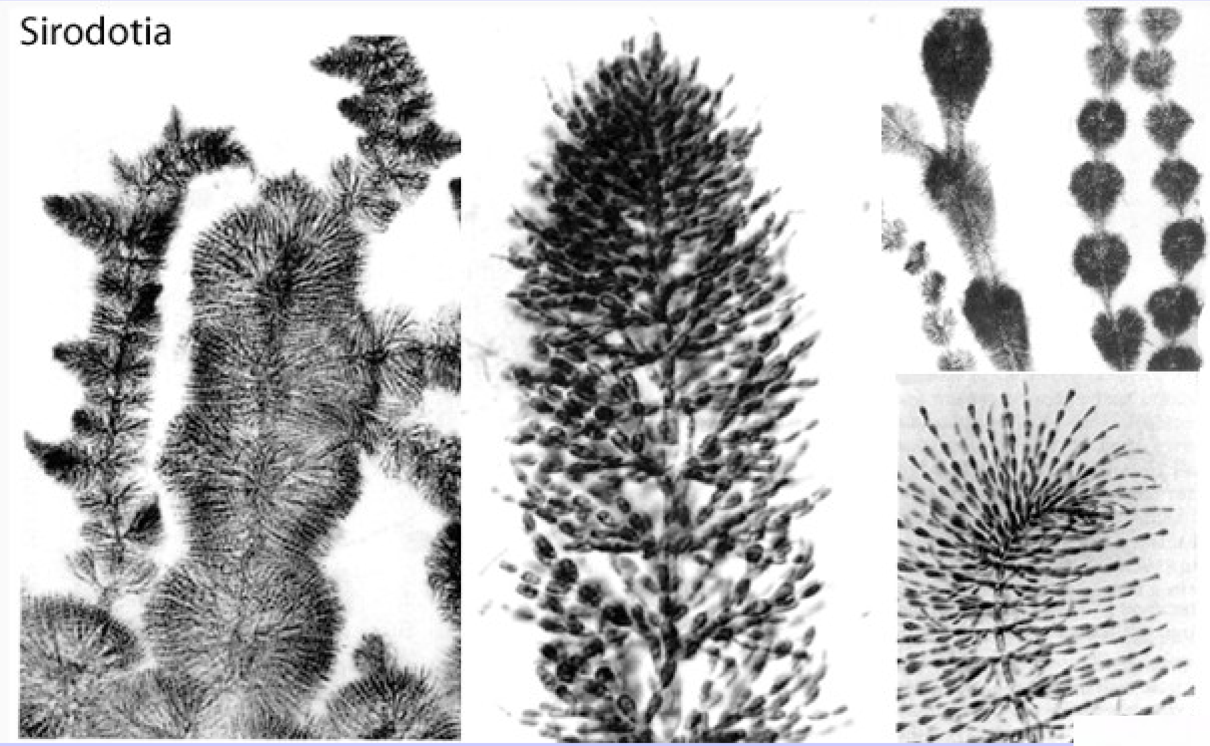

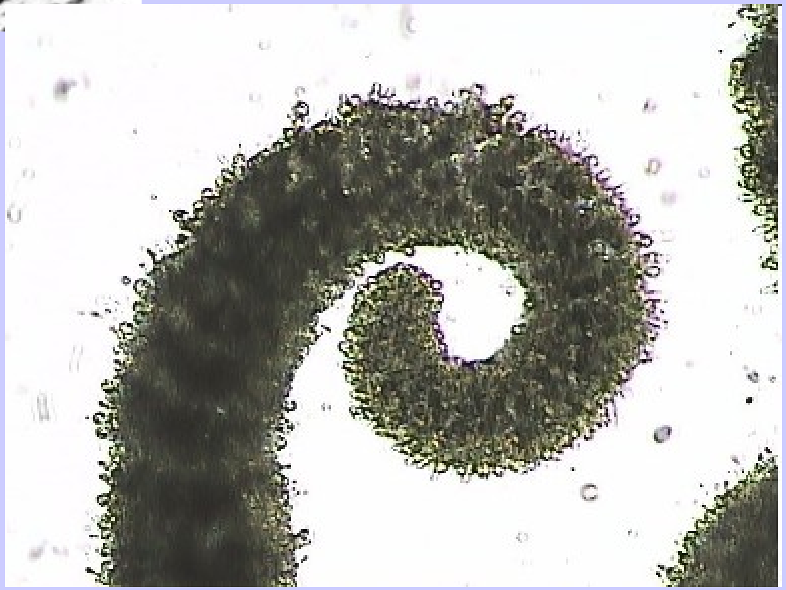

Tuomeya

Balbiania

formerly considered a member of Audouinella

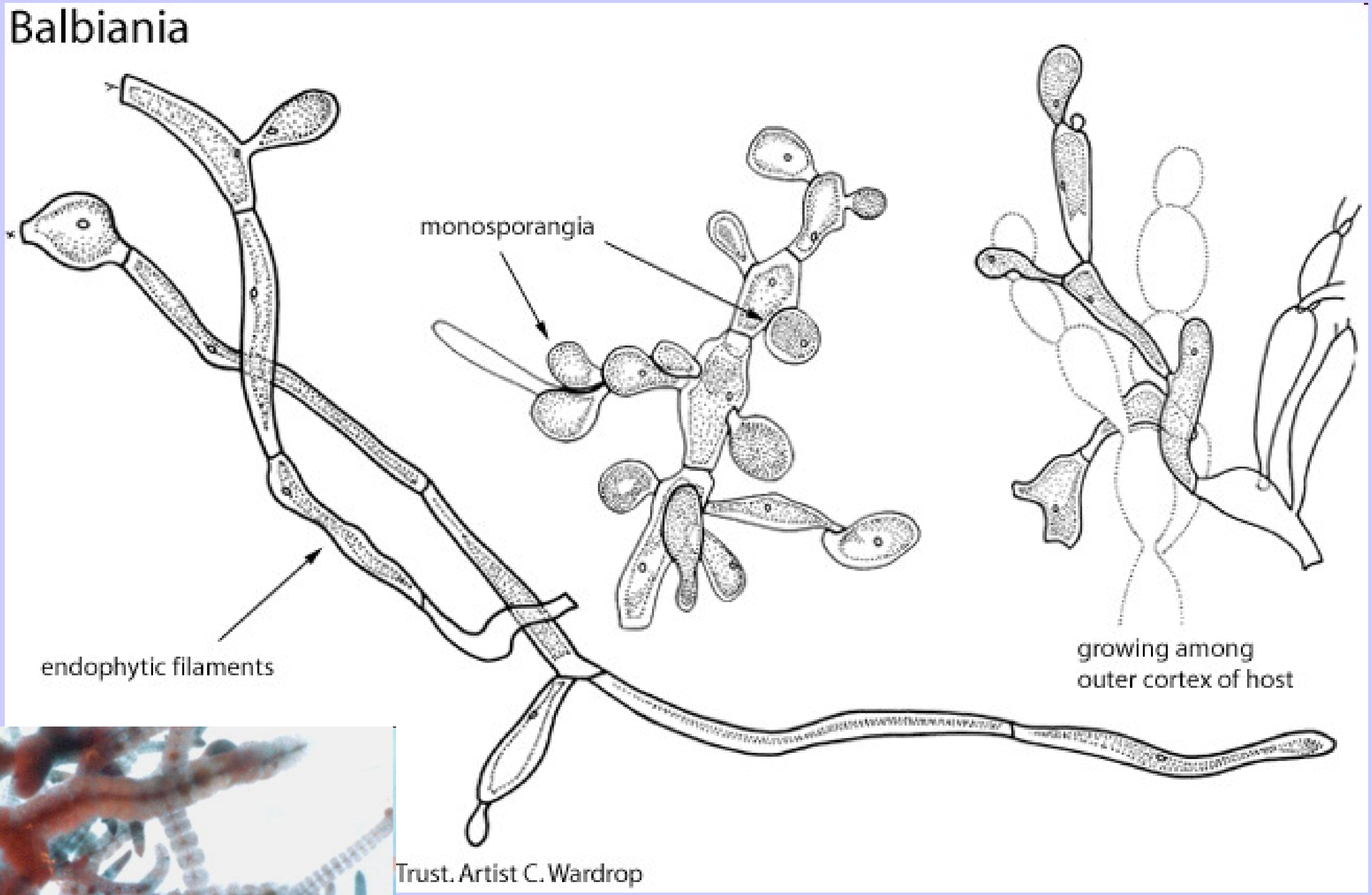

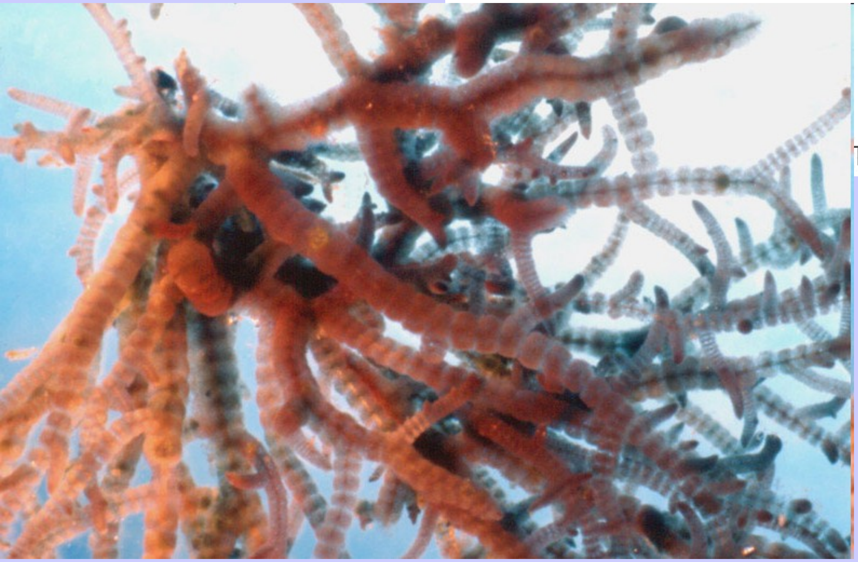

rare epiphyte and endophyte of freshwater rhodophytes (such as *Batrachospermum*)

(infragroup co-evolution of comensales and parasites)

reddish *Balbiania* growing on *Batrachospermum* (DE)

Thoreales

Thorea

the second freshwater order

often in freshwater aquaria
up to 200 cm long thalli
mostly tropics, rarely in Europe (GB)

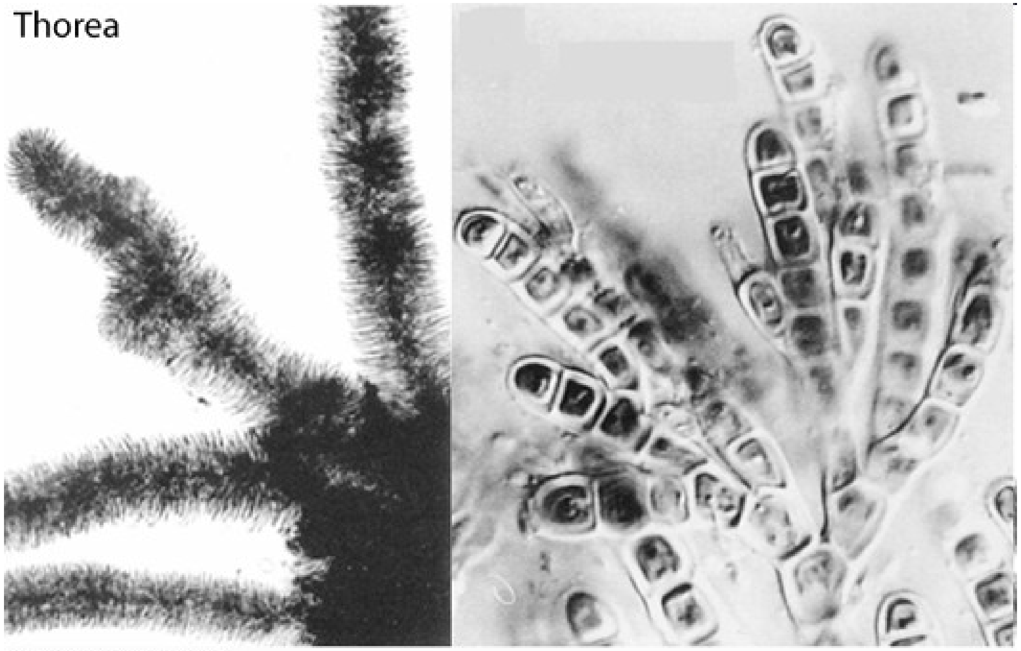

After Entwisle et al. (1999a)

Nemaliales

Nemalion

marine algae
often in supralittoral

(= emersed for the most tim
subatmophytic life strategy)

N. helminthoides

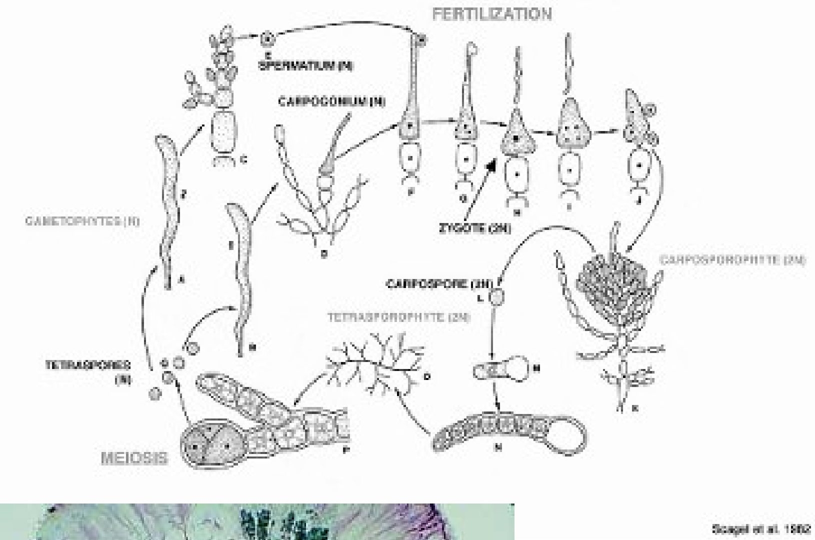

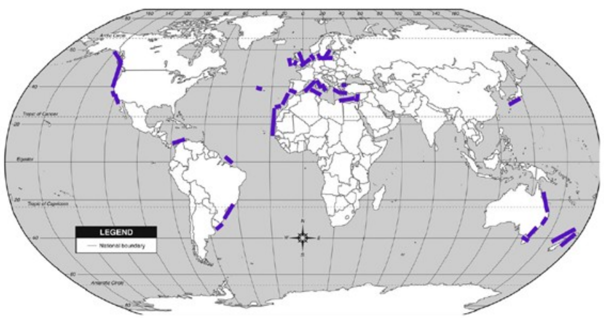

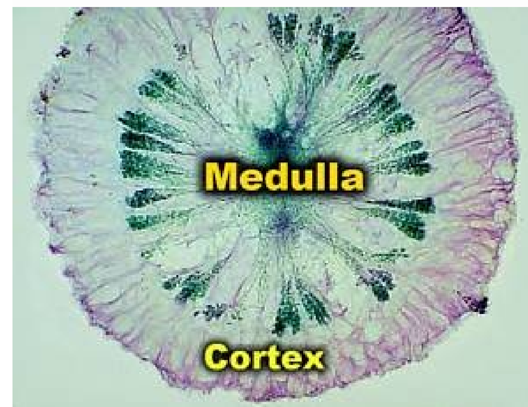

Galaxaura

calcified marine lineage from subtropical and tropical habitats

invasive in the E Mediterranean

G. rugosa
(photo: S Africa

Galaxaura

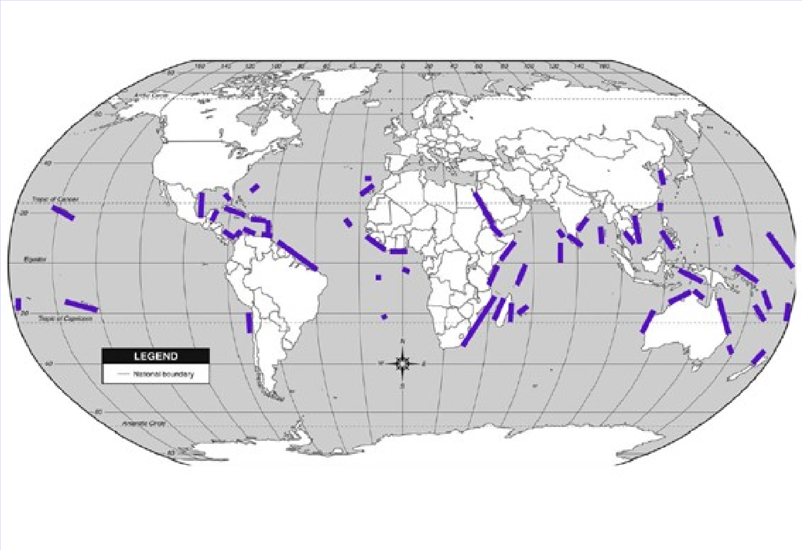

G. rugosa – pantropical species

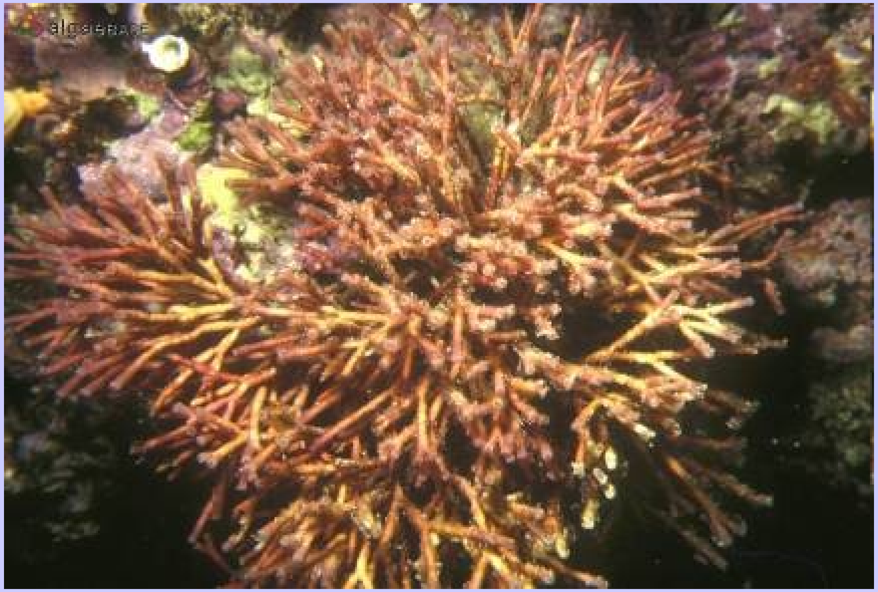

Corallinophycideae - “coral red algae”

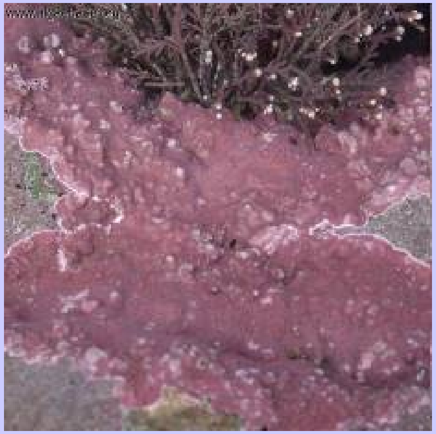

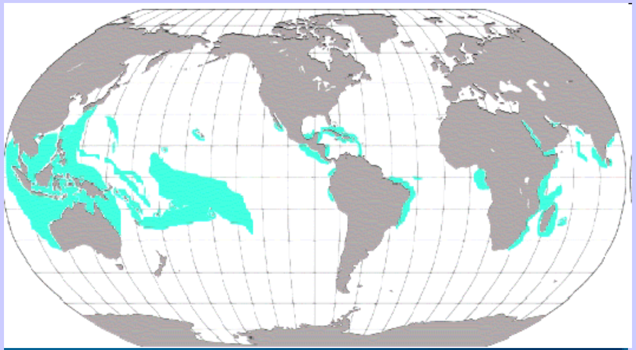

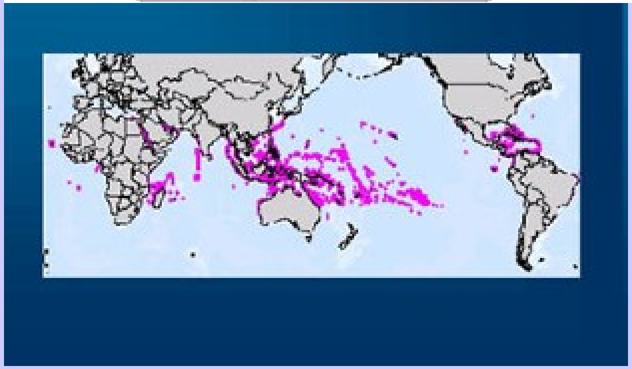

calcification, rhodolites

("coral red algae", "coralline red algae", "calcareous red algae", "CCA")

coralline red algae of coral ecosystems

- key agent in cementation of the reefs
- dominant especially in mesophotic habitats
- high diversity with significant proportion of undescribed taxa
- facilitating distribution of multiple other non-calcified red algae

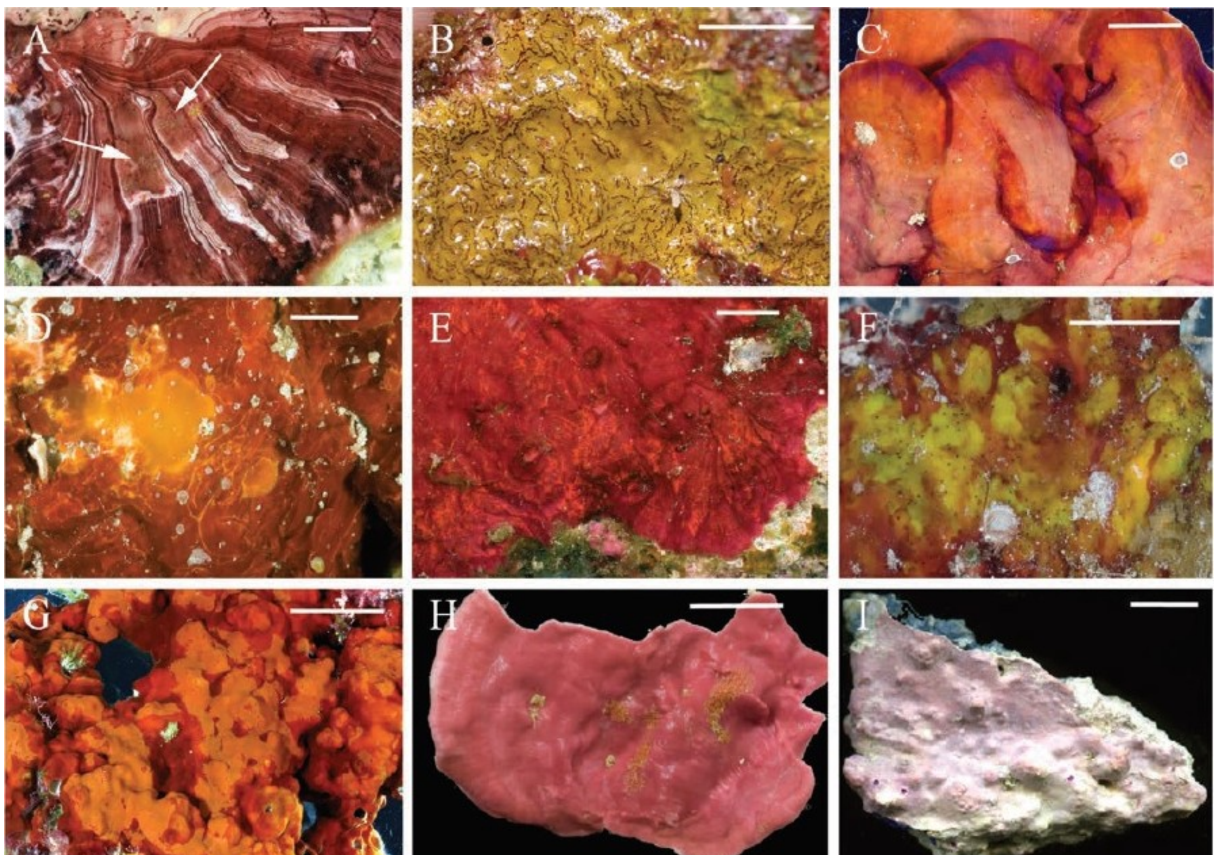

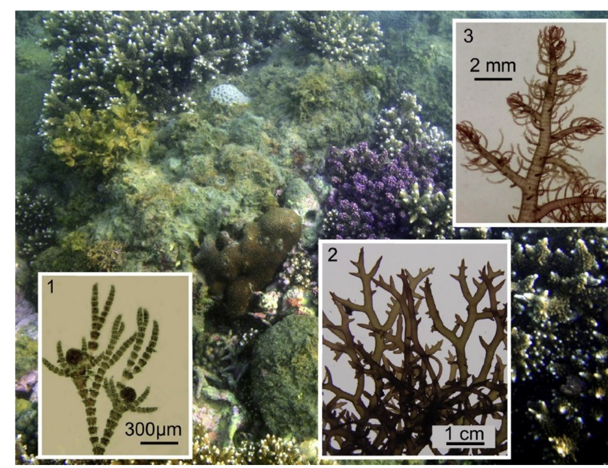

Loya et al., 2019,
Mesophotic Coral Ecosystems

Titlyanov et al., 2017

rhodolith beds [red algal ocean floor]

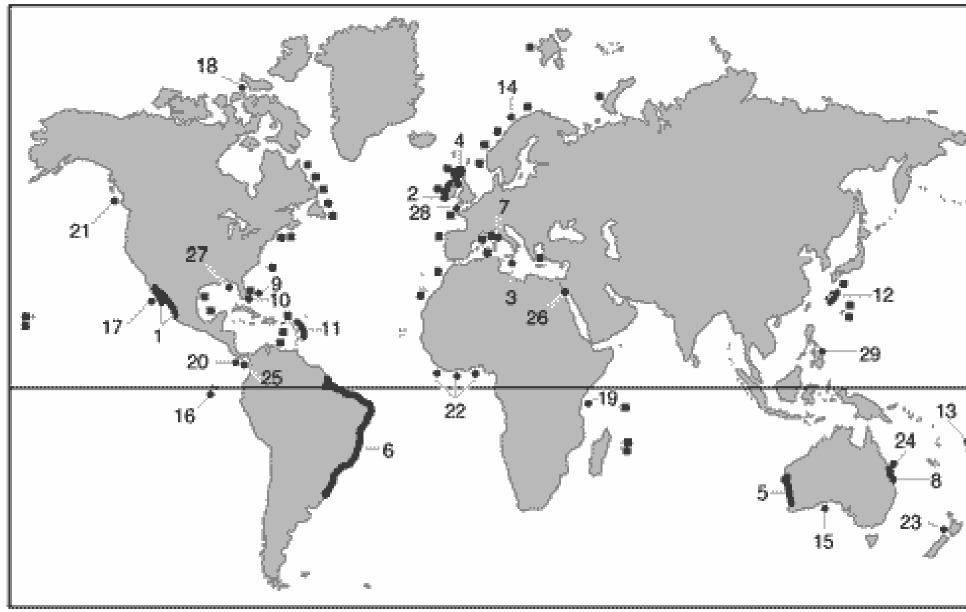

FIG. 4. The world distribution of living rhodolith beds. Squares are from map in Bosence (1983b; see for these references). Circles indicate locations of individual beds, and dark bands indicate large, continuous beds or numerous individual beds not included on the Bosence (1983b) map. No beds have been reported from Antarctica. Personal communication followed by more precise locations. 1. Foster et al. 1997, M. Foster, D. Steller & R. Riosmena, personal observation (eastern Gulf of California). 2. De Grave et al. 2000. 3. Borg et al. 1998 (Malta). 4. D. Donnan, Scottish Natural Heritage, personal communication (north & west Scotland). 5. James et al. 1999. 6. Kempf 1970, Milliman 1977. 7. Basso 1998. 8. Harris et al. 1996. 9. Littler et al. 1991. 10. Prager & Ginsburg 1989. 11. Reid & Macintyre 1988. 12. Tsuji 1993. 13. Scoffin et al. 1985. 14. Freiwald & Henrich 1994. 15. H. Kirkman, United Nations—East Asian Seas Regional Coordinating Unit, personal communication (Great Australian Bight). 16. C. Rigaud, Moss Landing Marine Laboratories, personal communication (Galapagos). 17. J. Harding, University of California at Santa Cruz, personal communication (Isla Cedros). 18. J. Oliver, Moss Landing Marine Laboratories, personal communication (Devon Island). 19. J. Waterbury, Woods Hole Oceanographic Institution, personal communication (Zanzibar). 20. T. Schaeffer, Moss Landing Marine Laboratories, personal communication (Costa Rica). 21. P. Thuringer, Archipelago Marine Research Ltd., personal communication (Queen Charlotte Islands). 22. Reviewed in John & Lawson 1991. 23. D. Schiel, University of Canterbury, personal communication (Kapiti Island). 24. A. Larkum, University of Sydney, personal communication (One Tree Reef). 25. Glynn 1974. 26. Piller & Rasser 1996. 27. McClintock et al. 1993. 28. Farnham & Bishop 1985. 29. D. James, Moss Landing Marine Laboratories, personal communication (Camiguin Island).

Riosmena-Rodríguez et al., 2017
Rhodolith Beds, Springer

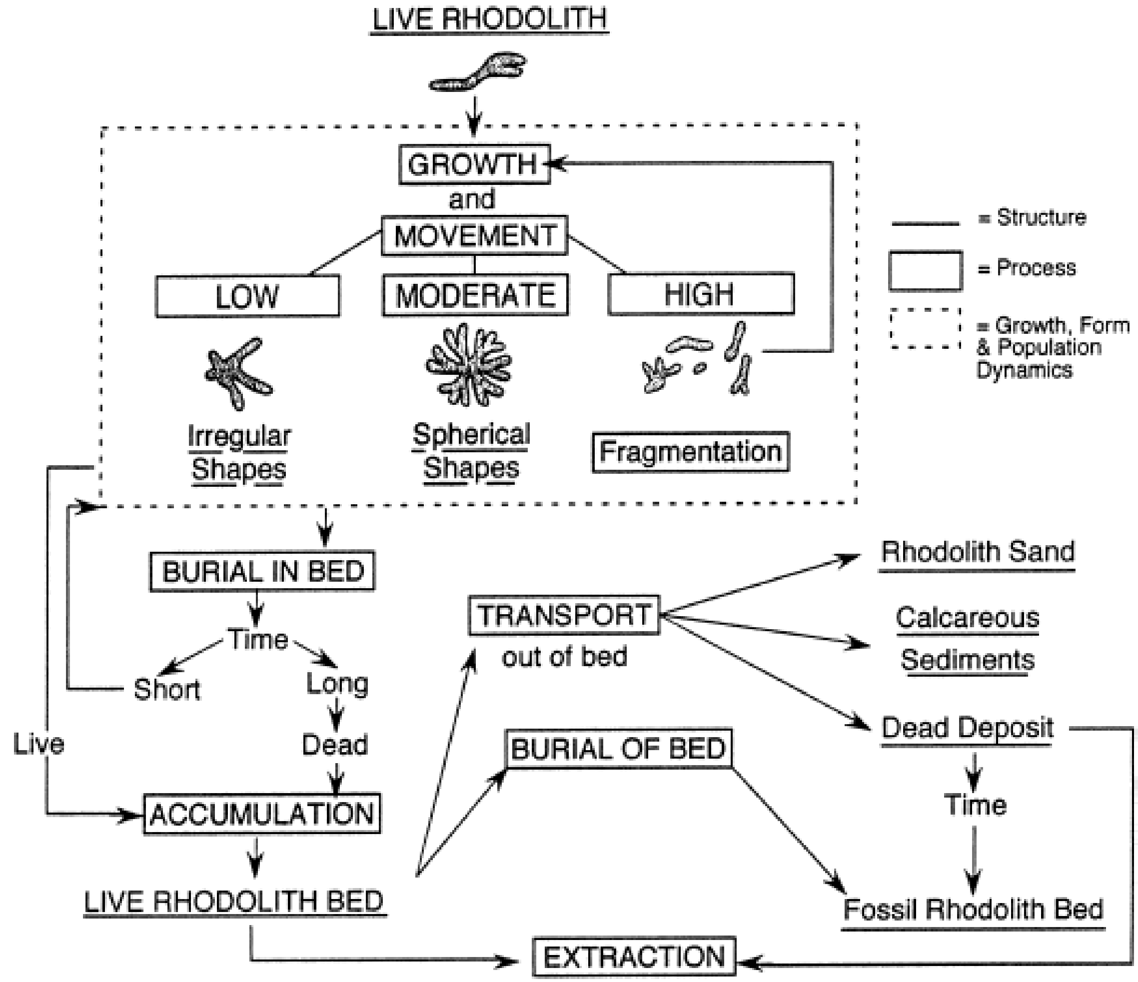

FIG. 2. A model for the structure and dynamics of rhodoliths, rhodolith beds, and geological structures derived from them. Living fragments can be produced in a bed or transported to it, and equivalent small plants can develop from spores. Growth rate and morphology may vary with light, nutrients, temperature, movement, and species. Fragments can be broken from larger thalli during movement from water motion, bioturbation, grazing, and trawling. These processes also produce sand and smaller calcareous particles. Burial in a bed can occur from sedimentation and disturbance from water motion and bioturbation. The effects of fouling may be similar to burial. Catastrophic sedimentation and changes in sea level can cause death/burial of entire beds.

Foster 2001, J. Phycol. – rhodolite dynamics

taxonomic structure of coralline red algae

Corallinales (ca 830 species) (Corallina, Jania, Bossiella, Amphiroa, Phymatolithon, Hydrolithon)
both geniculate and non-geniculate

Sporolithales (60) (Heydrichia, Sporolithon)
non-geniculate

Rhodogorgonales (ca 20)

Corallinapetrales (2) non-geniculate

evolutionary timeline

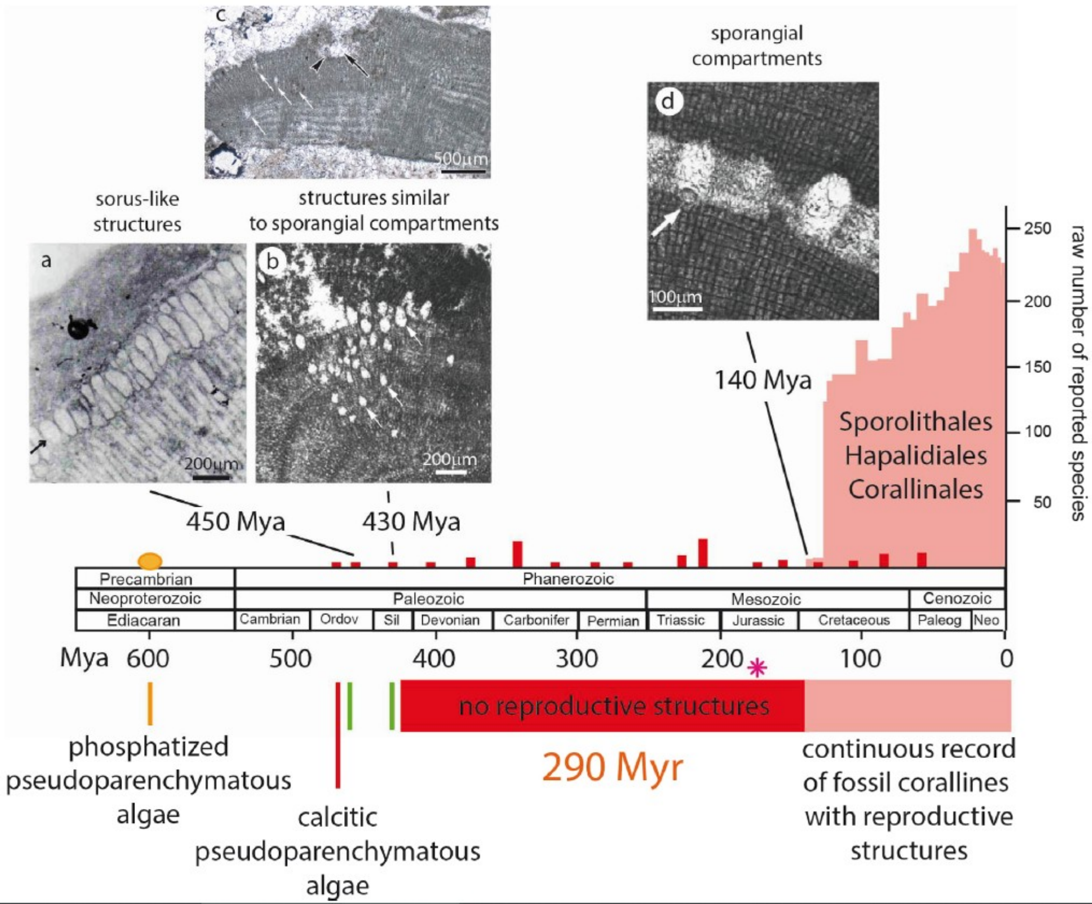

Pena et al., 2020, Mol. Phyl. Evol.

two basic life forms - geniculate and non-geniculate coralline algae

non-calcified *geniculae*
typical erect and branched morphology

typical crustose or rhodolithic morphology

Bossiella

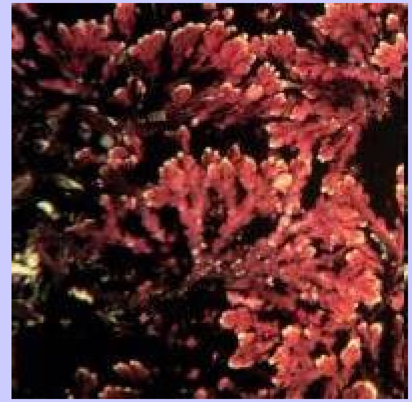

colder seas - kelps littoral ecosystems
entire Pacific coast of the Americas

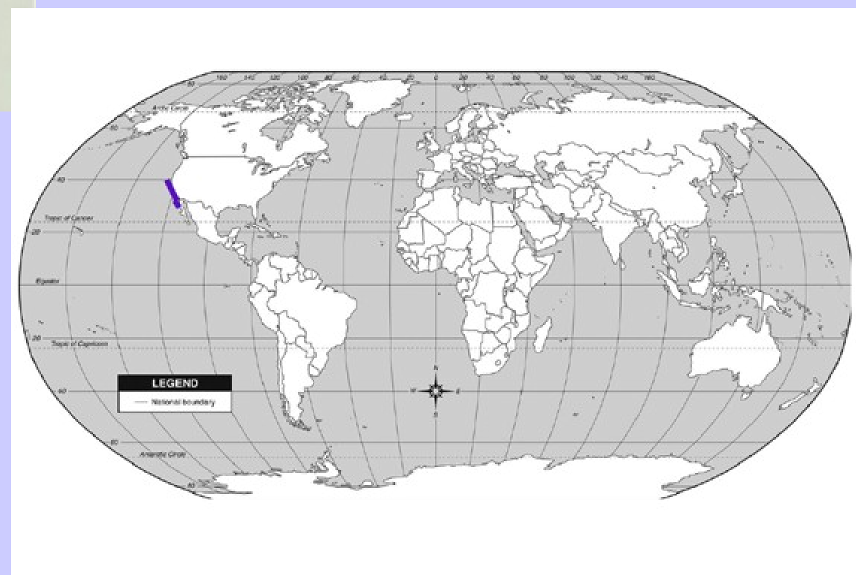

B. californica

Corallina

temperate to tropical seas; cosmopolitan

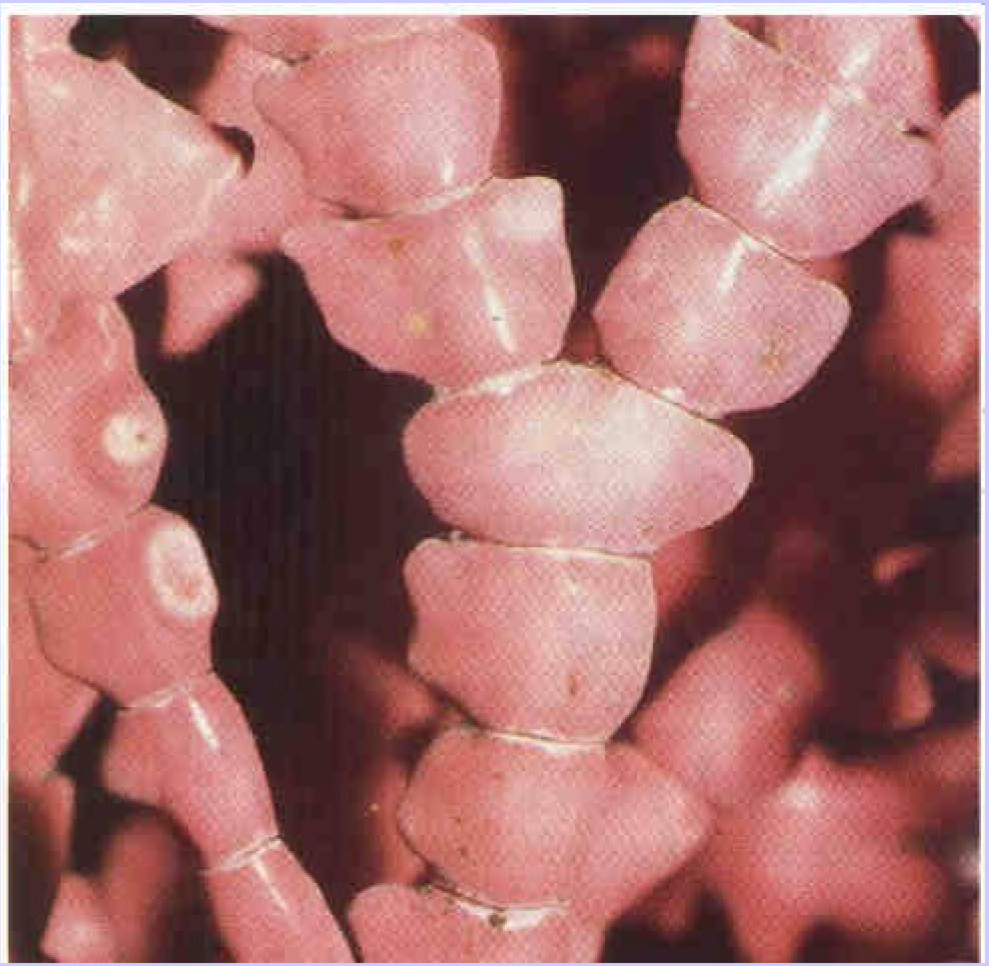

Jania

- dichotomically branched thalli
- cylindrical segments

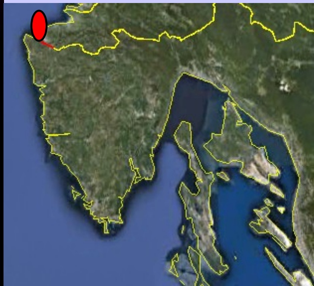

Amphiroa, Jania

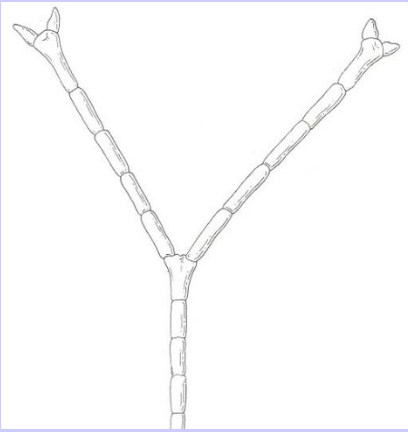

J. rubens

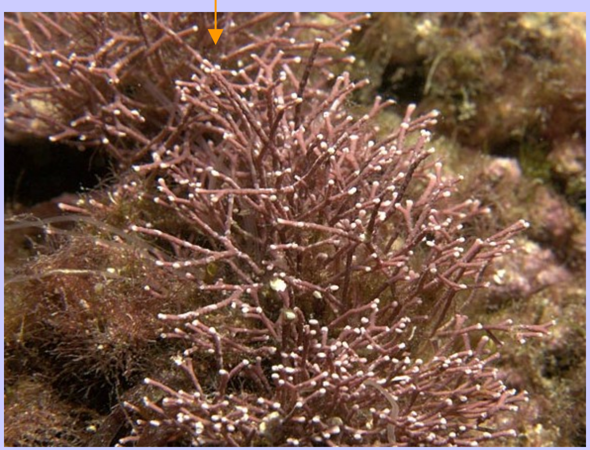

Amphiroa sp.

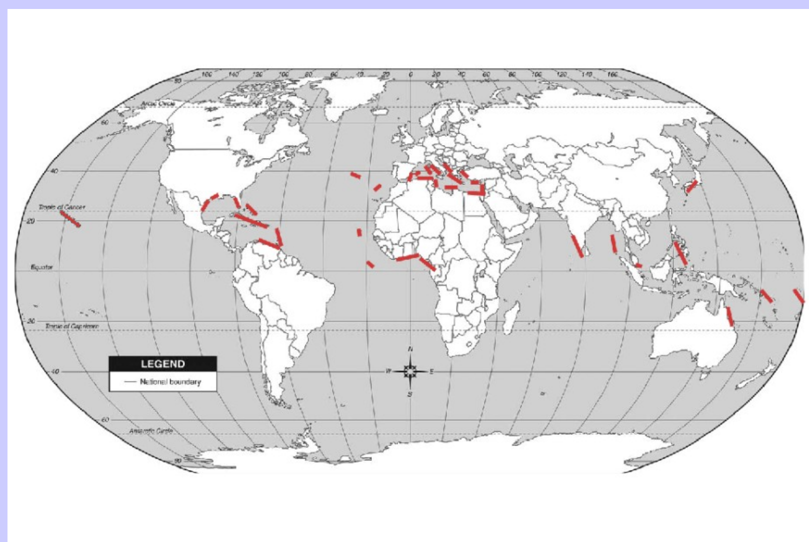

A. rigida

Haliptilon

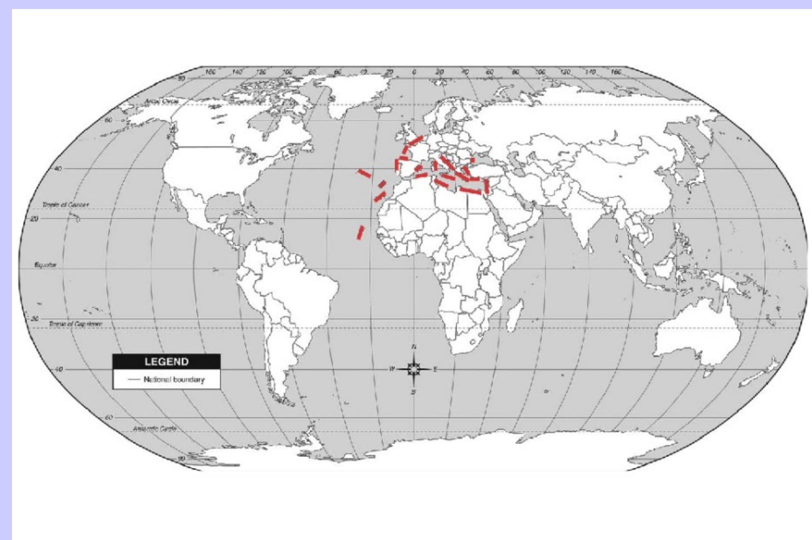

H. virgatum

phylogeny of geniculate corallines

non-monophyly of traditional Corallina

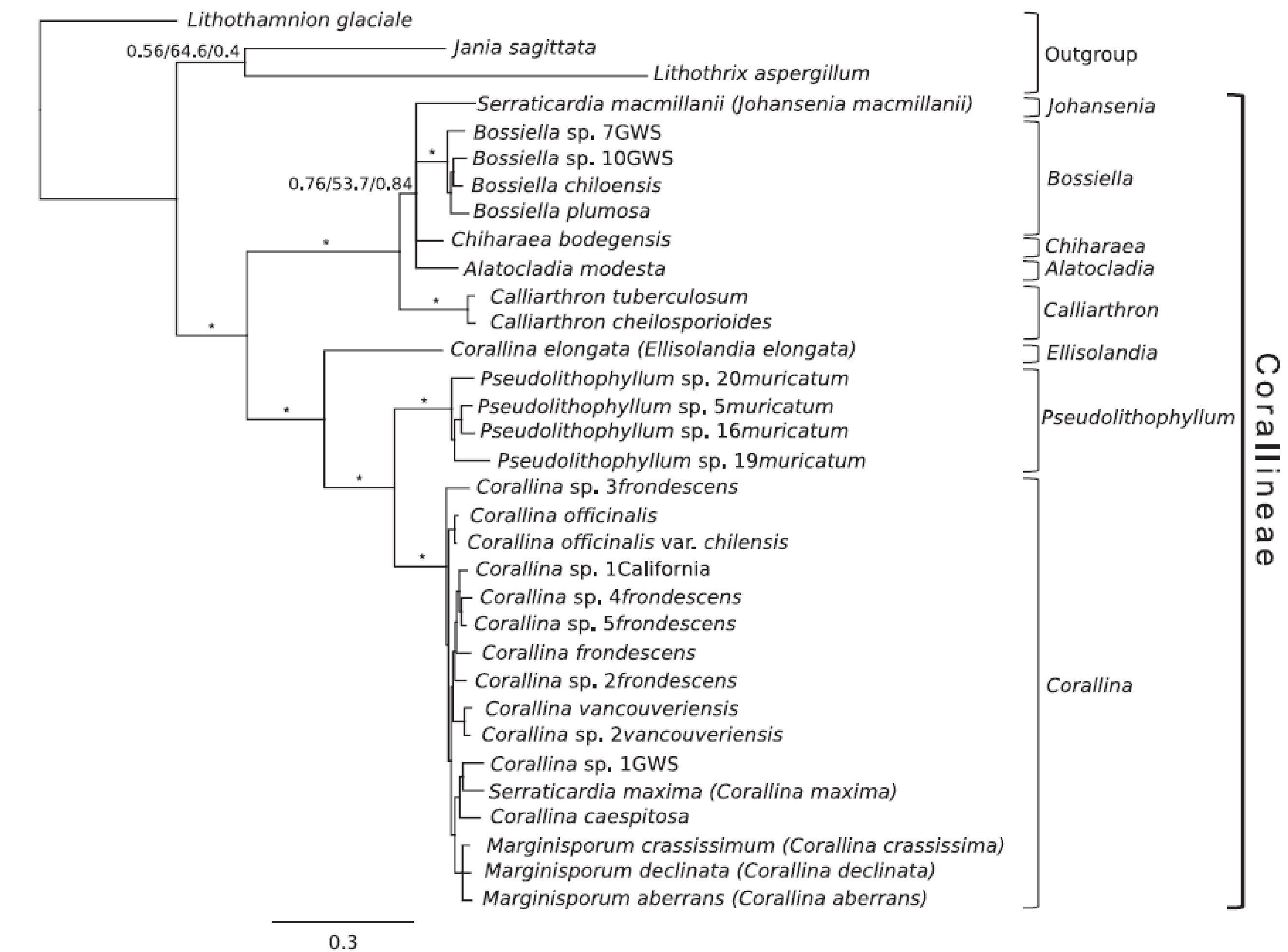

FIG. 1. Phylogram inferred by Bayesian analysis of concatenated COI-5P, *psbA*, and EF2 sequence data. Support values are listed as Bayesian posterior probabilities and bootstrap and aLRT values for maximum likelihood analyses, respectively. Asterisks denote nodes that are strongly supported (posterior probabilities = 1.0, bootstrap and aLRT values ≥ 0.95) in all analyses. Support values are not indicated for all nodes (i.e., among species within genera). Species names included in brackets are new combinations proposed in this study. Scale bar refers to substitutions per site.

Hind & Saunders, 2013, J. Phycol. 49

phylogeny of NE Atlantic geniculate corallines

non-monophyly of traditional Corallina

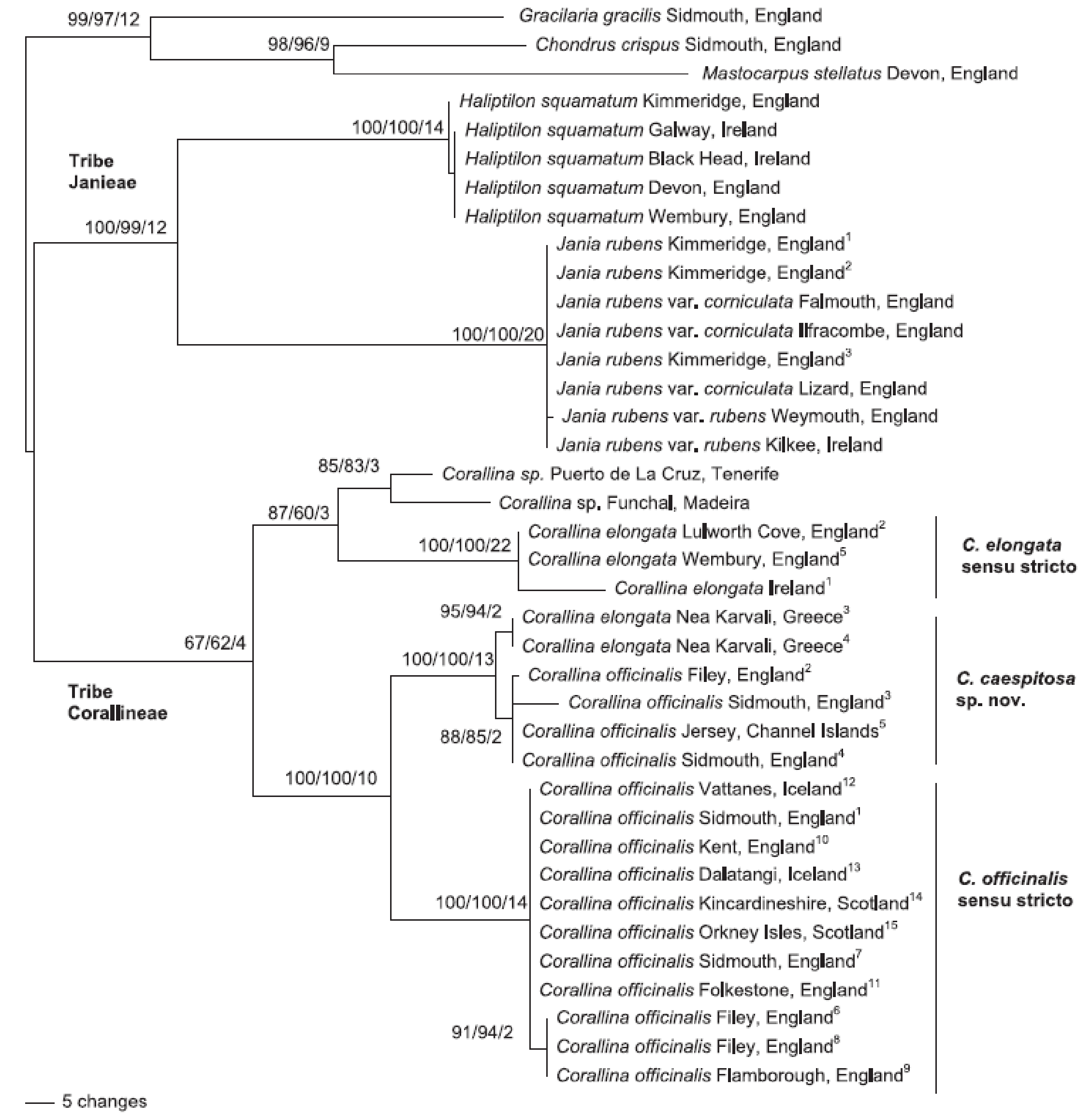

FIG. 1. Maximum-parsimony (MP) phylogram of the *cox*1 gene. Bootstrap support values for MP/bootstrap support values for ML/Bremer support values. ML, maximum likelihood. Superscript numbers refer to sample collection information in Table S1 (see the supplementary material).

Walker et al., 2009, J. Phycol. 45

European taxa of traditional *Corallina*

Ellisolandia elongata
– Atlantic coast, Mediterranean, Azores

C. officinalis – Atlantic (up to Greenland), Medit.,
other temperate coasts,
possibly cosmopolitan

C. caespitosa – rare, Atlantic coast, Azores, Medit.

coastal habitats with high herbivore pressure

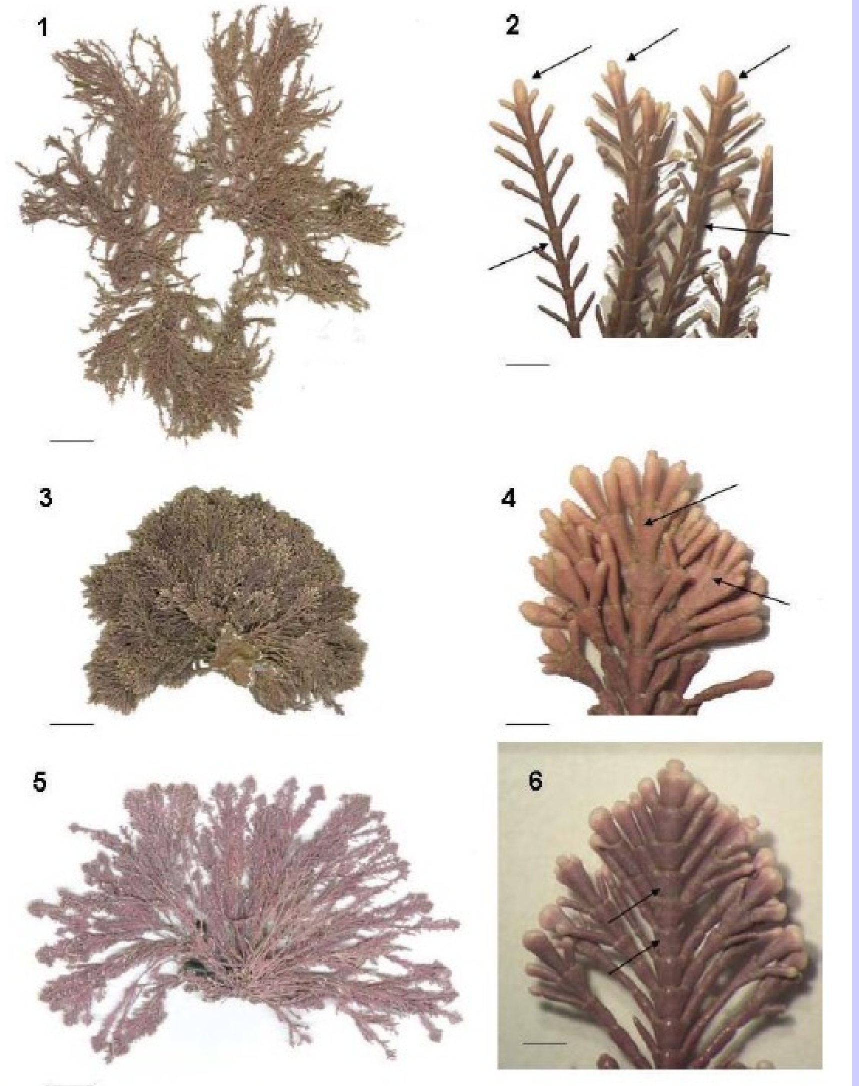

Figs 1-6. *Corallina officinalis*, *C. caespitosa* and *C. elongata*. **1.** *Corallina officinalis* Linnaeus: epitype. Scale bar = 7.5 mm. **2.** *Corallina officinalis* detail of apical intergenicula: upper arrows - trifurcate intergenicula; lower arrows – conspicuous gaps between lateral branchlets. Scale bar = 1 mm. **3.** *Corallina caespitosa* R.H. Walker, J. Brodie & L.M. Irvine: holotype. Scale bar = 7.5 mm. **4.** *Corallina caespitosa* detail of apical intergenicula: arrows – palm-like intergenicula with quadrifurcate apical intergenicula. Scale bar = 1.3 mm. **5.** *Corallina elongata* Ellis & Solander: epitype. Scale bar = 12 mm. **6.** *Corallina elongata* detail of apical intergenicula: arrows – tiny or non-existent gaps between lateral branchlets. Scale bar = 1.4 mm.

Brodie et al., 2013, Crypt. Algol. 34

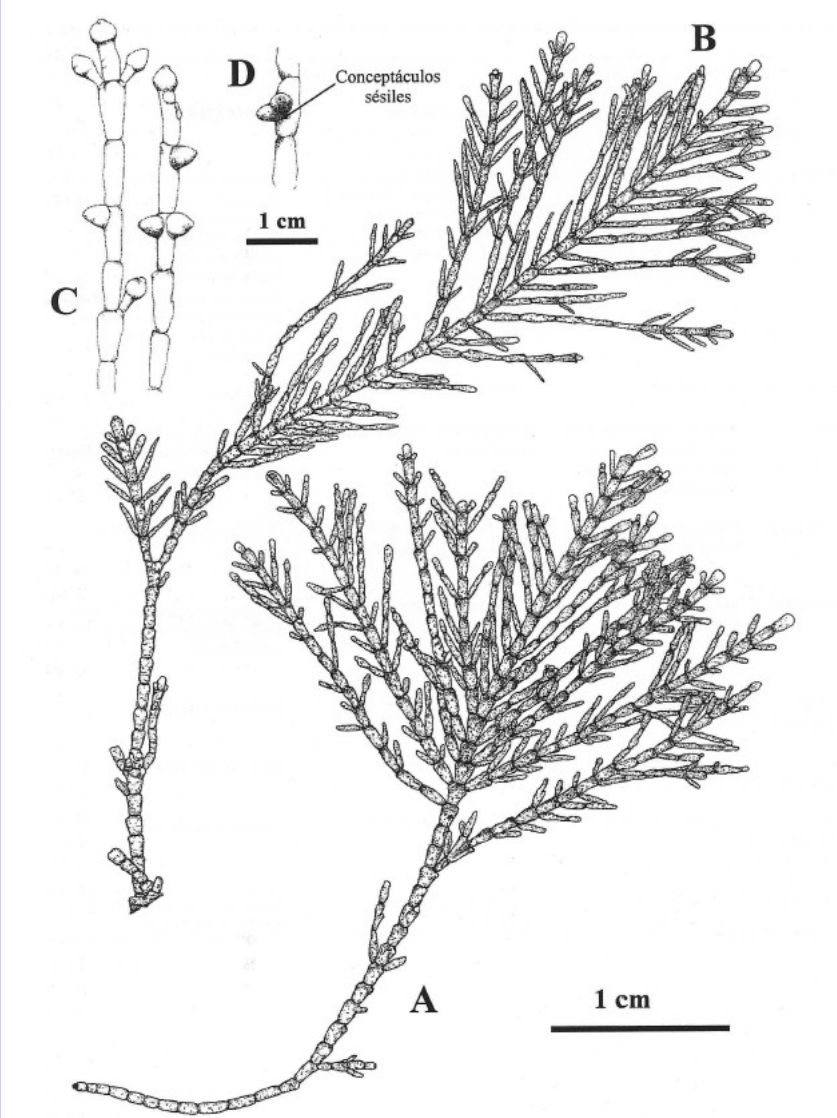

Fig. 1. *Corallina officinalis*. (**A,B**) Morfología de los talos. (**C,D**) Detalles de ramas reproductoras con conceptáculos terminales (pedicelados) y laterales (sésiles).

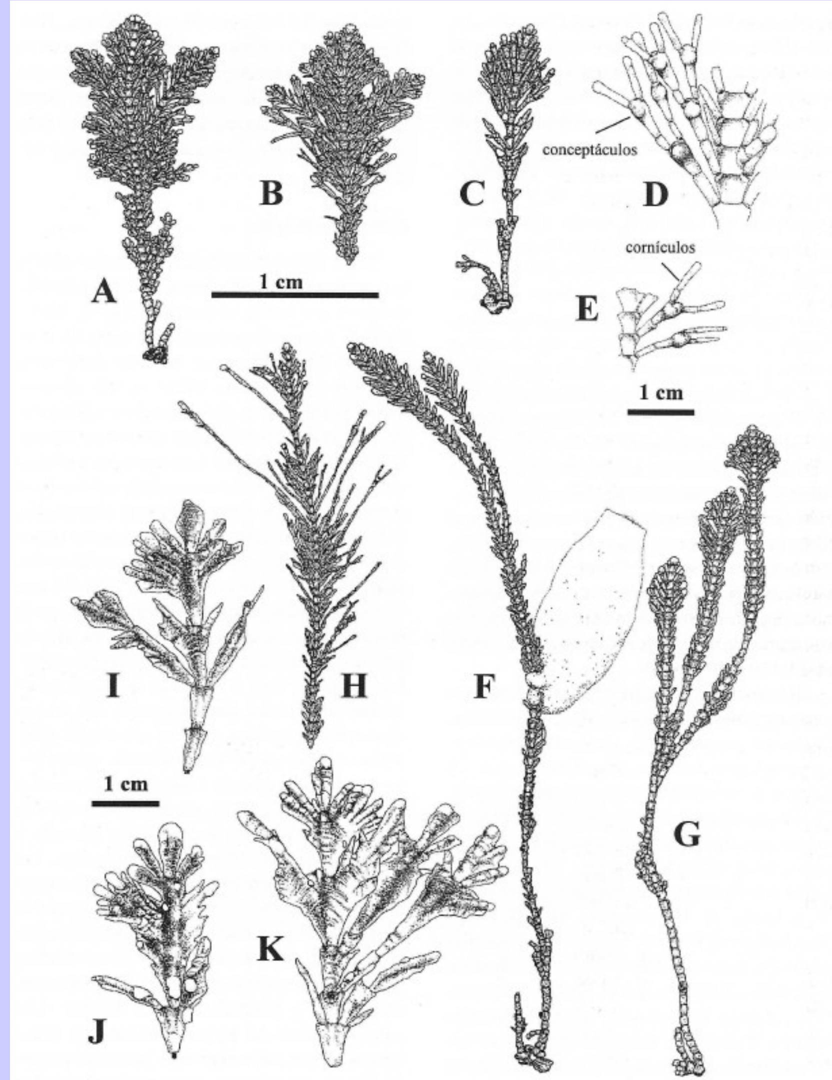

Fig. 2. *Corallina elongata*. (**A-C**) Morfología de talos característicos del intermareal medio. (**D,E**) Detalle de ramas reproductoras con conceptáculos provistos de cornículos. (**F-H**) Morfología de talos característicos de paredes verticales del intermareal inferior; en **F** asociada a la esponja *Grantia compressa*. (**I-K**) Variaciones morfológicas de artejos y grado extremo de aplanamiento del talo en la formación de expansiones laminares.

Beltrán & Bárbara, 2013, Nova Acta Cient. Compost. Biol. 13

morphology of conceptacles - classification of taxa in Crallinales and Sporolithales

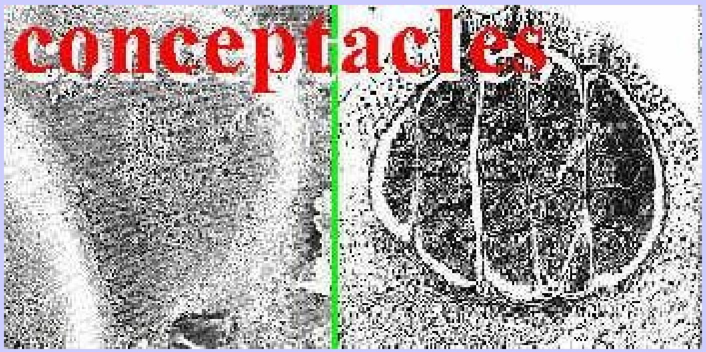

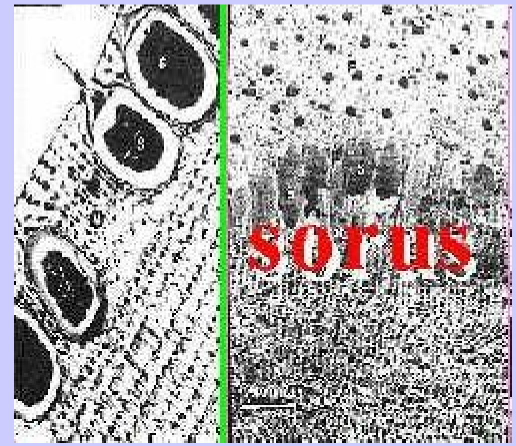

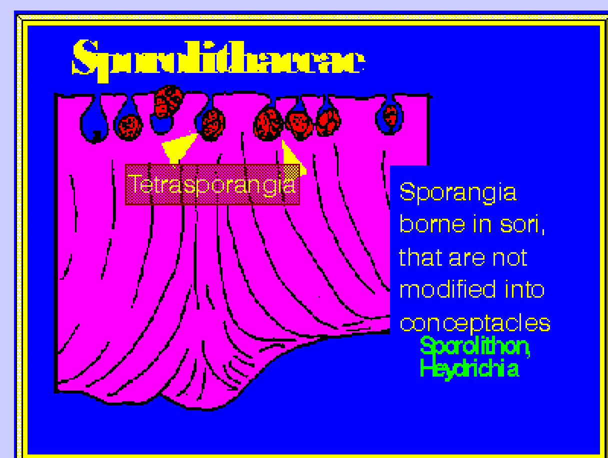

Lithophyllum and *Ezo*

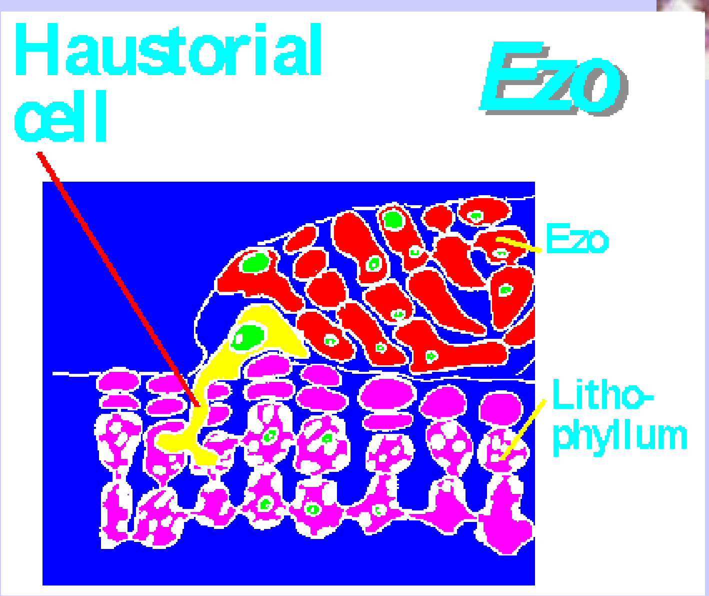

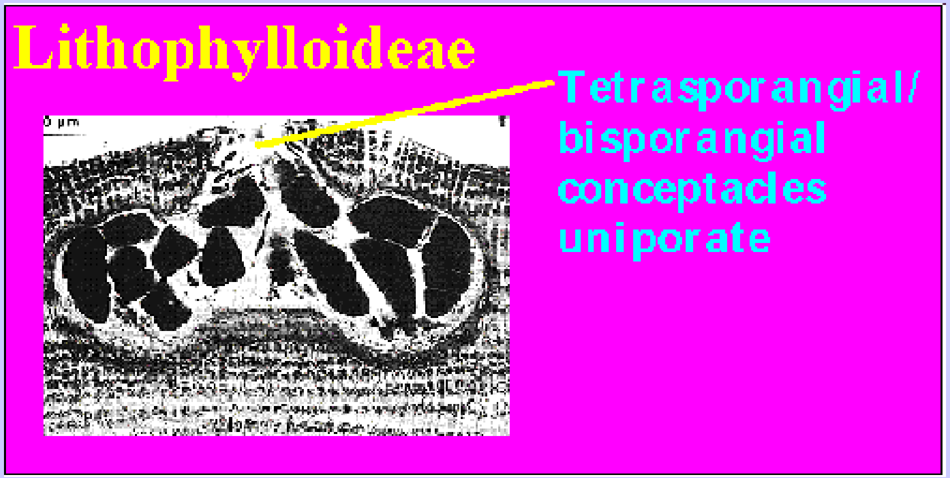

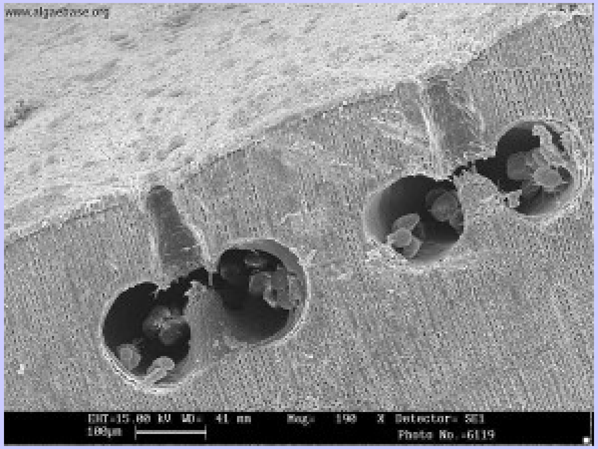

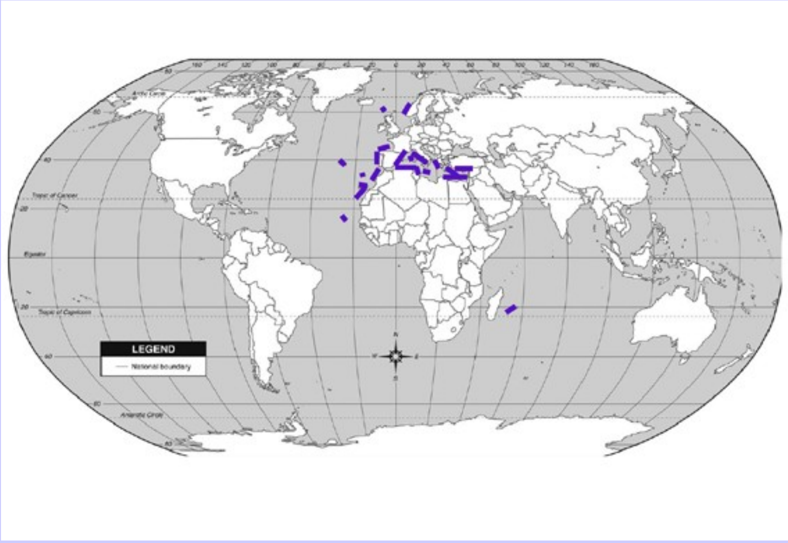

L. incrustans

Hydrolithon

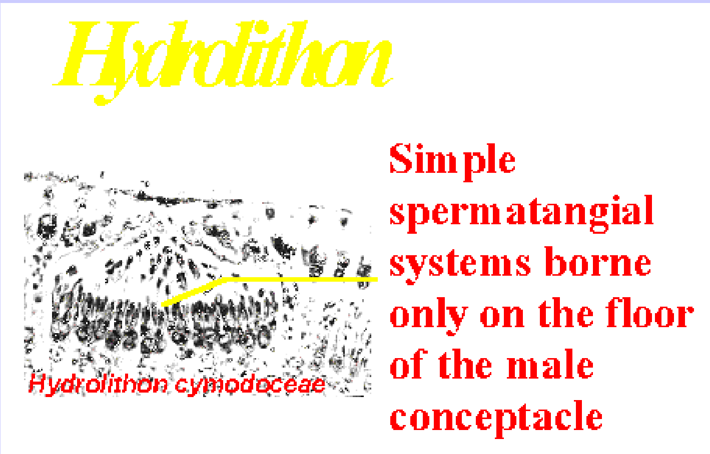

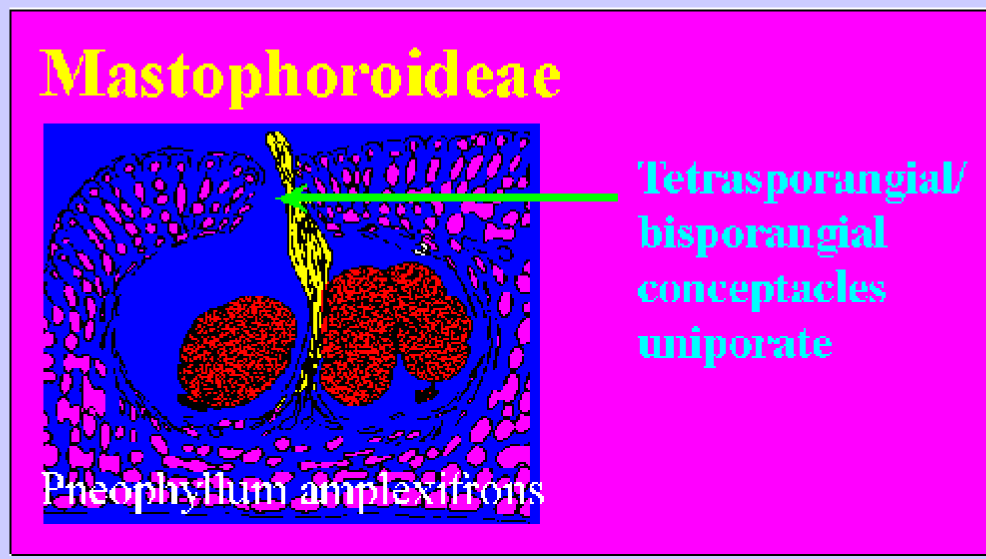

atoles, coral reefs

Heydrichia

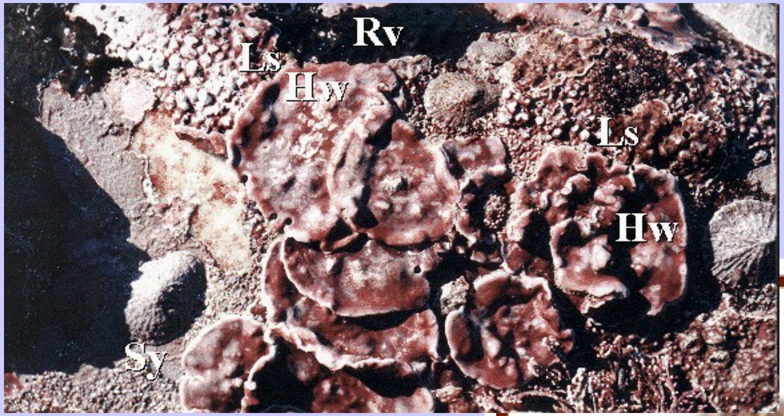

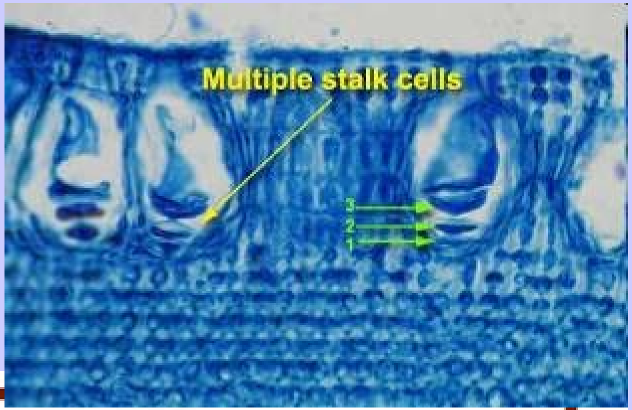

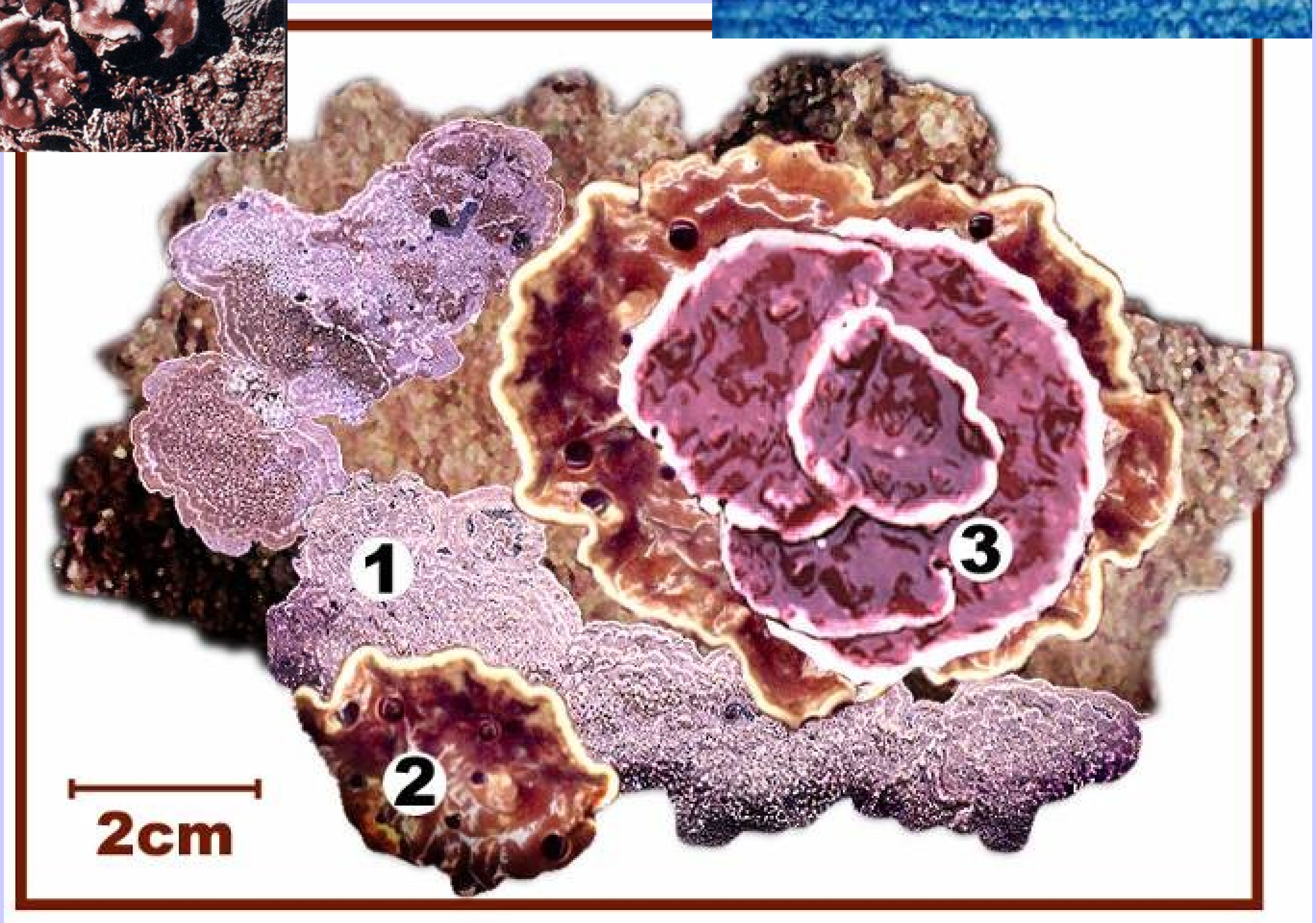

south Africa, Australia

Leptophytum foveatum - Mesophyllum engelhartii - Heydrichia woelkerlingii

Sporolithon

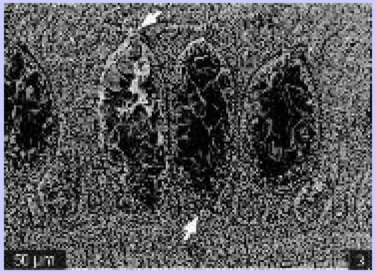

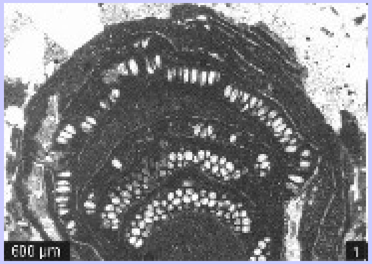

coral reefs, Pacific, Australia

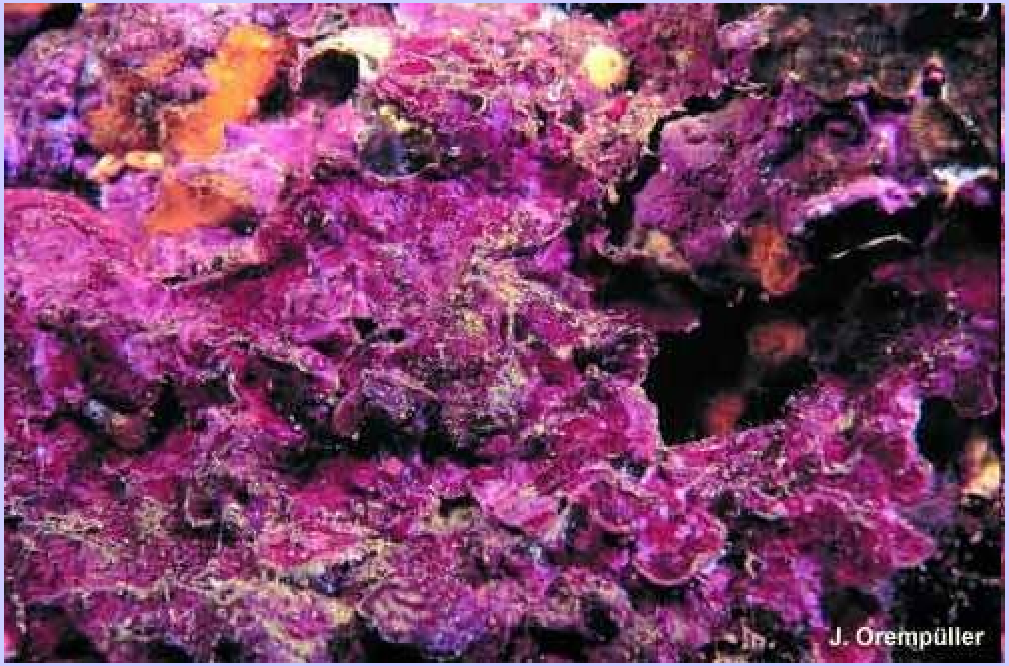

Sporolithon in the Mediterrean – formerly and now

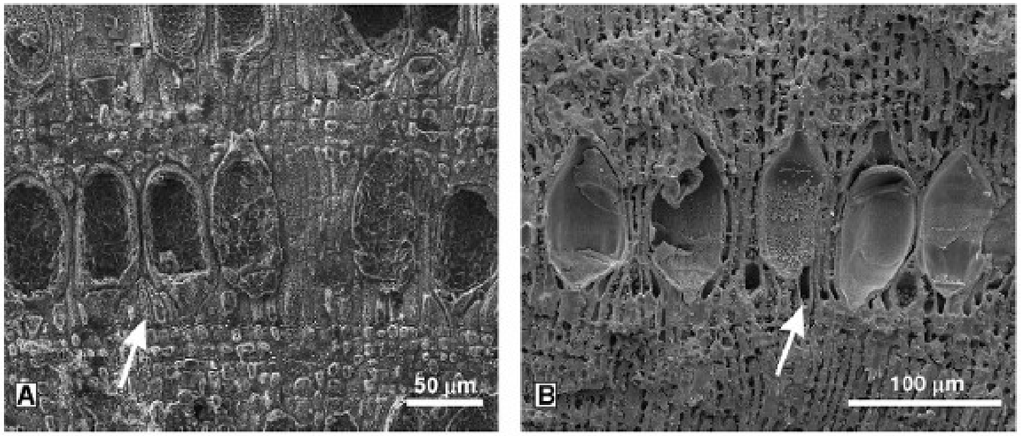

Fig. 6. *Sporolithon ptychoides* Heydrich (1897). SEM photos showing the row of elongated cells at the base of the reproductive structures (arrows). (A) Early Pleistocene, Torrente Enza, Northern Apennines, Emilia–Romagna, northern Italy. (B) Recent, Punta Javana, Cabo de Gata, Almeria, SE Spain.

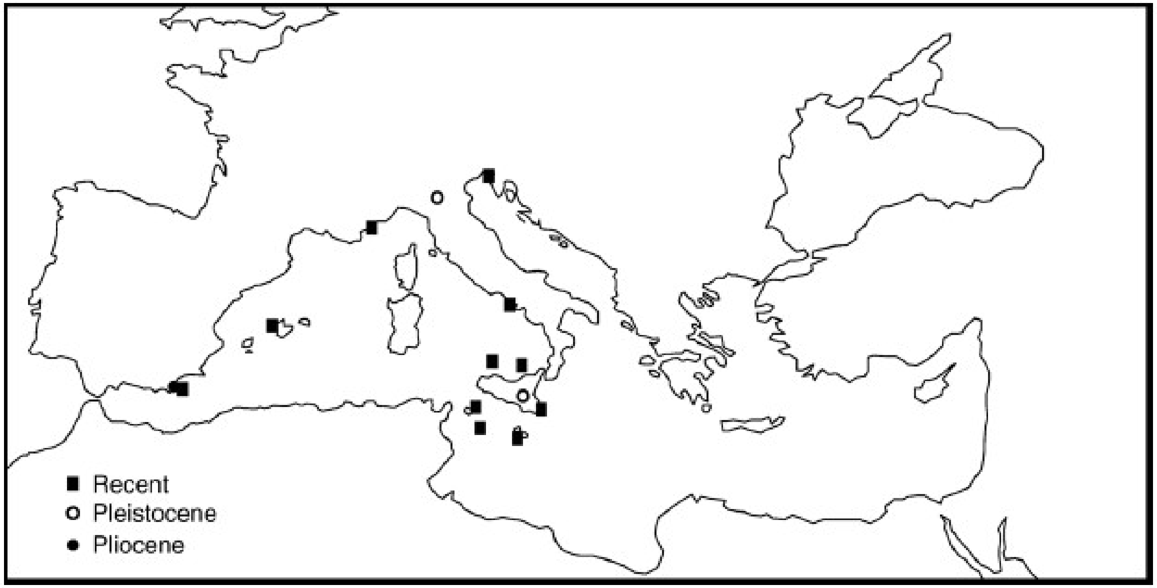

Fig. 3. Geographic location of *Sporolithon* records in the Mediterranean area from the Pliocene to the Recent. For details see Table 5 and Alongi et al. (1996).

Braga & Bassi, 2007, Palaeogeography, Palaeoclimatology, Palaeoecology 243: 189–203.

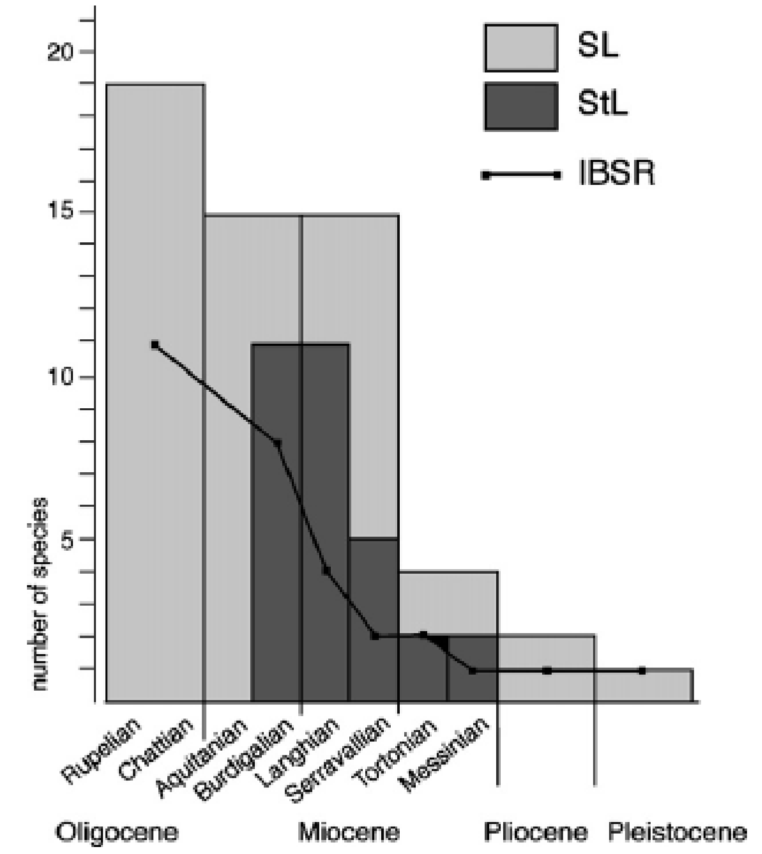

Fig. 4. Species number plots of *Sporolithon* from the Oligocene to the Pleistocene of the Mediterranean area at series level (SL) and stage level (StL). The 'Intra-Basin Species Richness' (IBSR) is also shown. At the series level, species richness decreased from the Oligocene to the Late Miocene and underwent an abrupt drop before the Pliocene. At the stage level there was a significant decrease within the Mid Miocene from the Langhian to the Serravallian, which continued within the Late Miocene. The IBSR shows a gradual decrease in the number of species from the Oligocene to the Messinian.

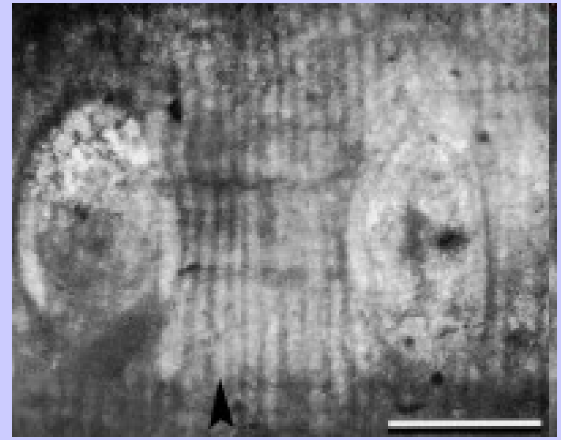

Rhodymeniophycideae – typical "bushy" macroscopic marine red algae

multiple orders, such as:

Ceramiales, Gelidiales, Gigartinales, Gracilariales, Halymeniales, Plocamiales, Rhodymeniales, etc.

- they are almost entirely marine algae (except for *Caloglossa* in Delesseriaceae, Ceramiales)

- they are almost entirely non-calcified (except for several species in *Peyssonnelia*)

- a lot of perennial macroalgae but some important taxa are secondarily simplified to ephemerous filamentous morphology (e.g. *Callithamnion*, *Aglaothamnion* in Ceramiales)

- parasitic lineages in Ceramiales - typical for adelphoparasitism

- pronounced latitudinal diversity gradient

- higher proportion on marine vegetation with increasing depth

- several key invasive taxa in marine coastal habitats (e.g. *Asparagopsis, Bonnemaisonia*)

- multiple taxa used as food source (e.g. Gracilaria, Gelidium, Plocamium) but others are often poisonous

- key genera for agar and karagen production (e.g. *Gelidium, Pterocladiella, Furcellaria, Coccotylus*)

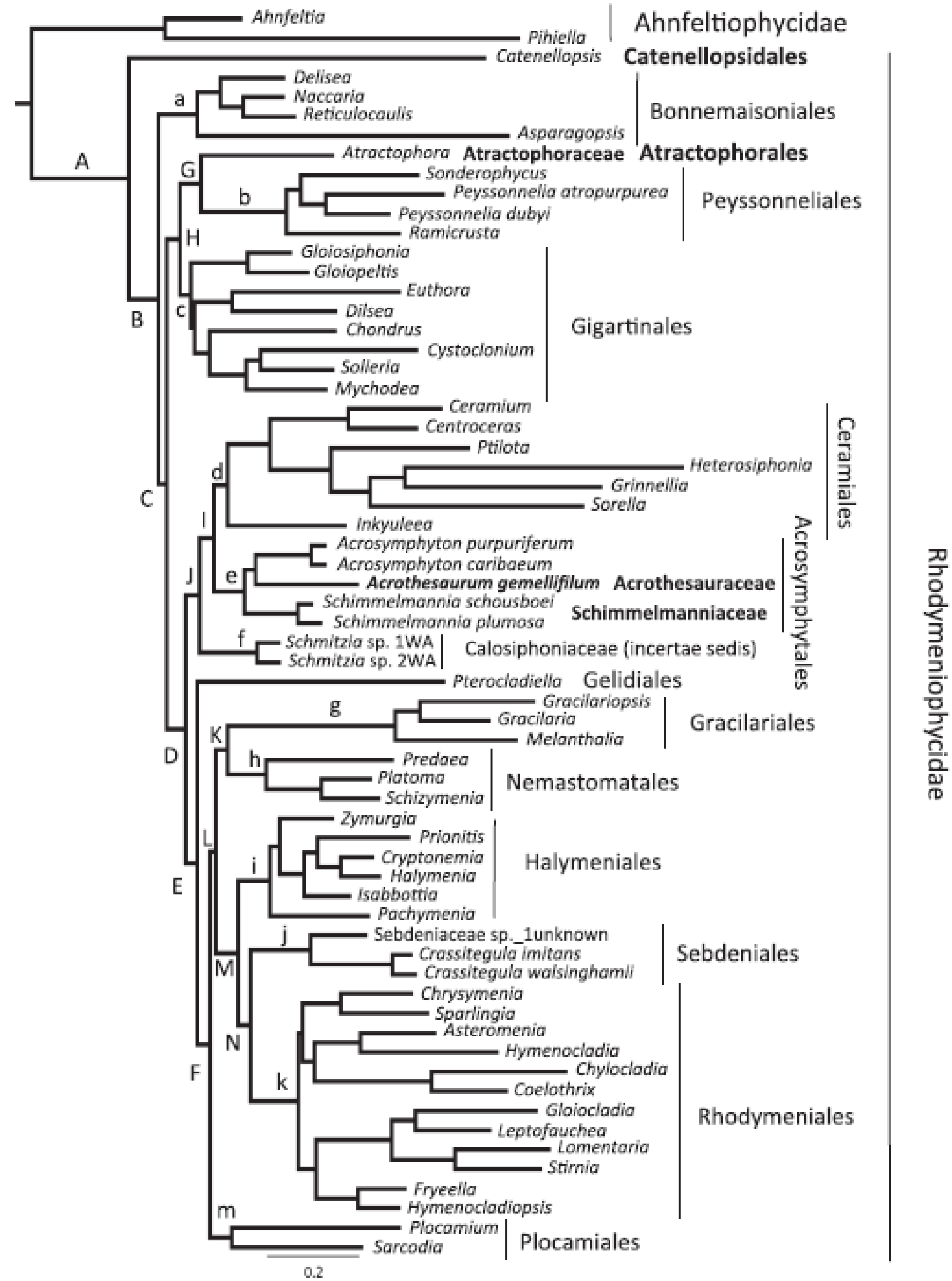

FIG. 1. Bayesian phylogeny for multigene alignment analyzed with full partitioning. Letters at nodes refer to respective support values in Table 1. New taxa in bold type. The outgroup Corallinophycidae have been cropped from the figure to facilitate presentation. Scale indicates substitutions per site.

Saunders et al., 2016, J. Phycol.

Gracilariales (Gracilaria, Gracilariopsis)

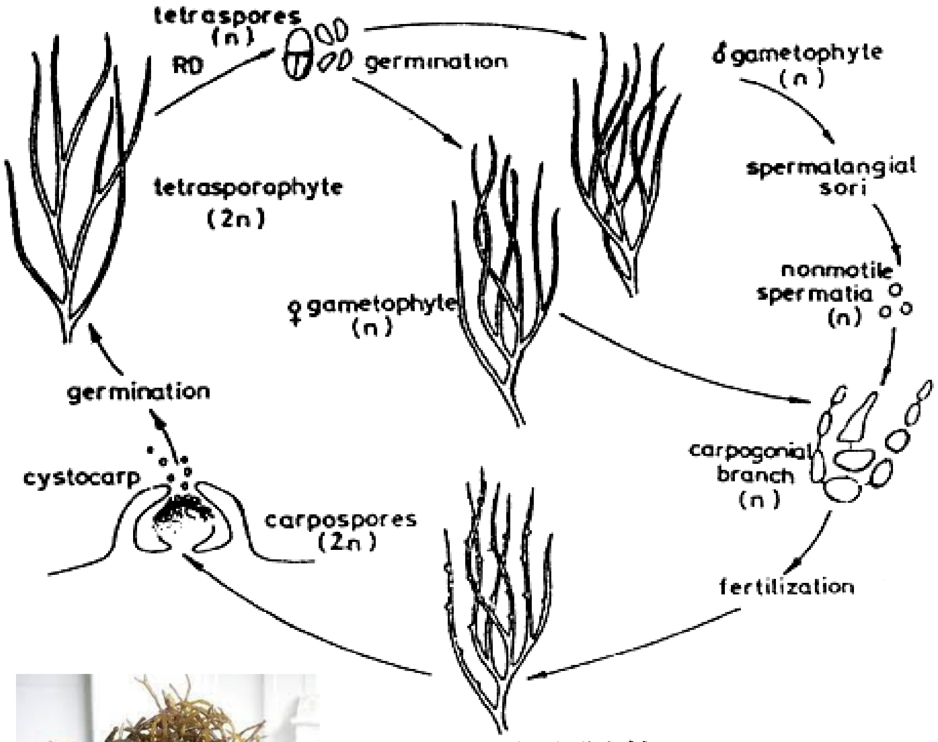

edible gracilarias - ogonori, hai tsai, nuoc-mam, Ceylon moss, etc.

Gracilariopsis vermicullophyla
an invasive species of European coasts

G. parvispora

(wikipedia)

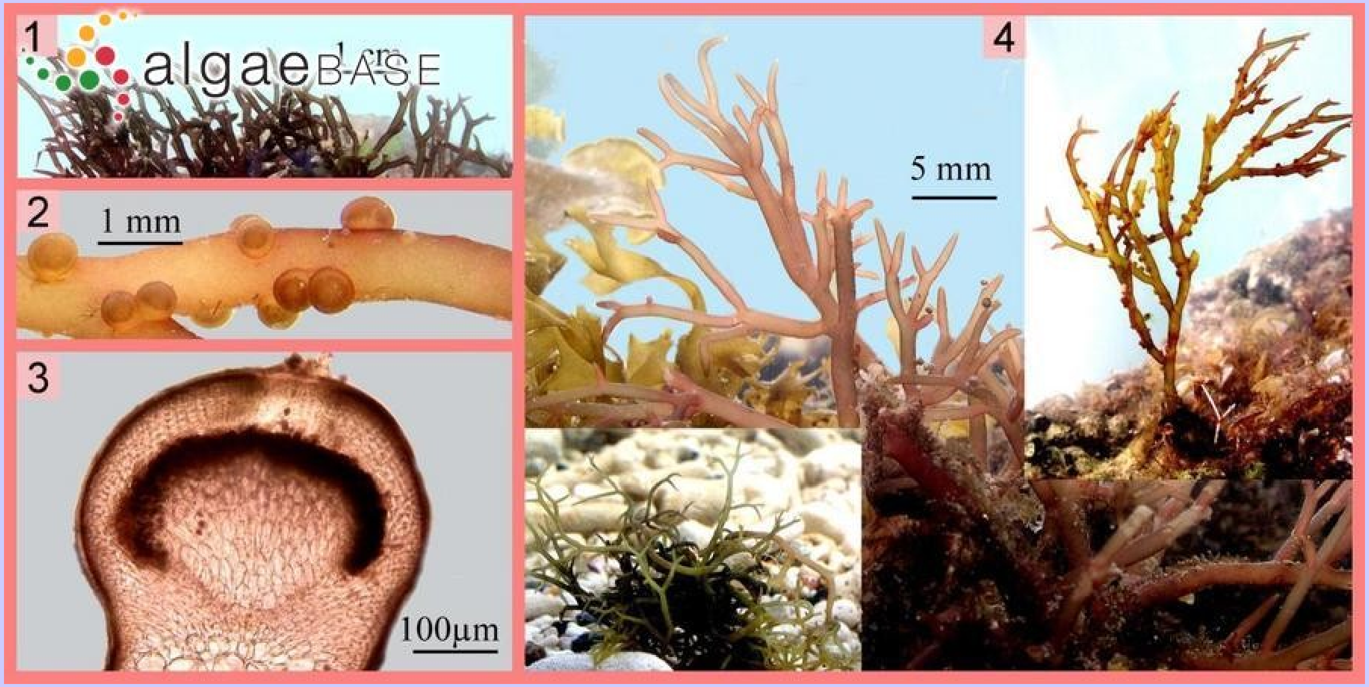

Hydropuntia (Gracilaria) edulis

Gigartinales
(Gigartina, Sphaerococcus, Furcellaria)

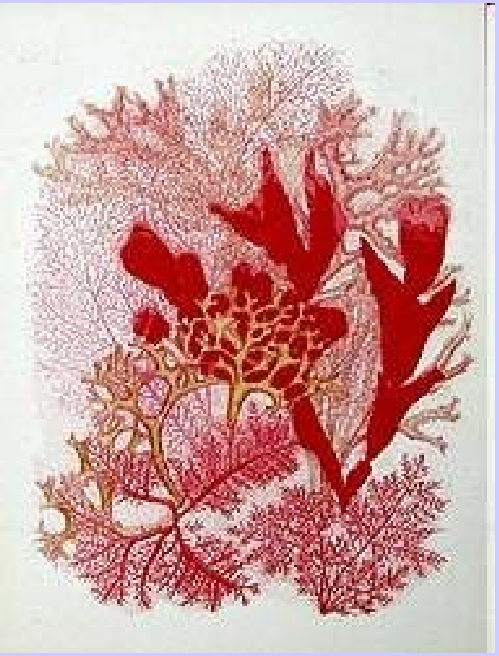

temperate and subtropical seas

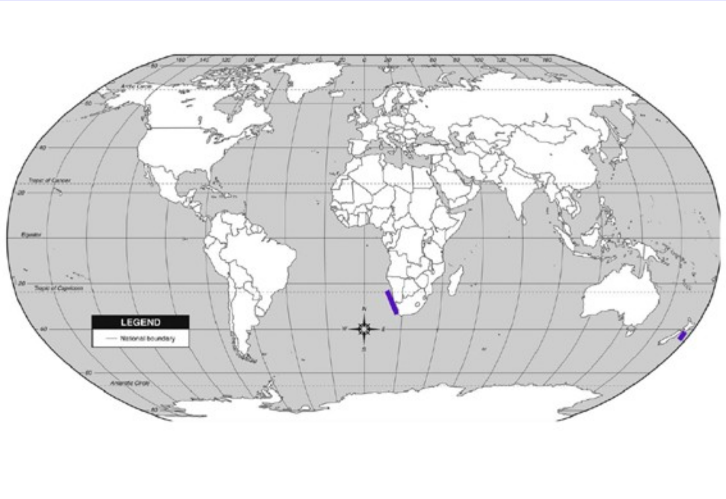

G. bracteata

Furcellaria lumbricalis

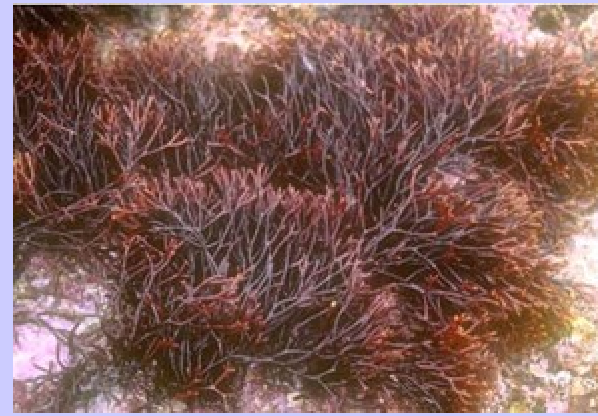

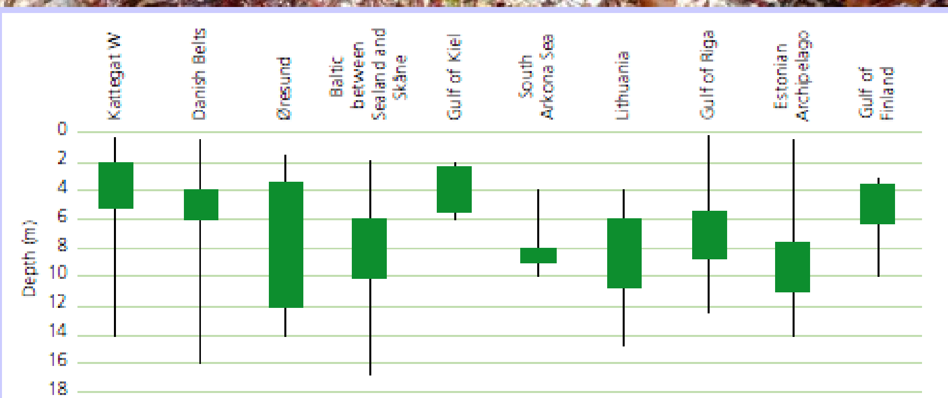

Figure 3.2.3. Maximum depth penetration of *Furcellaria lumbricalis* in different sea areas of the Baltic Sea. Boxes delimit the 25% and 75% percentiles and whiskers the minimum and maximum values. Data from 1989 to 2007 (CHARM database, national monitoring data).

one of the habitat forming algae in Baltic sea

e.g. 120 km2 of *loose-lying* thalli in lagunes close to western Estonian islands

distribution – western Mediterranean to Spitzbergen


Foto: Yvonne N.


Foto: Yvonne N.

Furcellaria has a triphasic l.c., but the carposporophyte lives on female gametophyte

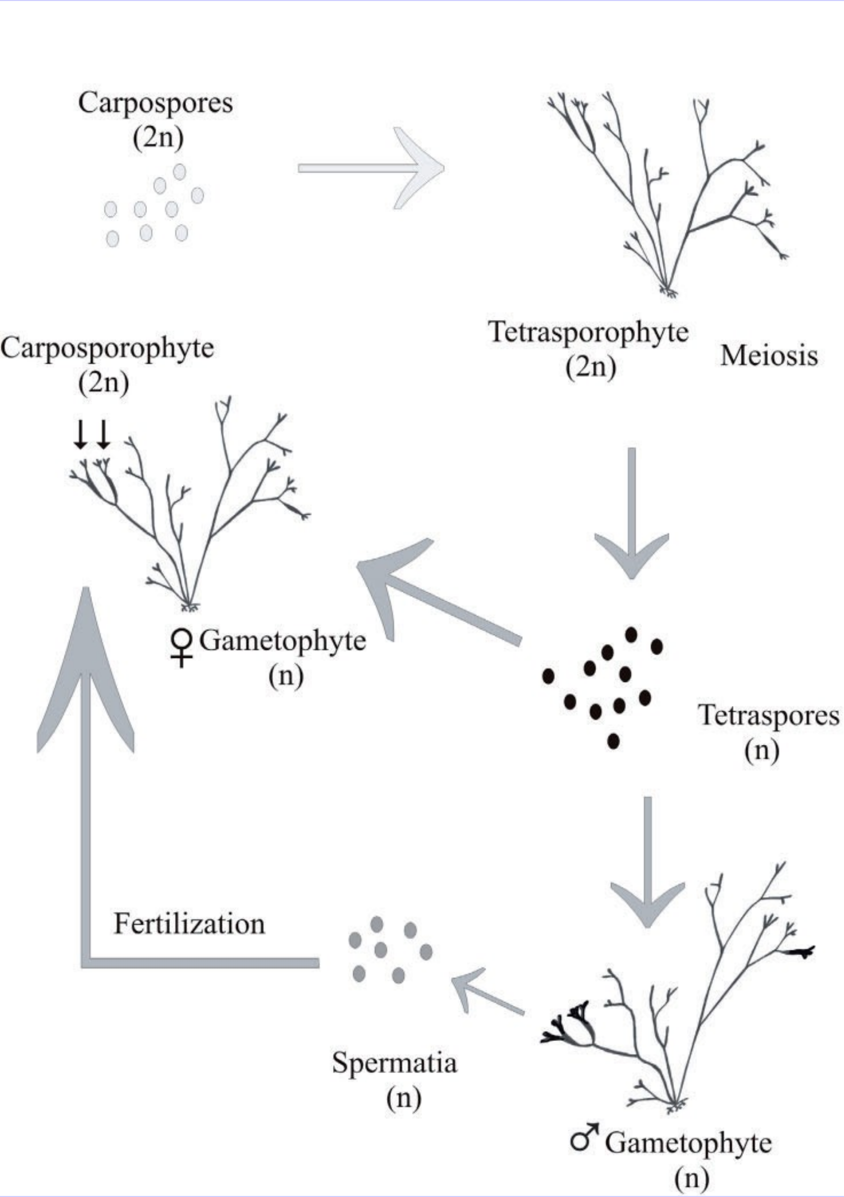

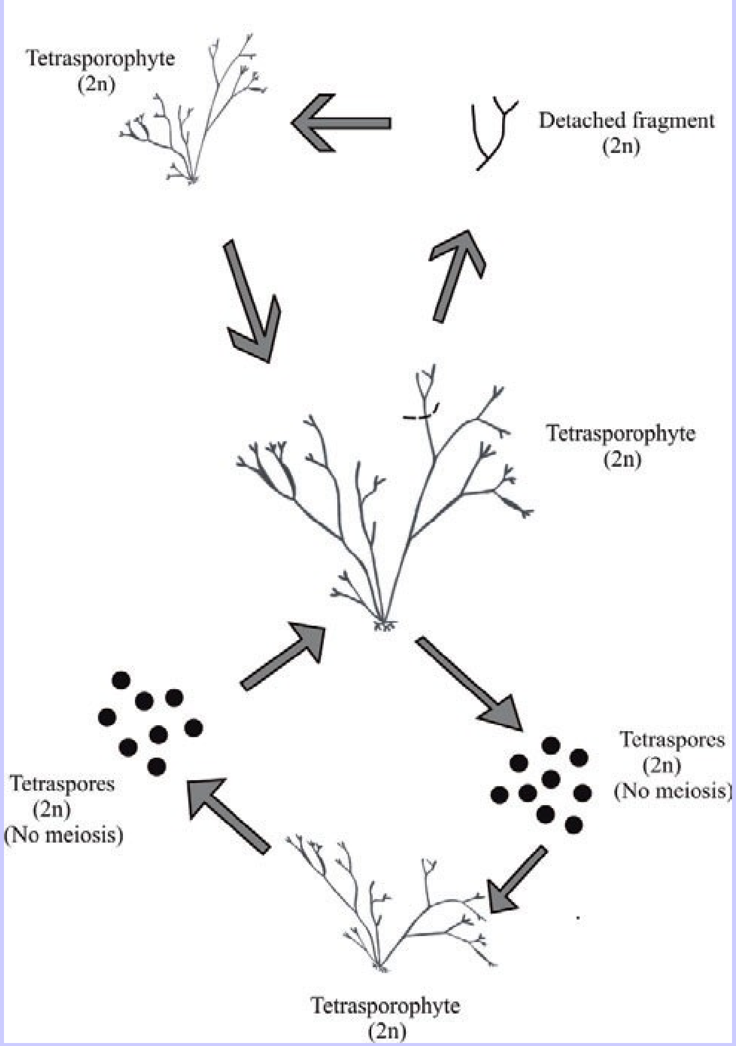

Kotsamo, 2008

<u>decreased salinity:</u>
tetrasporophytes only and only males;
<u>extremely decreased salinity:</u>
vegetative reproduction only

Coccotylus truncatus

(often occurs together with *F. lumbricalis*)

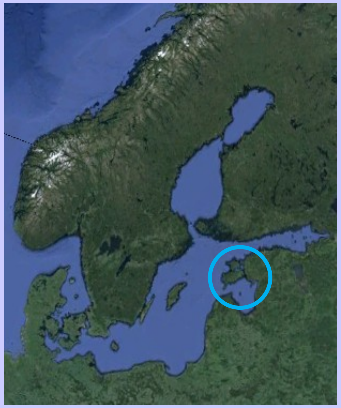

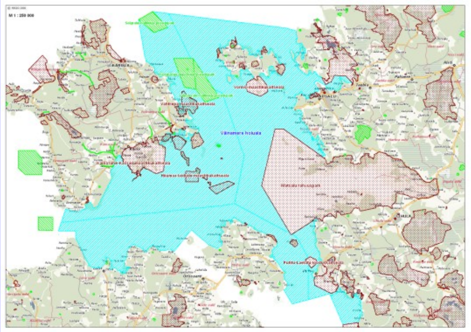

important part of the loose lying benthic communities in brackish lagunes
(such as Väinamere in the Baltic)

Chondrus

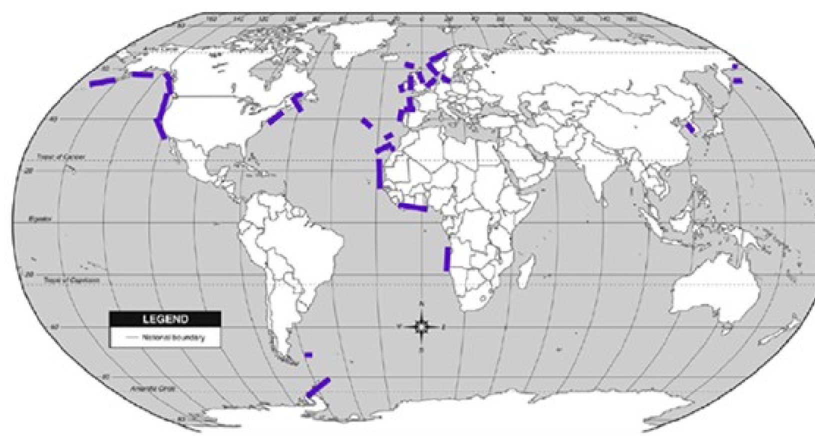

eulittoral of the cold temperate
European coasts

Ch.crispus

Gelidiales - e.g. *Gelidium, Pterocladiella, Gelidiella*

Gelidium sesquipedale (Foto: A. Santolaria)

Gelidium sesquipedale (Fot. A. Santolaria)

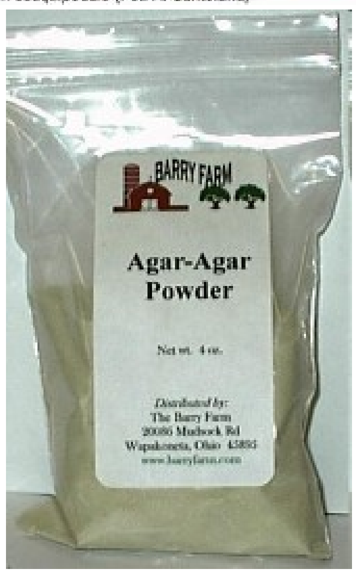

agar – from polysascharides of their cell walls

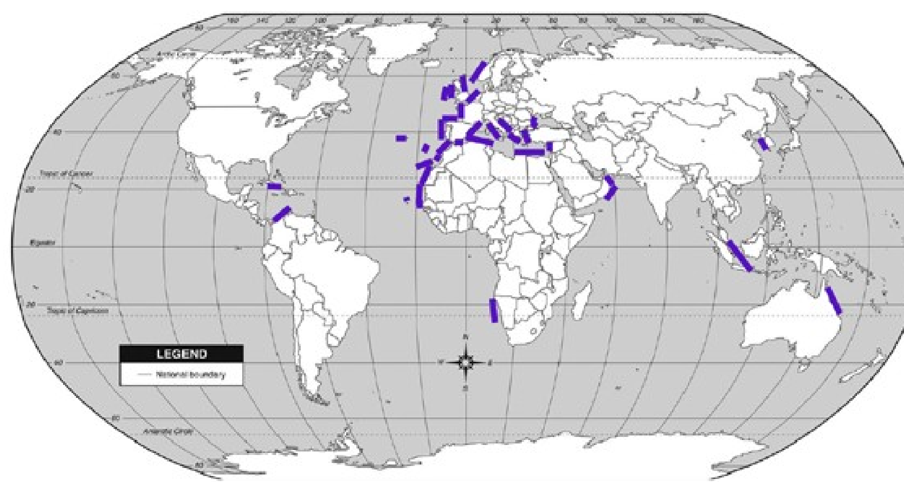

G. spinosum


Jersey
Ando

Bonnemaisoniales

Asparagopsis (armata / taxiformis)

macroscopic gametophyte,
filamentous microscopis tetrasporophyte (*Falkenbergia* stage)
antibacterial extract – examples…
cryptic diversity (invasive/local lineages)

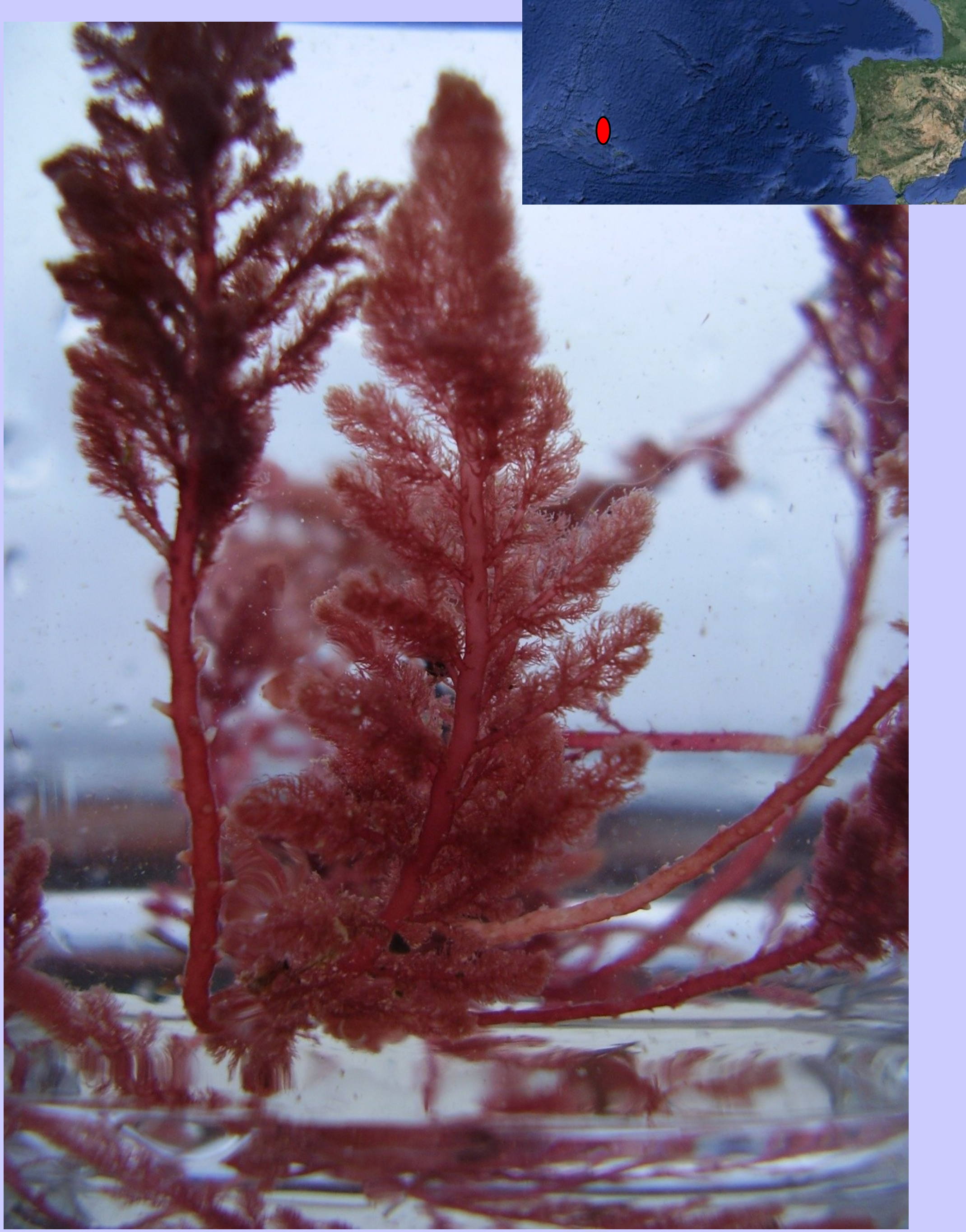

invasive red algae in subtropical seas (Mediterranean, Azores, etc.)

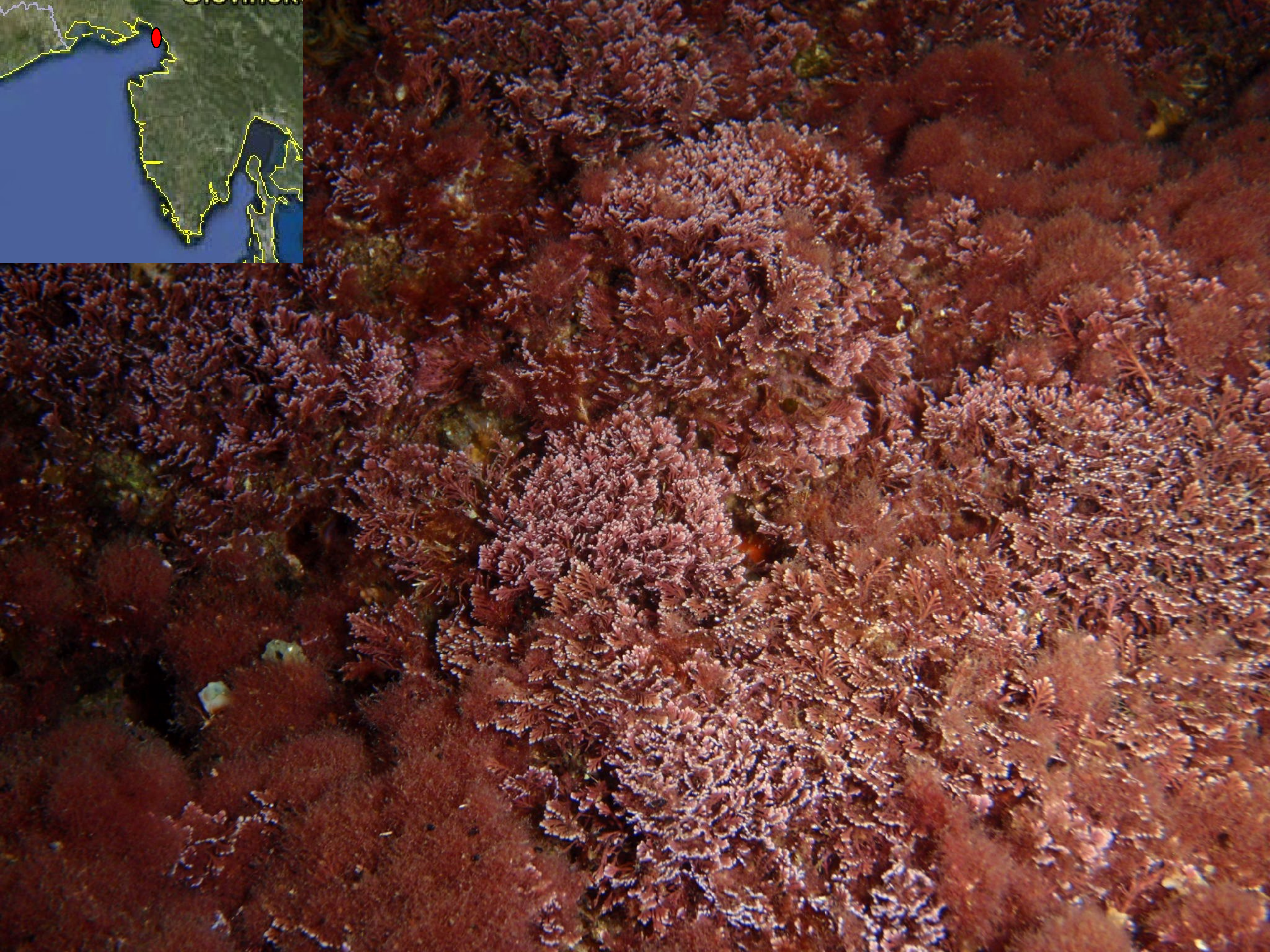

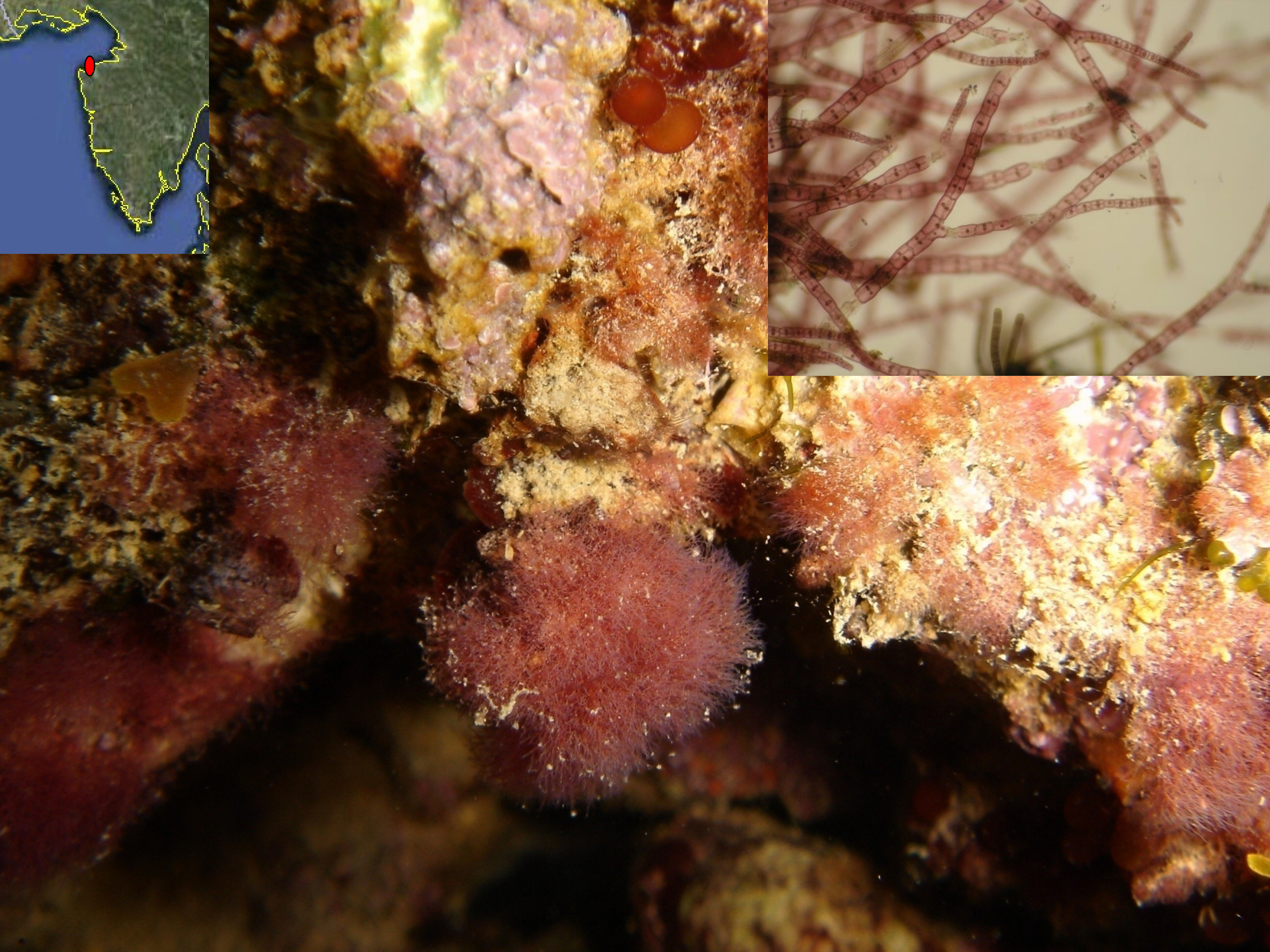

frequent world-wide introductions and invasions of cryptic *Asparagopsis* species

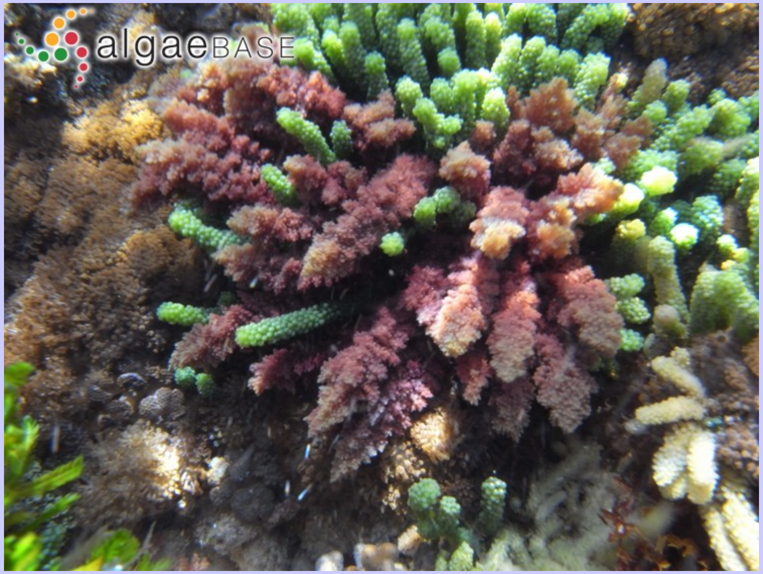

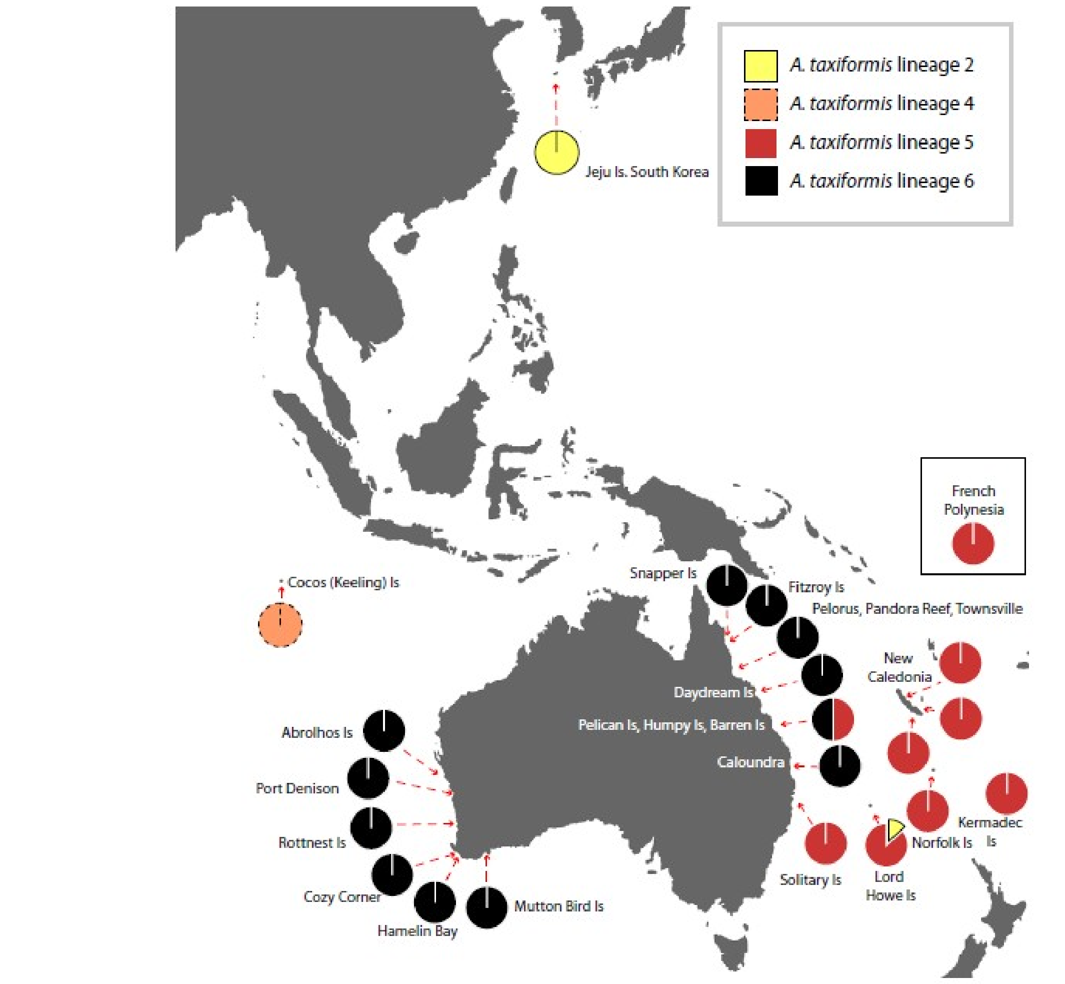

FIG. 1. Collection sites and mitochondrial lineage distribution of *Asparagopsis taxiformis* isolates analyzed in this study.

supposedly endemic lineages (5 and 6)
and globally invasive lineages (2) intermix
at the regional level

Andreakis et al., 2016, J. Phycol.

Halymeniales (Halymenia, Pachymenia)

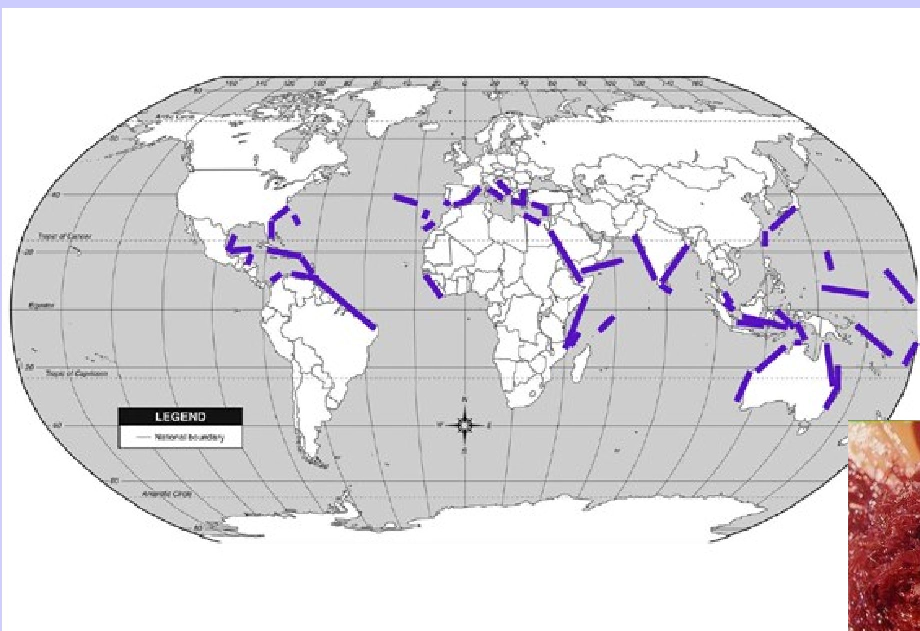

H. floresii

Pachymenia – jižní polokoule, N.Z.

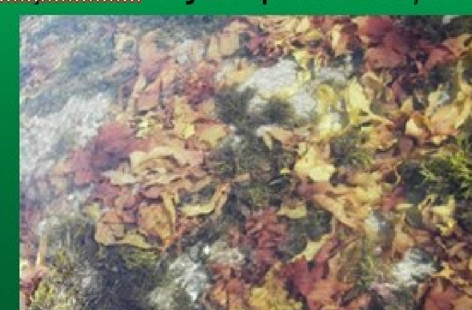

Plocamiales (Plocamium)

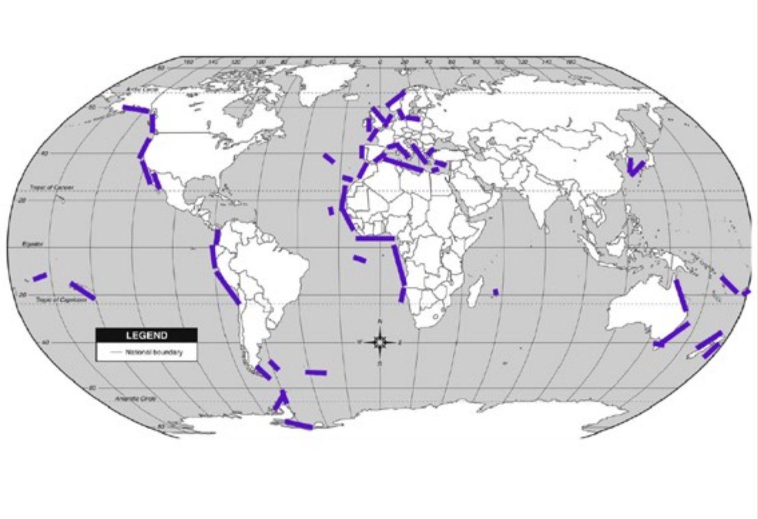

P. cartilagineum

Plocamium – lower sublittoral of temperate to tropical seas, cosmopolitan

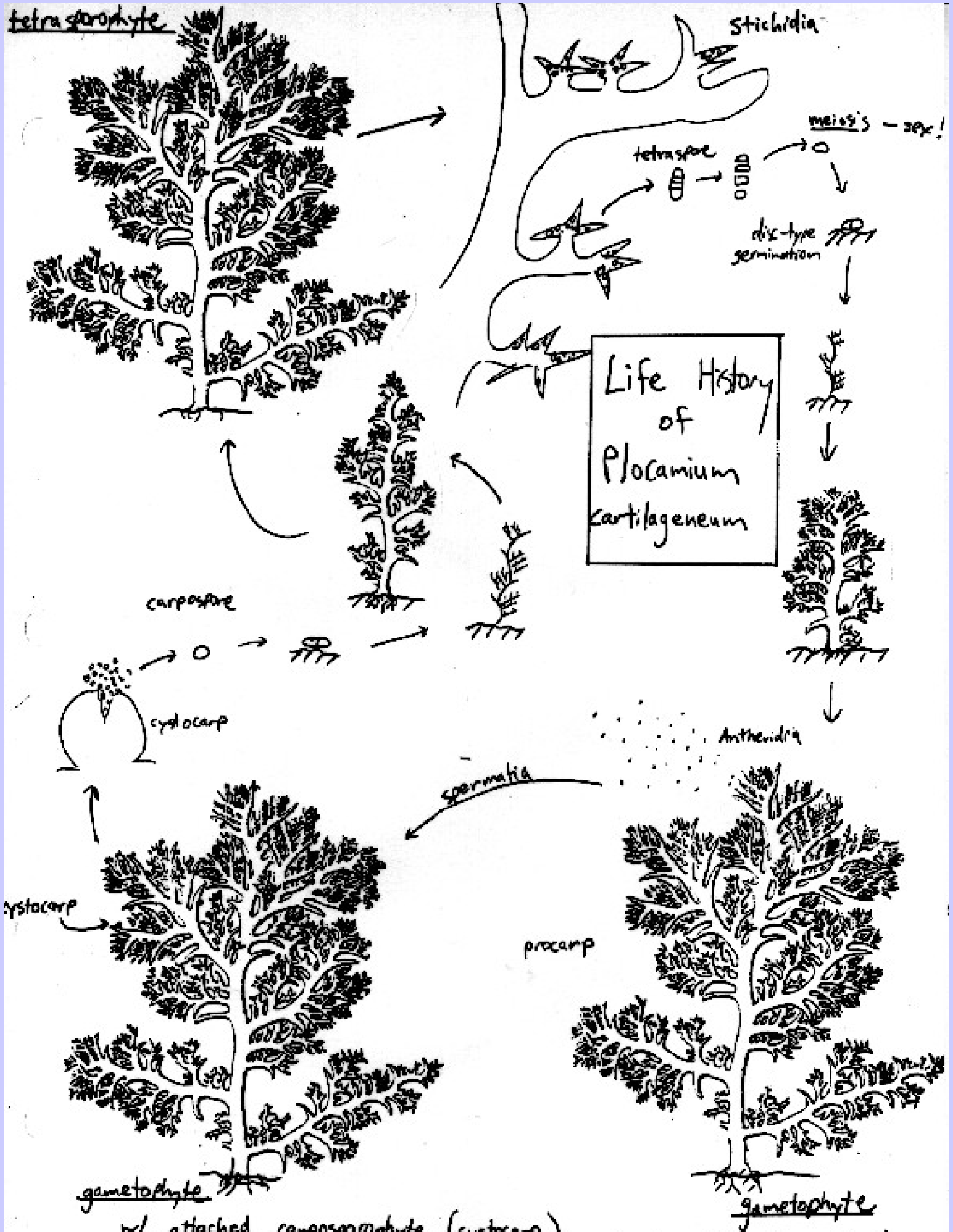

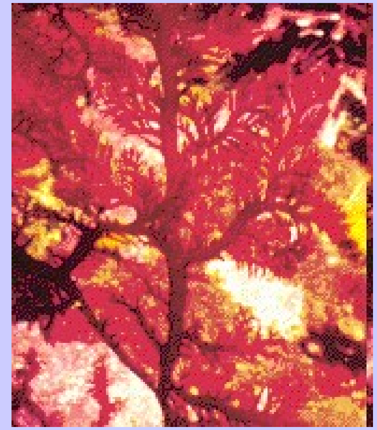

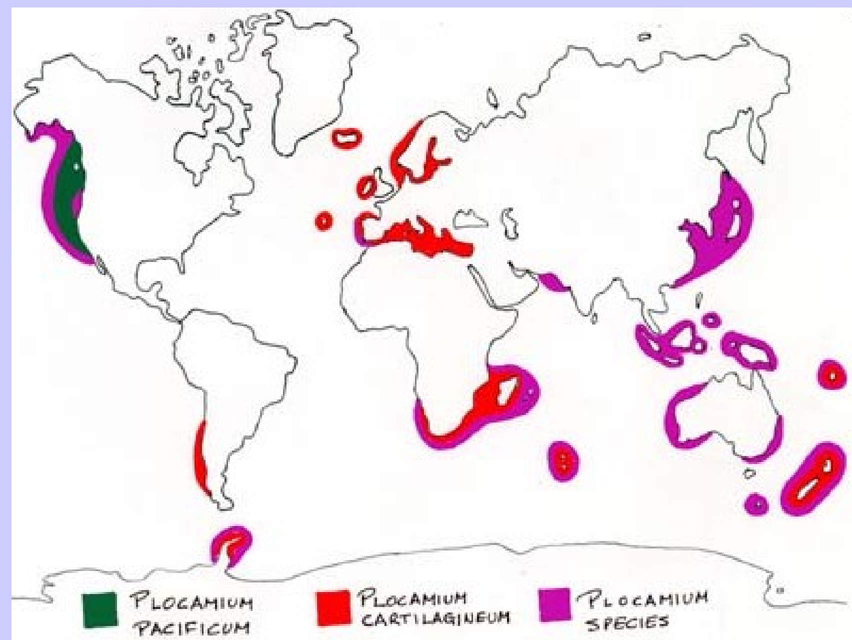

so far about 50 species

Ceramiales - an order with general tendency to secondarily simplified thalli

Ceramium

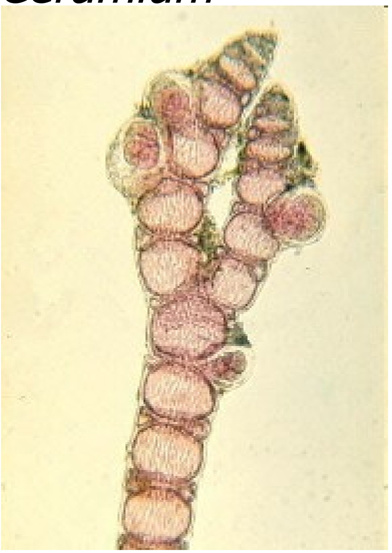

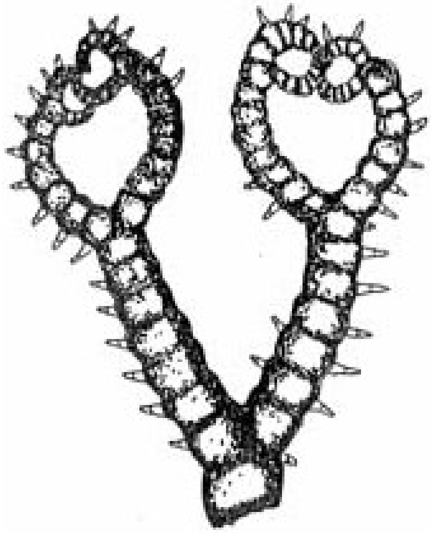

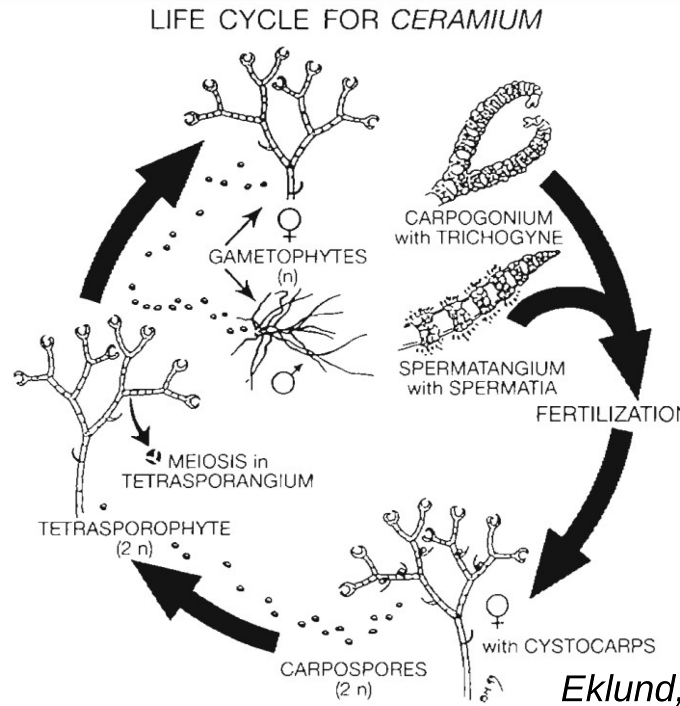

Eklund, 1998
Mar. Ecol. Progr. Ser.

ephemerous thalli

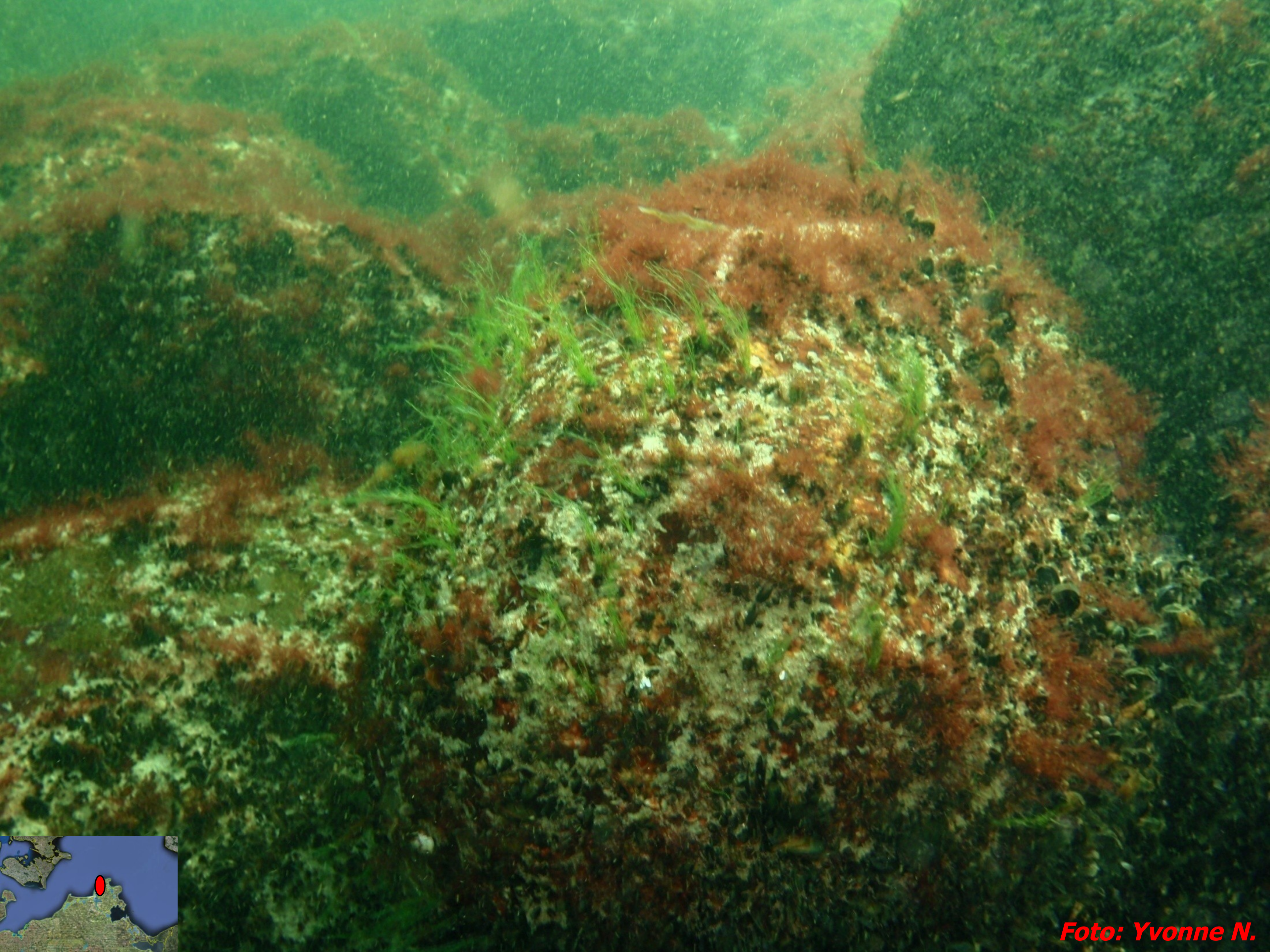
Foto: Yvonne N.

Callithamnion

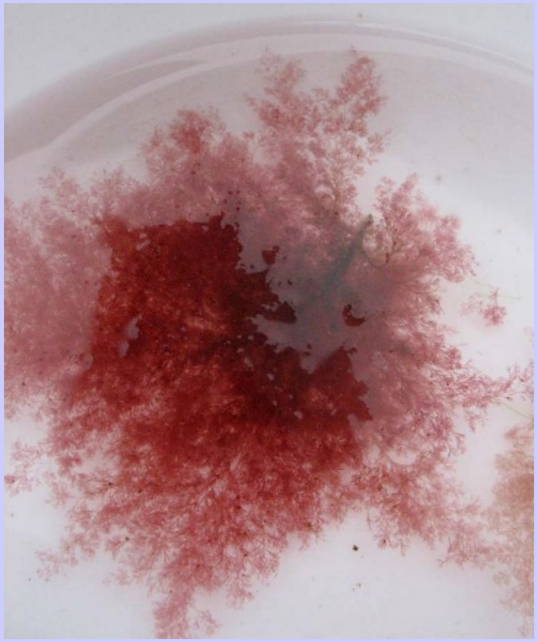

ephemerous thalli

epiphytes on perennial macroalgae or epilithic on stones

boreal and subtropical European coasts

Delesseria sanguinea

ephemerous phylloids growing repeatedly on perennial cauoid

lower sublittoral, cold European seas; pseudoparenchymatous thallus

Caloglossa

the delesseriacean lineage that also includes several freshwater and brackish species occurs in the tropics (and the freshwater aquariums as the „red moss")

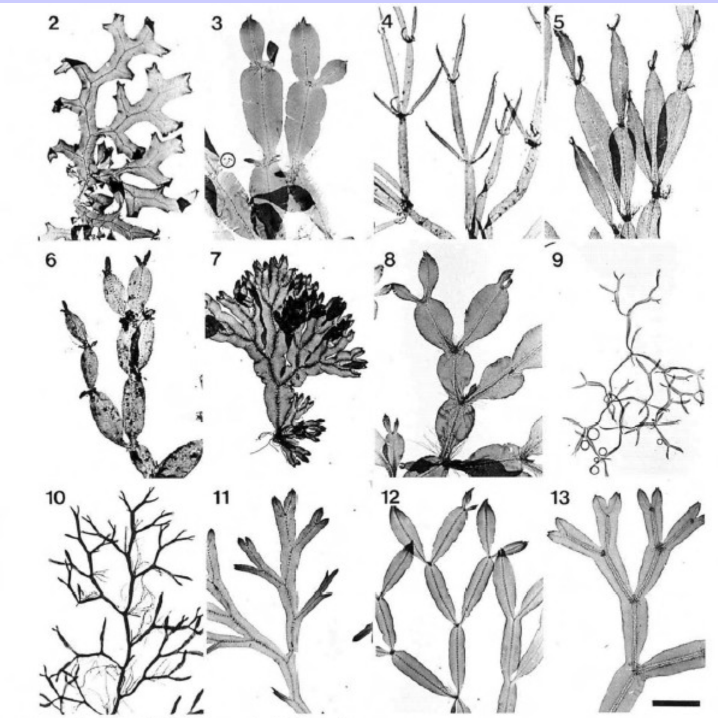

Figs 2–13. Vegetative thalli of *Caloglossa* species. Scale bar = 2mm.
Fig. 2. *Caloglossa adhaerens* from Isobe River, Ishigaki Island, Japan.
Fig. 3. *Caloglossa bengalensis* from Daintree River, Queensland, Australia.
Fig. 4. *Caloglossa ogasawaraensis* from Tone River, Chiba, Japan.
Fig. 5. *Caloglossa beccarii* from Sungai Kolok, Thailand.
Fig. 6. *Caloglossa stipitata* from Ambon, Indonesia.
Fig. 7. *Caloglossa monosticha* from Teluk Awang, Lombok, Indonesia.
Fig. 8. *Caloglossa monosticha* from São Paulo, Brazil.
Fig. 9. *Caloglossa saigonensis* from Sandakan, Sabah, Malaysia.
Fig. 10. *Caloglossa postiae* from Georges River, NSW, Australia.
Fig. 11. *Caloglossa continua* from Shiotsuka River, Fukuoka, Japan.
Fig. 12. *Caloglossa leprieurii* from Umlalazi, Natal, South Africa.
Fig. 13. *Caloglossa intermedia* from James Island, South Carolina, USA.

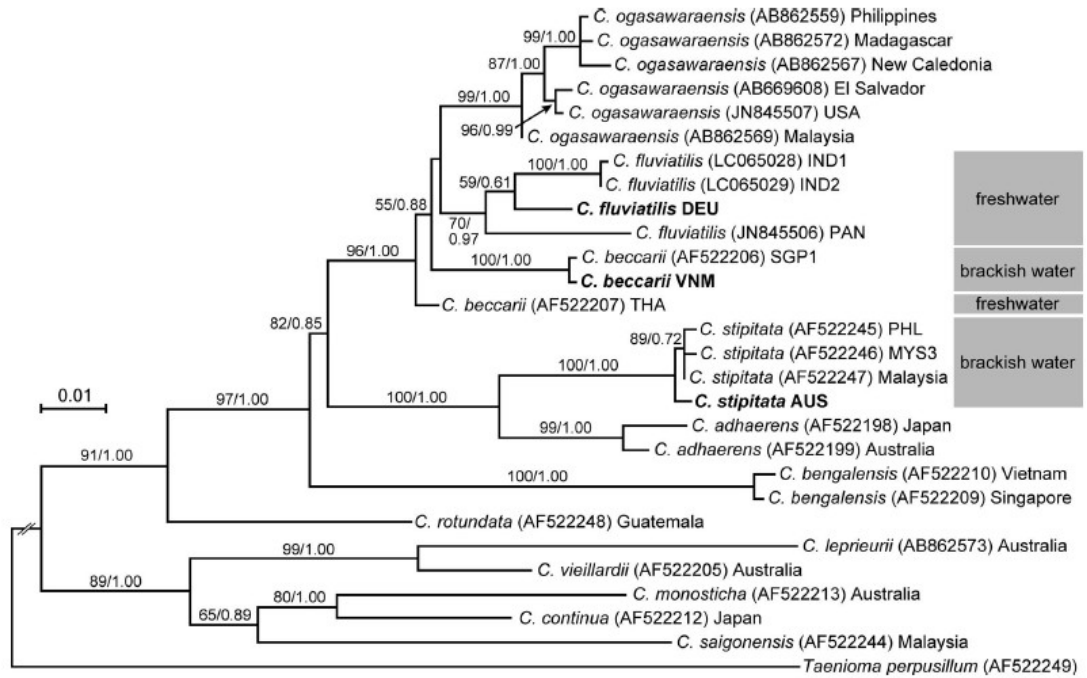

Fig. 1. Maximum-likelihood (ML) phylogeny of *Caloglossa* species inferred from the partial LSU rDNA gene sequences. *Taenioma perpusillum* was used as an outgroup. The bootstrap values for ML (> 50%; left) and posterior probabilities for Bayesian inference (BI) (≥ 0.50; right) are presented for each branch. Accession number is shown in each set of parentheses, and habitats of *C. beccarii* and related species are shown in gray boxes. Newly sequenced samples are shown in bold. See Table 1 for the information of abbreviations after species names.

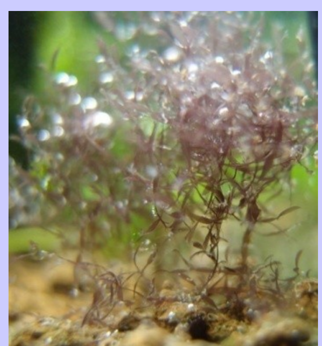

Kamiya et al., 2016, Phycologia
Kamiya et al., 2003, Phycologia

Claudea

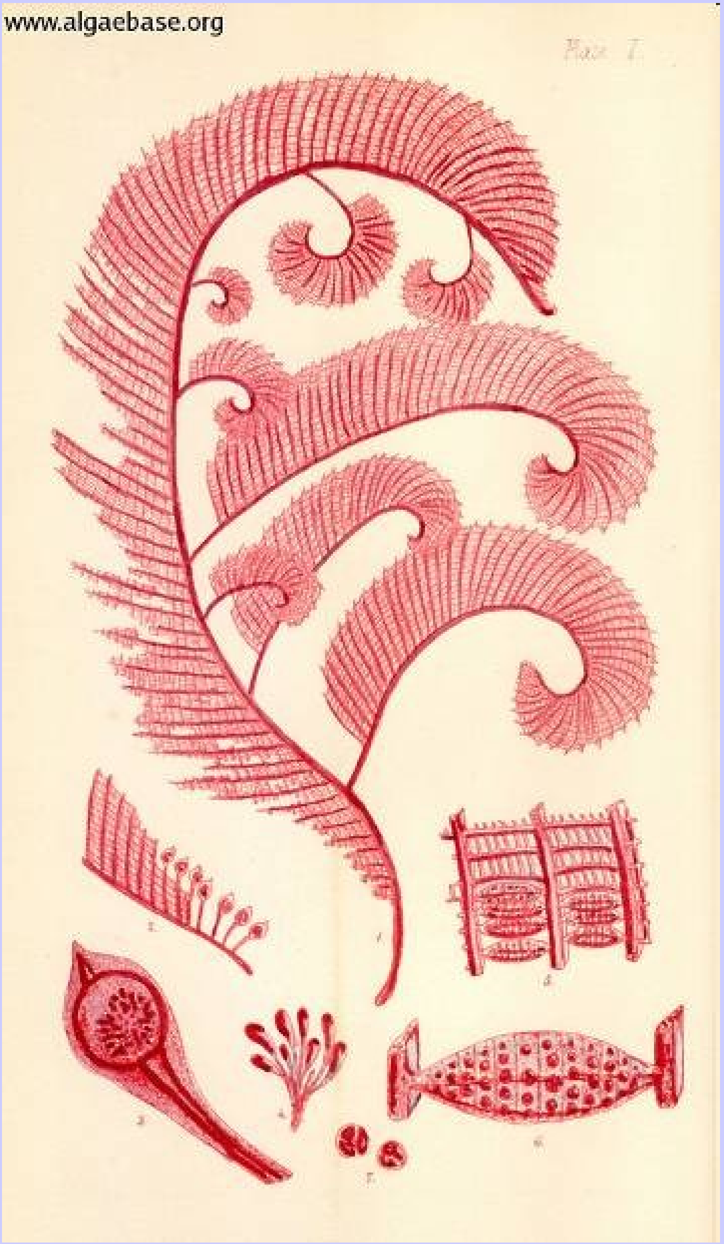

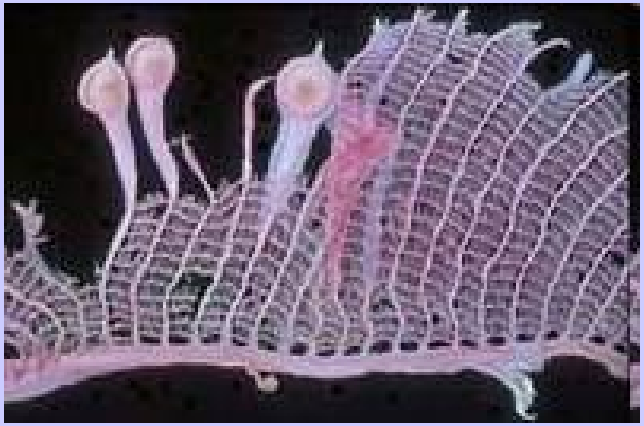

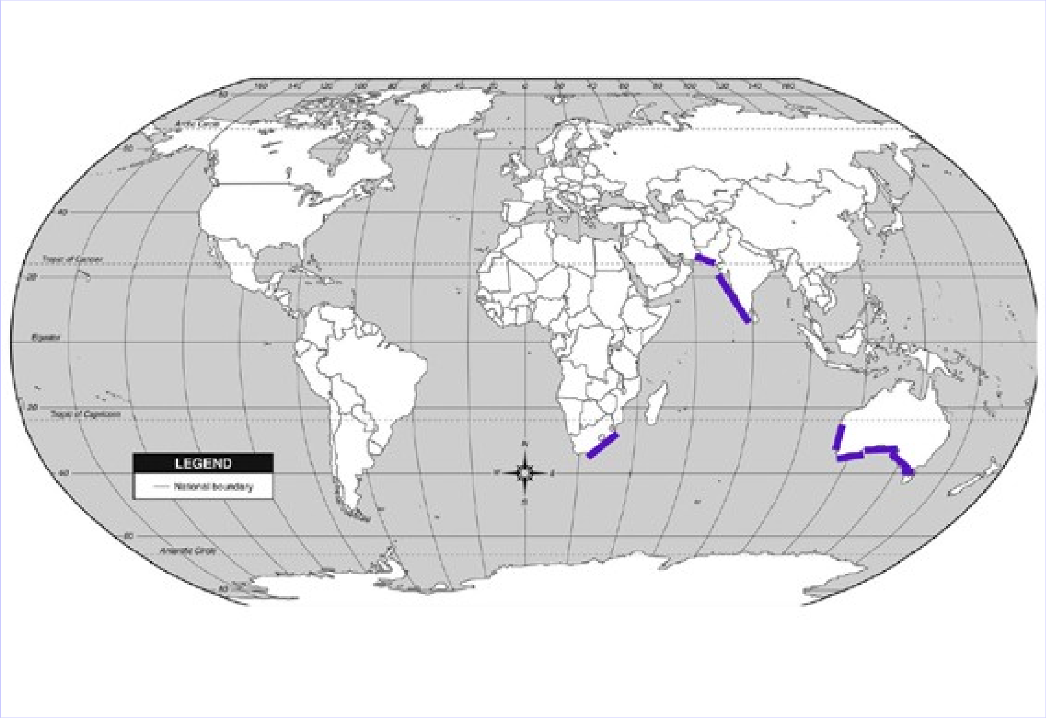

C. elegans

Polysiphonia (generic complex)

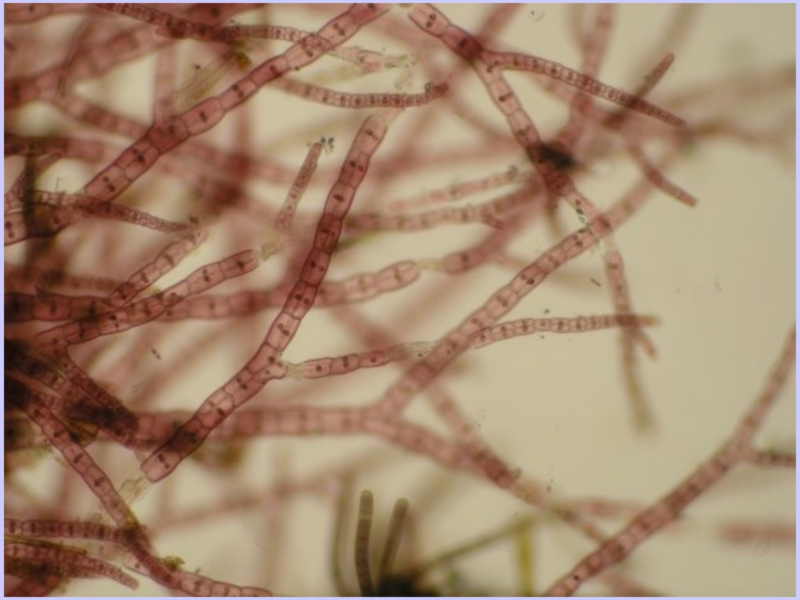

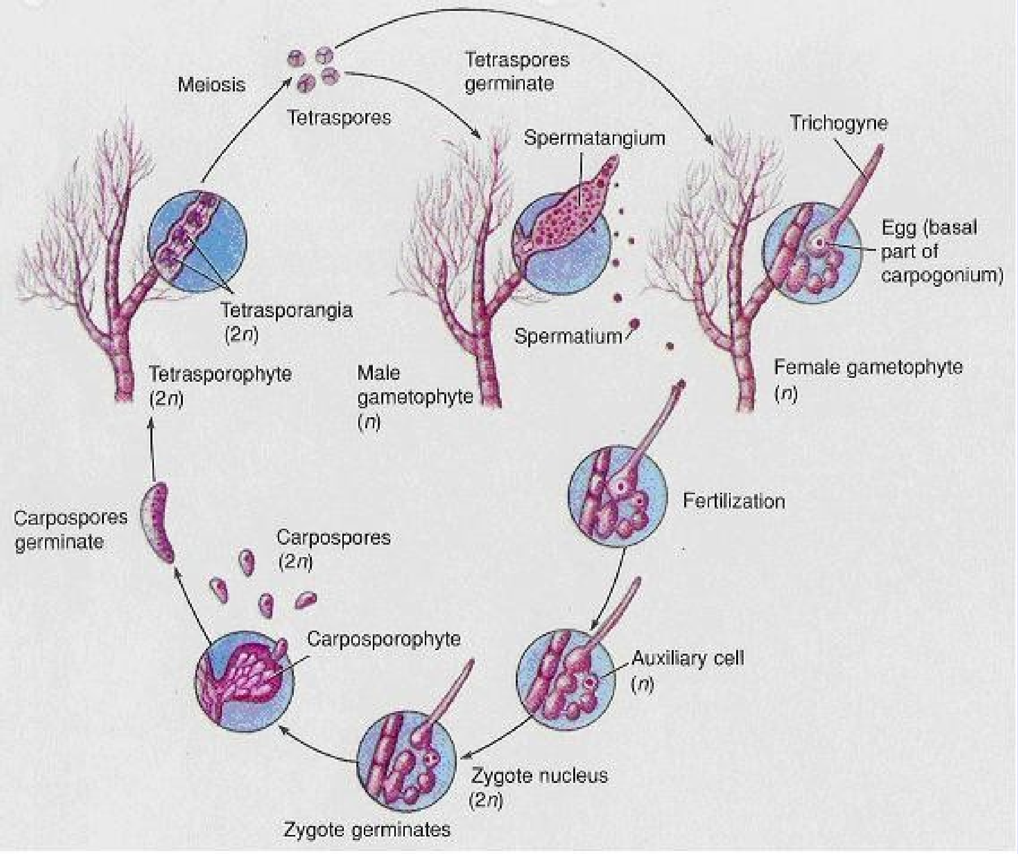

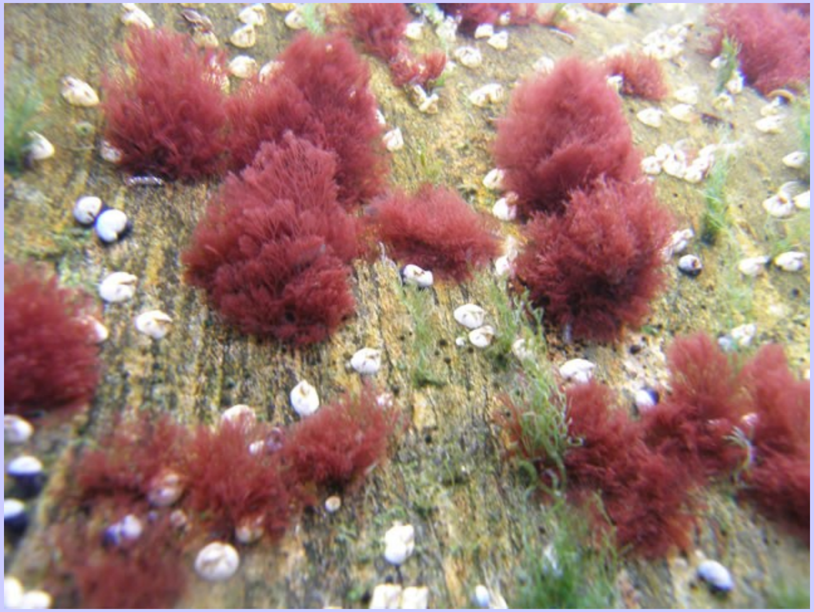

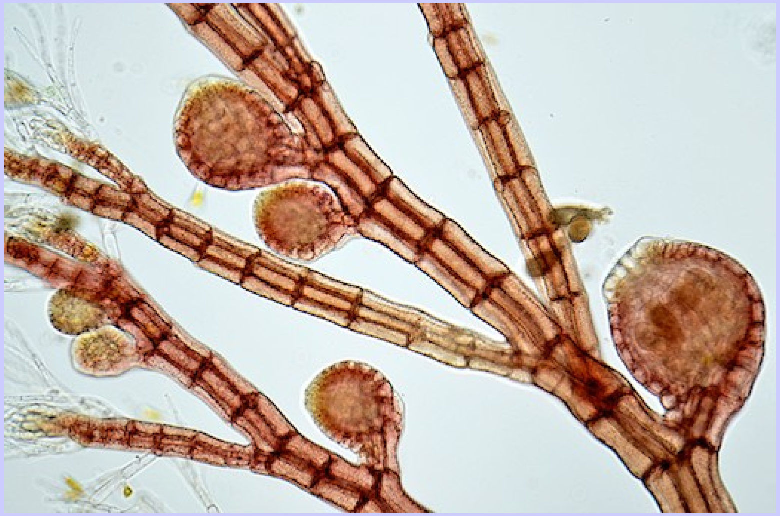


Foto: Yvonne N.

Vertebrata fucoides

European coasts;
inclusing brackish Batic Sea

Odonthalia

O. floccosa
Pacific coast of N Am

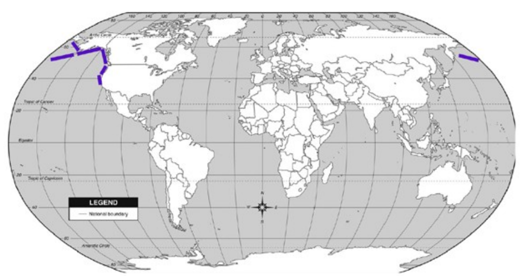

O. dentata
circumboreal distribution, incl. European N Atl

a cold water genus

Choreocolax, Plocamiocolax, Gracilariophila

obligatory parasites of other red algae, so called **adelphoparasites**
they eject their own nuclei into host cells where they replicate and, eventually, form spores

Choreocolax is also known to steal the plastids of the host alga (i.e. *Polysiphonia*)
but it still possesses its own very small plastid genome and a „ghost plastid"

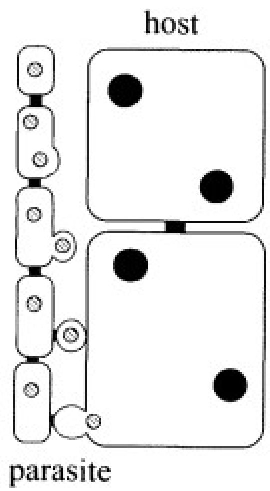

Figure 1. Process of Secondary Pit Connection between Cells of Parasitic Red Algae and Their Host.

Parasite nuclei are striped, light circles and host nuclei are black circles.

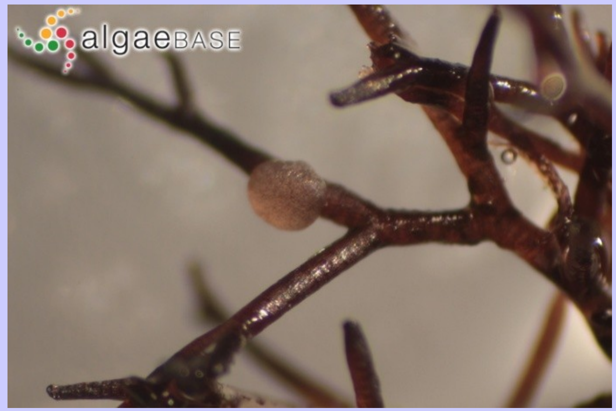

Choreocolax polysiphoniae

Plocamiocolax pulvinata

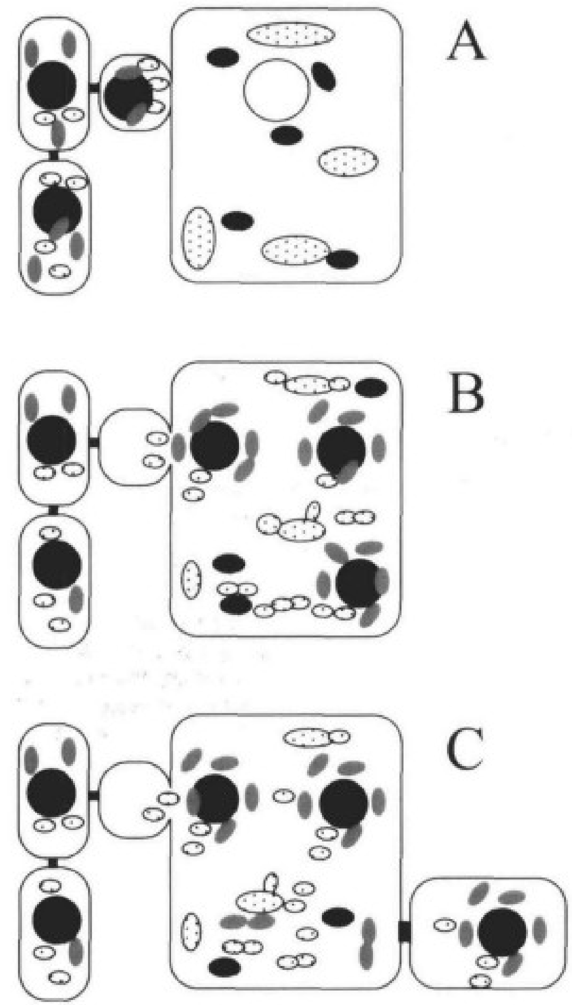

Figure 10. Transfer of Parasite Nuclei, Mitochondria, and Proplastids into a Host Cell.

(A) The parasite cells (left) have formed a conjunctor cell containing a parasite nucleus (black), mitochondria (gray), and proplastids (white with dots). This conjunctor cell fuses with the host cell (host nuclei are white, host plastids are dotted, and host mitochondria are black ovals) delivering the parasite organelles into the host's cytoplasm.
(B) The parasite nucleus and mitochondria replicate in the host cell, and the host plastids divide to form numerous proplastids. The host nuclei and mitochondria replicate in the host cell. The host nucleus may disappear or persist.
(C) Ultimately, a cell is cut off from the heterokaryotic host plus parasite cell. This cell contains a parasite nucleus, parasite mitochondria, and proplastids derived from the host plastids.

Goff & Coleman, 1995, Plant Cell
Salomaki et al., 2015, J Phycol

Rhodymeniales

Rhodymenia and allied genera – tropics and subtropics (Rhodymeniaceae)

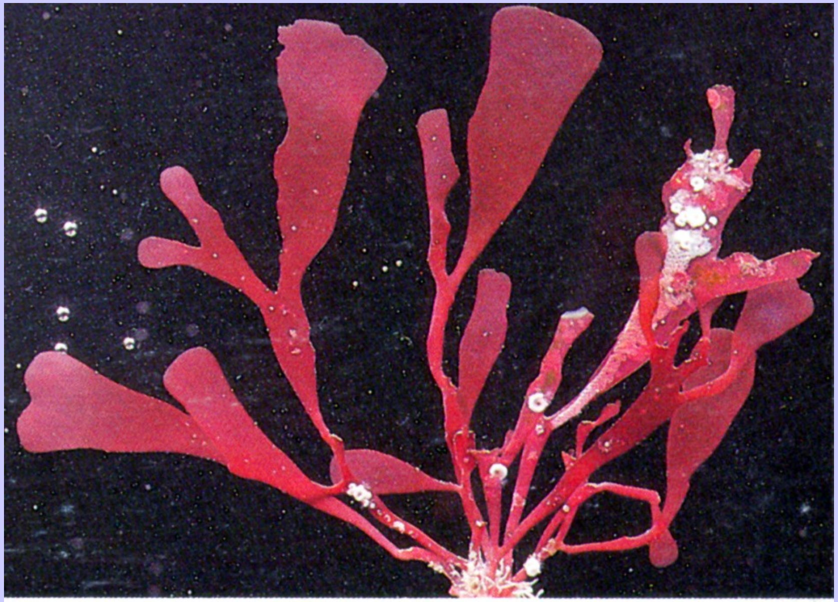

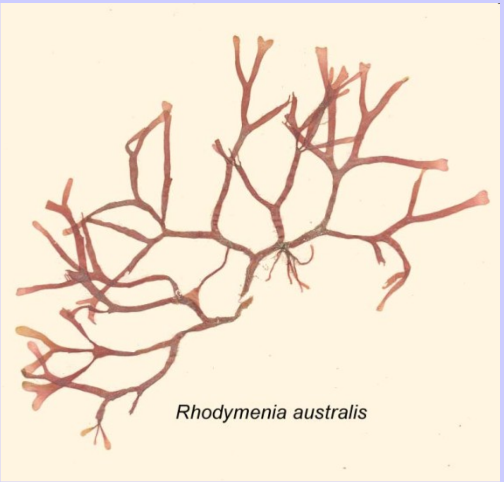

Sparlingia pertusa

Rhodymenia cf. pseudopalmata

Botryocladia

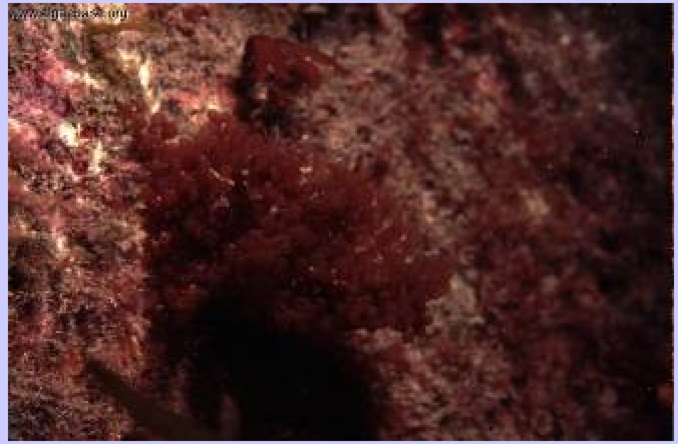

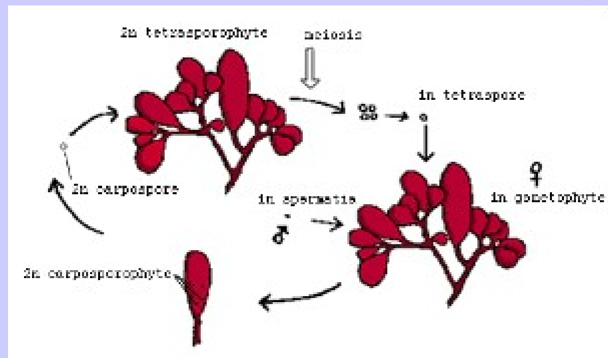

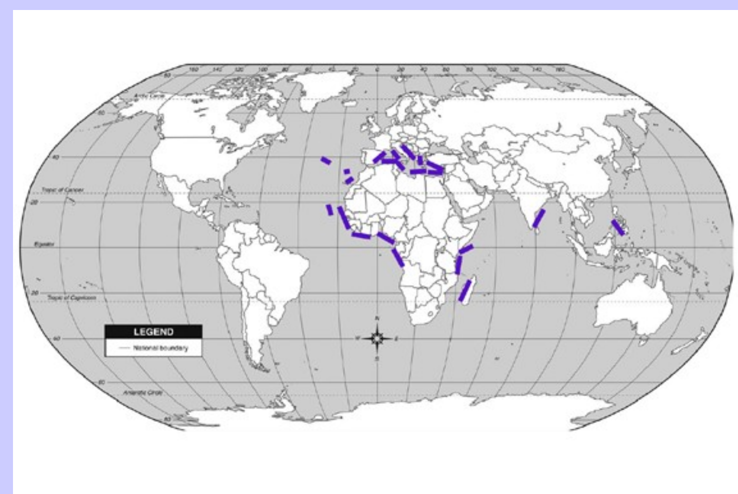

B. botryoides